

Sheffield Hallam University

The hydraulic bulge forming of tubular components.

BARLOW, Timothy James.

Available from the Sheffield Hallam University Research Archive (SHURA) at:

<http://shura.shu.ac.uk/19316/>

A Sheffield Hallam University thesis

This thesis is protected by copyright which belongs to the author.

The content must not be changed in any way or sold commercially in any format or medium without the formal permission of the author.

When referring to this work, full bibliographic details including the author, title, awarding institution and date of the thesis must be given.

Please visit <http://shura.shu.ac.uk/19316/> and <http://shura.shu.ac.uk/information.html> for further details about copyright and re-use permissions.

SHEFFIELD CITY
POLYTECHNIC LIBRARY
POND STREET
SHEFFIELD S1 1 7B

6829

TELEPEN

101 122 001 6



~~18/10.
20.41~~

~~8/6
17/54~~

~~20/6/95 10.39~~

~~18/9/95 20.36.~~

Sheffield City Polytechnic Library
REFERENCE ONLY

ProQuest Number: 10694197

All rights reserved

INFORMATION TO ALL USERS

The quality of this reproduction is dependent upon the quality of the copy submitted.

In the unlikely event that the author did not send a complete manuscript and there are missing pages, these will be noted. Also, if material had to be removed, a note will indicate the deletion.



ProQuest 10694197

Published by ProQuest LLC (2017). Copyright of the Dissertation is held by the Author.

All rights reserved.

This work is protected against unauthorized copying under Title 17, United States Code
Microform Edition © ProQuest LLC.

ProQuest LLC.
789 East Eisenhower Parkway
P.O. Box 1346
Ann Arbor, MI 48106 – 1346

ABSTRACT

THE HYDRAULIC BULGE FORMING OF TUBULAR COMPONENTS

T. J. BARLOW

The bulge forming process is a method for shaping tubular components using an internal hydrostatic pressure combined with an axial compressive force. Initial investigations involved carrying out an extensive literature survey to determine the components which could be formed and the types of machines which have been used. Subsequent to this, initial tests were carried out using a previously designed die and tool block in conjunction with a compression testing machine. In these tests copper tubes were formed into expander/reducers and cross pieces by manual adjustment of the axial force and internal pressure.

Having obtained experience of the difficulties associated with this die and tool block, and the loading requirements necessary for the forming process, a new bulge forming machine was designed. The design of the machine was based on the following main criteria:

- (i) The machine should be free standing and self contained.
- (ii) The axial deformation of the ends of the tube blank should be synchronised to allow the bulge to form centrally on the tube.
- (iii) The internal bulge forming pressure should be externally controllable during the forming process.
- (iv) The design should incorporate facilities for subsequent automatic control using a micro-processor/computer.

On the basis of these requirements, a machine was designed, built and commissioned.

After correcting a few problems encountered in the commissioning of the machine, a series of tests were carried out, forming tee and cross pieces from copper tube of two different wall thicknesses. These were found to be fairly easy to produce on this new machine. From the resulting components, formed at various combinations of internal pressure and axial compressive force, the limits for a successful forming operation were established. Further analysis of these components was then undertaken to evaluate the effects of the internal pressure and axial compressive force on the bulge height and the wall thickness in the deformation zone. From these results, which have been illustrated graphically, the greatest effect on the resulting bulge can be seen to be the axial compressive force.

An extension of a theoretical analysis has also been presented, which predicts the wall thickness distribution around the bulge zone. Comparison of these predictions with the experimental wall thickness distributions shows fairly good agreement, especially at the root and tip of the side branch.

THE HYDRAULIC BULGE FORMING

OF TUBULAR COMPONENTS

by

TIMOTHY JAMES BARLOW BSc

A Thesis submitted to the COUNCIL FOR NATIONAL ACADEMIC AWARDS

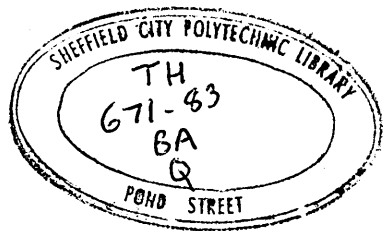
in partial fulfilment for the degree of

DOCTOR OF PHILOSOPHY

Sponsoring Establishment : Department of Mechanical and
Production Engineering,
Sheffield City Polytechnic,
Sheffield.

Collaborating Establishment : Yorkshire Imperial Metals Ltd,
PO Box 166,
Leeds.

December 1986



ACKNOWLEDGEMENTS

The author wishes to express his sincere gratitude to Dr R Crampton and Dr M S J Hashmi for their encouragement and helpful supervision during the course of this project.

The technical assistance offered by Mr R Teasdale and his staff was much appreciated and in particular the author wishes to thank Messrs R Sidebottom, D Woodhead, A Fletcher and L. Evans for the dedicated work they carried out constructing the bulge forming machine.

The author would also like to express his gratitude to Mr W Rushton of Yorkshire Imperial Metals Ltd for providing financial support and materials towards this research, and also for his encouragement.

Finally, a very sincere thanks goes to my parents for their understanding and encouragement during the whole course of this research.

DECLARATION

The author declares that no part of this work has been submitted in support of another degree or qualification to this or any other establishment. The author further declares that he not been a registered candidate or enrolled student for another award of the CNAA or other academic or professional institution during the course of the research programme.

T. J. Barlow

ABSTRACT

THE HYDRAULIC BULGE FORMING OF TUBULAR COMPONENTS

T. J. BARLOW

The bulge forming process is a method for shaping tubular components using an internal hydrostatic pressure combined with an axial compressive force. Initial investigations involved carrying out an extensive literature survey to determine the components which could be formed and the types of machines which have been used. Subsequent to this, initial tests were carried out using a previously designed die and tool block in conjunction with a compression testing machine. In these tests copper tubes were formed into expander/reducers and cross pieces by manual adjustment of the axial force and internal pressure.

Having obtained experience of the difficulties associated with this die and tool block, and the loading requirements necessary for the forming process, a new bulge forming machine was designed. The design of the machine was based on the following main criteria:

- (i) The machine should be free standing and self contained.
- (ii) The axial deformation of the ends of the tube blank should be synchronised to allow the bulge to form centrally on the tube.
- (iii) The internal bulge forming pressure should be externally controllable during the forming process.
- (iv) The design should incorporate facilities for subsequent automatic control using a micro-processor/computer.

On the basis of these requirements, a machine was designed, built and commissioned.

After correcting a few problems encountered in the commissioning of the machine, a series of tests were carried out, forming tee and cross pieces from copper tube of two different wall thicknesses. These were found to be fairly easy to produce on this new machine. From the resulting components, formed at various combinations of internal pressure and axial compressive force, the limits for a successful forming operation were established. Further analysis of these components was then undertaken to evaluate the effects of the internal pressure and axial compressive force on the bulge height and the wall thickness in the deformation zone. From these results, which have been illustrated graphically, the greatest effect on the resulting bulge can be seen to be the axial compressive force.

An extension of a theoretical analysis has also been presented, which predicts the wall thickness distribution around the bulge zone. Comparison of these predictions with the experimental wall thickness distributions shows fairly good agreement, especially at the root and tip of the side branch.

CONTENTS

ACKNOWLEDGEMENT	(i)
DECLARATION	(ii)
ABSTRACT	(iii)
INDEX TO FIGURES	(viii)
NOMENCLATURE	(xi)
1. INTRODUCTION	1
1.1. THE BULGE FORMING PROCESS	1
1.2. BULGE FORMED COMPONENTS	4
1.2.1. Axisymmetrical Components	4
1.2.2. Asymmetrical Components	6
1.2.3. Commercially Produced Components	8
1.2.4. Associated Applications	10
1.3. FAILURES OF THE PROCESS	13
1.4. PREVIOUS INVESTIGATIONS	14
1.4.1. Axisymmetric al Bulge forming	14
1.4.2. Asymmetric al Bulge forming	17
2. PRELIMINARY INVESTIGATION	23
2.1. THE PROTOTYPE BULGE FORMING MACHINE	23
2.2. EXPERIMENTAL PROCEDURE	24
2.3. DISCUSSION OF RESULTS	26
2.4. PROBLEMS ASSOCIATED WITH THE PROTOTYPE RIG	29
2.5. CONSIDERATIONS FOR THE DESIGN OF A NEW RIG	32

3. BULGE FORMING MACHINE DESIGN	40
3.1. OPERATING PARAMETERS	40
3.2. HYDRAULIC COMPONENTS	41
3.2.1. Hydraulics Supply Pressure	41
3.2.2. Hydraulic Cylinders Applying Axial Force	41
3.2.3. Hydraulic Cylinders Applying Clamping Force	42
3.2.4. Hydraulic Pump & Electric Motor	43
3.3. THE HYDRAULIC CIRCUIT	45
3.3.1. The Clamping Hydraulic Cylinder	46
3.3.2. The Hydraulic Cylinder Applying Axial Force	46
3.3.3. The Internal Pressurised Region of the Tube Blank	46
3.3.4. The Initial Circuit Design	47
3.3.5. The Actual Circuit Design	48
3.4. THE STRUCTURAL DESIGN OF THE MACHINE	50
3.4.1. The Clamping Force Restraint	51
3.4.2. The Axial Force Restraint	53
3.4.2.1. The Mounting Brackets	54
3.4.3. Assembly	56
3.4.4. Alterations to the Initial design	58
3.5. COMMISSIONING	59
3.5.1. Structural Problems	59
3.5.2. Hydraulic Problems	60
4. TEST PROCEDURE	84
4.1. TEST MATERIAL	84
4.2. OPERATING PROCEDURE	84
4.2.1. Fixed Internal Pressure During Bulging	86

4.2.2. Increasing Internal Pressure During Bulging	87
4.2.3. Increasing Internal Pressure in Stages	88
4.3. ANALYSIS OF THE FORMED COMPONENTS	90
4.4. RESULTS	91
4.4.1. Tee Pieces	91
4.4.1.1. Tee Pieces Formed from the Thicker Tube	93
4.4.1.2. Tee Pieces Formed from the Thinner Tube	96
4.4.2. Cross Pieces	98
4.4.2.1. Cross Pieces Formed from the Thicker Tube	99
4.4.2.2. Cross Pieces Formed from the Thinner Tube	100
5. THEORETICAL WALL THICKNESS DISTRIBUTION	143
5.1. THEORETICAL ANALYSIS	143
5.1.1. Expansion of a Curved Surface	147
5.1.2. Axisymmetric Expansion of a Tubular Blank	145
5.1.3. Asymmetric Bulging of a Tube into a Side Cavity	147
5.1.4. Bulging After $\rho = \rho_0$	149
5.1.5. The Effect of Axial Deformation	152
5.2. APPLICATION OF THE THEORY	154
5.2.1. For Case 1	155
5.2.2. For Case 2	156
5.2.3. For Case 3	157
5.2.4. The Effects of Axial Deformation	160
5.3. COMPARISON OF THEORETICAL AND EXPERIMENTAL RESULTS	164
5.3.1. Tee Pieces	165
5.3.2. Cross Pieces	167
5.4. DISCREPANCIES IN THE THEORY	169

6. DISCUSSION	217
6.1. THE DESIGN AND COMMISSIONING OF THE MACHINE	217
6.1.1. Operating Parameters and Design Considerations	217
6.1.2. Hydraulic System	218
6.1.3. Structural Design	221
6.1.4. Commissioning	223
6.2. EXPERIMENTAL RESULTS	226
6.3. THEORETICAL PREDICTIONS	230
6.4. FURTHER WORK	232
7. CONCLUSIONS	235
8. REFERENCES	237

APPENDIX 1:

THE HYDRAULIC COMPONENTS

APPENDIX 2:

THEORETICAL ANALYSIS COMPUTER PROGRAM

APPENDIX 3:

PAPER PUBLISHED

LIST OF FIGURES

<u>Fig. No.</u>		<u>Page</u>
1.	The bulge forming process.	20
2.a.	Schematic diagram of typical asymmetrical components.	21
2.b.	Schematic diagram of typical axisymmetrical components.	22
3.	Shrinkage, or recession of the joint, occurring during the forming process.	14
4.	The prototype bulge forming rig.	34
5.	Bulge height and wall thickness notation.	26
6.	Wall thickness distribution for axisymmetrical components - No axial deformation.	35
7.	Wall thickness distribution for axisymmetrical components - With axial deformation.	36
8.	The bulge heights of axisymmetrical components.	37
9.	Wall thickness distribution for asymmetrical components - No axial deformation.	38
10.	Wall thickness distribution for asymmetrical components - With axial deformation.	39
11.	Initial hydraulic circuit design.	62
12.	Actual hydraulic circuit design.	63
13.	Switch arrangement for solenoid valves.	64
14.	Arrangement of the hydraulic cylinders.	64
15.	Forces acting on the top plate.	65
16.a.	Forces acting on the mounting bracket.	66
16.b.	Position of the neutral axis.	66
17.	Flange reinforcement.	55
18.	Base plate, top plate and tie bars.	67
19.	Hydraulic cylinder brackets.	68

<u>Fig. No.</u>		<u>Page</u>
20.	Welded base assembly.	69
21.	Hydraulic cylinder bracket bolting arrangement.	70
22.	Plungers and plunger mounts.	71
23.	Assembly drawing.	72
24.	Stand assembly.	73
25.	Die block assembly.	74
26.	Top and bottom die holders.	75
27.	Die blocks.	76
28.	Plunger guides.	77
29.	The front view of the bulge forming machine.	78
30.	The back view of the bulge forming machine.	79
31.	The side view of the bulge forming machine.	80
32.	The top view of the bulge forming machine.	81
33.	The die blocks.	82
34.	Modified plunger mounts.	83
35.	Tee pieces formed to various stages.	102
36.	Cross pieces formed to various stages.	103
37.	Wall thickness measurement.	104
38.	Forming limits.	105
39.	Failure during the forming of tee pieces.	106
40.	The effect of internal pressure on the branch length of a tee piece.	107
41.	The effect of internal pressure on the cap radius of a tee piece.	108
42.-47.	Wall thickness distribution; tee pieces; thick walled.	109-116
48.-51.	Wall thickness distribution; tee pieces; thin walled.	117-123

<u>Fig. No.</u>		<u>Page</u>
52.	The effect of internal pressure on the branch length of a cross piece.	124
53.-58.	Wall thickness distribution; cross pieces; thick walled.	125-135
59.-62.	Wall thickness distribution; cross pieces; thin walled.	136-142
63.a.	Geometric expansion mode of a circular arc.	172
63.b.	Force equilibrium.	172
64.	Formation of a tubular branch.	173
65.	The effect of axial deformation.	174
66.	The various bulge formations.	175
67.	Theoretical wall thickness distribution along the bulge - without axial deformation.	176
68.	Theoretical wall thickness distribution along the bulge - with axial deformation.	177
Comparison of the experimental wall thickness distribution with theoretical predictions:		
69.-75.	Tee pieces; 85kN axial compressive force.	178-184
76.-82.	Tee pieces; 130kN axial compressive force.	185-191
83.-85.	Tee pieces; thin walled; 85kN axial compressive force.	192-194
86.-87.	Tee pieces; thin walled; 106kN axial compressive force.	195-196
88.-92.	Cross pieces; 106kN axial compressive force.	197-201
93.-98.	Cross pieces; 127kN axial compressive force.	202-207
99.-100.	Cross pieces; 148kN axial compressive force.	208-209
101.-102.	Cross pieces; thin walled; 63kN axial compressive force.	210-211
103.-106.	Cross pieces; thin walled; 85kN axial compressive force.	212-215
107.	Distinguishing the tubular branch and the spherical cap by linear interpretation of the wall thickness distribution.	216

NOMENCLATURE

a	semi-length of unsupported tube in the die cavity.
dx_1	initial semi-axial defomation causing thickening of the cap wall.
dx_2	secondary semi-axial defomation causing a tubular branch to form.
f	apparent strain factor.
h_1	initial height of an element prior to forming.
h_2	height of an element after forming.
h_e	height of an element on an expanded spherical cap from the junction of the spherical cap and the tubular branch.
H_1	initial height of the cap prior to forming.
H_2	height of the cap after forming.
H_s	height of a formed spherical cap.
H	height of a small cap.
L	length of the tubular branch.
L_b	length of the tubular branch formed from the axial defomation.
L_o	length of the tubular branch formed from the expansion of the spherical cap.
m	ratio between the meridional and circumfential strain.
p	internal pressure.
r_o	original radius of the tube.
t_o	original wall thickness of the tube.
t_L	wall thickness at the junction of the spherical cap and the tubular branch.
t'	wall thickness of an element on an expanded spherical cap.
t	wall thickness at any point.
x_o, x_1, x_2	meridional position of an element.
X	length of the tube.

X_0 original length of the tube.

y height of an element up the side branch from the root.

y_1, y_2 diameter of the circle, of which the cap is an arc of, minus the height of the cap.

ρ_θ radius of curvature of the cap in the circumferential direction.

ρ_L radius of curvature of the cap in the meridional direction.

ρ_s radius of curvature of the spherical cap.

σ stress.

ϵ logarithmic strain.

1. INTRODUCTION

1.1 THE BULGE FORMING PROCESS

The bulge forming process is a useful method for shaping tubular metal parts, by the use of internal hydrostatic pressure. This pressure is transmitted via a medium which can be liquid (e.g. hydraulic fluid), a soft metal (e.g. lead or lead alloy), or an elastomer (e.g. polyurethane). The tubular blank is subjected to this internal pressure while it is contained in a die bearing the shape of the component to be formed. Where the tube wall is unrestrained, expansion occurs until the required shape is formed.

However, bulge forming using only internal pressure causes excessive thinning of the tube wall, as would be expected. This leads to rupture of the tube at only moderate expansions. In order to be able to obtain larger expansions, metal has to be fed into the deformation zone during the forming process. This can be achieved by the application of a compressive axial force to the ends of the tube. If this axial force is great enough to cause axial deformation of the tube blank i.e. shortening of the tube length, a much greater expansion can be obtained with less tube wall thinning occurring. This method of forming is illustrated diagrammatically in Fig. 1.

The bulge forming process has now been in use for many years. As early as June 1940 a Patent, filed by Gray et al', was published by the United States Patent Office. This described an apparatus used for making wrought metal 'tees' from tubular blanks, cut from a length of standard commercial copper tubing. The apparatus used consisted of a die block split axially in relation to the tube, appropriately shaped for forming a

'tee'. In between these two die halves was placed the tube blank and the two halves were clamped together. A compressive axial force was then applied to the ends of the tube via plungers which entered the ends of the die block. The internal pressure was transmitted by a liquid through drilled passages in one of the plungers, using a pump to provide the pressure, and a check valve to maintain the pressure at a given level during forming. In order to fill the tube blank with liquid before forming, the die block was contained in a tank. This maintained the liquid level above the tube, with the side plungers passing through gasketed bushings in the side of the tank. The actual forming process involved increasing the internal pressure to an initial value of between 3000lbf/in² (21MPa) and 6000lbf/in² (41MPa) after the plungers had sealed the ends of the tube blank. As the plungers continue to advance, forced in by hydraulic rams, axial deformation occurs causing an increase in the internal pressure. The maximum value of this pressure was controlled by a preset pressure relief valve, set to a pressure of between 6000lbf/in² (41MPa) and 10000lbf/in² (69MPa) depending on the diameter and wall thickness of the tube used. This combination of axial force and internal pressure pushes the tube wall into the recesses of the die - so forming the tee piece. The formed tee piece exhibited thickening of the wall opposite the side branch and at the side branch junction. This provided added strength and reinforcement to the parts subjected to the greatest strain when the tee piece was in service. The only operations required to complete the manufacture of the component after forming was cutting off the cap of the formed branch, followed by drilling a socket into the branch and cutting the ends of the tube to equal length.

An article published in 1948 by Crawford² outlined a similar process for the production of tee pieces using a different pressure medium. This process, employed by a Canadian manufacturer, used a soft metal filler (a Bismuth, Lead and Tin alloy with a melting temperature of about 138°C) which was poured while molten into a straight copper tube blank to fill most of its length. When the filler had cooled and solidified, a compressive axial force was applied to both the metal filler and the ends of the tube, while contained in a suitably shaped die. After forming, the filler metal was removed by immersing the component in a hot oil bath. The tee pieces were formed from seamless copper tube of 12.7mm to 76.2mm nominal diameter, for use in heating and water supply systems.

However this type of forming process, using a cast metal filler as a pressure transmitting medium, does have its disadvantages which have been described in a Patent for an improved process filed by Stalter³. The casting technique required the use of expensive, complex equipment which was normally dirty, slow and smelly. Also after casting into the tube blank the filler material exhibited substantial shrinkage after cooling and solidified preventing the tube from being completely filled because of the shrinkage cavities created. This could result in the branch not being expanded enough after the bulge forming process, in which case the formed item would have to be scrapped.

The improved method detailed in the Patent used small pellets (approximately 1.6mm diameter.) of the filler metal (Woods Metal - an alloy of Bismuth, Lead, Tin and sometimes Cadmium) which were compacted into a slug and inserted into the tube blank prior to forming. Alternatively the slug could be compacted directly into the tube blank in the forming machine. Forming was carried out as before by subjecting the

metal filler and the ends of the tube to a compressive axial force, but independent control of the force on each was required. This was achieved by using plungers composed of a central plunger, to act on the metal filler, and an outer sleeve, to act on the ends of the tube. After forming the metal filler could be melted out and reformed into pellets for re-use.

1.2 BULGE FORMED COMPONENTS

The large variety of components that can be formed by the bulge forming process from open ended tube blanks fall into two groups namely:

1. Axisymmetrical components.
2. Asymmetrical components.

1.2.1. Axisymmetrical Components

Axisymmetrical components are those that have a uniform expansion over the whole circumference i.e. they exhibit symmetry around their axis. Examples of this group of components are shouldered hollow shafts and expansion/reduction pipe joints (where an expansion formed in the middle of a tube can be cut in half to form two joints.). In the forming of these components the relationship between the axial force and the internal pressure is very critical. Once a moderate expansion has occurred the resistance of the tube to the axial force decreases and buckling of the deformation zone can easily occur.

An investigation carried out by Al Qureshi⁴ compared the forming technique where a polymer was used and a hydraulic forming process for forming axisymmetrical components. Two different rigs were used - the

forming rig where polymer was used consisted of a horizontally mounted split die held together by a vertical hydraulic ram. Two horizontally mounted hydraulic rams were used to provide axial compression of a polyurethane rod inserted inside a tube blank, which was contained in the die. All three rams had a load capacity of 300kN. The hydraulic forming rig was not as sophisticated, simply consisting of a vertically mounted split die, and a vertical punch to provide axial compression. Results indicated that greater circumferential expansions and longitudinal drawing occurred when the polymer was used. The technique was simpler and cleaner to operate, and could perform more than one operation. However, as the hydraulic forming process allows the independent variation of axial force and internal pressure, the article concluded that it should be possible to obtain higher circumferential expansions with this process using a better developed forming machine.

In papers presented by **Limb et al^{5,6}** axisymmetrical components were formed using a hydraulic process. The forming rig consisted of a vertical hydraulic ram for clamping the die together and two horizontal rams, each with a 300kN capacity. Forming was carried out using 1½inch (38mm) O.D. seamless tube of commercially pure Aluminium, Aluminium alloy (HV9 - Al/Mag/Sil alloy), Copper, 70/30 Brass and low carbon Steel, in varying wall thicknesses - 0.048inch (1.22mm) to 0.080inch (2.03mm). In the forming of axisymmetrical components it was found that oil had to be continuously fed in to maintain the internal pressure, due to an increase in the internal volume during expansion. The most satisfactory method of forming thin walled tubes was found to be by increasing the internal pressure as a step function of the ram movement. This highlighted the need of a control system that would follow a preselected

relationship between internal fluid pressure and ram travel. The forming of axisymmetrical components was found to present a more difficult problem than the forming of tee pieces, and experience with the commercially pure Aluminium emphasized the fact that material properties are of greater importance when attempting a large radial expansion than when forming tee pieces.

1.2.2. Asymmetrical Components

Asymmetrical components are those that have a localised or sectional expansion, such as the tee piece pipe joint previously mentioned. Alternative methods of producing tee pieces would involve machining from a casting or from a welded design, since they could not be shaped with customary rigid tools. However these processes are more complex, requiring much more processing and would prove to be costlier than the bulge forming process. There is a very large number of variations in the shapes of components that can be produced. Components can be formed with various numbers of side branches in different diameters, angles and alignments to the main branch. Some of the typical components are illustrated in Fig. 2.

The variety of asymmetrical components are described in articles by Ogura and Ueda^{7,8} who reported on the work which has been done in Japan to produce components of various shapes using a bulge forming process. Tee pieces were produced in various sizes ranging from $\frac{1}{2}$ inch (12.7mm) to 12inch (305mm) outside diameter. For tee pieces up to 4inch (102mm) diameter a press was used with a 4000kN clamping force for holding the die halves together, and two 2500kN side rams for applying the axial compressive force. Multi capacity dies were used and the cycle times

ranged from 30 to 60 seconds. The larger tees were formed singularly on a machine with a 13MN clamping ram, and two 7000kN side rams, with a cycle time of 50 to 120 seconds. In order to avoid recession of the joint (or shrinkage - a gap between the surface of the tube and the die - see Fig. 3) or wrinkles in the main branch, a linear relationship was assumed between the amount of axial deformation and the minimum internal pressure required, during the forming process.

Also formed were components with two axially aligned but staggered side branches. These were found to be similar to form as the tees, but the tube blank had to be axially deformed twice as much to form side branches to the same height. The same was also true for the forming of components with two circumferentially aligned branches, except when the branches were 180° to one another i.e. a cross joint. In the forming of cross joints the component undergoes a different forming process, due to the symmetrical manner of plastic flow. This produces fewer variations in the deformation resistance and therefore less axial compressive force is required.

Problems were encountered when trying to form components with four branches, two of which were large, circumferentially aligned and very close to one another. Due to the large unsupported area, presented by the recess in the die for the two large branches, a relatively small pressure would result in fracture of the tube wall. This was overcome by controlling the rate of expansion of the two large branches during the forming process, preventing rapid bulging and thinning of the tube wall. To achieve this the die recesses contained sliding stoppers, the movement of which were controlled by a cam connected to the horizontal plungers,

to restrict and control the formation of the large branches (a bulge forming machine with this type of formation control is also described in a Patent Specification⁷ filed by a Japanese corporate body).

For the range of components that were formed, internal pressures of between 1000kg/cm² (98MPa) to 3000kg/cm² (294MPa) were used, depending on the diameter of the tube being formed. This internal pressure had to be sealed inside the tube using the end plungers. In order to obtain a good seal, the ends of the plungers - which butt up against the ends of the tube blank - were ground to a 'vee' around the ring in contact, resulting in a high pressure acting on a small sealing area.

The high pressure required for the forming process produced considerable friction forces between the tube and the die resulting in rapid die wear. Molybdenum disulphide was found to be a good lubricant for reducing the wear of the die, especially if permeated through bonderite treated die surfaces.

1.2.3. Commercially Produced Components

The main use of the bulge forming process for producing commercial products is for the production of asymmetrical components such as tee pieces. The process has been used for many years in Britain for the production of copper pipe fittings used for pipework systems (including domestic water and gas supplies). The only alternative methods of production of tee pieces is by machining from castings or from welded fabrications since they can not be shaped with customary rigid tools. The bulge forming process is much simpler, requiring less operations, and cheaper and quicker, especially when seamless components

are required. The process is not only restricted to the forming of copper tubes but can be applied to other materials as well e.g. mild steel, aluminium etc.

An article in 1978^e described a bulge forming press manufactured by a company based in Dorset, for producing steel tees in the range 1½inch (38mm) to 8inch (203mm) nominal bore. These hydraulic forming machines incorporate two 8500kN rams for applying the axial load to tubular blank, and a 10MN ram for keeping the axially split dies together during the forming process. The clamping ram also features a small inner ram for controlling the formation of the side branch of the tee piece.

Besides forming tee pieces the process is also used commercially in Britain for forming bicycle frame brackets from mild steel tubing, using a polymer insert as an internal pressure medium. However, in Japan the process has been highly developed and has been used for a great many applications. Besides the production of asymmetrical components of various shapes and number of branches previously mentioned^{7.e}, axisymmetrical components were also produced. One such component was a stepped shaft being used for an electric motor. This was found to be considerably cheaper to form from tube than turning down from a solid shaft, although a 10% increase in diameter was required. A problem encountered in forming these shafts was that a sharp radius was required at the edges of the step to accommodate the fitting of ball bearing races. The normal bulge forming process could only produce a relatively large radius. To overcome this problem the dies were modified so that the two ends could move together axially. These were hydraulically actuated inwards when the bulging process was completed to form the required

radius. It was also found possible to replace the central section of the die with the actual object to be fitted to the shaft.

A similar process was also used for forming flanged wheel hubs for bicycle wheels. Two axisymmetrical bulges were formed at the ends of a tube blank, which were then flattened into flanges by the inward movement of the die ends. Other examples of the application of the bulge forming process used in Japan is the production of rear axle casings for cars and small lorries. These were produced from steel, using 96mm diameter, 3.2mm wall thickness tube blanks for car rear axle casings and 132mm diameter, 6mm wall thickness tube for two ton lorry casings.

1.2.4. Associated Applications.

Besides the use of the bulge forming process for forming axisymmetrical and asymmetrical components from open ended tube, it has also had been used in various other applications. One variation of the process is its use for production of Brass kitchen tap spouts, as detailed in an article by Smith', from lengths of tube bent into a 'U' shape. The bent tube was placed into an appropriately shaped die and pressurised internally using water as the pressure transmitting medium. Load was then applied to the two ends of the tube to push them in, thus forming the tube into the shape of the die. However, with this process only 'U' shaped parts could be formed. An improved process was then introduced in which the internal fluid pressure was increased after the ends of the tube had been pushed in, forcing the metal into the extremities of the die. With this improved process, extreme configurations could be obtained, with expansions of over 100% obtained

from Brass tubing. The components formed replaced ones which previously could only be made by casting or combining several machined parts.

Another application is the use of the process for bending pipe and forming elbow fitting. A device for this process is described in two Patent specifications filed by a Dutch organisation^{12,13}. This consists of two die blocks that can slide across one another, perpendicular to the tube blank that is placed through them both. The tube contained in the dies is filled with a substantially incompressible medium in the form of oil, rubber or a similar material and pressurised at each end by a pressure transmitting plunger. The two die halves are so shaped that, when the tube is loaded to such an extent that plastic deformation occurs, one half is forced to slide across the other due to the forces on the tube. Using this process, two 'square' elbows are obtained from one tube blank. Alternatively, slightly differently shaped dies can be used and forced to slide across one another using an external force during the process. In this case curved elbows are obtained. The advantages of using this process is that elbows can be obtained with very small radiused bends with the wall thickness remaining almost equal to the original around the tube at the bend. Using previous methods to make elbows by bending tube, it has been extremely difficult, or even impossible, to produce very small radiused bends. Those which can be produced by bending usually result in an extreme decrease in the wall thickness on the outside of the bend.

The use of the process was reported by Remmerswaal¹⁴ who used an elastic medium for transmitting the internal pressure. His conclusions were that using this forming process smaller bend radii could be obtained than by conventional processes. Also less thinning of the wall occurred

outside the bend and less thickening of the wall occurred inside the bend. In the process used by Boyd¹⁵, water was used as the internal pressure medium with 2.7inch(69mm) O.D. tubes used in dies with 3.5inch(99mm) bores. However buckling occurred using this combination due to the infeed compressive loads applied to the tube ends. This was corrected by changing from water to oil as the pressure medium, which could be pressurised independantly. The resulting components thus formed exhibited less change in wall thickness than by forming from conventional methods.

Powell¹⁶ used the process for forming bends in 1inch(25mm) O.D. Aluminium tube using an internal oil pressure of up to 10000psi.(69MPa). The internal forces alone were used to force the die halves to slide across one another but it was discovered that restraining the dies from sliding would result in an increase in the wall thickness of the tube wall. A theory was provided equating the external forces to the power dissipation due to the internal shear, frictional loss, and the restraint loss. The final equation was used to calculate the internal pressure from the flow stress, relative wall thickness and the geometry given by the bend angle. A sound product was produced at a pressure just less than that predicted by the analysis.

Another use of the bulge forming process is that for bulging deep drawn articles. An article by Woo¹⁷ details the use and operation of a machine developed to form Aluminium and Pewter vessels from circular blanks. Using one rig, the blank is deep drawn through a 'tractrix' die, passed through an ironing die, and finally filled with oil and bulged into the required shape using internal pressure and axial load.

1.3. FAILURES OF THE PROCESS

There are two main modes of failure that can occur during the bulge forming process. One is the fracture of the component during expansion. This is due to excessive thinning of the tube wall which may be caused due to too large an internal pressure, or an inadequate axial deformation occurring when trying to produce a large expansion. Theoretically the expansion process could go on indefinitely if more metal is being pushed into the deformation zone continuously, and the internal pressure is kept at a suitable value. However with inadequate axial deformation, the wall thickness of the tube in the deformation zone decreases until rupture occurs.

The other main type of failure is the buckling of the component due to an excessive axial deformation load or to insufficient internal pressure to support the tube. This results in wrinkles appearing in the main branch if the effect is only mild, but if the effect is severe, buckling will occur down the length of the tube and the expanded branch will be mishaped. Should fracture of the tube occur, when using oil as the pressure transmitting medium, and the axial deformation continued, then buckling of the tube will also occur due to the loss of internal pressure.

Besides these two main types of failure, 'shrinkage' of the expansion can also occur when forming around a radius in the die. This is illustrated in fig. 3 which shows a tee joint being formed. In order to form a good quality component the wall of the tube must be in contact with the die walls. However, when a small radius is encountered, the tube wall may come away from the die wall resulting in 'shrinkage'. There are two reasons why this can occur. One is that the radius of draw is too

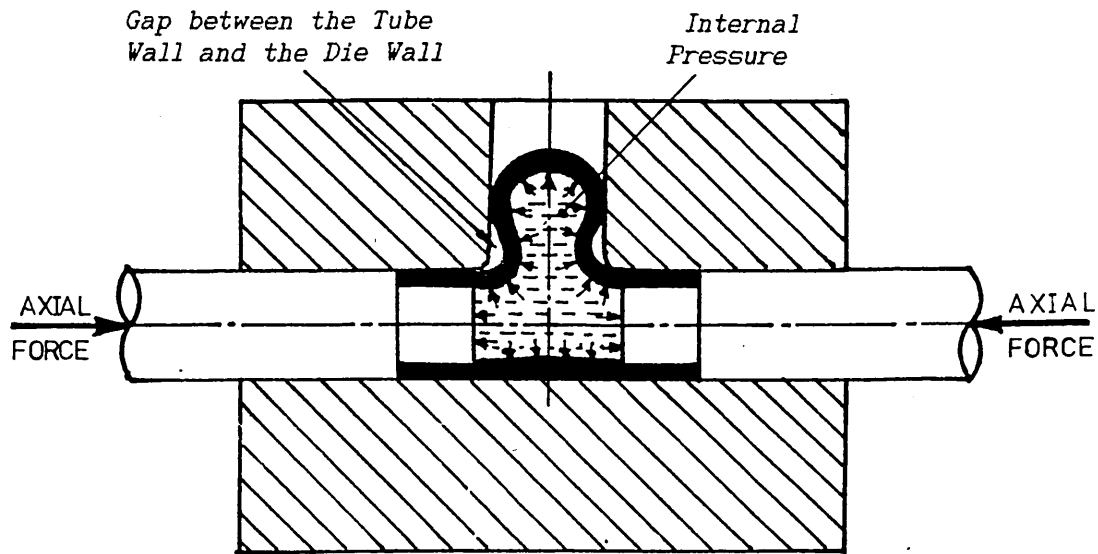


Fig. 3 'Shrinkage' or Recession of the Joint occurring during the forming process.

small which can be corrected by the redesign of the dies to provide a larger radius. The second is due to insufficient internal pressure in proportion to the axial deformation which can be corrected by increasing the internal pressure to force the tube wall against the die.

Therefore, in order to produce a good product, the process is dependant on the relationship between the internal pressure and the axial deformation.

1.4. PREVIOUS INVESTIGATIONS

1.4.1. Axisymmetrical Bulge Forming

The use of the bulge forming process to form axisymmetrical components has been subject to a number of investigations and the application of several theories. In a paper presented by Woo¹⁸ in 1973, a theory was provided for the free expansion process under internal hydraulic pressure and axial compressive force. This theory used the relationship between the circumferential strain and the thickness strain,

for processes in which the whole length of the bulged tube was in tension. Comparison of the theoretically produced results showed reasonably good agreement with experimental results, when the stress-strain properties obtained from the bulging process were used. The use of stress-strain properties obtained from tensile tests resulted in large discrepancies. Problems were also encountered in satisfying the boundary conditions in the numerical solution used i.e. zero circumferential strain at the end of bulge zone. In a later paper by Woo and Luci¹⁹, published in 1978, this problem was overcome by introducing the anisotropy of the tube material into the theory.

In 1975 Banerjee²⁰ reported on work carried out on the limiting deformations of fixed lengths of aluminium tubes for the free bulging process using internal hydraulic pressure only. The tubes were formed slowly until rupture occurred. The values of maximum pressure and bulge height were then compared with those obtained from a theory derived from the stress and strain at instability, taking into account strain hardening. Good agreement was obtained for the maximum pressures values, but there was a discrepancy for the bulge height values.

An article in 1976 described the experimental work carried out by Kandil²¹ into the axisymmetrical bulge forming of Brass, Aluminium and Copper tubes using internal hydraulic pressure only. Various radii of the die at the edge of the forming zone (radius of draw) were used, as well as various tube diameters. From the results an empirical relationship was obtained, derived from the forming pressures, the stresses and the die and tube geometry.

In 1978 Badran and Emara²² presented a theory in 1978 for the forming of axisymmetrical components using rubber as the internal

pressurising medium, with no axial load applied to the tube apart from frictional force between the rubber insert and the tube wall. This theory provided equations for predicting the internal pressure required for various increments in the deformation. An assumption used was that the deformed area forms the arc of a circle in the axial direction. Equations for the value of the wall thickness after deformation were also provided. This theory was used to produce graphs predicting the values of internal pressure for any deformation, both neglecting and including the effect of work hardening. However, no experimental results were provided to compare with the theoretical predictions.

In the same year Saver et al²³ published their work which dealt with the theory of the failure of bulged tubes due to buckling and fracture. This was applied to the forming of parts with very pronounced bulges such as rear axle casings. A numerical solution was used to compute values of axial load and internal pressure from increments in the diameter of the bulge. The algorithm used was based on five principles - Strain-displacement relationships, incompressibility, effective stresses and strains (Plasticity Theory), equations of equilibrium, and boundary conditions. Experimental work was carried out on a rig that could apply axial load and internal pressure at a finely adjustable ratio in order to apply various constant stress ratios. The tubular blanks - 1½inch(38mm) O.D. with the wall thickness turned down in the region of bulging to a thickness of 0.050inch(1.27mm) - were slowly bulged until failure occurred. The results showed a favourable comparison between the predicted and actual forces required to produce each step in the curvature of the bulge between load increments, although the actual strains to produce fracture were higher than those predicted.

1.4.2. Asymmetrical Bulge Forming

The forming of asymmetrical components has not had as many investigations carried out as for axisymmetrical components. There have been a few articles published dealing with the various axisymmetrical components that it is possible to form such as those by Ogura et al^{7,8} previously mentioned. There has, however, been only a small number of articles dealing with experimental work investigating the process.

In the work carried out by Limb et al^{5,6} into the forming of axisymmetrical components previously mentioned, some work was also carried out in the forming of tee pieces. These were found to be easier to form than axisymmetrical components and during forming, the internal hydraulic pressure was increased as a function of the ram position. On the formed tees those formed without lubrication had a very pronounced dome, but with lubrication the dome was much flatter, and the length of the side branch increased by as much as .20%. The best lubricant was found to be P.T.F.E. film but it was rather expensive, Colloidal Graphite and Rocal AS giving the next best results. The worst lubricant was found to be Tellus 27. The tees were formed from 1½inch(38mm) diameter seamless tubes of commercially pure Aluminium, HV9(al-mag-sil alloy), Copper, 70/30 Brass, and low carbon Steel in an initial annealed conditioned. The softer materials were formed with little or no thinning of the side branch wall thickness whereas the stronger materials showed considerable reductions in the wall thickness, although for the latter formation continued after the end of the ram movement. The conclusions to the articles highlighted the need of a control system that would follow a

preselected relationship between internal fluid pressure and ram travel during forming.

An article in 1980 by Lukanov et al²⁴ described a process for forming tee pieces which minimises the amount of wall thickening that occurs in the main branch, opposite the side branch. The method involves forming two tees from a single tube blank, with side branches staggered on opposite sides of the tube. In the tees thus formed the increase in wall thickness was found to be reduced to 15% and a greater branch was obtained. This allowed the initial tube blank to be reduced in length by 4% compared with just forming one tee twice.

1.5 AIMS OF THE CURRENT INVESTIGATION

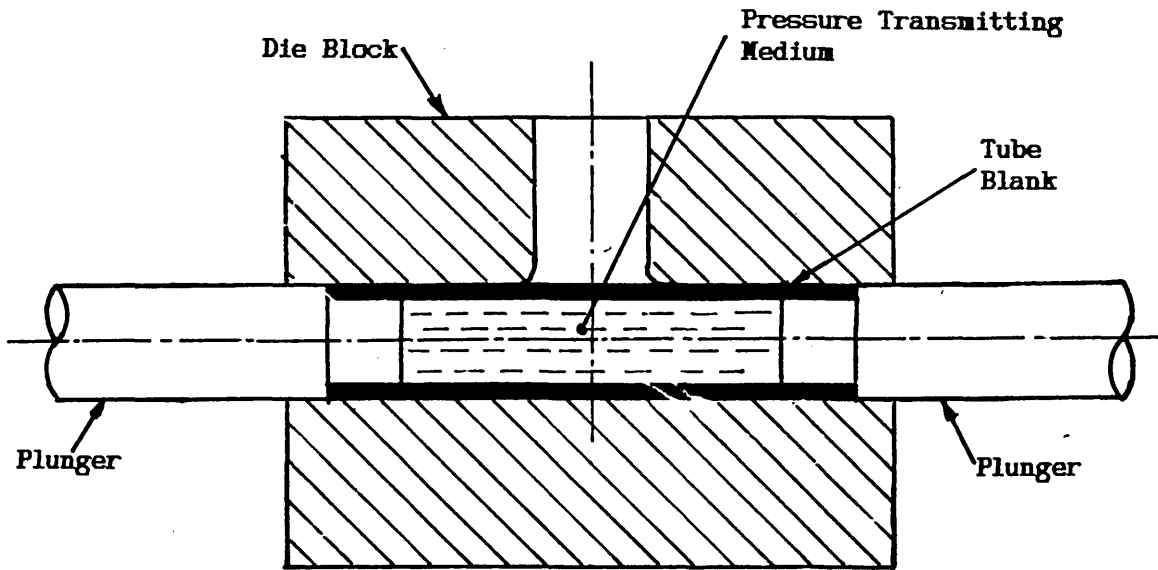
The investigation carried out initially involved a literature survey in order to assess the previous work carried out into the bulge forming of tubular components. This survey also highlighted the various components that were formable using a bulge forming process, and the machines and the forces required for their production.

As an introduction to the actual forming process, tests were carried out on a simple prototype machine on which axisymmetrical and asymmetrical components were produced. These tests allowed the requirements of the process to be assessed and highlighted the problems associated with the prototype rig and the bulge forming process.

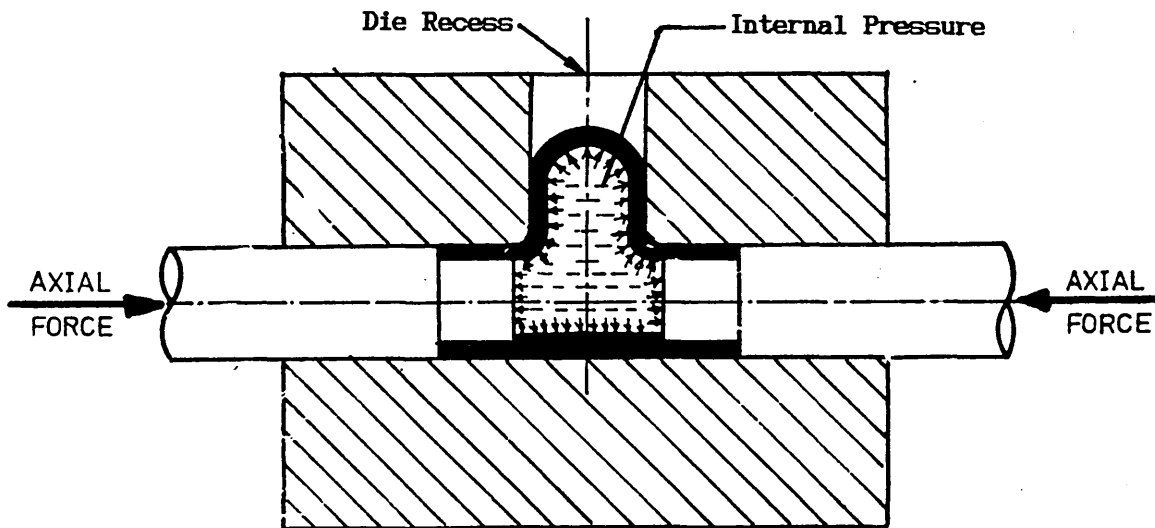
With this information the aims of the investigation are:

1. Design a new bulge forming machine on which various shaped tubular components can be formed.

2. Commission the completed bulge forming machine, followed by alteration/modification of the machine in order to correct any problems that are highlighted.
3. Evaluate the limits of the operating parameters (axial compressive force and internal pressure) required to produce a good component, by a series of tests forming both tee and cross pieces
4. Analyse the formed components to show the effects of the various combinations of internal pressure and axial compressive force on the bulge height and the wall thickness around the deformation zone.
5. Compare the geometry of the formed component with theoretical predictions.



a, Prior to forming with tube blank in position.



b, Component formed with axial deformation.

Fig. 1

The Bulge Forming Process

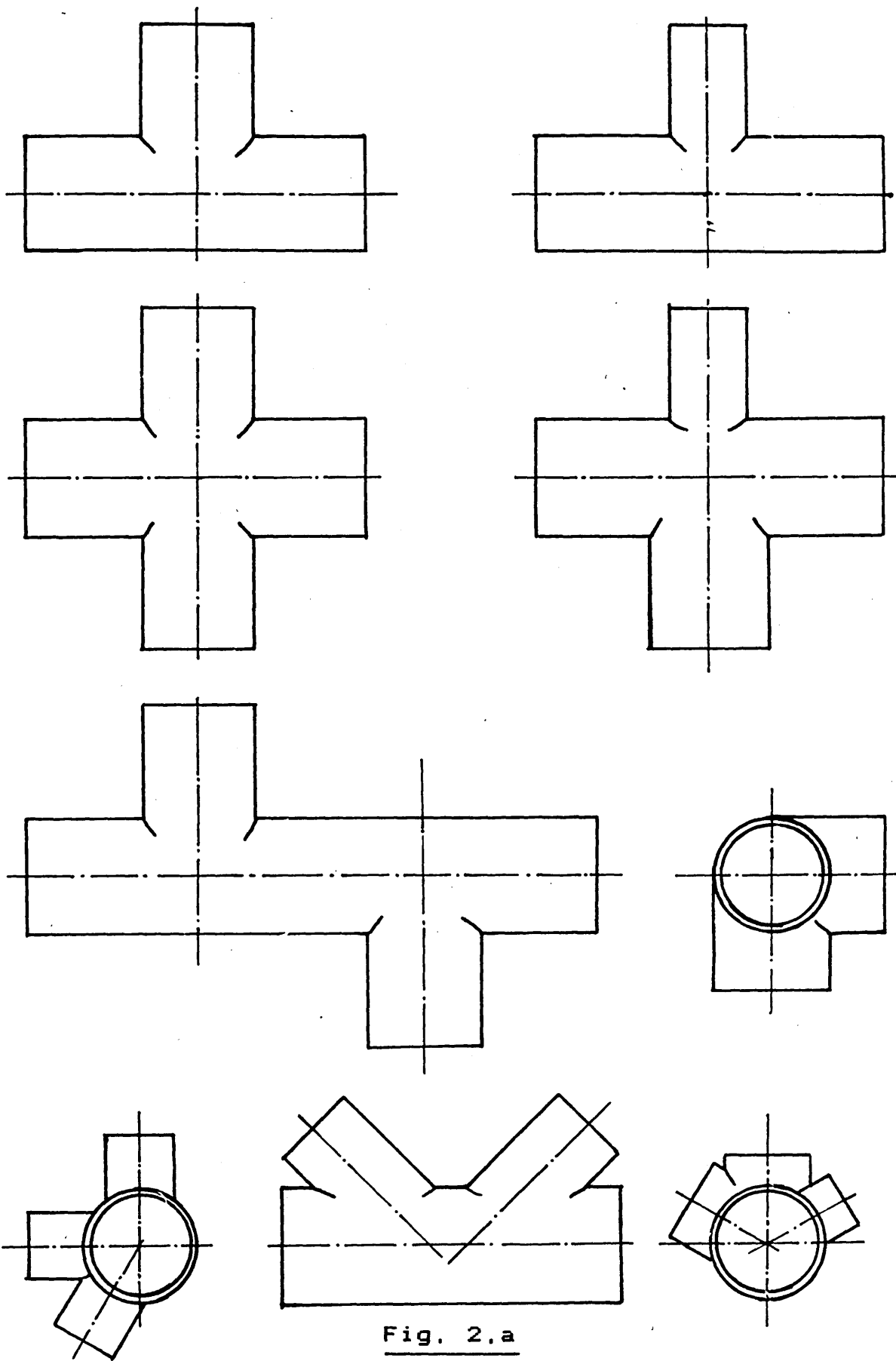


Fig. 2.a

Schematic Diagram of Typical
Asymmetrical Components

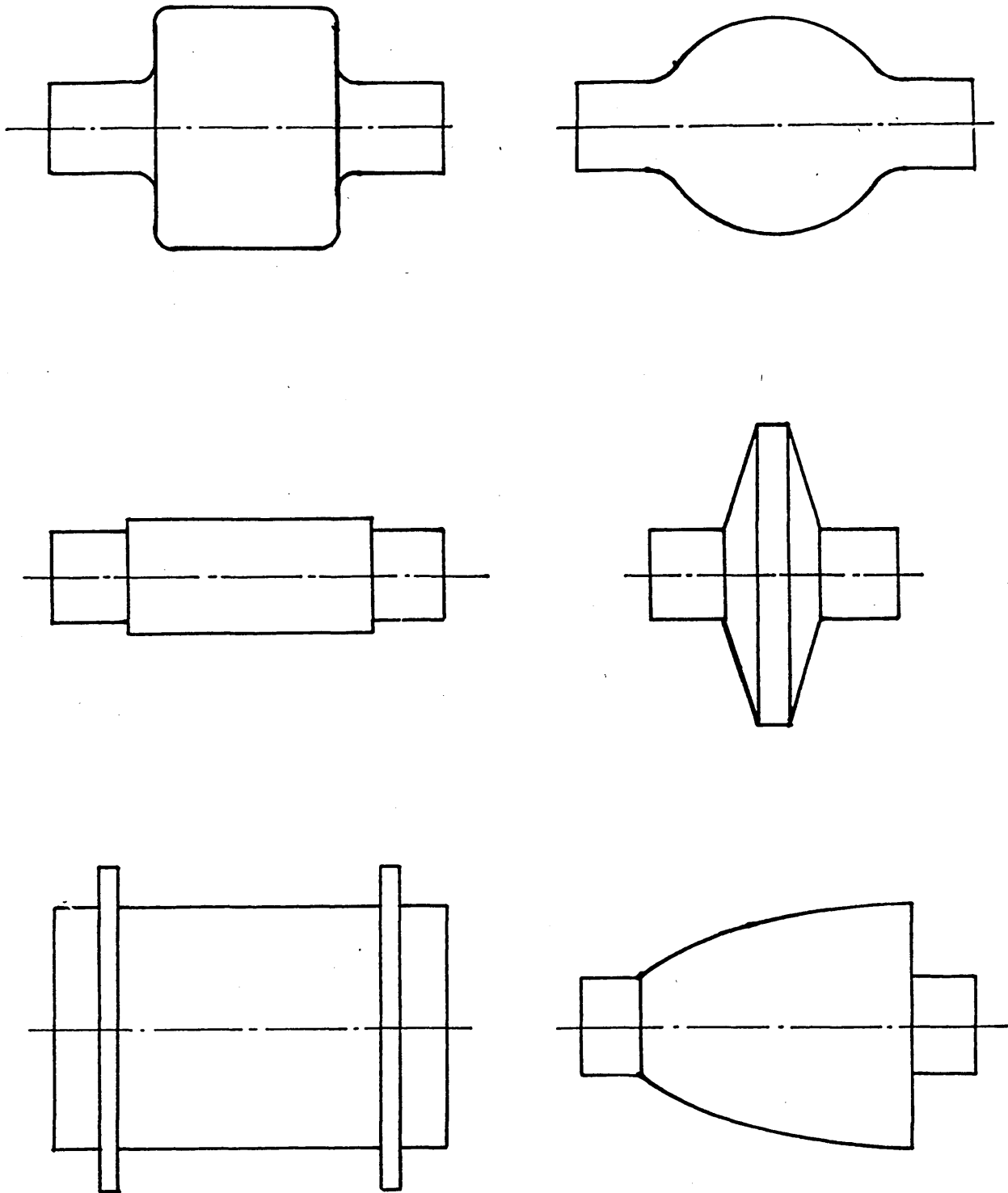


Fig. 2.b
Schematic Diagram of Typical
Axisymmetrical Components

2. PRELIMINARY INVESTIGATION

2.1 THE PROTOTYPE BULGE FORMING MACHINE

A series of tests were initially carried out using a simple rig, previously designed and built for a student's final year project. This consisted of two die halves each mounted in a robust die holder, which split laterally in relation to the tube - see Fig. 4. The actual dies could be removed from their holders so that different shaped dies could be used to form axisymmetrical or asymmetrical components (the actual axisymmetrical components formed were tee and cross pieces). Each die half was bored through, to allow the insertion of the tube blank when the two halves were together. An axial compressive force could be applied to the ends of the tube by means of plungers, one at each end, which entered the ends of the dies to butt up against the tube. Each plunger was turned down at the end so that they would locate inside the tube. This part of the plunger also housed an 'O' ring to seal against the inside of the tube in order to contain the internal pressure. To keep these two plungers in line with the dies, each one was mounted on a guide plate, with the die block suspended between the two using heavy duty springs. The plungers also contained drilled passages down their length, through which oil could be passed.

To provide the axial compressive force, a 200kN *Denison* compression testing machine was used. Before each forming test the rig had to be assembled on this machine, with a copper tube blank positioned inside the die blocks. During forming, therefore, a compressive force could be applied to the plungers and hence to the ends of the tube blank.

The internal pressure was provided by a hydraulic hand pump, complete with pressure gauge. This was connected to the bottom plunger via an adjustable pressure relief valve, in order to regulate the maximum internal pressure. The drillings through the top plunger were used in order to bleed the tube blank of air during filling, prior to forming. This was sealed after expulsion of all the air.

Testing was carried out on copper tube with an outside diameter of 24mm, in three different wall thicknesses - 0.9mm, 1.17mm and 1.6mm (a different pair of plungers were used with each thickness). The tube blanks were prepared for forming by cutting them to a nominal length of 100mm and annealing at 500°C.

2.2 EXPERIMENTAL PROCEDURE

In order to carry out a bulge forming test, the rig had first of all to be mounted on the compression testing machine. This included fitting a copper tube blank, the length, thickness and diameter having been noted. The compression testing machine was then operated in order to seal the plungers against the ends of the tube, so that the inside could be pressurised. After preloading the tube with a force of approximately 0.5kN, the hydraulic oil was introduced into the tube, by means of the hand pump, while air was bled from the top. After filling with oil, the air bleed was sealed and the internal pressure was increased until the desired starting pressure was reached. Axial compression of the tube could then be started by increasing the force acting on the plungers from the compression testing machine. The deformation of the tube was allowed to continue until the required degree of deformation was obtained, or the tube burst.

Some of the tests carried out involved only internal pressure, and no axial force. In these cases the internal pressure was just increased up to the required pressure using the hand pump, having previously sealed the ends of the tube with just an initial end load.

In the tests carried out involving axial compression, the deformation of the tube would cause an increase in the internal pressure. In order to avoid an excessive pressure from being generated the relief valve was set beforehand to a suitable value depending on the tube wall thickness and the shape of the component to be formed. The initial and final internal pressures were noted during the test, as was the final axial force, indicated on the compression testing machine.

On completion of the test the internal pressure and end load were released, and the plungers withdrawn from the die blocks. This allowed the die blocks to be split, from which the formed component could be removed. After removal from the rig, the length of the component was measured, and after cutting into suitable sections, the thickness around the deformation zone and the bulge heights were measured.

The sequence used for the experimental procedure was as follows:

1. Assemble the rig on the compression testing machine complete with premeasured tube blank.
2. Preload tube blank by operation of the compression testing machine in order to seal the tube.
3. Fill tube with oil and bleed the air out.
4. After sealing the air bleed, increase the internal pressure until the desired initial pressure is obtained.

5.a Increase the axial force acting on the tube in order to cause axial deformation, until the required amount of deformation is obtained.

Or

5.b Increase the internal pressure by operation of the hand pump up to the required pressure, with only the preload axial force acting on the tube.

6. Release the axial force and internal pressure, and withdraw the plungers from the die blocks.

7. Dismantle the rig, separate the two die halves and remove the formed component.

2.3 DISCUSSION OF RESULTS

The measurements taken from the formed components, after cutting into suitable sections, are illustrated in several graphs. The notation used is shown in Fig. 5. Figs. 6 and 7 show the amount of wall thinning (t/t_0) that occurs from the root of the bulge ($h_2/H_2 = 0$) to the tip of it ($h_2/H_2 = 1$). These graphs have been produced from the forming of axisymmetrical components with various bulge heights.

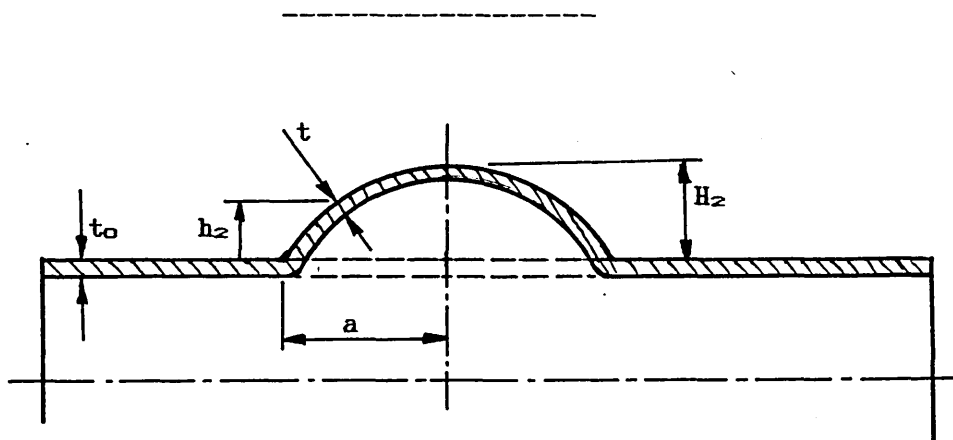


Fig. 5 Bulge Height and Wall Thickness Notation.

The graph in Fig. 6 shows the effect on the wall thickness of the bulge when there is no axial deformation. At the root of the bulge the wall thickness has not altered (at $h_2/H_2 = 0$, $t/t_0 = 1.0$). However moving up towards the top of the bulge, the amount of wall thinning that has occurred increases until the tip of the bulge is reached where the wall is it's thinnest. By comparison, Fig. 7 shows the measurements from bulged components, with similar maximum bulge heights, produced using axial deformation. This time, at the root of the bulge, thickening of the tube wall has occurred (at $h_2/H_2 = 0$, $t/t_0 > 1.0$). At one point up the bulge the thickness has not altered, and above this point thinning occurs. However comparison of the two graphs show that less wall thinning has occurred around the bulged region when axial deformation is present.

The actual bulge heights that were achieved when forming axisymmetrical components are shown in Fig. 8, in ratio form, plotted against the internal pressure. The graph shows results obtained with and without axial deformation, for various initial tube thicknesses. It can be seen that without axial deformation, increasing internal pressure is required to increase the bulge height. However, with axial deformation an increase in the bulge height can be achieved at the same pressure by just increasing the amount of deformation. Also, when utilising axial deformation, greater expansions are achieved using lower internal pressures.

The improvement to the process is also emphasized in Table 1. This shows the maximum bulge heights that could be obtained before rupture of the tube occurred. The values are given for the forming process under pure internal pressure (no axial force except for an initial preload to seal the tube), and also for those formed with axial compression (the f

value also given is the apparent strain factor resulting from the axial compression - original length of tube divided by final length - this is 1.0 when there is no axial deformation). The bulge heights of the latter exhibit an increase in their bulge height of at least 25% compared to the former.

TUBE THICKNESS	SIMULTANEOUS AXIAL COMPRESSION		PURE INTERNAL PRESSURE
mm	H_z/a	f	H_z/a
0.9	0.44	1.1	0.33
1.16	0.46	1.12	0.36
1.6	0.5	1.1	0.4

Table 1. Maximum Bulge Heights Obtained Before Fracture of the Tube Occurred.

The results obtained from forming asymmetrical components are shown in Figs. 9 and 10. These were obtained from forming cross pieces (or double tee pieces) from tubes of two different initial wall thicknesses, and again show the variation in the wall thickness around the deformation zone. As for the axisymmetrical components, thinning occurs at the top of the bulge, but in this case far greater wall thickening occurs near the root of the bulge - as much as a 40% increase. The graphs plotted for the various bulge heights do not, however, follow the same trends, but cut across one another. This is likely to be due to difficulty in the control of the internal pressure during the forming process, and the inability to keep the process constant for each test.

2.4. PROBLEMS ASSOCIATED WITH THE PROTOTYPE RIG

As previously mentioned the rig had first to be assembled on the compression testing machine before each test could be carried out. After each test the rig then had to be dismantled in order that the formed component could be removed. All this involved moving heavy lumps of metal about. To make things more difficult the die blocks split laterally in relation to the tube. During the bulge forming process, as well as the tube bulging in the unrestricted area, bulging also occurred down the rest of it's length to a small extent, forcing the tube wall against the die wall. This meant that the tube was stuck firmly into the two halves of the die, making separation of the dies and removal of the component extremely difficult. In order to free the component the two die halves had to be removed as a unit from the rig and separated with the aid of drifts and a stout hammer. Because of this each test could take over half an hour to complete from set-up to extraction of the formed component.

Another problem was the method used for sealing the tube ends. This involved the use of 'O' rings located at the end of the stepped plungers as shown in Fig. 4. These worked alright initially, but because of their position the 'O' rings invariably became damaged by the ends of the copper tube and would have to be replaced after only one or two tests. During some of the tests carried out complete sealing could not be achieved. In such cases the internal pressure had to be maintained during the test by the constant use of the hydraulic hand pump. In some cases, however, the rig had to be dismantled and the 'O' rings replaced before the test could be carried out.

Leakage was not so much of a problem, though, when large compressive axial forces were obtained during the process. These occurred when forming tee and cross pieces especially when using the thickest walled tube. The high pressure acting between the step of the plunger and the end of the tube ensured a good seal. This, however, sometimes led to another problem. The large compressive axial force being used caused deformation of the ends of the tube. Consequently the tube would form into the recess at the end of the plungers containing the 'O' rings. This would prevent the plungers from being withdrawn from the tube at the end of the test. The removal of the plungers was again obtained with the use of a hammer, but with caution this time since the springs between the die block and the guide plates were held in a compressed state.

These heavy duty springs located between the die block and the guide plates were used in order to keep the two halves of the die block together during forming. A secondary use was to keep the die block central between the two guide plates so that the bulge would form centrally on the tube. Unfortunately this did not always work and the resulting bulge would be formed off central, due to one plunger meeting a greater resistance than the other during forming. The bulge thus formed would also be mishaped as well as not central due to more forming occurring at one side than the other.

As well as these problems in assembling and dismantling the rig there was also a lack of control during the actual bulging process as well as a lack of instrumentation. This caused a large variation in the components formed and made accurate recording of the process difficult. The strain rate for the axial compression could be set/altered on the compression testing machine. However there was little control over the

internal pressure during the process apart from setting its maximum value with the pressure relief valve and its initial value. With the variations in the quality of the tube sealing for each test, it was extremely difficult to carry out a series of tests with similar internal pressure conditions.

The only values recorded during the test, apart from the dimensions of the copper tube, were the :

- i. initial and final internal pressure,
- ii. initial and final axial force.

The internal pressure was taken from a pressure gauge mounted on the hand pump and was not very precise. If leakage was occurring the pressure would be changing all the time, making recording the final value very difficult if the maximum pressure set by the relief valve was not achieved.

In order to overcome these problems the following points were needed to improve the prototype bulge forming rig :

1. improved machine design in order to make tests easier and quicker to perform,
2. better tube sealing arrangement,
3. greater machine/process control,
4. better instrumentation.

At this stage it was decided to design a new bulge forming rig taking into consideration the problems encountered with the prototype rig.

2.5. CONSIDERATIONS FOR THE DESIGN OF A NEW RIG

In order to shorten the time required for each test and to make it easier to perform, the need to assemble and dismantle large heavy blocks of metal had to be avoided. This meant that the new rig should be free standing and self contained. The main part of the rig would be the die block in which the actual forming occurs. In the prototype this was split laterally in relation to the tube, which resulted in problems in extracting the formed component. Splitting the die blocks axially would overcome this problem, but the two halves would have to be clamped together during the process in order to resist the internal pressure trying to force them apart. It was decided to use a hydraulic ram for this purpose which could also be used to open and close the dies to allow access for placing/removing the copper tube.

Hydraulic rams could also be used for applying the axial compressive load to the ends of the tube. With the prototype rig problems were encountered with the bulge not forming centrally on the tube. Therefore two hydraulic rams would have to be used, one at each end, that were synchronised together so as to provide equal deformation and strain rate of each end of the tube.

Using hydraulic rams would mean the need of a hydraulic power pack i.e. pump and electric motor, to power them. This could also be used to provide the internal pressure, although this pressure was likely to be a lot higher than the supply pressure. Running the hydraulic system at the same pressure as the maximum internal pressure required would prove to be very costly. Alternatively, a lower supply pressure could be chosen and this pressure increased through a pressure intensifier to provide the forming pressure.

The design of the plungers that transmit the axial compressive force to the ends of the tube would preferably do away with the need of 'O' rings to seal in the internal pressure. Again the ends should be stepped so as to locate inside the ends of the tube, but the actual sealing should be due to the pressure acting on the end of the tube. The end of the plunger could also be a tight fit inside the tube, to help with the sealing, until the axial force is great enough to cause sealing at the tube end.

The use of hydraulics in the process would also allow more control to be achieved, through the use of pressure reducing, flow control, directional control valves etc. The use of solenoid valves would also allow the application of a micro processor/computer to the control and sequencing of the process.

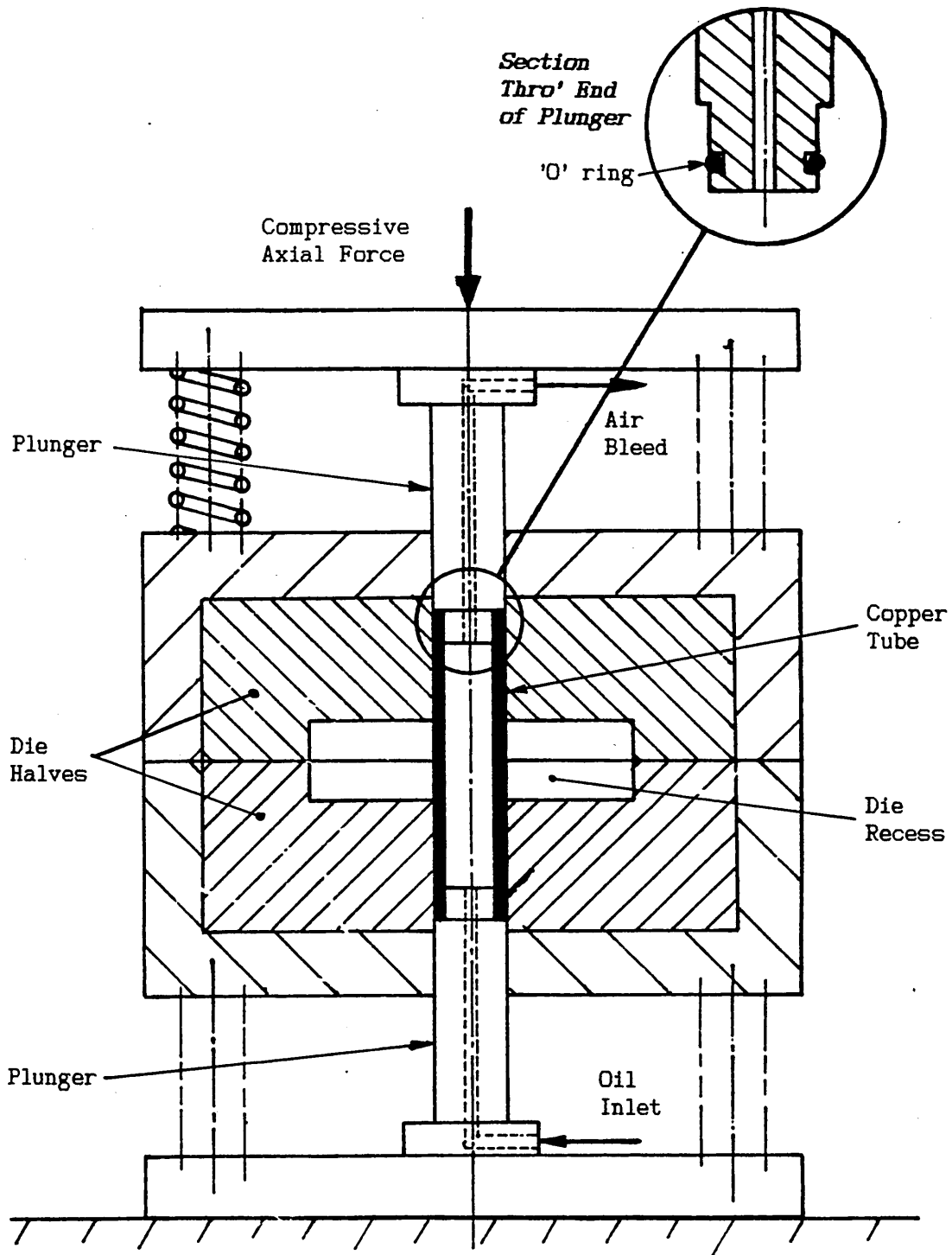


Fig. 4
Prototype Die and Tool System
for Bulge Forming

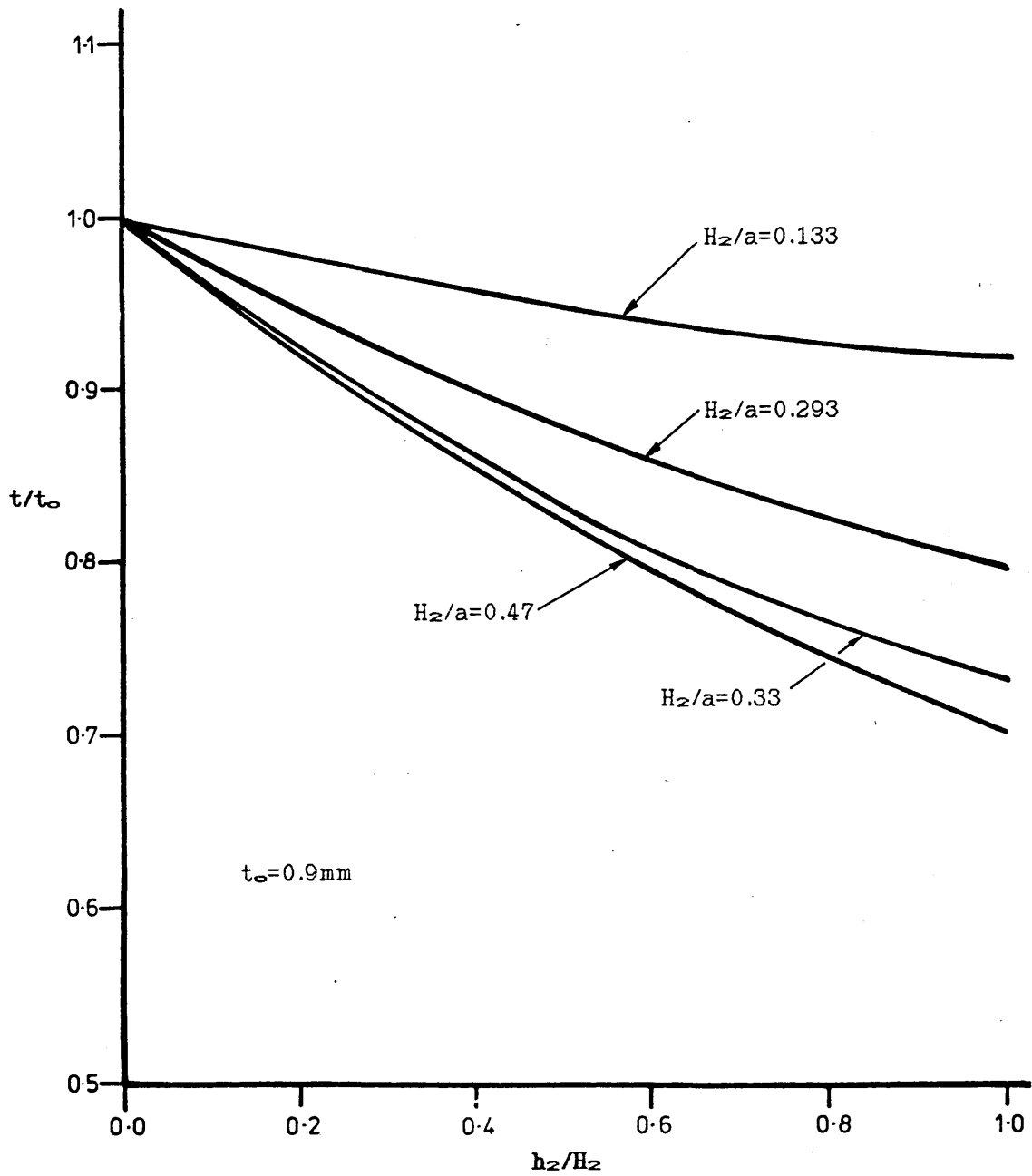


Fig. 6.
 The Wall Thickness Distribution for Axisymmetrical
 Components - Without Axial Deformation.

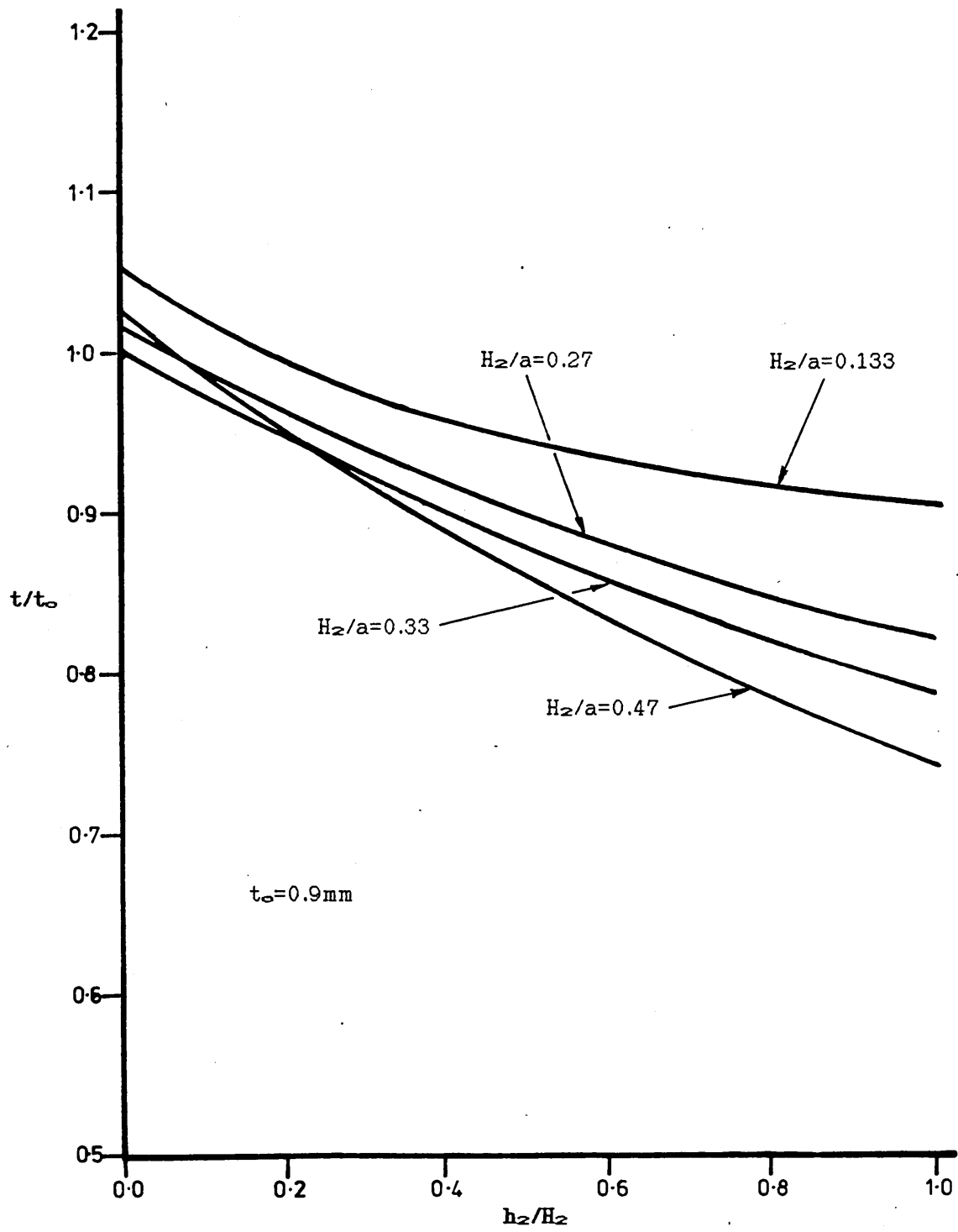


Fig. 7.
 The Wall Thickness Distribution for Axisymmetrical
 Components - With Axial Deformation.

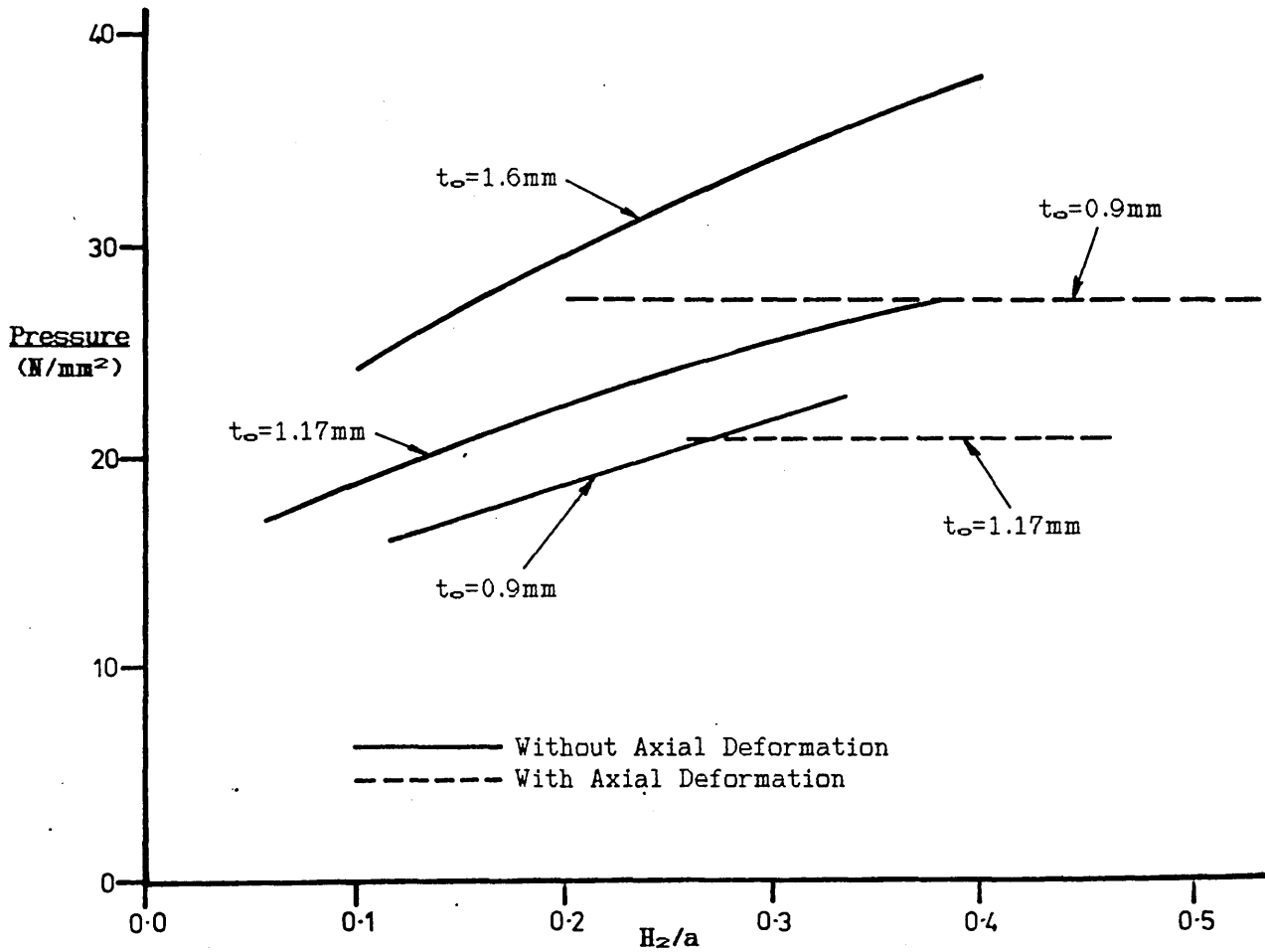


Fig. 8.
 The Effect of Internal Pressure on the Bulge Height
 of Axisymmetrical Components -
 with and without Axial Deformation.

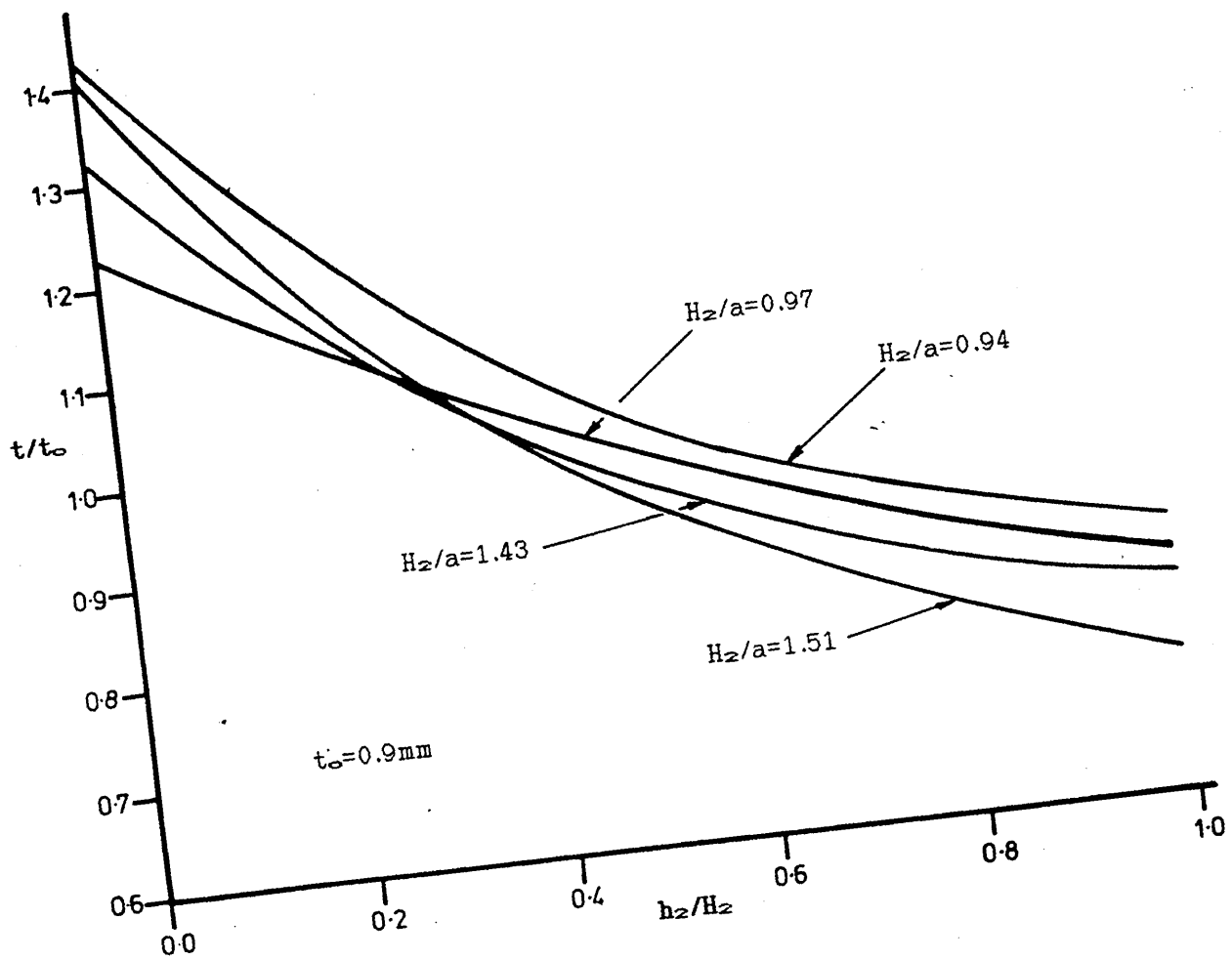


Fig. 9.
The Wall Thickness Distribution for Tee Pieces -
With Axial Deformation.

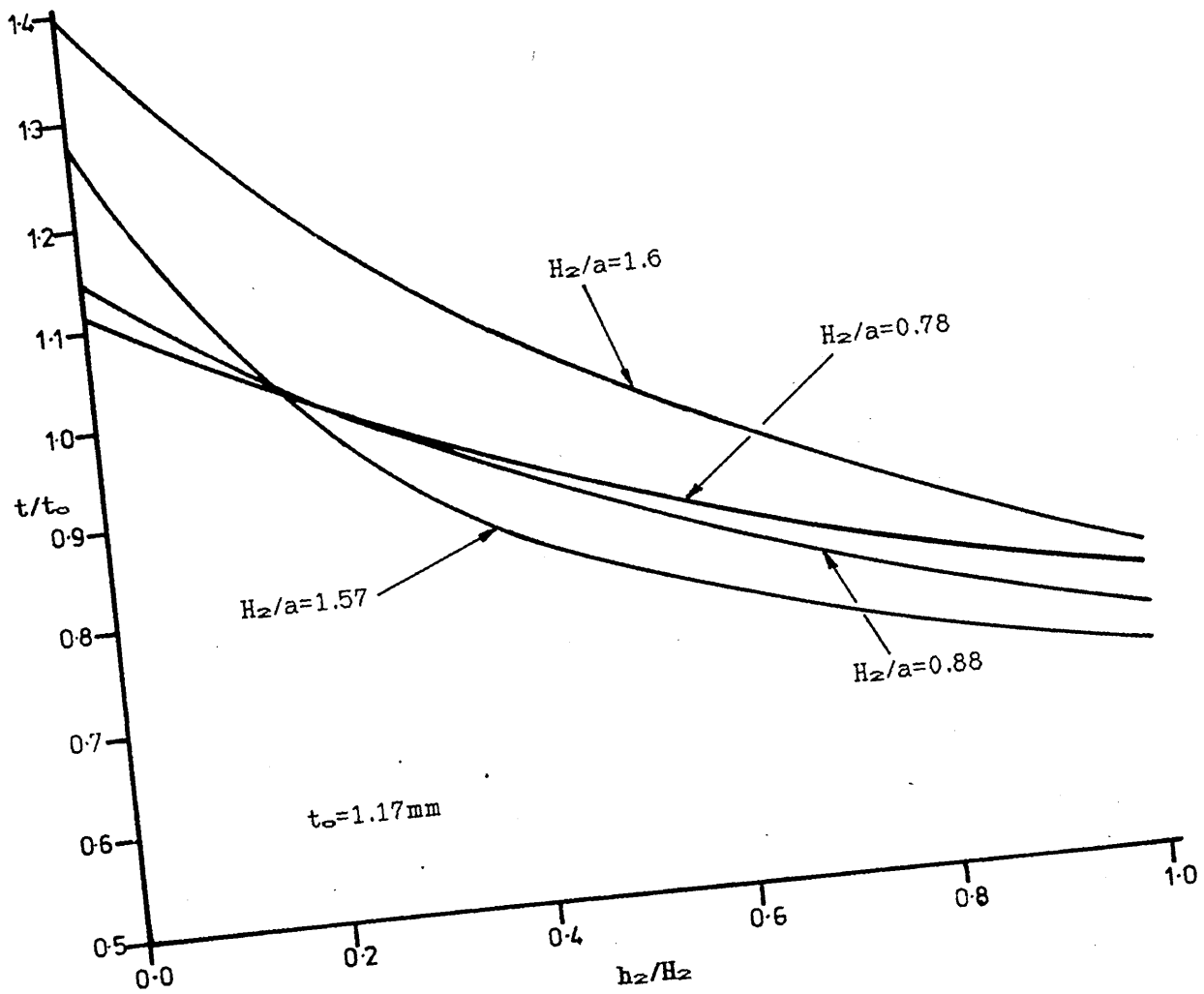


Fig. 10.
 The Wall Thickness Distribution for Tee Pieces -
 With Axial Deformation.

3. BULGE FORMING MACHINE DESIGN

3.1. OPERATING PARAMETERS

The operating parameters used in the design of the new machine were based on the findings of the preliminary investigation. With the prototype rig, a maximum internal pressure of 5500 psi. (38 N/mm²) and an axial compressive force of 110 kN were involved in the forming of axisymmetrical components. These values were obtained when forming the thickest tubes (1.6 mm wall thickness).

The new machine was required to provide sufficient internal pressure and axial compressive force to form copper tube and possibly stronger materials eg. mild steel, brass etc. For these reasons a nominal internal pressure of 10000 psi. (69 N/mm²) and axial force of 200 kN were chosen. The clamping force holding the two die halves together needs to restrain this internal pressure, and was considered assuming a tube blank of 25 mm diameter and 150mm length. The force acting to split the two die halves at maximum internal pressure (neglecting the resistance from the tube wall, and the wall thickness) was calculated to be :

$$\begin{aligned} \text{Projected Area} &= 150 \times 25 \text{ mm}^2 \\ \text{Pressure} &= 69 \text{ N/mm}^2 \\ \text{Force on Projected Area} &= 69 \times 150 \times 25 \text{ N} \\ &= \underline{260 \text{ kN}} \end{aligned}$$

The nominal value for the clamping force was chosen to be 300 kN in order to restrain this force.

3.2. HYDRAULIC COMPONENTS

3.2.1. Hydraulic Supply Pressure

Before the sizes of the hydraulic cylinders could be considered, a value for the hydraulic circuit pressure first had to be chosen. A maximum internal pressure of 10000 psi. (69 N/mm²) is required for the forming process. However, operating at this pressure would make the cost of the hydraulic components very expensive. Alternatively, a lower supply pressure could be chosen and this pressure increased through a pressure intensifier to provide the forming pressure. The second route was taken, with a main circuit pressure of 2500 psi. (17 N/mm²) - sufficiently high as to reduce the size of the hydraulic cylinders to a manageable size, but not too high as to make the hydraulic circuit very expensive.

3.2.2. Hydraulic Cylinders applying Axial Force

In order to provide axial deformation of the tube during forming, two hydraulic cylinders would be required, each providing a maximum axial compressive force of 200 kN. The size of the cylinders required to provide this force was calculated as follows:

$$\begin{aligned} \text{Force Required} &= 200 \text{ kN} \\ \text{Supply Pressure} &= 17.2 \text{ N/mm}^2 \\ \text{Area of Piston} &= \frac{\text{Force Required}}{\text{Supply Pressure}} \\ &= \frac{200 \times 10^3}{17.2} \text{ mm}^2 \\ \text{Diameter of Piston} &= 2 \times \sqrt{\frac{200 \times 10^3}{17.2} \cdot \frac{1}{\pi}} \text{ mm} \\ &= \underline{122 \text{ mm}} \end{aligned}$$

The actual cylinders used on the machine are two "Mecman" Series 203 cylinders with a diameter of 125 mm and a stroke of 100 mm. This stroke was considered suitable to allow insertion of a 150 mm tube blank into the die with the plungers withdrawn and to provide sufficient axial deformation of it during forming. It also allows the use of longer tube blanks which may be required for more complicated component shapes.

3.2.3. Hydraulic Cylinder applying Clamping Force

The size of the cylinder required to keep the two halves of the die together during forming was calculated in the same way. However, this cylinder was required to provide a force of 300 kN in order to restrain the internal pressure. Hence :

$$\begin{aligned}
 \text{Force Required} &= 300 \text{ kN} \\
 \text{Supply Pressure} &= 17.2 \text{ N/mm}^2 \\
 \text{Area of Piston} &= \frac{\text{Force Required}}{\text{Supply Pressure}} \\
 &= \frac{300 \times 10^3}{17.2} \text{ mm}^2 \\
 \text{Diameter of Piston} &= 2 \times \sqrt{\frac{300 \times 10^3}{17.2} \cdot \frac{1}{\pi}} \text{ mm} \\
 &= \underline{149 \text{ mm}}
 \end{aligned}$$

This led to the choice of a "Mecman" Series 206 cylinder with a diameter of 160 mm (150 mm was not available) and a stroke of 150 mm. In this case the stroke determined how far the dies could be opened. The dies blocks were required to open in order to place a tube blank in position, and to remove the formed component after forming. A gap of about 150 mm between the two was determined to be sufficient to allow access. However, in order to provide a clamping force not all of the

stroke is used up, and the actual gap between the two die blocks is about 140 mm.

3.2.4. Hydraulic Pump and Electric Motor

The power source for the hydraulic system is a "Sperry Vickers" variable displacement piston pump - model PVB 5 - driven by a 7.5 kW electric motor. This pump is capable of operating at pressures of up to 21 N/mm², but is set at an operating pressure of 17.5 N/mm².

Therefore, the maximum theoretical forces that can be applied by the hydraulic cylinders are as follows (neglecting any losses).

For the cylinders applying axial compressive force:

Area of Piston (from manu. spec.)	= 123 x 10 ² mm ²
Pressure	= 17.5 N/mm ²
Maximum Force	= 123 x 10 ² x 17.5 N
	= <u>215 kN</u>

For the clamping cylinder:

Area of Piston (from manu. spec.)	= 201 x 10 ² mm ²
Pressure	= 17.5 N/mm ²
Maximum Force	= 201 x 10 ² x 17.5 N
	= <u>352 kN</u>

The maximum flow rate of the hydraulic pump is 32 l/min according to the manufacturers specifications, but less than this will be obtained when operating at 17.5 N/mm² and using only a 7.5kW motor. This gives a maximum theoretical flow rate of:

Driving Power	= 7.5 kW
Operating Pressure	= 17.5 N/mm ²

$$\begin{aligned} \text{Delivery Flow Rate} &= \frac{7.5 \times 10^3}{17.5 \times 10^6} \text{ m}^3/\text{s} = 0.429 \times 10^{-3} \text{ m}^3/\text{s} \\ &= \underline{25.7 \text{ l/min}} \end{aligned}$$

The actual delivery flow rate will in fact be a little less than this due to the volumetric efficiency of the pump being less than 100%, and due to losses in the circuit between the pump and the cylinders. However, this value can be used to calculate the approximate maximum velocities of the pistons of each cylinder. For the clamping cylinder, assuming all the flow is directed to it, the velocity during the outward stroke (closing the two die halves) is:

$$\begin{aligned} \text{Area of Piston} &= 201 \times 10^{-4} \text{ m}^2 \\ \text{Delivery Flow Rate} &= 0.429 \times 10^{-3} \text{ m}^3/\text{sec} \\ \text{Piston Velocity} &= \frac{0.429 \times 10^{-3}}{201 \times 10^{-4}} \text{ m/sec} \\ &= \underline{21 \text{ mm/sec}} \end{aligned}$$

Hence a full stroke of 150 mm will be completed in just over 7 seconds. For the return stroke (opening the die) the velocity will be faster, due to the smaller piston area around the piston rod.

$$\begin{aligned} \text{Area of Pull Side} \\ \text{of Piston} &= 137 \times 10^{-4} \text{ m}^2 \\ \text{Piston Velocity} &= \frac{0.429 \times 10^{-3}}{137 \times 10^{-4}} \text{ m/sec} \\ &= \underline{31 \text{ mm/sec}} \end{aligned}$$

This gives a return stroke time of under 5 seconds.

For the cylinders applying the axial compressive force a similar approach is used again assuming all the flow is directed to them (in practice, however, some of the flow will be directed to the internal pressure). For the outward stroke (causing axial deformation) the velocity is:

$$\begin{aligned} \text{Area of Piston} &= 123 \times 10^{-4} \text{ m}^2 \\ \text{Delivery Flow Rate} &= \frac{0.429 \times 10^{-3}}{2} \text{ m}^3/\text{sec} \\ \text{to One Cylinder} & \\ \text{Piston Velocity} &= \frac{0.429 \times 10^{-3}}{2 \times 123 \times 10^{-4}} \text{ m/sec} \\ &= \underline{17 \text{ mm/sec}} \end{aligned}$$

And for the return stroke:

$$\begin{aligned} \text{Area of Pull Side} &= 84.2 \times 10^{-4} \text{ m}^2 \\ \text{of Piston} & \\ \text{Piston Velocity} &= \frac{0.429 \times 10^{-3}}{2 \times 84.2 \times 10^{-4}} \text{ m/sec} \\ &= \underline{25 \text{ mm/sec}} \end{aligned}$$

This gives an outward stroke time of under 6 seconds and a return stroke time of 4 seconds to complete the 100 mm stroke of both cylinders.

3.3. THE HYDRAULIC CIRCUIT

The hydraulic circuit for the bulge forming is required to perform three functions i.e. to connect the power unit and to control the supply to:

1. the hydraulic cylinder clamping the two die halves together,
2. the two hydraulic cylinders providing the compressive axial force,
3. the internal pressurised region of the tube blank.

These have to be controlled independantly of each other and each has different control requirements.

3.3.1. The Clamping Hydraulic Cylinder

The function of the hydraulic circuit providing the clamping force is simply one of extending and retracting the cylinder rod. The basic component of this part of the hydraulic circuit is thus simply a directional control valve with three positions - one position to extend the ram (to close the two die halves and when together to provide the clamping force), one to stop it, and one to withdraw it (to open the die).

3.3.2. The Hydraulic Cylinders Applying Axial Force

This second requirement needs some extra control as well as a directional control valve. As previously mentioned one of the considerations for the design of the new rig was that the two hydraulic cylinders providing the compressive axial force should move in unison to one another, in order to produce equal deformation of each end of the tube and so form the bulge centrally on the tube. This can be achieved approximately by the use of a flow divider in the circuit between the pump and the hydraulic cylinders. This will divide the flow from the pump into equal parts regardless of the load on each cylinder, and so synchronise the movement of the two cylinders. A pressure reducing valve is also required in order to control the force being applied to the ends of the tube. Again a directional control valve will control extending and withdrawing the cylinders.

3.3.3. The Internal Pressurised Region of the Tube Blank

This third requirement is needed to provide the internal pressure in order to form the tube into the shape of the die. As previously mentioned in the operating parameters, a maximum pressure of

10000 psi. (69 N/mm^2) is required for the forming pressure. This can be achieved from the supply pressure (17 N/mm^2) by the use of a pressure intensifier between the pump and the high pressure circuit. Again a pressure reducing valve is required to control the pressures being generated, and also a directional control valve but this time its functions are:

1. to bypass the pressure intensifier (in order to fill the tube blank, prior to forming, quickly at the lower supply pressure),
2. to stop the supply, and
3. to supply the pressure intensifier, and thus generate a high forming pressure.

Also needed on this high pressure circuit is a valve connected to the opposite end of the tube in order to bleed the air while filling the tube with oil.

3.3.4. The Initial Circuit Design

A circuit diagram for the initial design of the hydraulic circuit is shown in Fig. 11. This illustrates the allocation of the directional control valves, pressure reducing valves, flow divider and pressure intensifier previously mentioned. Also included in the circuit, and not previously mentioned, is a non-return valve in the part of the circuit supplying the internal pressure. This protects the rest of the circuit from the high pressures generated by the pressure intensifier, but also allows fluid to flow through it when bypassing the intensifier in order to fill the tube.

3.3.5. The Actual Circuit Design

Using the initial design as a basis, the final design for the hydraulic circuit was arrived at after consultation with experts in the field. The circuit actually used on the forming machine is illustrated in Fig. 12. As can be seen, filters have been added to both inlet and outlet sides of the hydraulic pump in order to prevent the ingress of dirt, which would affect the operation of some of the valves. Also to protect the circuit, a relief valve (RV1) has been included which can be varied according to need.

Considering the part of the circuit controlling the clamping cylinder (A) a small change has been made to the directional control valve (V1). In its central position ie. stopping the movement of the cylinder, this valve acts as a dump valve returning all the fluid flow back to the tank. This allows the hydraulics to be kept in a standby state with the pump still running, without generating a lot of heat by passing all the fluid through the relief valve. Variable flow control valves (FC4) have also been added so that the speed of the opening and closing of the dies can be adjusted. To prevent accidental closure of the die when the circuit is in the standby state or the supply is turned off, a pilot operated check valve (CV1) has been included in the circuit, which locks the cylinder in the up position until pressure is applied to force it down.

For the cylinders applying the axial compressive force (B), the hydraulic circuit has been split into two, each half having its own directional control valve (V2 & V3), pressure reducing valve (PR1 & PR2) and flow control valves (FC1 & FC2). This is because the movement of

these cylinders is required to perform several tasks. First of all the cylinders must move the plungers, through which the compressive forces are transmitted, up to the ends of the tube and seal them. This must be performed fairly quickly, so as to minimise the time for the production of each component, and should apply only a small axial compressive force - sufficient enough to seal the ends of tube but without causing axial deformation. Secondly, the cylinders have to apply an axial compressive force large enough to cause axial deformation of the tube, while it is subjected to internal pressure. This force will vary depending on the wall thickness of the tube and the shape of the component that it is being formed into. Lastly the speed of the cylinders (strain rate) might have to be altered. With the supply circuit split into two halves these two operations can be achieved with the pressures and flow rates preset without the need to adjust any of the valves once set.

In Fig. 12 the two directional control valves (V2 & V3) are shown in the unenergised state which causes retraction of the cylinders. Once the solenoid on valve V2 is energised the cylinders will extend with the fluid pressure and flow rate determined by valves PR1 and FC1 respectively. This should be at low pressure and at high speed in order to bring the plungers into contact with the tube and to seal the ends. Energising the solenoid on valve V3 will then cause axial deformation to occur with the pressure and flow rate set by valves PR2 and FC2 respectively. These will be set at a higher pressure and perhaps at a lower flow rate. The flow from both halves of the circuit still pass through a flow divider (FD) in order to synchronise the movement of the two cylinders. Unenergising the solenoids on both directional control valves will then cause the cylinders to be retracted again.

The high pressure part of the circuit, providing the internal pressure, remains similar to the initial circuit diagram apart from the addition of a pressure relief valve (RV2) and an extra check valve (CV4). These are required because during the forming process the axial deformation causes an increase in the internal pressure. A pressure relief valve prevents this pressure from becoming too large which might cause rupture of the tube being formed or more importantly damage to the hydraulic circuit. The additional check valve (CV4) prevents this larger pressure thus generated from reaching the outlet side of the pressure intensifier (PI).

All the solenoids operate on a 24V DC supply, which initially will be controlled manually by switches. The switch arrangement is illustrated in Fig. 13. At a later date these switches could be replaced by relays controlled by a micro processor or a micro computer to allow the automatic control of the process.

3.4. THE STRUCTURAL DESIGN OF THE MACHINE

Having decided on the size of the cylinders to be used on the bulge forming machine, the overall design could then proceed. The layout of the cylinders was partly predetermined by the actions required of them. The two cylinders applying the axial compressive force have to be located on opposite sides of the die block acting in line and inwards towards each other. With the die block splitting axially in relation to the tube blank, the clamping cylinder would have to be mounted perpendicular to the other two cylinders. The obvious arrangement for these cylinders then would be to mount the clamping cylinder vertically acting downwards onto the die block, with the other two cylinders mounted

horizontally, on either side of the die block, acting inwards. This is illustrated in Fig. 14 along with the general mounting arrangements. The restraints for the two different forces have been separated - the clamping force being contained by four tie bars and the axial compressive force by a beam. These shall therefore be dealt with separately.

3.4.1. The Clamping Force Restraint

The clamping cylinder is mounted on a plate supported by four tie-bars each of diameter 50mm. The ends of these tie-bars are turned down with M30 threads to connect to the plates. The maximum stresses in these end threads when the tie-bars are subjected to the maximum tensile force of 352 kN are as follows:

$$\text{Maximum Load in each Tie-bar} = \frac{352 \text{ kN}}{4} = 88 \text{ kN}$$

$$\text{Tensile Stress Area of M30 Bolt} = 621 \text{ mm}^2$$

$$\text{Stress} = \frac{88 \times 10^3}{621} = 142 \text{ N/mm}^2$$

$$\text{Yield Stress of EN8} = 385 \text{ N/mm}^2$$

$$\text{Proof Load for M30 Nut} = \frac{392 \times 561}{1000} = 220 \text{ kN}$$

The top plate onto which the cylinder is mounted has been considered as a simply supported beam onto which a uniformly distributed load is acting - see Fig. 15. With a 60 mm depth the following stresses occur.

$$\begin{aligned} \text{Bending Moment} &= 176 \times 0.2 - \frac{352}{0.280} \times 0.140 \times \frac{0.140}{2} \\ &= 22.88 \text{ kNm} \end{aligned}$$

$$\begin{aligned} \text{Second Moment of Area} &= \frac{bd^3}{12} = \frac{0.4 \times 0.06^3}{12} \\ &= 7.2 \times 10^{-6} \text{ m}^4 \end{aligned}$$

$$\begin{aligned} \sigma_{\max} &= \frac{My}{I} &= \frac{22.88 \times 10^3 \times 0.03}{7.2 \times 10^{-6}} \\ & &= 146 \text{ N/mm}^2 \end{aligned}$$

Under full load conditions the maximum deflection occurring at the centre of this plate would be as follows:

$$\begin{aligned} R &= \frac{EI}{M} &= \frac{207 \times 10^9 \times 7.2 \times 10^{-6}}{22.88 \times 10^3} \\ & &= 65 \text{ m} \\ \text{Deflection at centre} &= 65 - \sqrt{65^2 - 0.2^2} \text{ m} \\ & &= 0.3 \text{ mm} \end{aligned}$$

The bottom of these tie bars locate in a similar plate, with depth 53 mm, on top of which is mounted the die blocks. The stresses occurring in this plate are calculated in a similar manner:

$$\begin{aligned} \text{Bending Moment} &= 176 \times 0.2 - \frac{352}{0.150} \times 0.075 \times \frac{0.075}{2} \\ & &= 28.6 \text{ kNm} \\ \text{Second Moment of Area} &= \frac{0.4 \times 0.053^3}{12} \\ & &= 4.96 \times 10^{-6} \text{ m}^4 \\ \sigma_{\max} &= \frac{My}{I} &= \frac{28.6 \times 10^3 \times 0.0265}{4.96 \times 10^{-6}} \\ & &= 152 \text{ N/mm}^2 \end{aligned}$$

the deflection occurring at the centre of this bottom plate when subjected to the maximum clamping force will be as follows:

$$\begin{aligned} R &= \frac{EI}{M} &= \frac{207 \times 10^9 \times 4.96 \times 10^{-6}}{28.6 \times 10^3} \\ & &= 35.9 \text{ m} \\ \text{Deflection at centre} &= 35.9 - \sqrt{35.9^2 - 0.2^2} \text{ m} \\ & &= 0.56 \text{ mm} \end{aligned}$$

These values have been obtained by considering the plates as simply supported beams, with a uniformly distributed load acting upon them. In fact these plates are bolted to the tie-bars and have the hydraulic cylinder and die block bolted to them. This will tend to strengthen the plates and decrease the amount of deflection that will occur at maximum loading.

3.4.2. The Axial Force Restraint

The force produced by the two hydraulic cylinders applying the axial compressive force is restrained by two channel section beams, serial size 305 x 102 mm. These are positioned back to back with a small gap between them, and the cylinders are attached to them by mounting brackets which locate onto the top flanges. The beams are subject to a bending moment due to the force exerted by the cylinders which, under full load conditions, is:

$$\begin{aligned} \text{Bending Moment} &= 215 \times [0.170 + 0.1524] \text{ kNm} \\ &= 69.3 \text{ kNm} \end{aligned}$$

The second moment of area for this size channel section is 8214 cm⁴ and hence the stresses in each beam at the outer fibres, where the maximum stresses occur, are:

$$\begin{aligned} \sigma_{\max} &= \frac{My}{I} = \frac{69.3 \times 0.1524}{2 \times 8214 \times 10^{-8}} \\ &= 64 \text{ N/mm}^2 \end{aligned}$$

It was originally intended to attach the cylinder mounting brackets to these beams by welding. However, machinery large enough to machine the faces of these mounting brackets square, once they were attached to the

beams, was not available. Instead the brackets were bolted to the channel sections in order to avoid distortion occurring. The use of bolts weakens the channel section beams, causing the second moment of area to be reduced, and increasing the stress occurring at the location of the bolt holes to approximately 71 N/mm².

The maximum deflection of the channel sections occurring in the middle will be:

$$\begin{aligned}
 R &= \frac{EI}{M} &= \frac{207 \times 10^9 \times 8214 \times 10^{-8}}{\frac{69.3}{2} \times 10^3} \\
 & &= 491 \text{ m} \\
 \text{Deflection} & &= 491 - 491^2 - 0.420^2 \text{ m} \\
 & &= 0.18 \text{ mm}
 \end{aligned}$$

3.4.2.1. The Mounting Brackets

The hydraulic cylinders are bolted to the mounting brackets, and therefore the forces acting on these brackets can be considered to be point loads. The values of these forces and their location are illustrated in Fig. 16.a, under full load conditions. Subjected to these forces the maximum bending moment will occur at the bottom of the bracket, which is evaluated to be:

$$\begin{aligned}
 \text{Bending moment} &= 27 \times 0.0525 + 54 \times [0.087 + 0.170 + 0.253] \\
 & \quad + 27 \times 0.2875 \\
 &= 36.7 \text{ kNm}
 \end{aligned}$$

In order to evaluate the stresses exerted on these brackets, first the position of the neutral axis has to be determined. Referring to Fig. 16.b - taking moments of area about X-X gives:

$$[330 \times 25 + 2 \times 300 \times 15] \bar{y} = 25 \times 330 \times 12.5 + 2 \times 300 \times 15 \times 175$$

$$\bar{y} = \frac{25 \times 330 \times 12.5 + 2 \times 300 \times 15 \times 175}{330 \times 25 + 2 \times 300 \times 15}$$

$$\bar{y} = 97.3 \text{ mm}$$

Therefore $I = \frac{330 \times 97.3^3 - 300 \times 72.3^3 + 2 \times 15 \times 227.7^3}{3}$

$$= 1.82 \times 10^{-4} \text{ m}^4$$

The maximum stresses will occur in the outer edges when $y = 227.3 \text{ mm}$ and will be compressive. The maximum tensile stress will occur at $y = 97.3 \text{ mm}$ and will be less than half the compressive stress.

$$\sigma_c = \frac{My}{I} = \frac{36.7 \times 10^3 \times 0.2273}{1.82 \times 10^{-4}}$$

$$= 46 \text{ N/mm}^2$$

As previously mentioned, each mounting bracket is bolted to the two channel section beams. Six M24 cap head screws are used for this purpose, and in order for the top flanges of the channel sections to be able to bear the loads acting on these screws, a reinforcement block is welded to the underside of the flanges in these areas. This is illustrated in Fig. 17. The stresses experienced by the bracket and the reinforced flange are as follows:

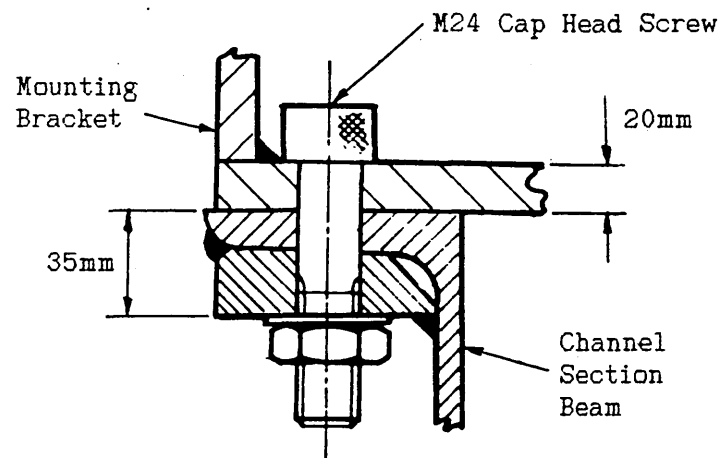


Fig. 17.
The Channel Section Flange Reinforcement.

$$\text{Load acting on each bolt} = \frac{215}{6} = 35.8 \text{ kN}$$

$$\text{Nominal Stress Area} = 384 \text{ mm}^2$$

$$\begin{aligned} \text{Shear Stress} &= \frac{35.8 \times 10^3}{384} \\ &= 93 \text{ N/mm}^2 \end{aligned}$$

$$\begin{aligned} \text{Bearing Stress in Bracket} &= \frac{35.8 \times 10^3}{24 \times 20} \\ &= 74.6 \text{ N/mm}^2 \end{aligned}$$

$$\begin{aligned} \text{Bearing Stress in Flange} &= \frac{35.8 \times 10^3}{35 \times 24} \\ \text{and Reinforcing Plate} & \\ &= 10.2 \text{ N/mm}^2 \end{aligned}$$

3.4.3. Assembly

The arrangement of the bulge forming machine is shown in Fig. 23, which is a reduced reproduction of the original assembly drawing- a full size reproduction of this, and the rest of the drawings, should be found at the back of this thesis. This drawing shows the two channel section beams onto which are attached the two horizontal cylinders which apply the axial compressive forces. Mounted in the centre of these channel sections is the bottom plate, containing the bottom die block and the four tie bars. At the top of these tie bars is the top plate supporting the hydraulic cylinder providing the clamping force. This is connected to the top half of the die block which is shown in the closed position.

When closed it is important that the two halves of the die blocks align with each other, otherwise the tube and plungers may be trapped by the large clamping force, or the bulge formed may be distorted. In order to insure alignment, the die blocks are mounted in a "Desoutter" Die Set.

This consists of two steel plates, the top one being guided by bushes which slide along pillars attached to the bottom plate. This can be seen in the drawing shown in Fig. 23, and can be seen in close up in Fig. 33 which is a close up photograph of the die blocks. This photograph, and Figs. 25, 26 & 27, show how the die block is made up - a central removable die block contained in a larger holder. In the photograph the die block is one to form cross pieces, and is shown with a tube blank in position prior to forming. The plastic tube at the front of the die block holder is to drain away some of the excess oil that is left in the die block after removing the formed component.

On either side of the die block holder are mounted two plunger guides, which support the plungers when the die blocks are opened. Drawings of these plungers and the guides are shown in Figs. 22 and 28. The plungers mount onto the ends of the horizontal cylinders and transmit the compressive axial force to the ends of the tube. Where they are in contact with the copper tube, the plungers are stepped, so they will locate inside the tube. This part is also tapered, as shown in Fig. 22, to help in sealing the end of tube when the inside is pressurised with oil. To allow the oil in, and the air out, both plungers are drilled through, one being connected to a flexible hydraulic hose, and the other to a bleed valve.

In order to provide a reasonable working height and to support the machine, the whole assembly is mounted on a framework made up of angle iron. Fig. 29 shows a photo of the front view of the machine in which the framework can clearly be seen together with the channel section beam mounted within it.

Fig. 30 shows a view of the back of the machine. In this photograph, part of the high pressure circuit can be seen in the foreground - the pressure intensifier and relief valve, with the flexible hydraulic hose leading off to one of the plungers. Above this can be seen the flow divider, with the two pipes leading off to the two horizontally mounted hydraulic cylinders. In the background at the top is mounted the stack containing most of the valves in the hydraulic circuit, connected to the pump and motor visible in the bottom of the photograph (the pump is mounted underneath the motor inside the oil tank).

3.4.4. Alterations to the Initial Design

The main alteration in the design, as previously mentioned, was the use of bolts instead of welding, for joining the cylinder mounting brackets to the channel section beams. Both cylinders have to be mounted horizontally and in line with each other. If the brackets had been welded to the channel sections, the mounting faces would have to be machined afterwards to correct any distortion that may have occurred due to the heat. Because of the size of the assembly this was impractical so the brackets were bolted on instead. Similarly, instead of welding the bottom plate, onto which the die block is mounted, it was clamped to the channel section by two long bolts stretching from the bottom plate to two blocks of metal located underneath the beams.

Another alteration was a change in the way the die block holders were mounted onto the "Desoutter" die sets. The drawings in Figs. 25 and 26 show bolt holes through each die block holder. These were not used, however, because of the difficulty it would have involved in trying to bolt the top half into position. Instead four recesses were cut into the

ends of each half, so that the die block holders could be clamped onto the die sets. This can be seen in Fig. 33, a photograph of the die blocks - the clamps are located on either side of the plunger guides. This method of attachment allows the top half of the die block holder to be attached with the dies in the closed position, and so also allows the alignment of the two halves prior to clamping fully tight in position.

3.5. COMMISSIONING

After completion of the machine and the hydraulic circuit, tests were carried out by forming copper tube into tee pieces in order to highlight any problems associated with it. The problems encountered fall into two categories - Structural and Hydraulic.

3.5.1. Structural Problems

Before any testing could be carried out, the first problem had to be rectified. The two plungers which were attached to the horizontal cylinders were not aligned properly. These plungers were attached to the cylinders by bolts passing through them and connecting to a plunger mount screwed onto the end of the cylinder rod. Some linear misalignment was allowed for by having oversize bolt holes drilled in the plungers, but a slight angular misalignment was also present. To allow for this a floating connection was required, which was achieved by discarding the mounting bolts and fitting a collar over the end of the plunger which is bolted to the plunger mount - see Fig. 34. This allows movement of the plunger within it.

A second problem encountered in the same area, was rotation of the cylinder rods during extension and retraction. This caused a problem

because of the part of the hydraulic circuit attached to the ends of them. This rotation was prevented by machining a flat onto the plunger mounting collars, and mounting a piece of angle iron along side each one. The contact between the flat on the collar and the angle iron during extension and retraction thus prevents rotation of the cylinder rods.

3.5.2. Hydraulic Problems

Once the structural problems had been rectified the forming of tee pieces could proceed. The first problem on the hydraulic side showed itself immediately - a high internal pressure could not be achieved indicating a faulty pressure intensifier. On removal and examination of the pressure intensifier the fault was traced. A pipe fitting screwed into one of the ports was too long and had covered and blocked a small port inside the intensifier. Shortening the pipe fitting rectified the fault and allowed a high internal pressure to be obtained.

Another problem with the internal pressure was the slow operation of the pressure relief valve. The pressure would only drop very slowly to the value set by the relief valve which allowed very high pressures to be accidentally obtained. Replacement of the high pressure relief valve did not effect its operation, and the original one was tested on a test bench and worked perfectly. The fault was finally traced to be due to the drain pipe, which returned the oil to the tank. On its way back to the tank, the pipe from the relief valve joined the drain pipe from the pressure intensifier and the return pipe from the rest of the circuit. Seemingly a large back pressure was building up in the drain pipe from the pressure relief valve, preventing the valve from operating properly. Providing the relief valve with its own drain pipe all the way back to

the tank prevented this problem and allowed the valve to operate correctly.

After carrying out several tests a less serious problem also showed itself, in that the bulges formed on the tube were not central. This indicated that the flow divider was not producing equal movement of the two hydraulic rams providing the axial compressive force. This was simply cured by removing and cleaning the flow divider. When replaced the bulges were formed approximately central on the tube. The fault was likely to be due to the ingress of dirt during the assembly of the hydraulic circuit.

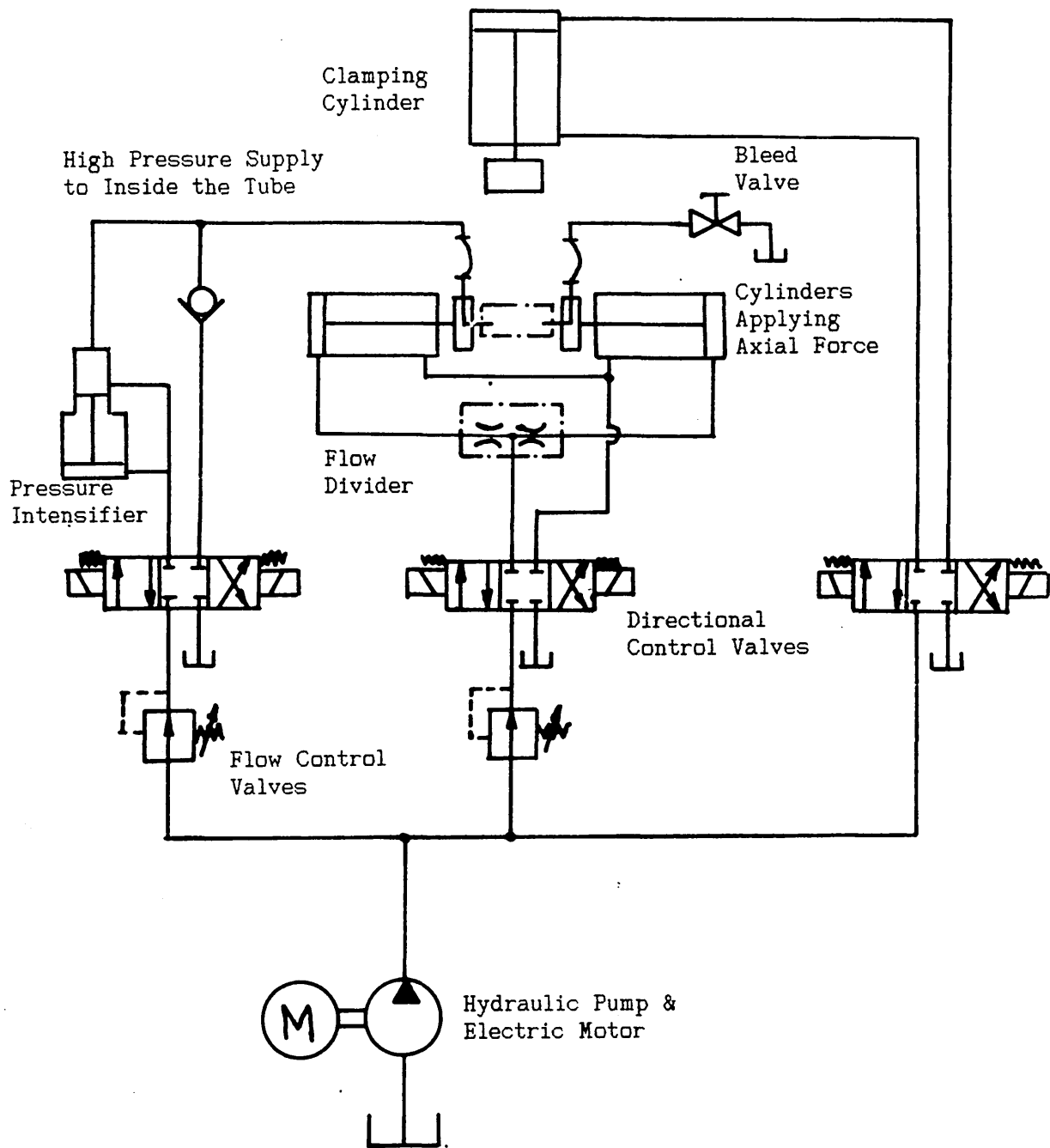
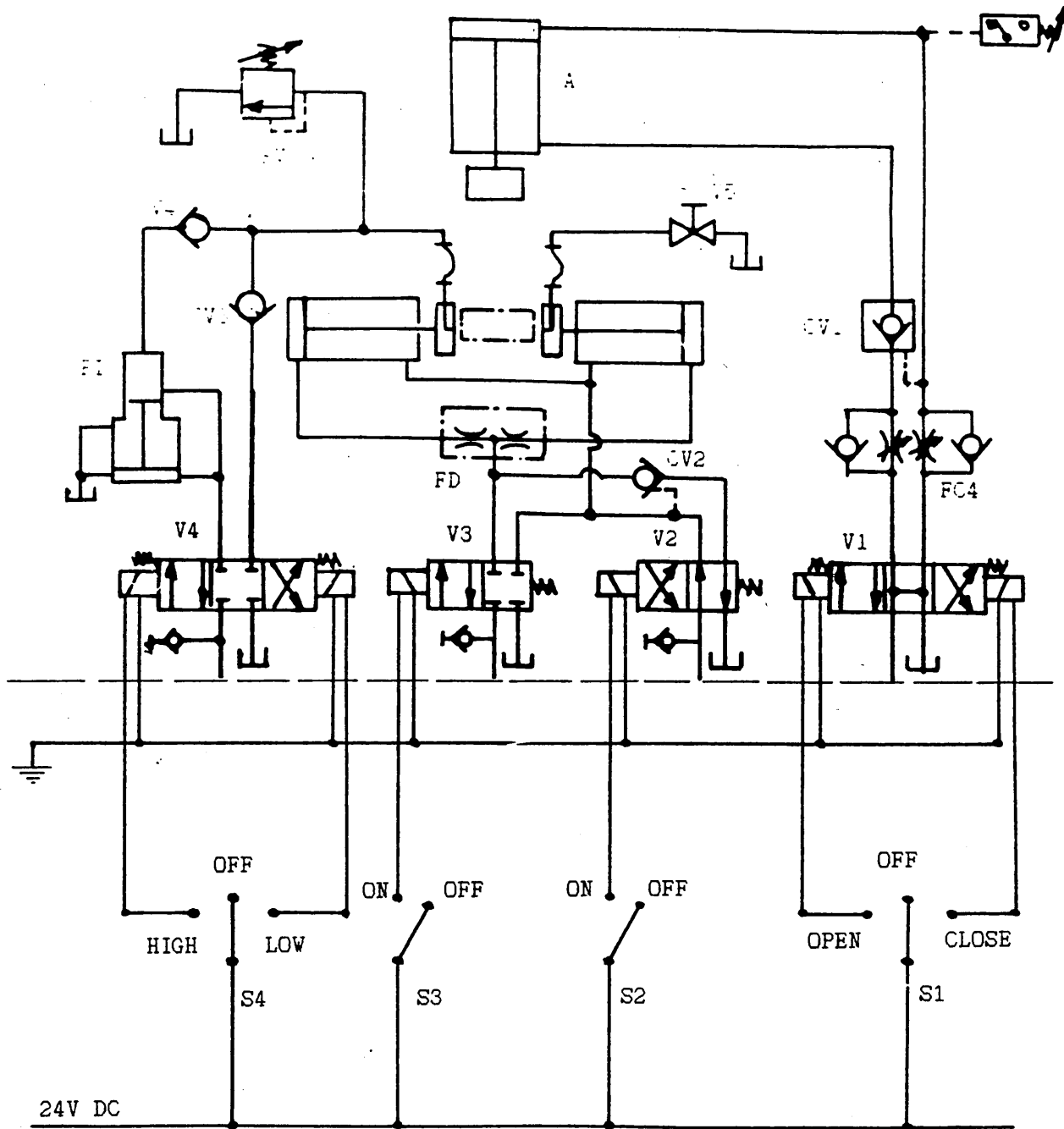


Fig. 11.
The Initial Design of the Hydraulic Circuit.



24V DC

S4		S3		S2		S1	
POSITION	ACTION	POSITION	ACTION	POSITION	ACTION	POSITION	ACTION
HIGH	Supply fluid to the pressure intensifier.	ON	Extend plungers using a large axial compressive force to cause deformation.	ON	Extend plungers using a small force for initial sealing.	OPEN	Open the die block to allow access to the forming area.
OFF	No flow.					OFF	Standby state.
LOW	Bypass the Pressure intensifier for initial filling.	OFF	No flow.	OFF	Retract plungers to allow release of the formed component.	CLOSE	Close and clamp the die halves together.

Fig. 13.
The Switch Arrangement for the Solenoid Valves.

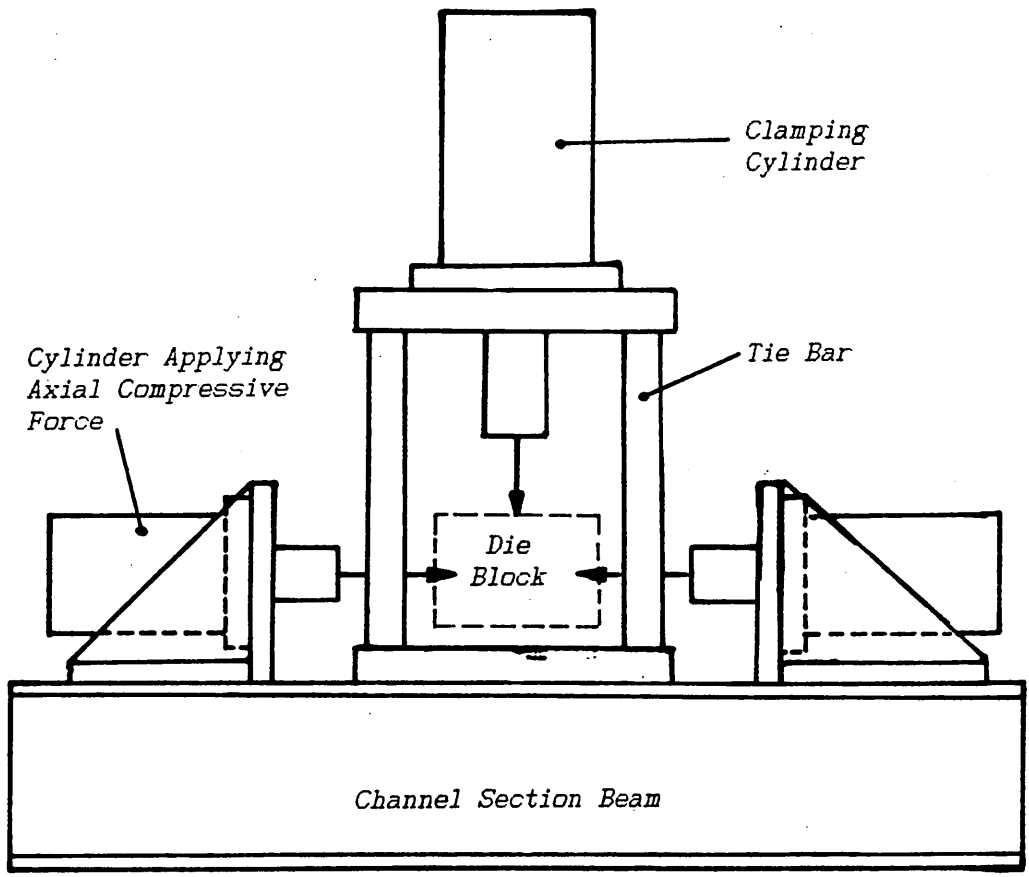


*Fig. 14
Arrangement of the Hydraulic Cylinders*

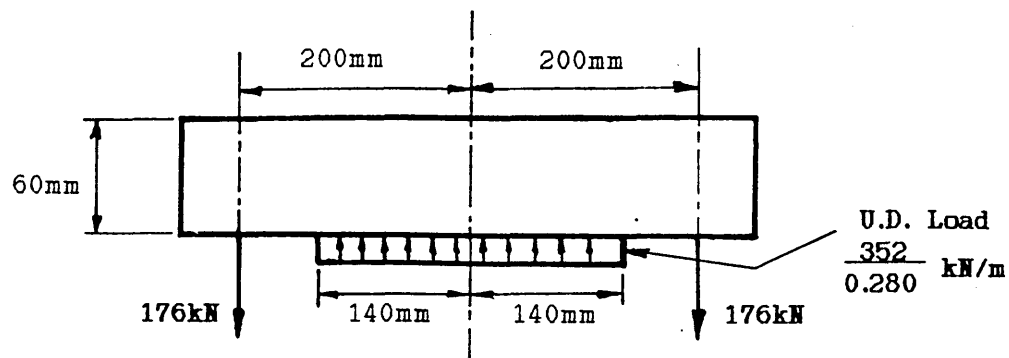


Fig. 15.
The Forces Acting on the Top Mounting Plate.

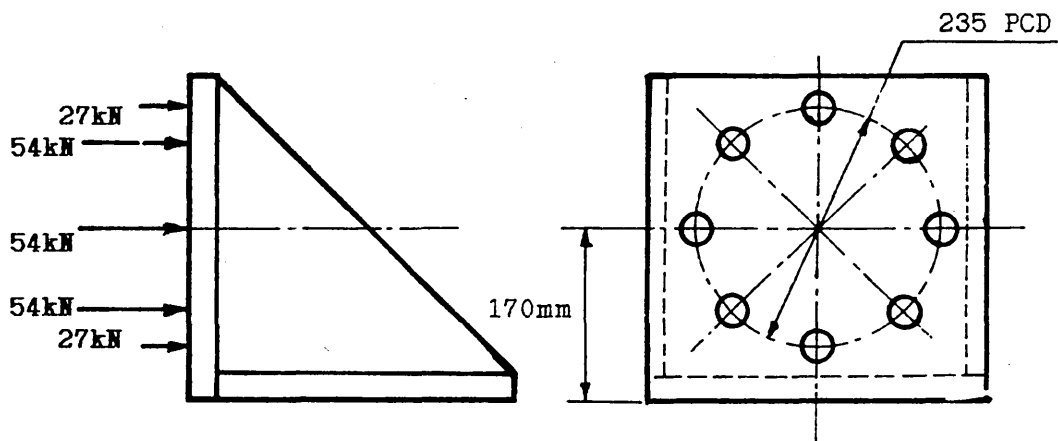


Fig. 16.a.
The Forces Acting on the Mounting Brackets.

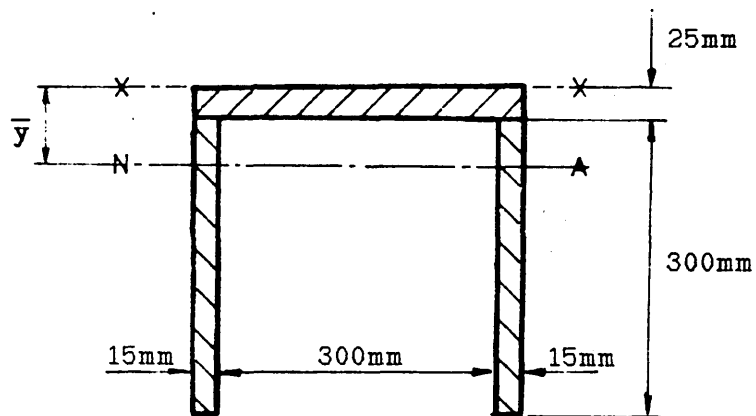
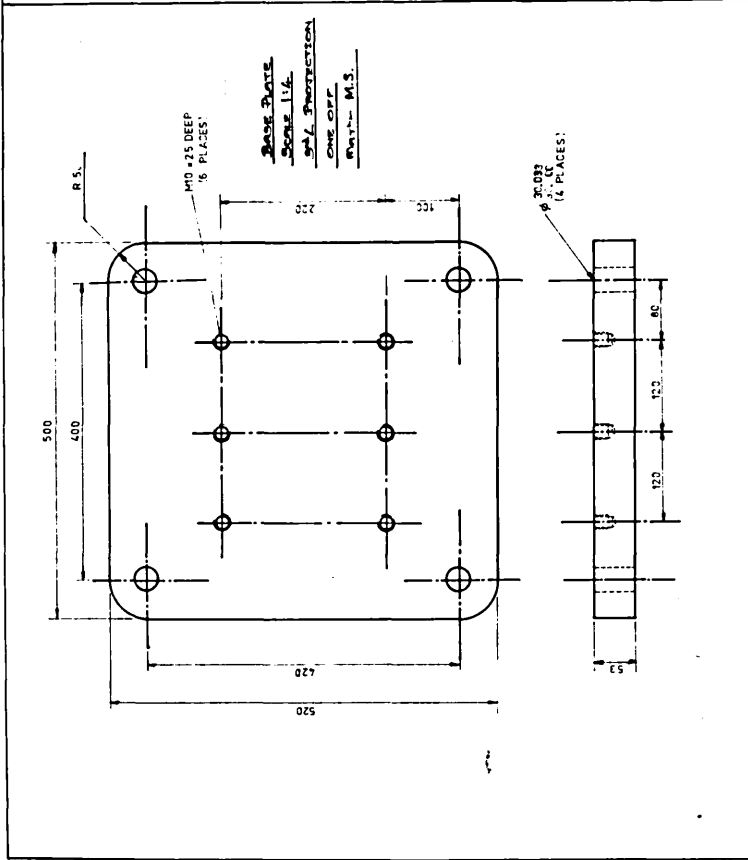
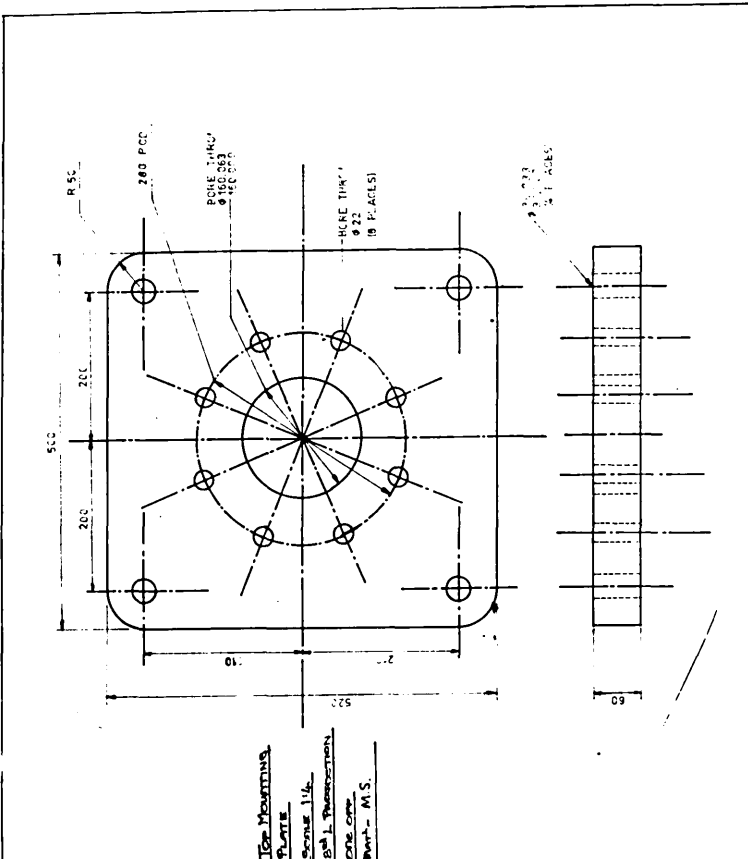


Fig. 16.b.
The Position of the Neutral Axis.

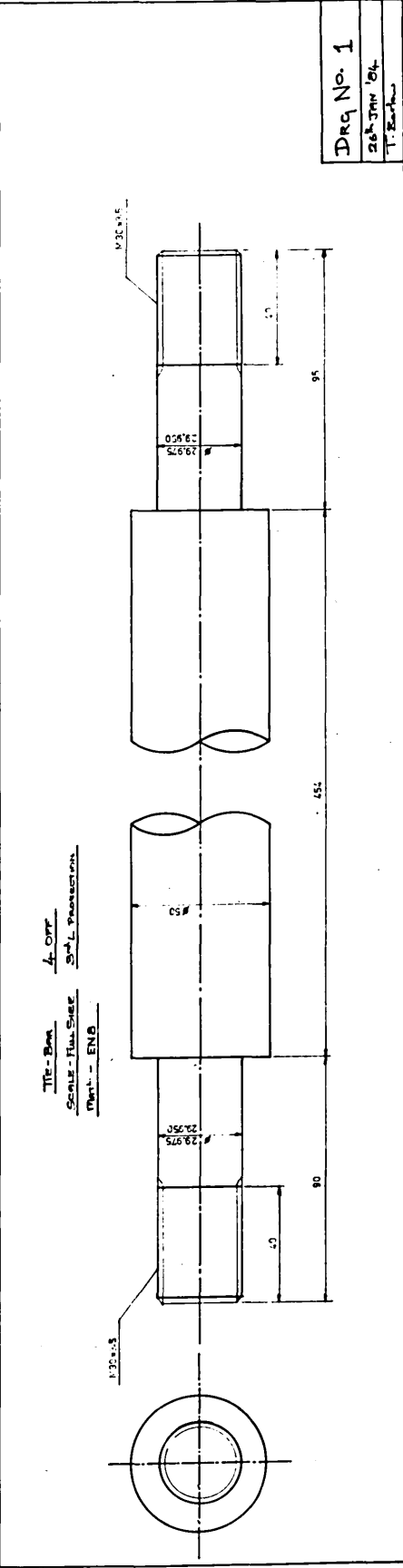
Fig. 18 The Base Plate, Top Plate and Tie Bars.



ICE MOUNTING PLATE
 SCALE 1/4"
 S¹/4 PROJECTION
 ONE OFF
 PART-- M.S.



ICE MOUNTING PLATE
 SCALE 1/4"
 S¹/4 PROJECTION
 ONE OFF
 PART-- M.S.



TEE-BAR
 SCALE 1/4"
 S¹/4 PROJECTION
 ONE OFF
 PART-- END

DRG No. 1
 26 JAN '04
 T. B. B.

Fig. 19. The Hydraulic Cylinder Brackets

HYDRAULIC CYLINDER BRACKET

7 th Feb '84	Scale - 1:2	T. S. Sadas
Matl - M.S.	2 OFF	
3 rd L PROTECTION	DRG. No. 2	

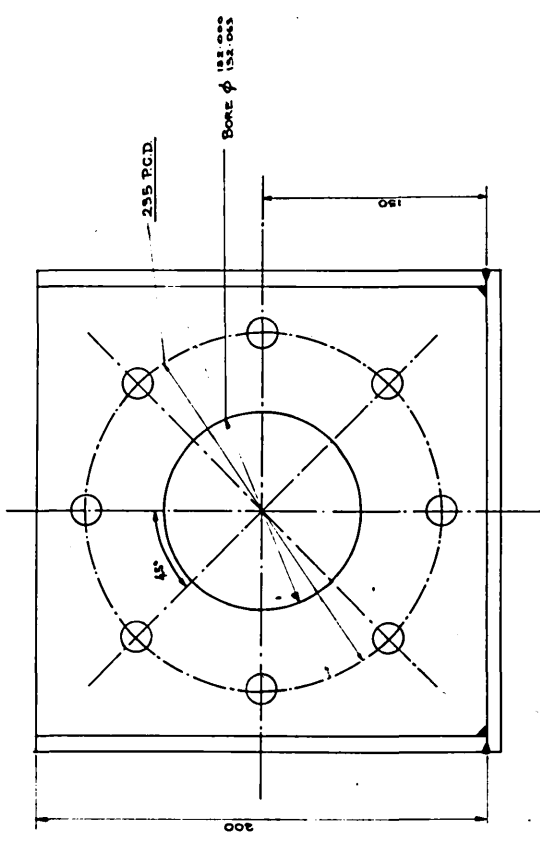
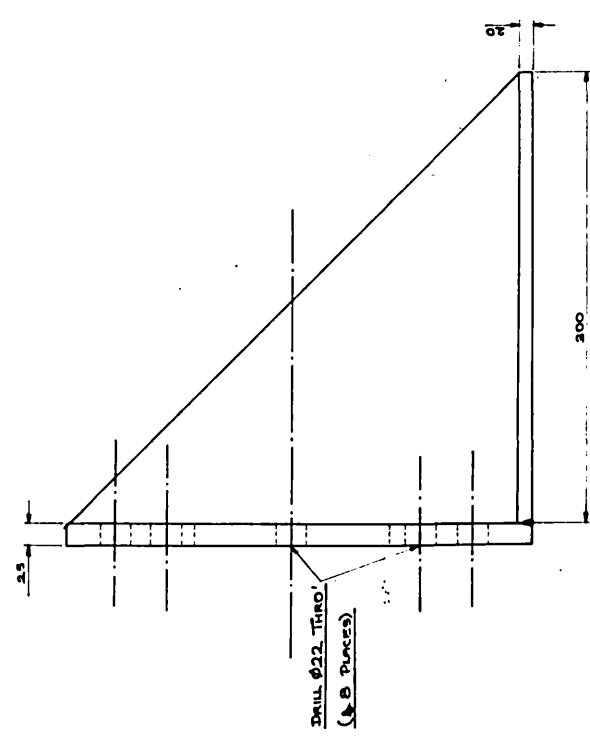
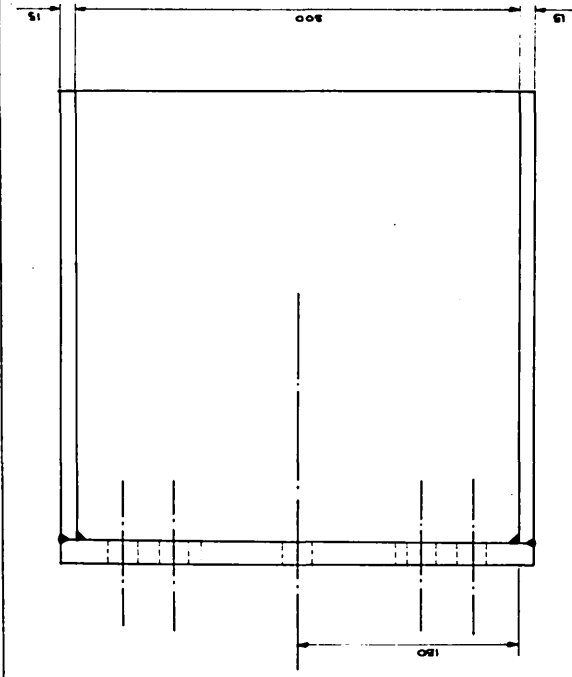
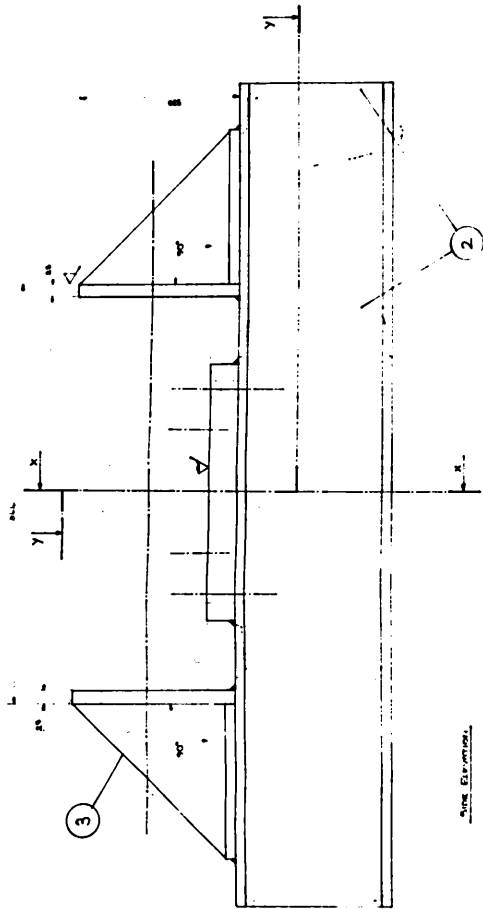
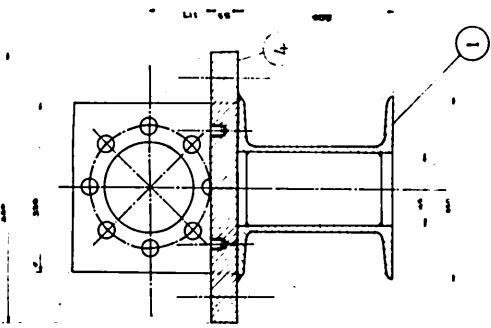


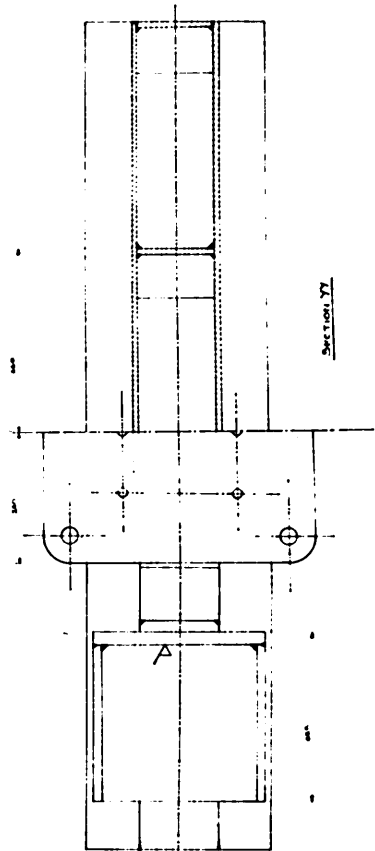
Fig. 20. The Welded Base Assembly.



Side Elevation



Section XX



Section YY

NO.	DESCRIPTION	QTY	UNIT	REMARKS
1	STEEL PLATE	1	SQ. FT.	3
2	STEEL CHANNEL	2	LINEAL FT.	2
3	STEEL RIVETS	4	NO.	—
4	STEEL BOLTS	2	NO.	—

PROPOSED BRIDGE REMOVAL, R.I.
 ALBANY BRIDGE, SOUTHWEST CORNER

DRAWING NO. 2
 SHEET NO. 2
 DATE 1/1/24

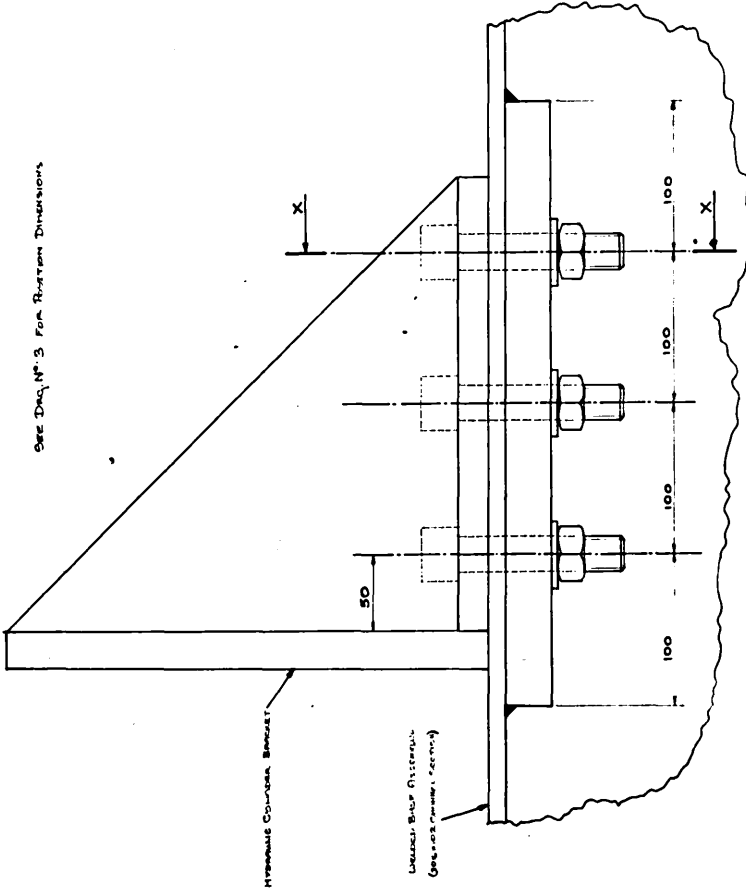


Fig. 21. The Hydraulic Cylinder Bracket Bolting Arrangement

HYDRAULIC CYLINDER BRACKET BOLTING ASSEMBLY

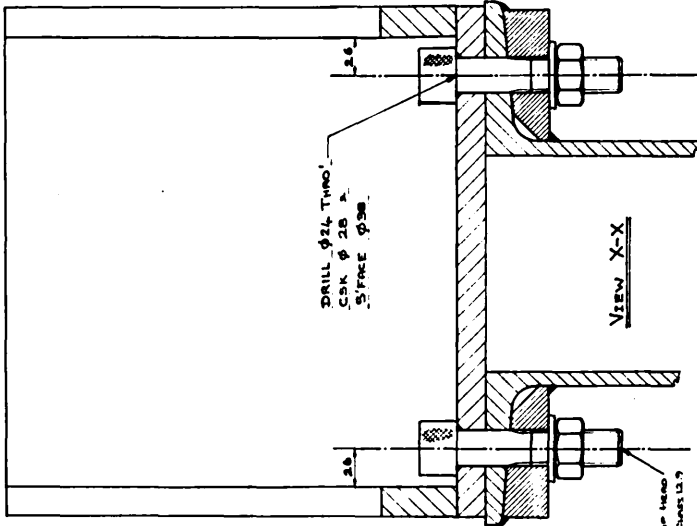
Scale 1:2 10th Edition T. B. B. & S.
 pt. 4. Mechanical Des. No. 28

See Des. No. 3 For Bracket Dimensions



Hydraulic Cylinder Bracket

Washer Bolt Nutwash
 (See Des. No. 12 for Detail)



DRILL Ø 21. THRU
 CSK Ø 28 P.
 5 PACE Ø 38

VIEW X-X

100-110 (100) One Head
 100-110 (100) One Head
 12. OFF

REINFORCING BLOCK
END VIEW

Mat. - M.S. 90-87-400
 4 OFF
 Scale - Full Size

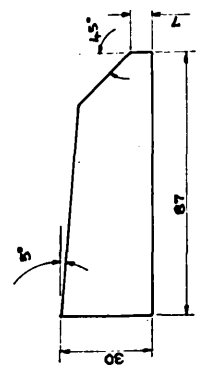
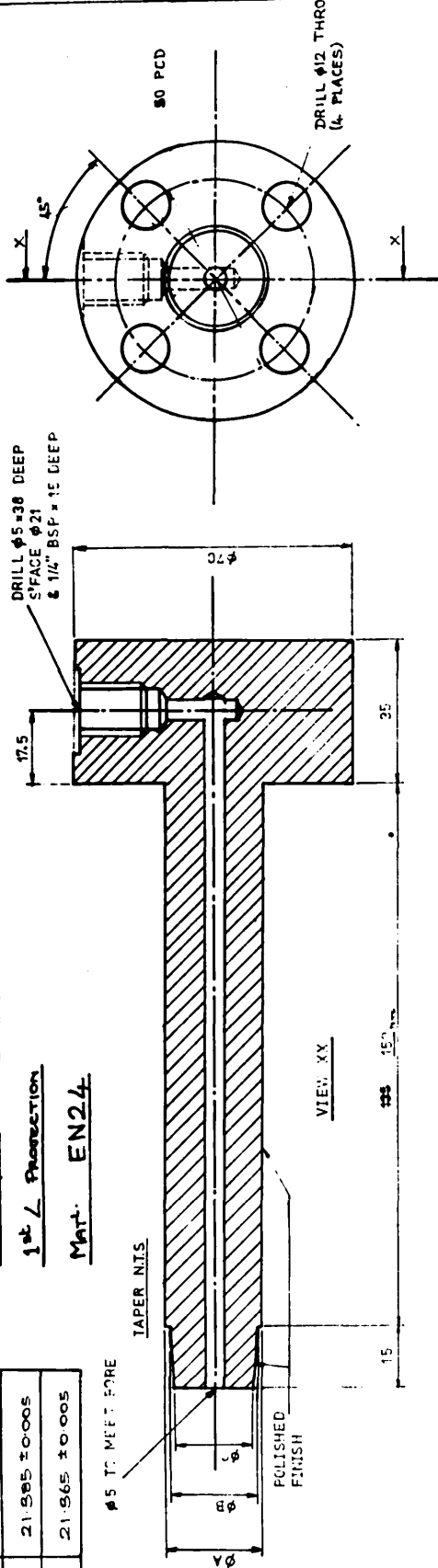


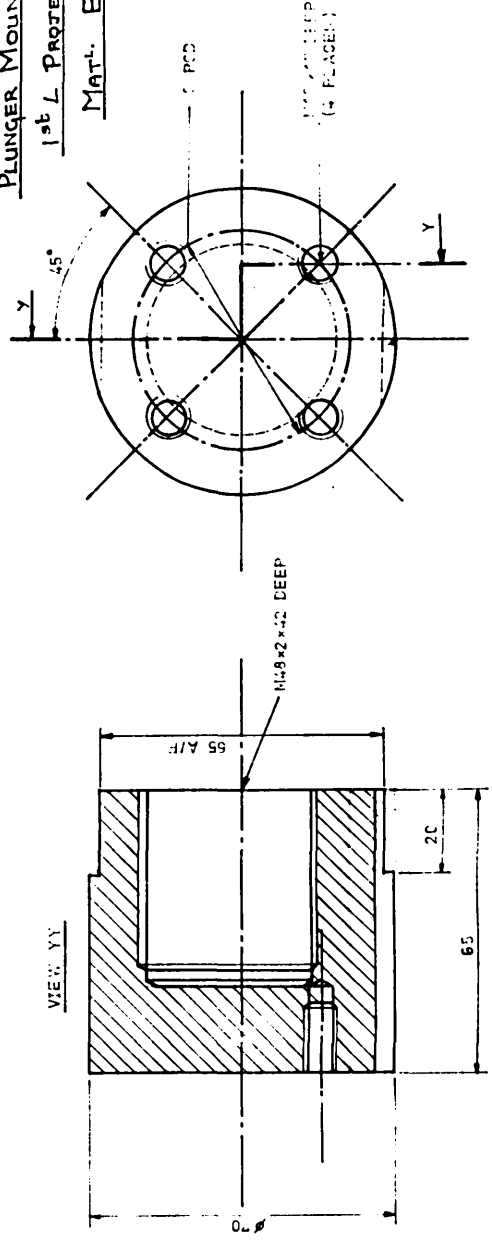
Fig. 22. The Plungers and Plunger Mounts

φA	24.120 ± 0.001
φB	21.985 ± 0.005
φC	21.965 ± 0.005

PLUNGER 2 OFF
1st L PROTECTION
MAT. EN24

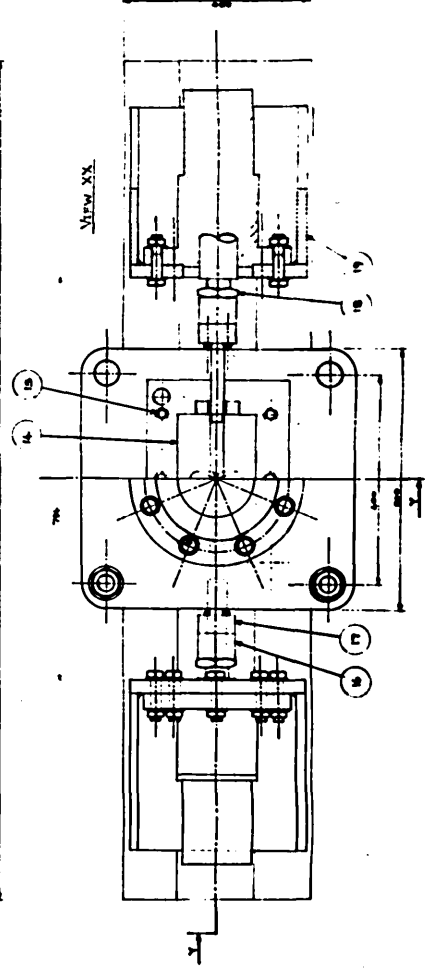
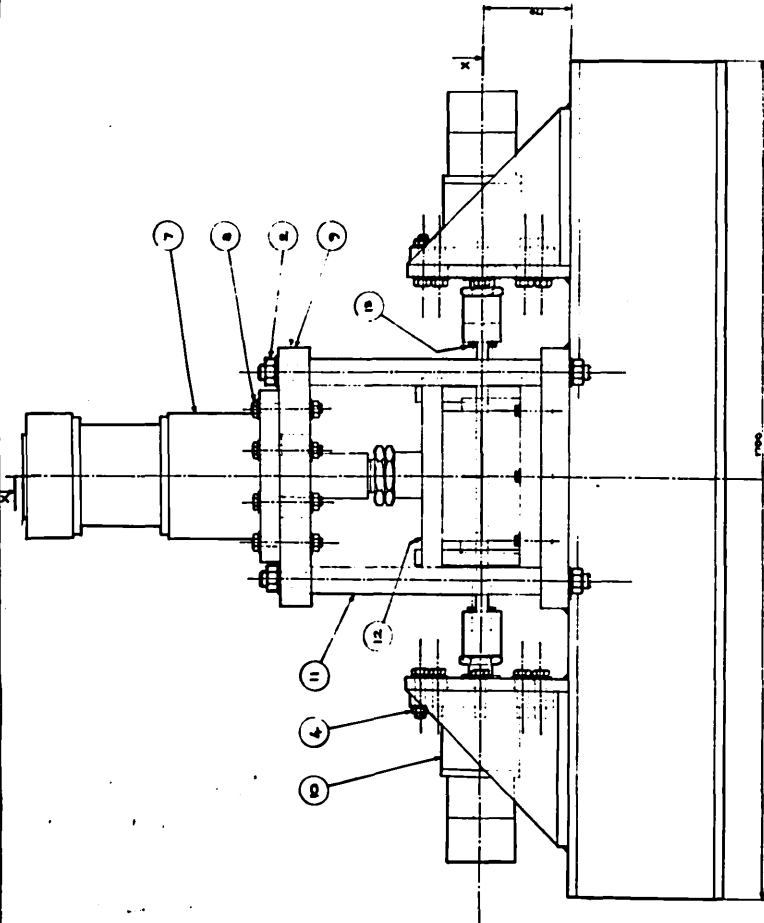
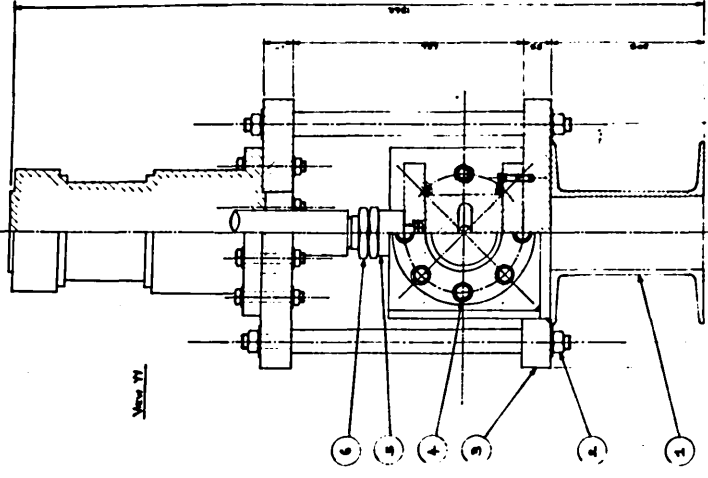


PLUNGER MOUNT 2 OFF
1st L PROTECTION
MAT. EN 8



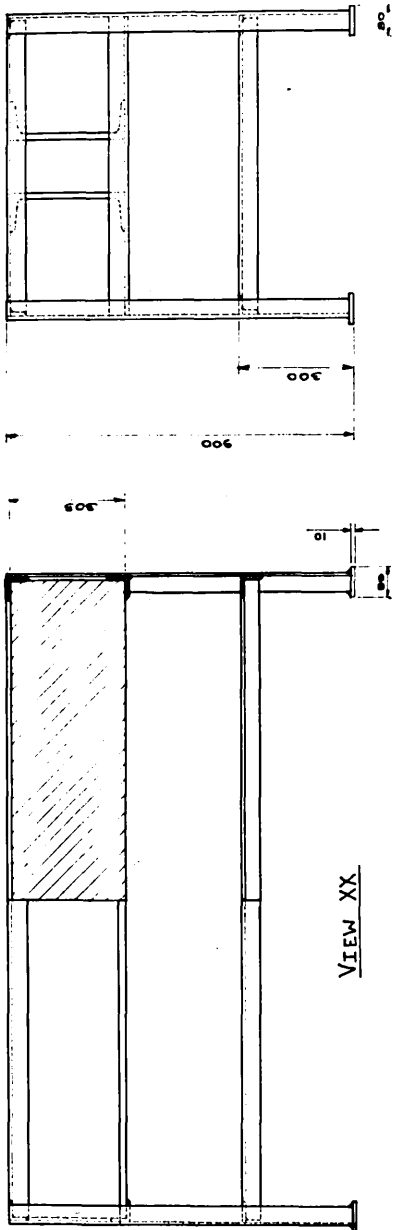
DRG No 4
25th JAN 64
T. Barber

Fig. 23. Assembly Drawing.



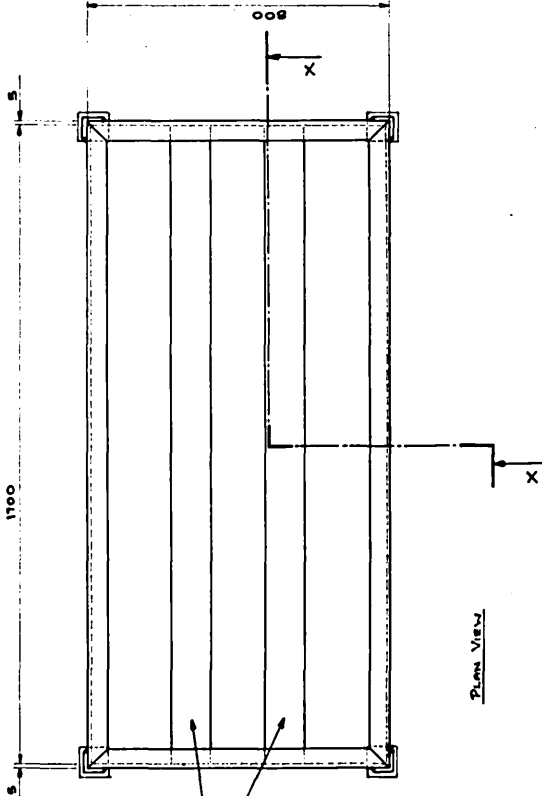
1. Title 2. Date 3. Author 4. Check No. 5. Drawing No. 6. Scale 7. Material 8. Quantity 9. Remarks		10. Part No. 11. Part Name 12. Part Description 13. Part Material 14. Part Quantity 15. Part Remarks	16. Part No. 17. Part Name 18. Part Description 19. Part Material 20. Part Quantity 21. Part Remarks	22. Part No. 23. Part Name 24. Part Description 25. Part Material 26. Part Quantity 27. Part Remarks	28. Part No. 29. Part Name 30. Part Description 31. Part Material 32. Part Quantity 33. Part Remarks	34. Part No. 35. Part Name 36. Part Description 37. Part Material 38. Part Quantity 39. Part Remarks	40. Part No. 41. Part Name 42. Part Description 43. Part Material 44. Part Quantity 45. Part Remarks	46. Part No. 47. Part Name 48. Part Description 49. Part Material 50. Part Quantity 51. Part Remarks	52. Part No. 53. Part Name 54. Part Description 55. Part Material 56. Part Quantity 57. Part Remarks	58. Part No. 59. Part Name 60. Part Description 61. Part Material 62. Part Quantity 63. Part Remarks	64. Part No. 65. Part Name 66. Part Description 67. Part Material 68. Part Quantity 69. Part Remarks	70. Part No. 71. Part Name 72. Part Description 73. Part Material 74. Part Quantity 75. Part Remarks
--	--	---	---	---	---	---	---	---	---	---	---	---

Fig. 24. Stand Assembly.



END VIEW

Mat. - 50x50x5mm Thick Angle Section
+ 10mm Thick M.S. Plate



PLAN VIEW

Welded Base
Sub-Assembly
See Dwg No 8

Hydraulic Bulge Forming Rig			
STAND ASSEMBLY			
10 th Feb '84	Scale 1:8	T.T. Sankar	
DRG. No.	6		

Fig. 25. The Die Block Assembly.

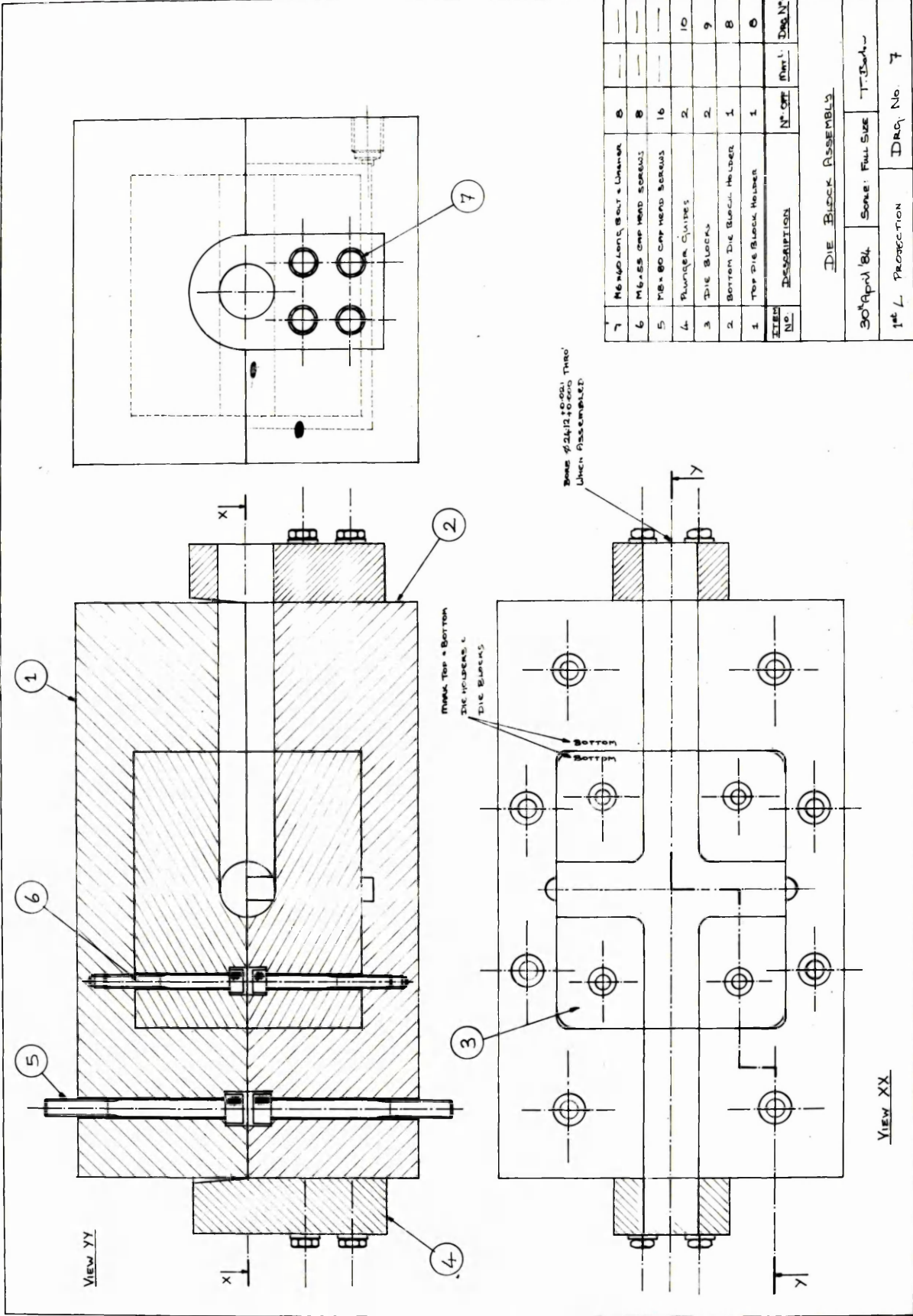
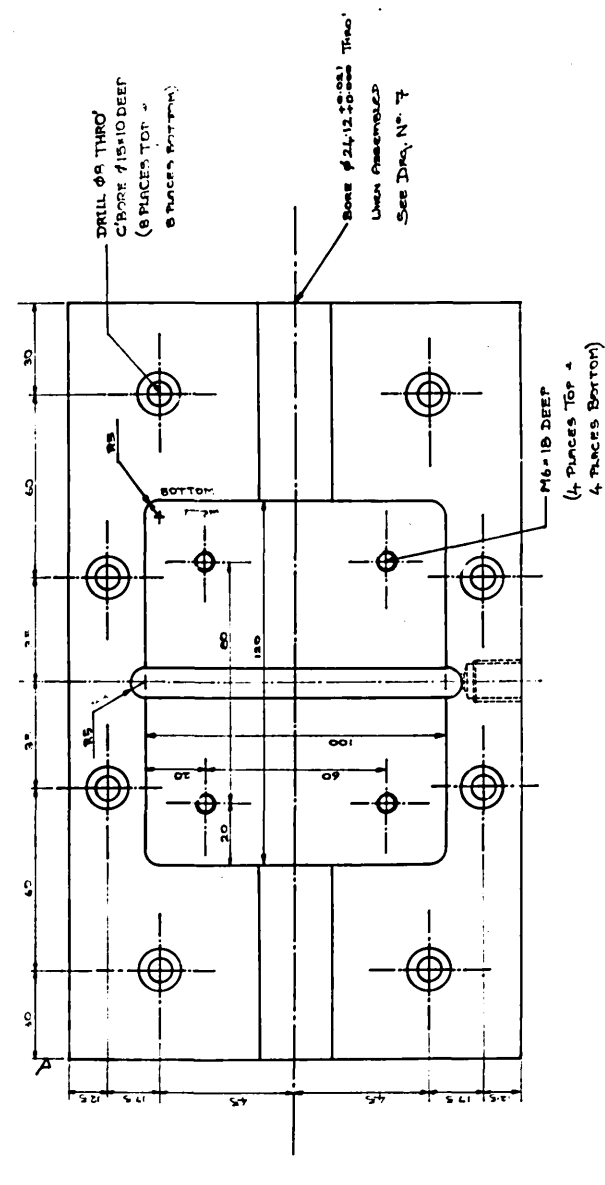
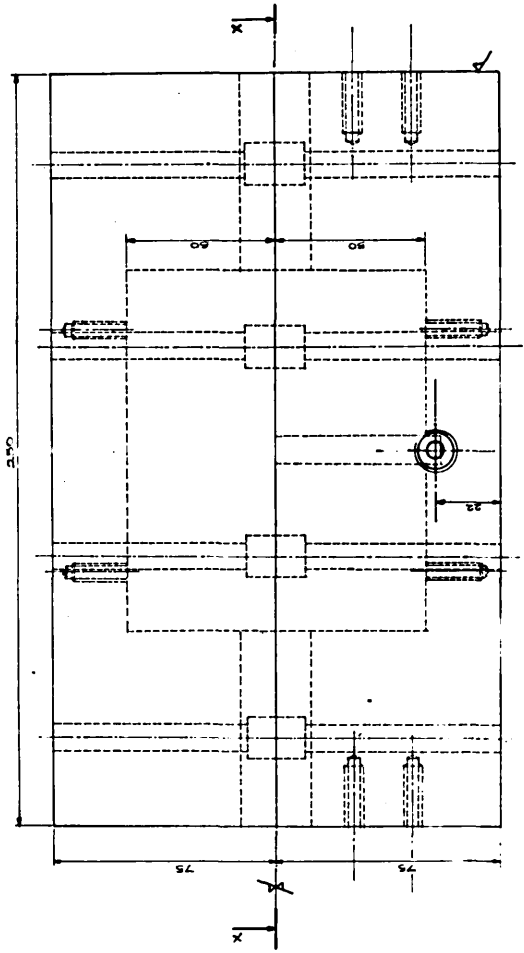
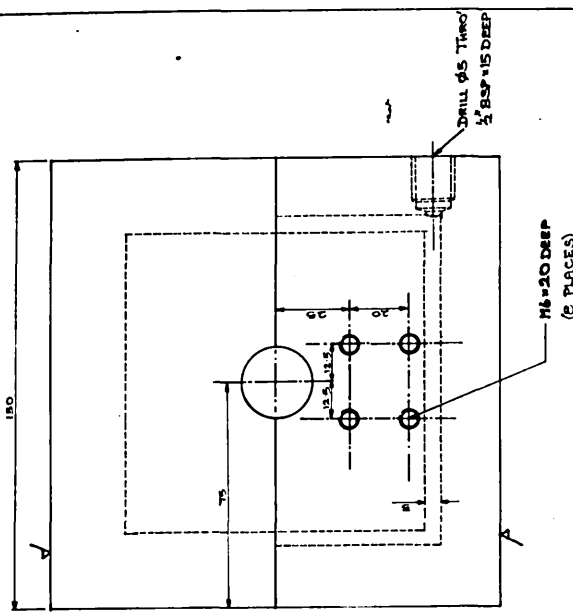


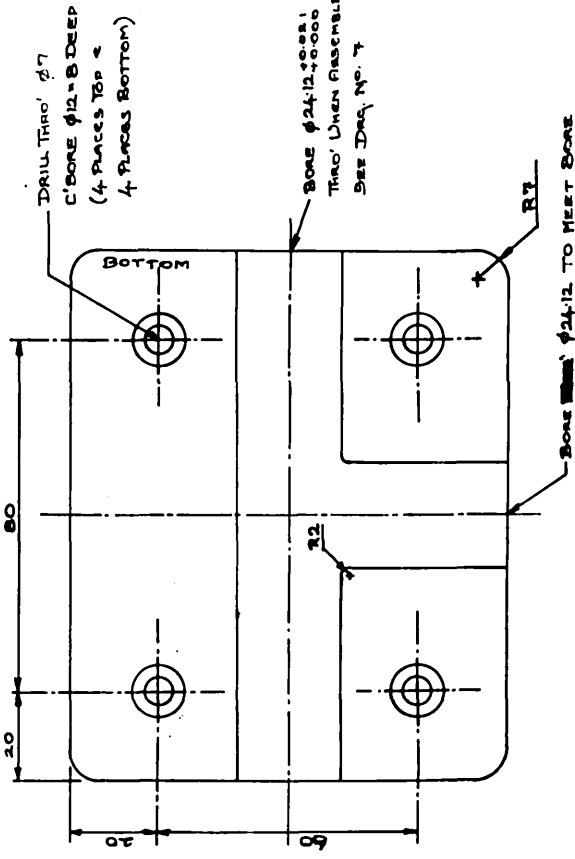
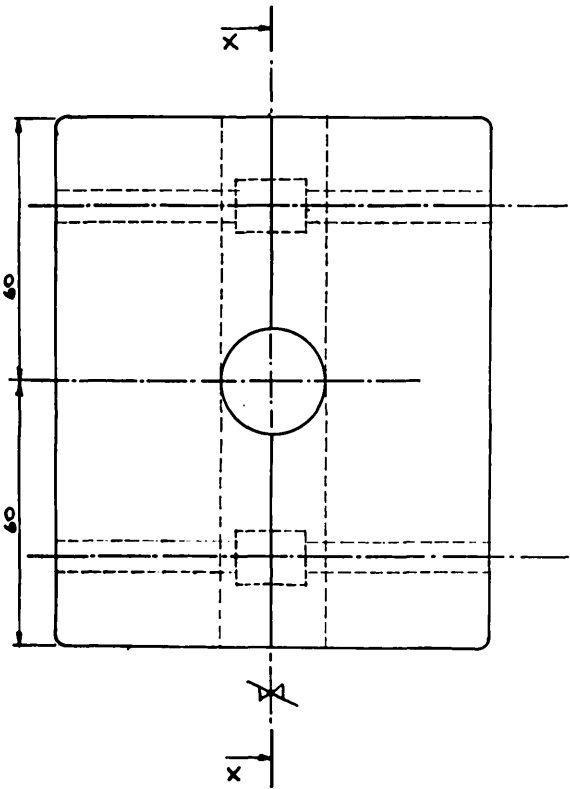
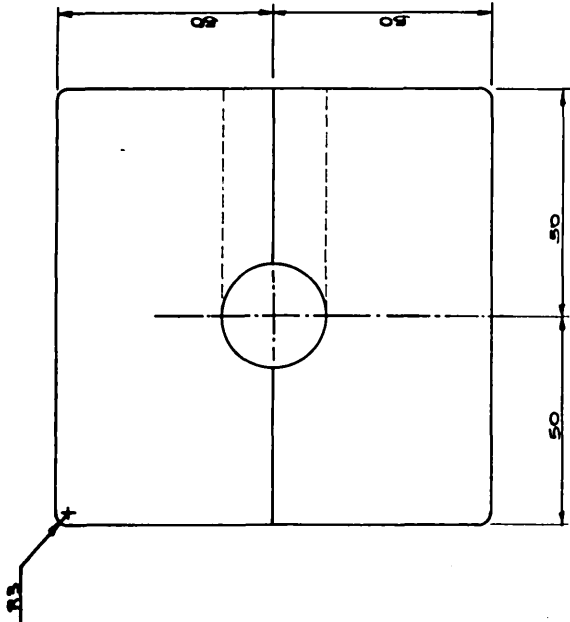
Fig. 26. The Top and Bottom Die Holders.



Top - Bottom Die Block Hobbers	
30° Angl 1/4	Seals - Full Size T.R. Barrels
Matl. - M.S.	1 OFF
1st Projection	Draw No. 8

7

Fig. 27. The Die Blocks.



VIEW XX

<u>DIE BLOCKS</u>		
3 rd May '84	SCALE: FULL SIZE	T. Barber
Mat'l.:		1 OFF
1 st L PRODUCTION		DRS. NO. 9A

PLUNGER GUIDES

30th April 84 J. Barlow

2 OFF SCALE FULL SIZE

1st L PROJECTION

DRG. No. 10

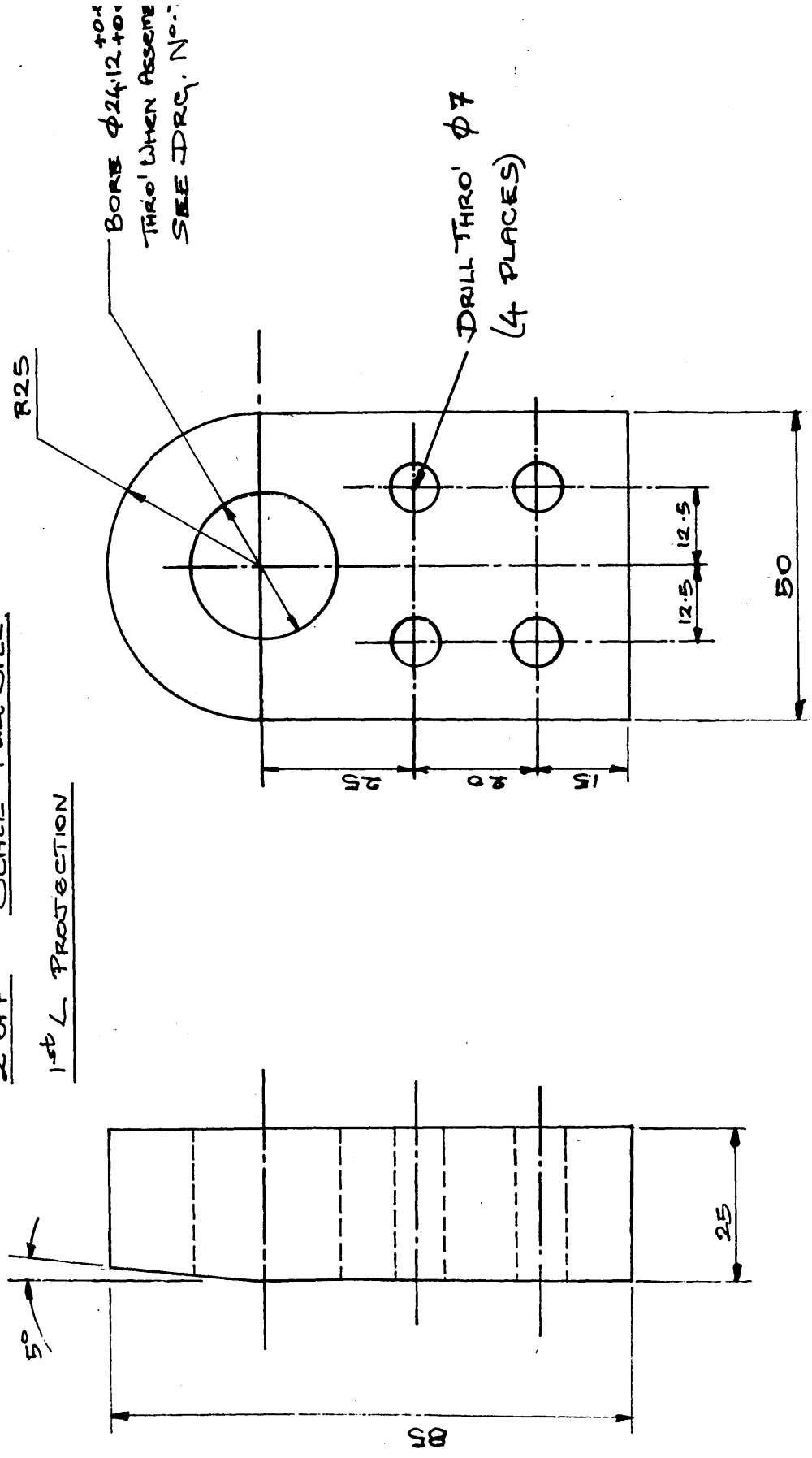


Fig. 28. The Plunger Guides

Clamping
Cylinder



Cylinder
Applying
Axial
Compressive
Force



Die Block

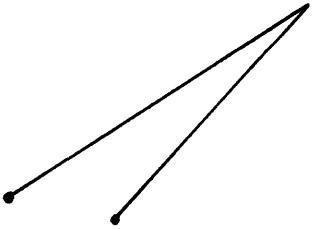
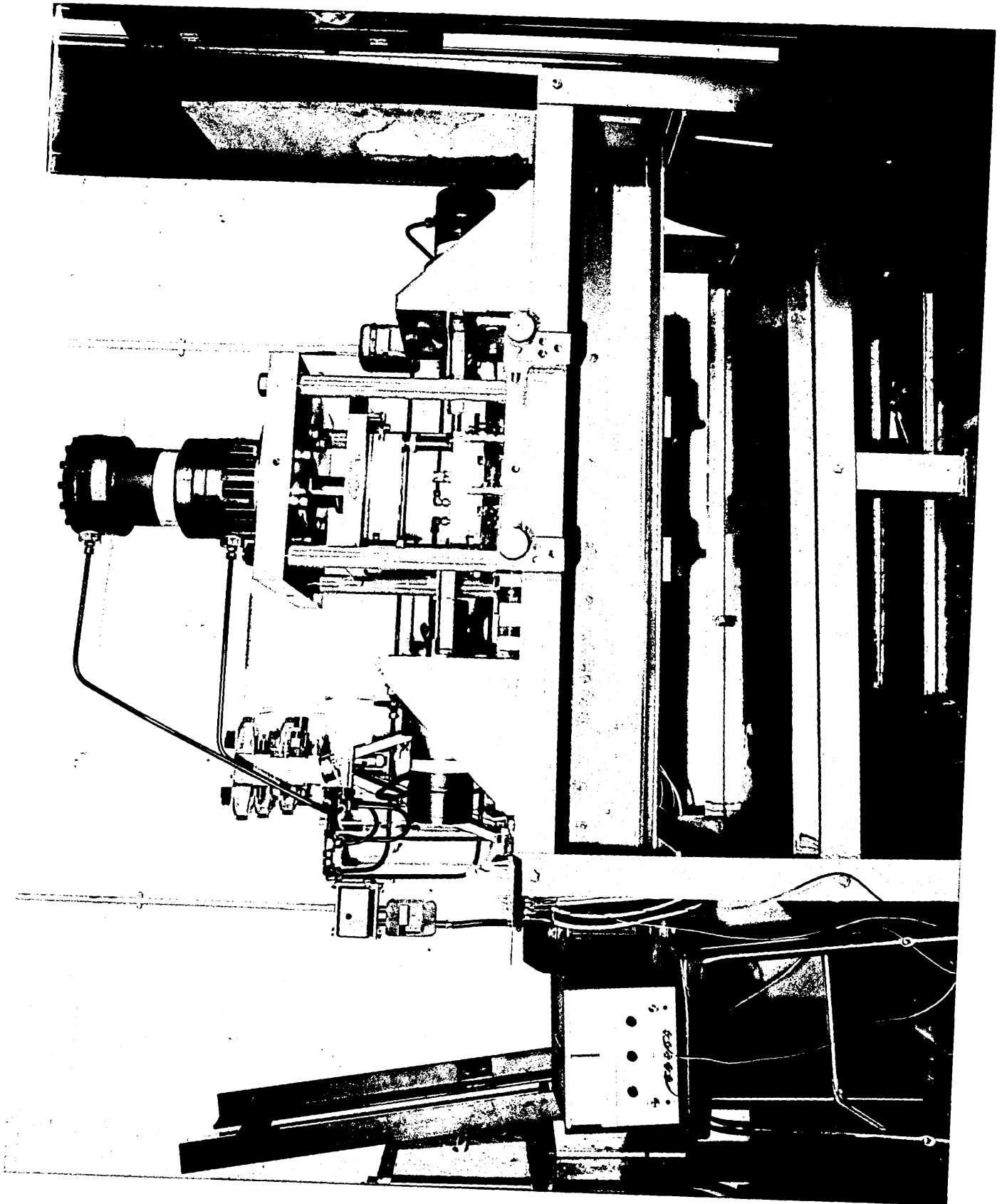


Fig. 29. The Front View of the Bulge Forming Machine.



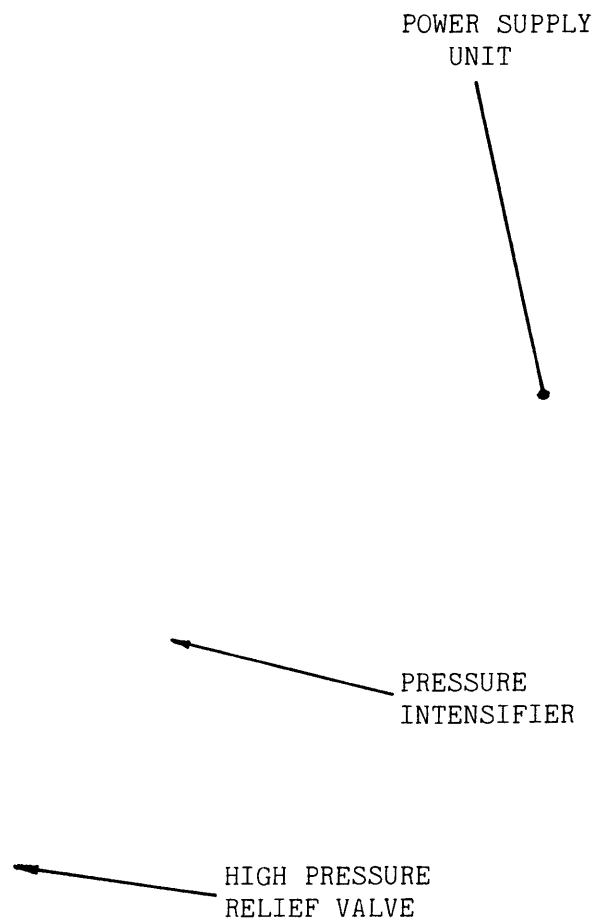
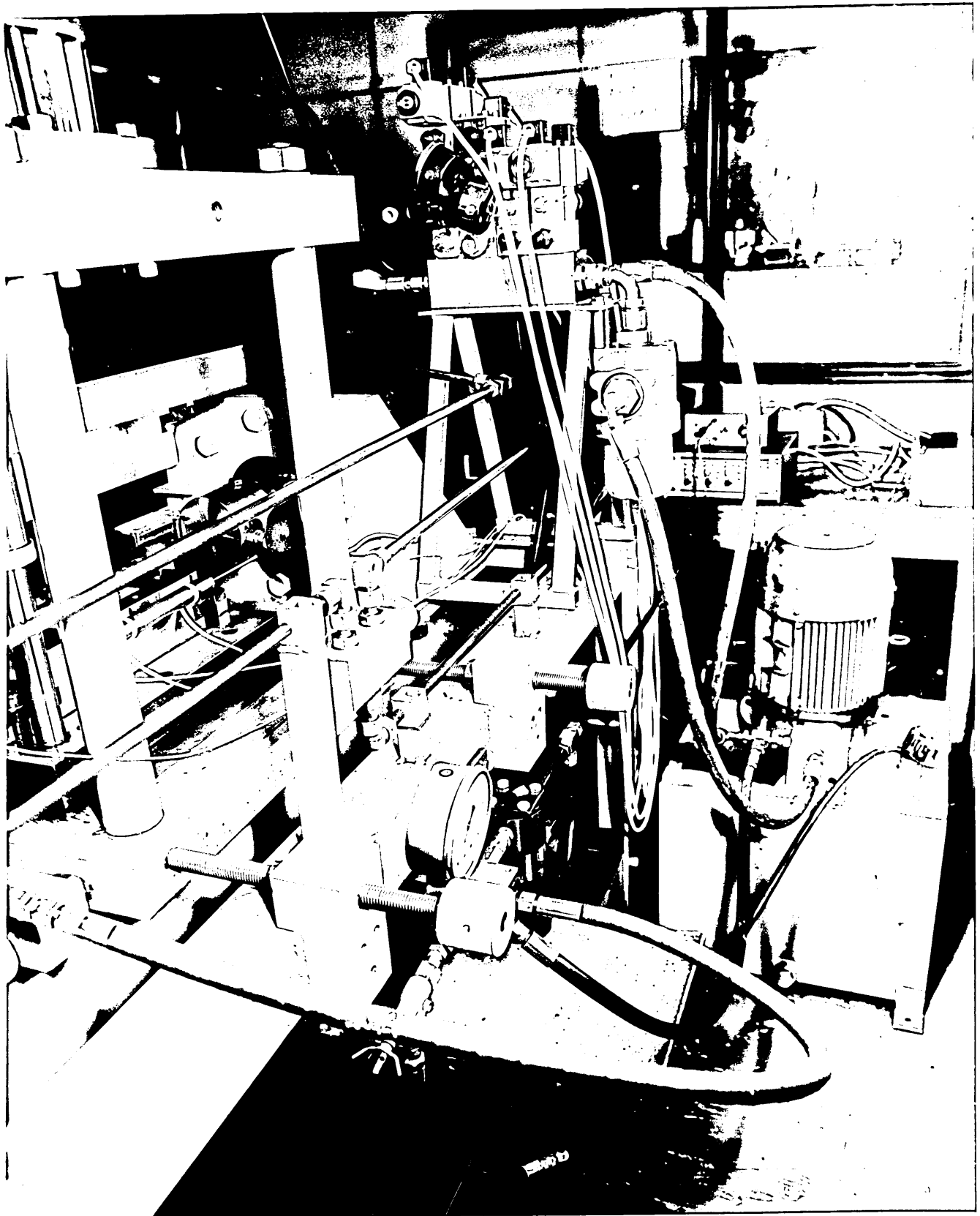
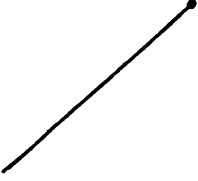


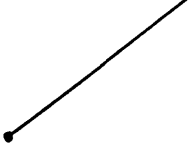
Fig. 30. The Back View of the Bulge Forming Machine.



HYDRAULIC
VALVES



CLAMPING
CYLINDER



CYLINDER APPLYING
AXIAL COMPRESSIVE
FORCE



Fig. 31. Side View of the Bulge Forming Machine.

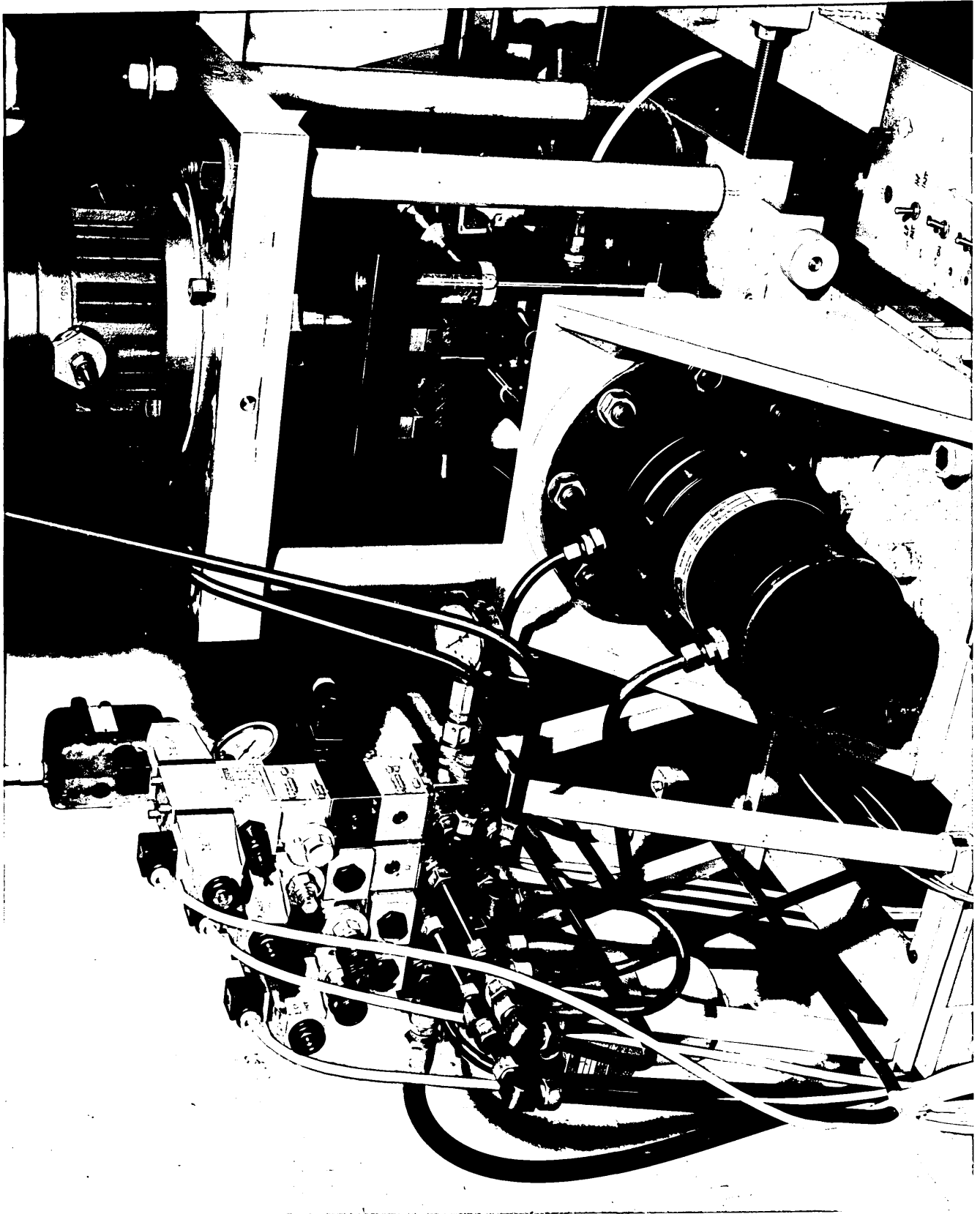
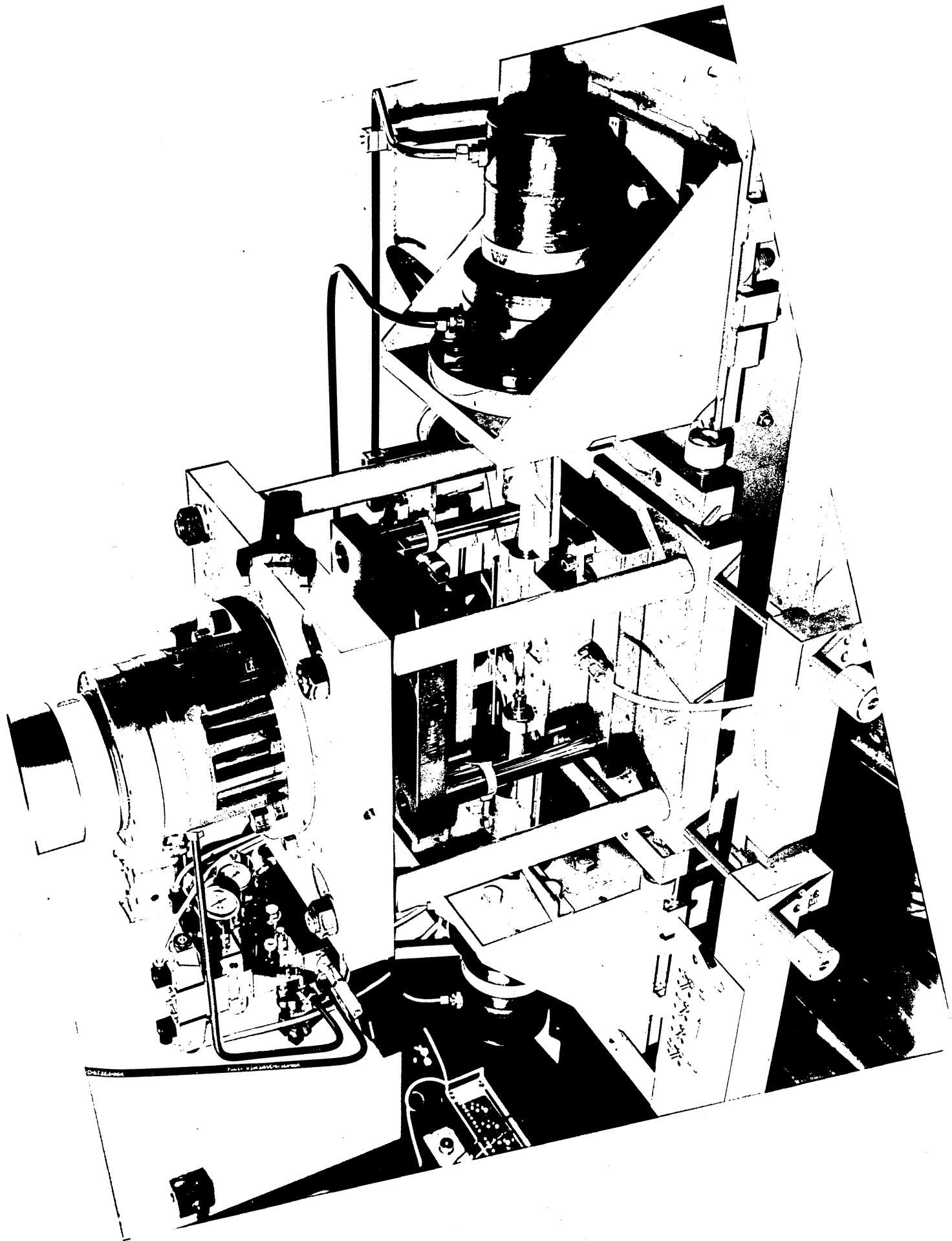


Fig. 32. The Top View of the Bulge Forming Machine.



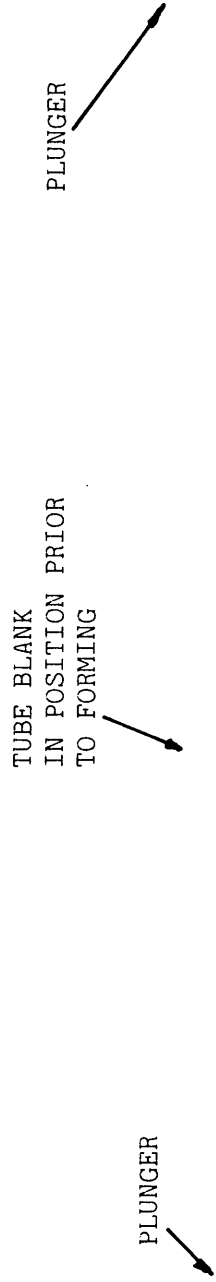
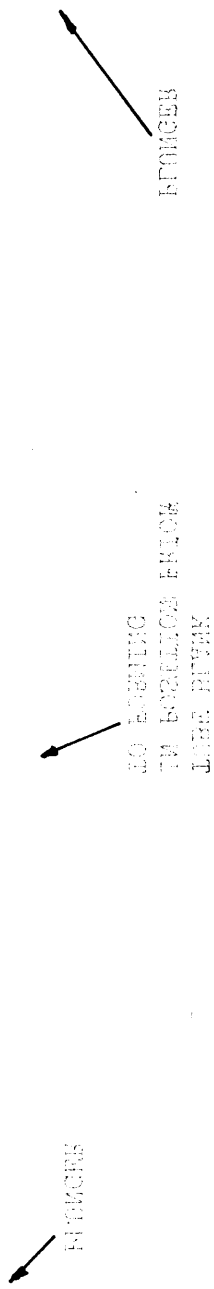
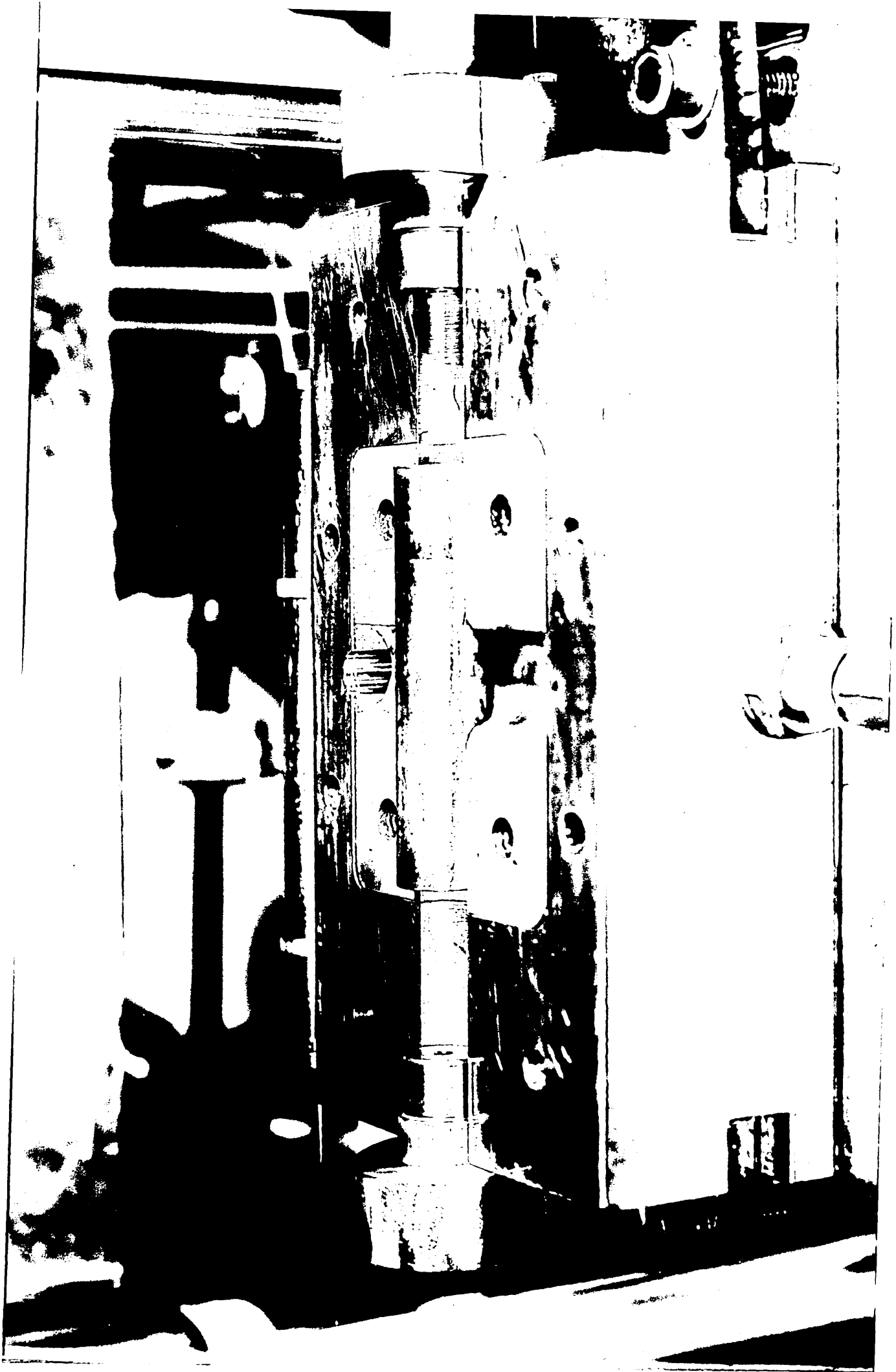


Fig. 33. The Die Blocks.

Fig. 33. The Die Blocks.





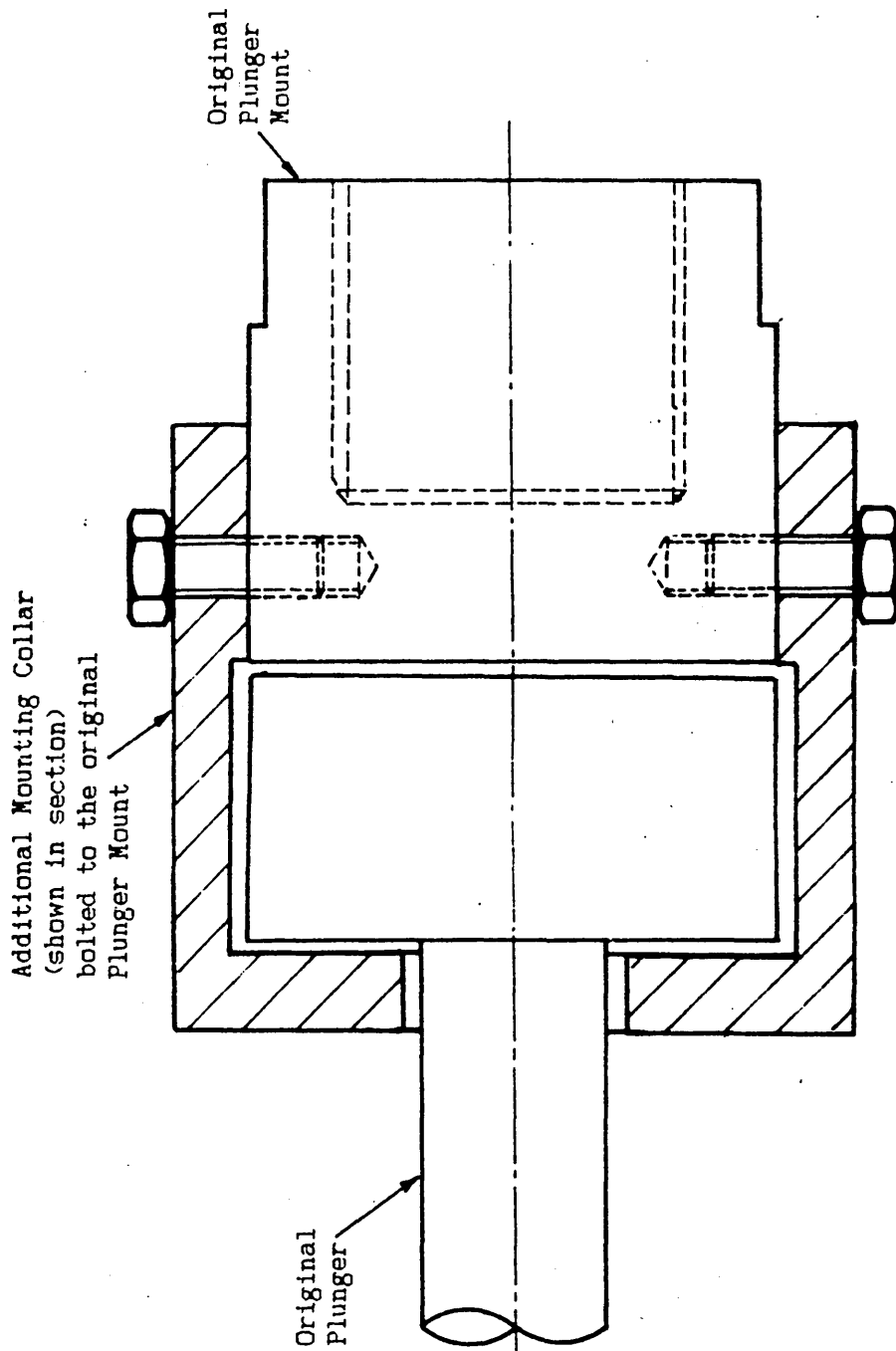


Fig. 34.
The Modification to the Plunger Mount to allow a Floating Connection.

4. TEST PROCEDURE

4.1. TEST MATERIAL

The initial stages of the design of the bulge forming rig involved estimating the size of the tube blank to be used in the forming operation. This was so that the forces involved could be calculated, and an approximate size for the die block could be allowed for in the rest of the design. For design considerations a nominal value of 25mm diameter and 150 mm length was chosen. The actual tube blanks used for the tests was decided on at a later time before the final dimensioning of the dies and plungers. These tubes were of copper and had an outer diameter of 24.12mm with a wall thickness of 1.37mm. These were supplied in an annealed state in lengths of 107mm. To provide a comparison another wall thickness tube was also used. This had the same outer diameter of 24.12mm but the wall thickness was thinner being 1.03mm. These tubes were supplied in a work hardened state in lengths of 127mm and before forming were annealed at 500°C.

4.2. OPERATING PROCEDURE

Forming components using the bulge forming machine required clamping the die block closed with a tube blank contained inside, and subjecting it to internal pressure and an axial compressive force.

The design of the machine is such that these forces can be varied to form components to various stages of expansion and various procedures can be used relating to the internal pressure used. The high pressure part of the hydraulic circuit is equipped with a pressure reducing valve and also a pressure relief valve to control the internal pressure. In the forming of tee and cross pieces, as previously mentioned, there is a

decrease in the volume inside the tube, due to the axial deformation, which generates a high pressure. Thus, the pressure reducing valve can be used to set the initial internal pressure which can be allowed to increase to a maximum value determined by the pressure relief valve. Alternatively, the relief valve can be used to set the initial pressure, resulting in a constant pressure throughout the forming process.

During the process, the application of the axial compressive load, if great enough, results in the axial deformation of the tube, i.e the tube gets shorter. As would be expected the greater the axial force the more deformation occurs. Therefore to take the control of the internal pressure a stage further during the process, the axial deformation can be carried out in stages. During each stage the internal pressure is set to a constant value, and at the end of each stage, when deformation has stopped, both the internal pressure and the axial compressive force are increased.

The test procedures for these different processes are the same at the start of the procedure which is as follows (the hydraulic components and switches refer to Figs. 12. & 13. respectively):

1. Connect the control board controlling the solenoid valves to a 24V DC supply and turn on the isolator to the electric motor and start it.
2. Open the die by moving switch S1 to the OPEN position (during periods of rest, when the motor is still running, the switch should be returned to the central - STANDBY - position to prevent excess heat from being generated in the main relief valve).

3. Place centrally on the bottom die a tube blank, the length, diameter, and wall thickness of which have already been noted.
4. Close the die block by moving switch S1 to the CLOSE position.
5. Move switch S2 to extend the horizontal hydraulic cylinders, and so bring the plungers into contact with the tube blank. The forces acting on the tube are controlled by the pressure reducing valve PR1 which should be set to provide sufficient force to seal the ends of the tube without causing any axial deformation.
6. Having sealed the ends of the tube, it can then be filled with oil by moving switch S4 to the LOW pressure position, causing the pressure intensifier to be by-passed to fill the tube quickly at low pressure. At the same time the valve V5 should be opened to allow the air to escape from the tube. Once clear oil starts to flow out, this valve can then be shut off to allow internal pressure to be generated.

The rest of the procedure depends on the mode of operation required. This will be dealt with separately for the three different variations.

4.2.1. Fixed Internal Pressure During Bulging

For this mode of operation the internal pressure is kept constant throughout the forming process, controlled by the high pressure relief valve RV2. After operations 1-6 have been completed the procedure is as follows:

7. Move switch S4 from the LOW pressure position to the HIGH pressure, which causes the pressure intensifier to be activated, generating a high pressure inside the tube blank.

This pressure is controlled by the adjustment of the relief valve RV2, with the pressure reducing valve PR3 adjusted to provide a pressure just greater than that required.

8. Once the tube is subjected to an internal pressure, the axial compressive force should be applied. This is achieved by moving switch S3. The forces acting on the ends of the tube are controlled by the pressure reducing valve PR2 which should be set sufficiently high as to cause axial deformation.
9. On completion of the forming process, when the forming plungers stop moving, or the tube bursts, switches S2, S3 & S4 are moved to the OFF position. This causes the plungers to be retracted, and stops the supply to the internal pressure. This pressure is released as soon as the plungers move apart. To open the dies to gain access to the formed component, switch S1 is moved to the OPEN position.

Having removed the formed component the machine is then ready for another blank to be placed in the dies for the next forming operation. As an alternative to the process just described, step 8 can be omitted, causing the tube to be formed due to internal pressure alone. In this case the axial force is just used to seal the tube and not to deform it, although this only produces small bulges.

4.2.2. Increasing Internal Pressure During Bulging

For this process the initial pressure is set by the pressure reducing valve PR3, and increases during the process to a value determined by the relief valve RV2. Ideally the relief valve RV2 should be set before hand, either at the end of a previous test or by subjecting

a blank to the required pressure. Again this procedure follows on after operations 1-6 have been completed.

7. Move switch S4 from the LOW to the HIGH pressure position. The pressure inside the tube blank is controlled by the pressure reducing valve PR3 which should be varied to produce the required initial internal pressure.
8. Once the tube is subjected to the internal pressure, the axial compressive force should be applied by moving switch S3 to the ON position. The force acting on the ends of the tube is controlled by the pressure reducing valve PR2. During forming the internal pressure will increase, due to the decrease in internal volume, until it reaches the value set by the relief valve RV2. A constant pressure will be maintained once this pressure is reached, until the completion of the forming process, after which it will drop due to leakages.
9. After completion of the forming process switches S2, S3 & S4 should be moved to the OFF position, and the dies opened by moving switch S1 to the OPEN position.

4.2.3. Increasing Internal Pressure in Stages

This process is similar to forming a component with a fixed internal pressure, but at the end of the deformation the internal pressure and axial force are increased to produce another deformation. The first axial force applied to the end of the tubes should thus be fairly small, to allow it to be later increased to produce a further deformation. Again Steps 1-6 should be followed.

7. Move switch S4 from the LOW pressure position to the HIGH pressure, which causes the pressure intensifier to be activated, generating a high pressure inside the tube blank. This pressure is controlled by the adjustment of the relief valve RV2, with the pressure reducing valve PR3 adjusted to provide a pressure just greater than that required.
8. Once the tube is subjected to an internal pressure, the axial compressive force should be applied. This is achieved by moving switch S3. The forces acting on the ends of the tube are controlled by the pressure reducing valve PR2 which should be set to a suitable value for the initial deformation.
9. When the deformation has stopped, i.e. the plungers have stopped moving, the internal pressure can be increased by adjustment of the relief valve RV2 (the pressure reducing valve PR3 may also require adjustment so that a large enough pressure is being produced from the pressure intensifier).
10. After increasing the internal pressure, the axial deformation can be continued by adjusting the pressure reducing valve PR2, so as to increase the axial force acting on the ends of the tube.
11. When this next deformation has stopped, steps 9 and 10 can be repeated - increasing the internal pressure and axial force again - or the component can be removed from the machine, by moving switches S2, S3 & S4 to the OFF position, and moving switch S1 to the OPEN position to open the dies.

4.3. ANALYSIS OF THE FORMED COMPONENT

Once formed and removed from the machine, the final length of the component and the length of the side branch(es) were measured. Further analysis involved cutting the component into two halves so that the wall thickness could be measured around the bulge profile. A band saw was used, and the components cut lengthwise down the centre of the bulge(s). Figs. 35. and 36. show sectioned tee and cross pieces produced by the machine at varying degrees of deformation. Once sawn in half, one half was then cleaned up and measured as shown in Fig. 37.a. Considering the tube in a horizontal position, readings were taken in steps vertically upwards from the root of the bulge to the top. This was done on both sides and a final wall thickness was measured at the tip of the bulge.

However, in components that were formed using internal pressure only - i.e. no axial deformation - the bulge formed was not large enough to be divided up in this way for measurement. Therefore for small bulges an alternative method for measuring the wall thickness was used. This is shown in Fig 37.b. Instead of dividing up the bulge vertically, it is divided horizontally. After first estimating the centre line, measurements were made in steps either side of the centre line.

4.4. RESULTS

4.4.1. Tee pieces

Tests were carried out on the bulge forming machine to form tee pieces from copper tube in the two wall thicknesses - 1.37mm and 1.03mm. These were conducted using constant axial deformation forces, achieved by setting the pressure reducing valve (V3) supplying the two horizontal cylinders to a set value. For each constant deformation force, various internal pressures were applied, and the effect of this internal pressure on the formed component was noted. In some cases buckling of the tube occurred, or the tube fractured. From these tests it was possible to derive the forming limits for the tube blanks used.

The forming limits are shown in graphical form in Fig 38. For the thicker tube, Fig 38.a applies. This shows the relationship between the axial deformation force and the Internal Pressure, and is split up into four areas. Failure of the forming process will occur if the forming conditions fall into areas C or D. Area C indicates that the the axial deformation force is too high, or the internal pressure is too low, resulting in buckling of the tube occurring. Fracture of the tube wall will occur in area D. This was found to occur in the dome formed by the internal pressure, and the fracture would lie in an axial orientation. Fracture will also occur if the initial conditions fall into area B. In order to form a perfect component, the conditions have to fall into area A. However, after the deformation has been partly completed, the forming conditions may move into area B. This is most probably due to the work hardening of the copper allowing it to restrain a larger pressure. Testing tubes with only a small axial force, sufficient to seal the ends, resulted in the tube fracturing with an internal pressure of

about 7500psi (52N/mm²) and above. However, after severe deformation due to a large deformation force, tube of the same original size was able to resist the maximum internal pressure available (10,000psi-69N/mm²). Fig. 39. shows components that have failed during forming, due to fracture and due to buckling.

The axial deformation forces have been calculated from the pressures applied to the hydraulic cylinders e.g for a pressure of 1000psi (6.9N/mm²), the force exerted by each cylinder is:

$$\begin{aligned} \text{Area of Cylinder (from Manu. Spec.)} &= 123 \times 10^2 \text{ mm}^2 \\ \text{Pressure} &= 1000 \text{ psi} \\ &= 6.9 \text{ N/mm}^2 \\ \text{Force Applied by Cylinder} &= 123 \times 10^2 \times 6.9 \text{ n} \\ &= 85 \text{ kN} \end{aligned}$$

The actual forces that are applied to the ends of the tube may be a little less than this due to losses between the pressure reducing valve (where a pressure reading is obtained) and the output from the cylinder. These are likely to occur because of flow losses occurring in the pipework and friction in the cylinders and plungers.

It also should be noted that the axial deformation of the tube is proportional to the axial compressive force, and, therefore, this graph also represents axial deformation against internal pressure. Hence this graph could be used to indicate how the internal pressure can be increased during the process.

Fig. 38.b similarly shows the forming limits for the thinner walled tube. This has the same areas, but these have moved in towards the origin of the axis. The area in which perfect forming occurred is considerably smaller than previously and this was reflected in the

difficulty experienced in trying to form good components. The thicker tube was found to be easier to form than the thinner walled tube, the values of axial force and internal pressure not being so critical.

4.4.1.1. Tee Pieces Formed From The Thicker Tube

The lengths of the side branches obtained when forming tee pieces are shown in Fig. 40. This is for various axial deformation loads - 26, 85, and 130kN, and shows the bulge height ratio ($(H_s+L)/R_o \times 100\%$) against the internal pressure. With only a small axial force the maximum bulge height ratio is only 38% at the maximum internal pressure possible before rupture occurs (7000psi - 48N/mm²). However with increasing axial forces, much greater expansions can be obtained with smaller internal pressures. Using an axial force of 130 kN, a height ratio of 170% was obtained with the same internal pressure. This indicates the importance of applying an axial compressive force when attempting to produce a component with a significant branch length. To increase the length of the branch formed, larger axial compressive forces have a more significant effect than an increase in internal pressure.

The branch formed can be split into two parts - H_s and L (see Fig. 37.a) where H_s is the height of the domed portion and L is the length of the tubular portion. The effect of increasing the axial compressive force seems to be an increase in the length of L . Increasing the internal pressure increases H_s with little effect on the value of L . This increase is achieved by the domed portion being bulged further out, and is indicated in Fig. 41. This shows a graph of the radius of the crown portion plotted against the internal pressure that formed it, for the three different axial forces. For small axial forces (85kN) there is a

large change in the radius with increasing pressure. With larger axial forces (130kN) the effect is not as great, but still significant with the radius decreasing with increasing internal pressure until it reaches a value of about 15mm when little change occurs (the minimum value it could reach is 12mm - the radius of the side branch). With very low pressures the graph indicates that the radii goes towards infinity ie. the branch is formed flat topped. This did occur on some of the components formed with a low internal pressure. At even lower pressures buckling of the tube would occur, and in some cases the dome of the branch would be formed concave in the axial direction.

The effect the internal pressure has on the wall thickness across the domed portion is illustrated in Figs. 42, 43 & 44, in graphs of percentage of original wall thickness ($t/t_0 \times 100\%$) against x (see Fig. 37). Fig. 42 shows the variation in the wall thickness for components formed with an axial force of 26kN (used as a sealing force and not to cause axial deformation). The centre of the bulge is represented by $x=0$ and as x moves towards 14mm and -14mm, this represents the edge of the domed portion and the root - where the side branch joins the main branch - measured in the axial direction. The original wall thickness is shown by the dashed horizontal line. The graph is plotted for various values of internal pressure, and it can be seen that increasing this pressure causes a decrease in the wall thickness across the dome. The thickness at the edges and at the root remains almost unchanged when forming at these conditions.

Fig. 43 is a similar graph but the measurements have been taken from components formed with an axial force of 85kN. Again thinning of the wall across the dome occurs, with increasing internal pressure. A

minimum thickness of 73% of original occurs when the internal pressure is 6000psi (41N/mm²). The thickness across the central part of the dome is fairly constant for each component. However, for this end load thickening of the wall occurs at the root due to the axial deformation. A comparison of the thickness distribution for components formed with axial compressive forces of 26kN and 85 kN is shown in Fig. 44. These were both formed with an internal pressure of 6000psi (41N/mm²). With the higher axial force, greater wall thinning has occurred across the dome, but at the root the wall is a lot thicker than the component formed with a small axial force.

In the commercial manufacture of tee pieces, the thickness of the domed cap is of little importance, so long as it does not fracture. After forming it would most probably be cut off to leave an open side branch. The wall thickness up the side of the branch is of greater importance. Figs 45-47, therefore, deal with the variation in the wall thickness up the side of the branch. This is shown in graphs of the percentage of original wall thickness against:

- a. the branch height ratio ($y/(H_s+L)$), and
- b. the height in mm (y).

Fig. 45.a is for the same components as in Fig.43, but this time the wall thickness is plotted against the height ratio. At the root of the side branch ($y/(H_s+L) = 0.0$) thickening of the wall occurs and is fairly constant for all the values of internal pressure. Gradually the thickness decreases moving up the side of the branch, until it reaches a minimum value at the tip of the dome ($y/(H_s+L) = 1.0$). Again the larger the internal pressure that was used to form the component the thinner the tube wall is.

The same data is plotted in Fig. 45.b, but this time against y . For all the components, the wall thickness is fairly constant at the bottom of the branch. At a height of about 4mm the graphs start to separate with the thinnest walled branch being the one with the highest internal pressure. This graph also shows the effect of the internal pressure on the height of the branch - the last value plotted being the thickness at the tip of the branch. Increasing the internal pressure causes an increase in the length of the side branch formed.

Similarly Figs. 46.a and 46.b show the variation in the wall thickness for components formed using an axial compressive force of 130kN. This time far greater wall thickening has occurred at the root of the branch. In Fig. 46.a the decrease in wall thickness with increasing internal pressure can be seen, when comparing height ratios, especially at the tip. However, in Fig 46.b the wall thickness follow the same trends for the various internal pressures, the variation occurring in the branch length and the wall thickness at the tip of the branch.

A comparison of forming with different axial compressive forces is shown in Fig. 47. Here the wall thicknesses of components formed with axial compressive forces of 85kN and 130kN, are plotted against y . The increase in the axial force causes an increase in the length of the branch and also thickening at the root of the branch. However, the wall thickness at the tip of the branch remains similar.

4.4.1.2. Tee Pieces Formed From The Thinner Tube

Forming tee pieces using the thinner tube (1.03mm wall thickness) was found to be more difficult than with the thicker tube. Smaller internal pressures had to be used to prevent rupture of the tube wall.

However, because of this, and because the walls were only thin, buckling would occur if large axial compressive forces were involved. This is where the third operating procedure, described previously, was found useful. This involved partly deforming the tube at one internal pressure (eg. forming with an axial force of 85kN and an internal pressure of 3000psi (20N/mm²)). At the end of the first deformation the internal pressure and axial compressive force would be increased to complete the deformation (eg. increasing the axial force to 106kN with an internal pressure of 5000psi (35N/mm²)). In this way a large internal pressure, which would have burst the tube if applied initially, can be used partway through the deformation to support the walls and prevent buckling occurring.

Again the wall thickness distribution is presented in graphs of percentage of original wall thickness against the height ratio and the height (y) in Figs. 48-50. Fig 48.a shows the results from components formed with an axial compressive force of 26kN. With the thinner tube, there is a much greater variation in the wall thicknesses for the components formed at different pressures, compared to the results obtained with the thicker walled tube. Again the root thickness is approximately the same as the original wall thickness, and the wall thickness gets less towards the tip of the branch. However, only a small internal pressure causes substantial thinning of the wall - with an internal pressure of 4500psi (31N/mm²) the wall thickness at the tip is reduced to 65% of the original thickness.

With an axial compressive force of 85kN the wall thickness at the root of the branch is greatly increased, as shown in Figs. 49.a and 49.b. Comparison of Fig. 49.a with Fig. 46.a, show that similar wall thickening

at the root is obtained from the thicker tube but a higher axial force of 130kN is required to achieve this. However the branch height of the thinner tube is not as great as those obtained from the thicker tube, as a comparison of Figs. 49.b and 46.b shows.

The greatest axial force that was possible, before buckling of the tube became very severe, was 106kN. The results obtained from forming with this axial compressive force are shown in Figs. 50.a and 50.b. The wall thickness at the tip of the branch remains similar to those obtained from forming with smaller axial forces, but there is an increase in the thickness at the root, and an increase in the length of the branch. Note that the results from one component are vastly different from the other two, having a much larger root thickness, and a longer branch. The reason for this is unknown - all forming conditions were identical except for the variation in the internal pressure - but may be due to variations in the original wall thickness around/along the tube blank.

A comparison of the wall thickness distribution obtained from forming at different axial compressive forces is shown in Fig. 51. This shows a large difference in the wall thicknesses of components formed at 26kN and 85kN, but only a small difference between components formed at 85kN and 106kN.

4.4.2. Cross Pieces

Forming cross pieces was found to produce results similar to forming tee pieces. The forming limits were found to be the same as those for forming tee pieces (Figs. 38.a and 38.b). The branch height produced was also found to be similar. In Fig. 52, the branch height, expressed as a percentage of the tube radius, is plotted against the

internal pressure for various values of axial compressive force. Comparison of the values obtained from axial compressive forces of 26kN, 85kN and 127kN, with Fig. 40 - the same graph plotted for tee pieces - shows similar branch heights have been achieved. For the cross pieces two extra compressive forces have been used - 106kN and 148kN. At 106kN the resulting branch heights are similar to those formed with an axial compressive force of 127kN. The results obtained from the highest axial compressive force of 148kN differ from other results in that a very steep line is produced. This indicates that with this high axial compressive force the internal pressure has a much greater effect on the resulting length of the branch. At low pressures buckling occurs, preventing the full length of the branch to be achieved. It may be that at higher internal pressures the line will level off and follow similar trends to the other axial compressive forces.

4.4.2.1. Cross Pieces Formed From The Thicker Tube

Similar graphs have been plotted for the cross pieces as for the tee pieces. Figs. 53-57 are graphs of wall thickness - expressed as a percentage of the original wall thickness - against:

- a. the height ratio ($y/(H_s+L)$), and
- b. the height in mm (y).

Fig 53.a and 53.b are for an axial compressive force of 26kN, used just as a sealing force. The graphs show the decrease of the wall thickness at the tip of the branch with increasing internal pressure. At the root of the branch the wall thickness remains approximately the same as the original wall thickness. Figs 54, 55, 56 and 57 correspond to axial compressive forces of 85kN, 106kN, 127kN and 148kN respectively.

Increasing the axial compressive force results in an increase in the length of the branch, and thickening of the tube wall at the root of the branch. For each compressive force, the wall thickness up the branch remains fairly similar for various values of internal pressure, except at the tip, where increasing the internal pressure decreases the wall thickness.

The results obtained from all five different axial compressive forces is shown in Fig. 58. Comparison of wall thicknesses shows that increasing the axial compressive force simply increases the root thickness and the branch height, while the wall thickness at the tip of the bulge remains almost constant. The data in Fig. 58 was obtained by producing components using two internal pressures - 6000psi (41N/mm²) and 7000psi (48N/mm²). The smallest wall thickness at the tip of the branch is obtained when using only the sealing force of 26kN, ie. when there is no or little axial deformation.

4.4.2.2. Cross Pieces Formed From The Thinner Tube

Again the thinner tube was found to be harder to form than the thicker tube. Similar results were obtained in forming cross pieces as were obtained forming tee pieces from the thinner walled tube. Figs. 59, 60 and 61 show the results obtained from forming with axial compressive forces of 26kN, 63kN and 85kN respectively. At the lowest axial force there is similarity between the wall thickness distribution of the cross piece and the tee piece, and can be seen by comparison of Figs. 59.a and 48.a. Again, increasing the axial force causes an increase in the wall thickness at the root together with an increase in the length of the branch, and is illustrated by Figs. 60.a and 60.b.

The results obtained from forming with an axial force of 85kN shows quite a few discrepancies - see Figs. 61.a and 61.b. Two of the components show considerable thickening of the wall at the root. However, the other three have hardly any wall thickening occurring at the root. This again may be due to variations occurring in the original wall thickness (perhaps due to variations in annealing), or may be due to errors during the measurement of the components.

A comparison of the components formed from the three different axial compressive forces is shown in Fig. 62. Ignoring the discrepancies occurring at the root of the components formed with an axial force of 85kN, it can be seen that increasing the axial force again causes a thickening of the wall at the root as well as an increase in the length of the branch.

Fig. 35. Tee Pieces Formed to Various Stages.

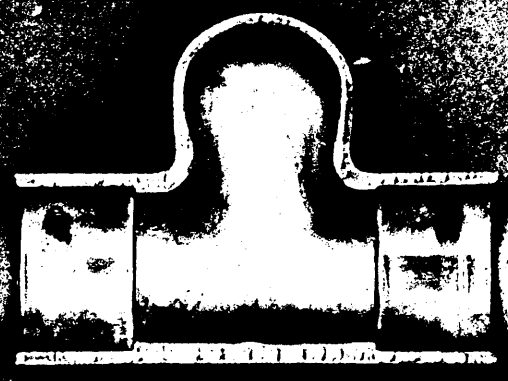
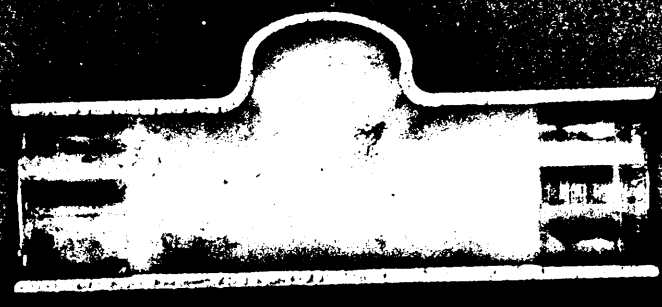
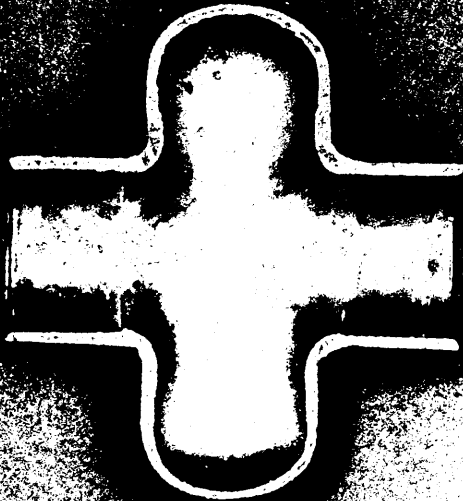
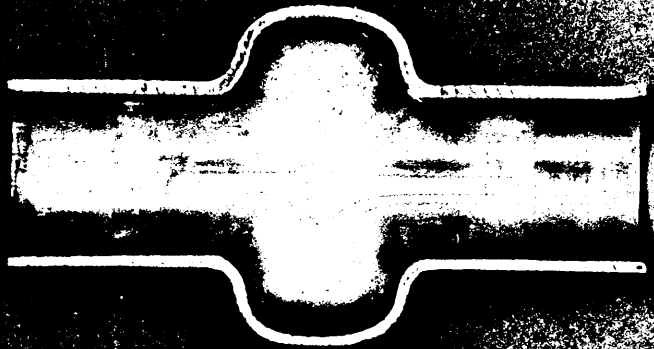
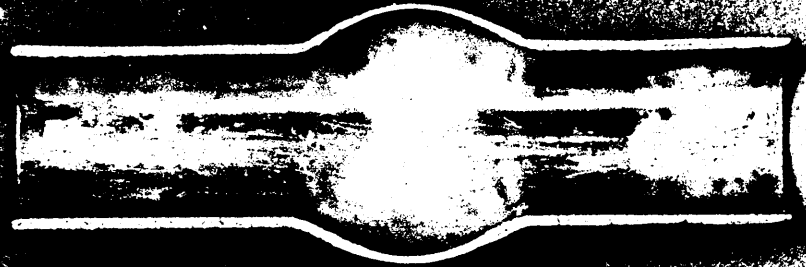
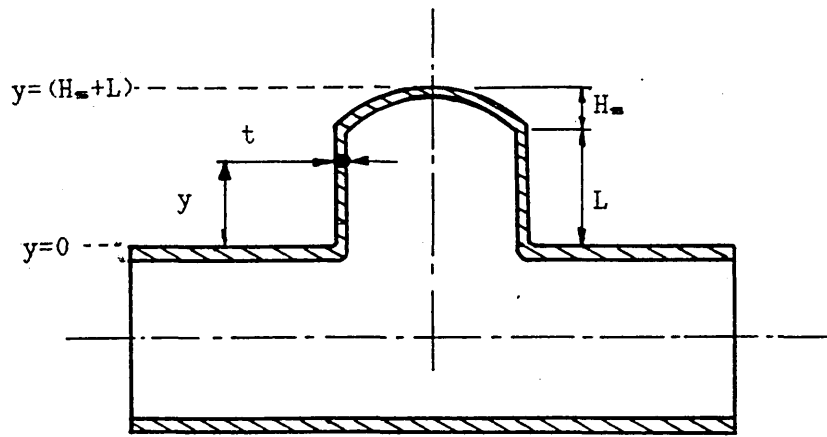
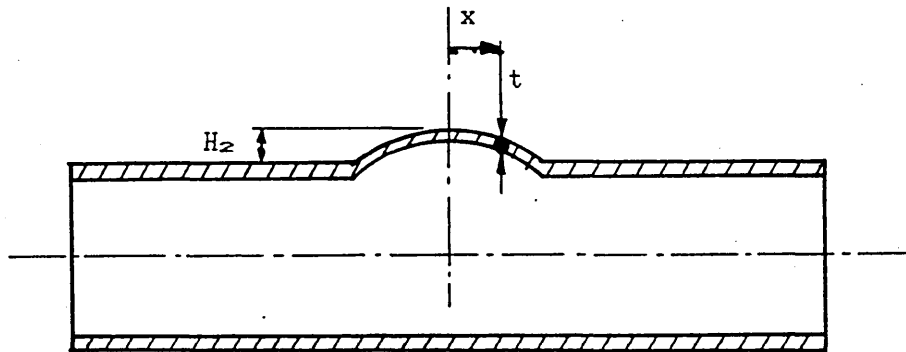


Fig. 36. Cross Pieces Formed to Various Stages.





a. For Prominent Bulges.



b. For Small Bulges.

Fig. 37.
The Methods of Wall Thickness Measurement.

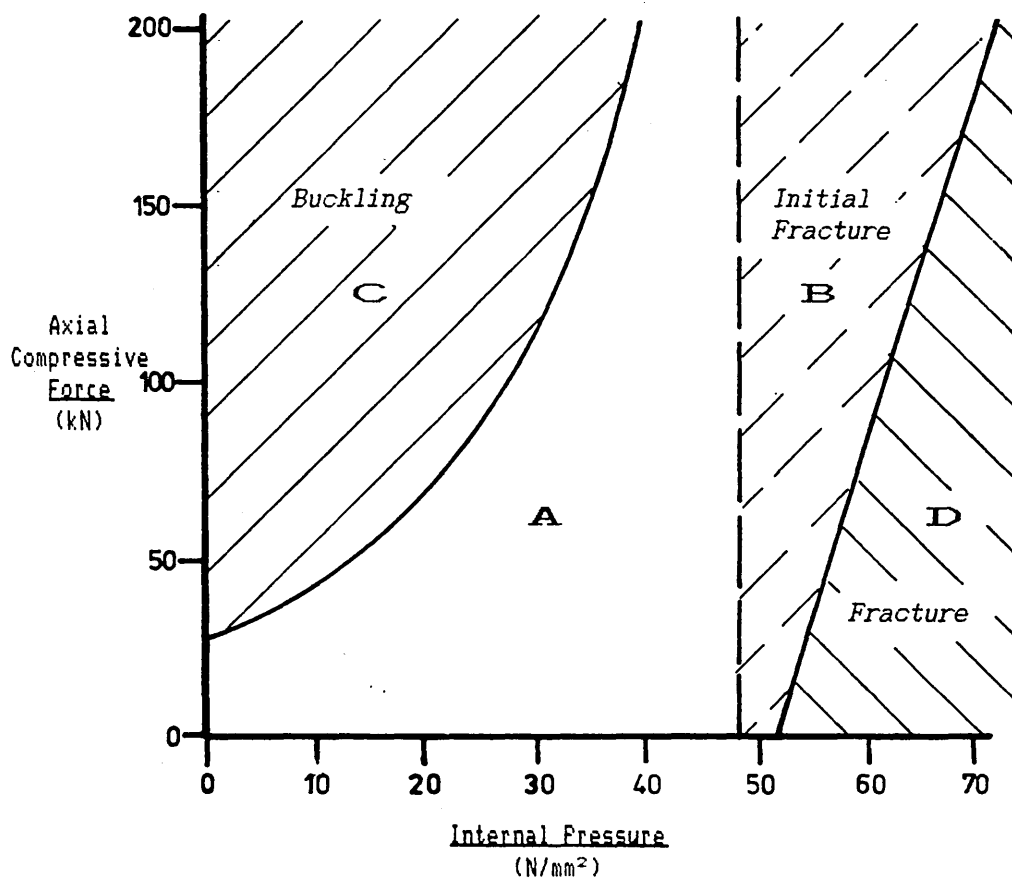


Fig. 38.a.
Forming Limits for Tube of Wall Thickness: $t_o=1.37\text{mm}$

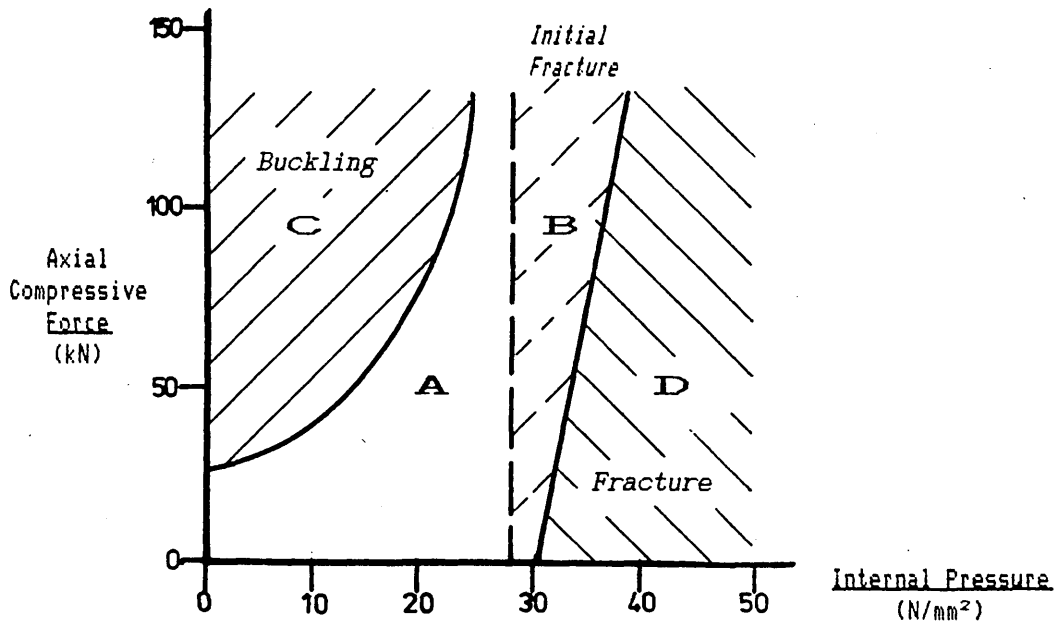


Fig. 38.b.
Forming Limits for Tube of Wall Thickness: $t_o=1.03\text{mm}$

Bulge Off Centre but Fairly Well Formed

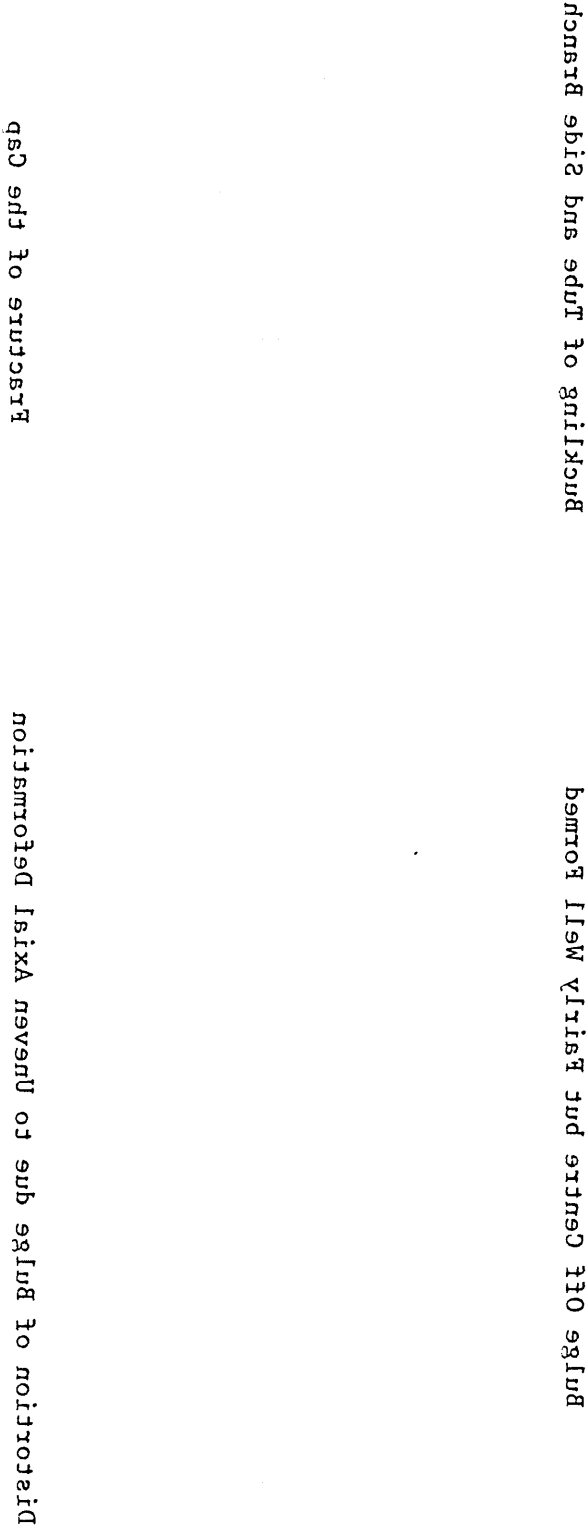
Buckling of Tube and Side Branch

Distortion of Bulge due to Uneven Axial Deformation

Fracture of the Cap

Fig. 39. Failure During the Forming of Tee Pieces.

Fig. 30. Failure During the Forming of Tee Pieces.



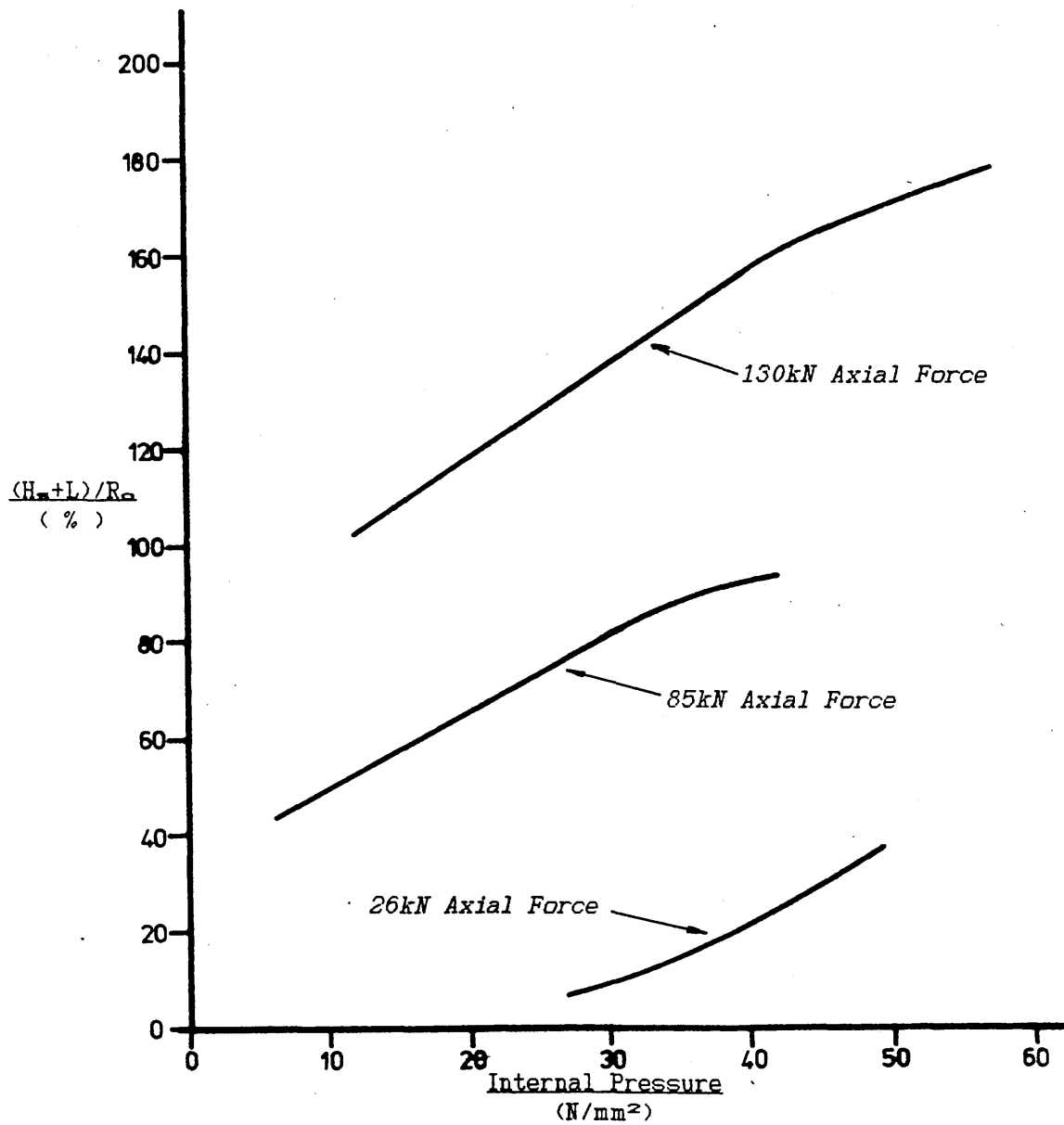


Fig. 40.
*The Effect of Internal Pressure on the Branch Length
of a Tee Piece.*

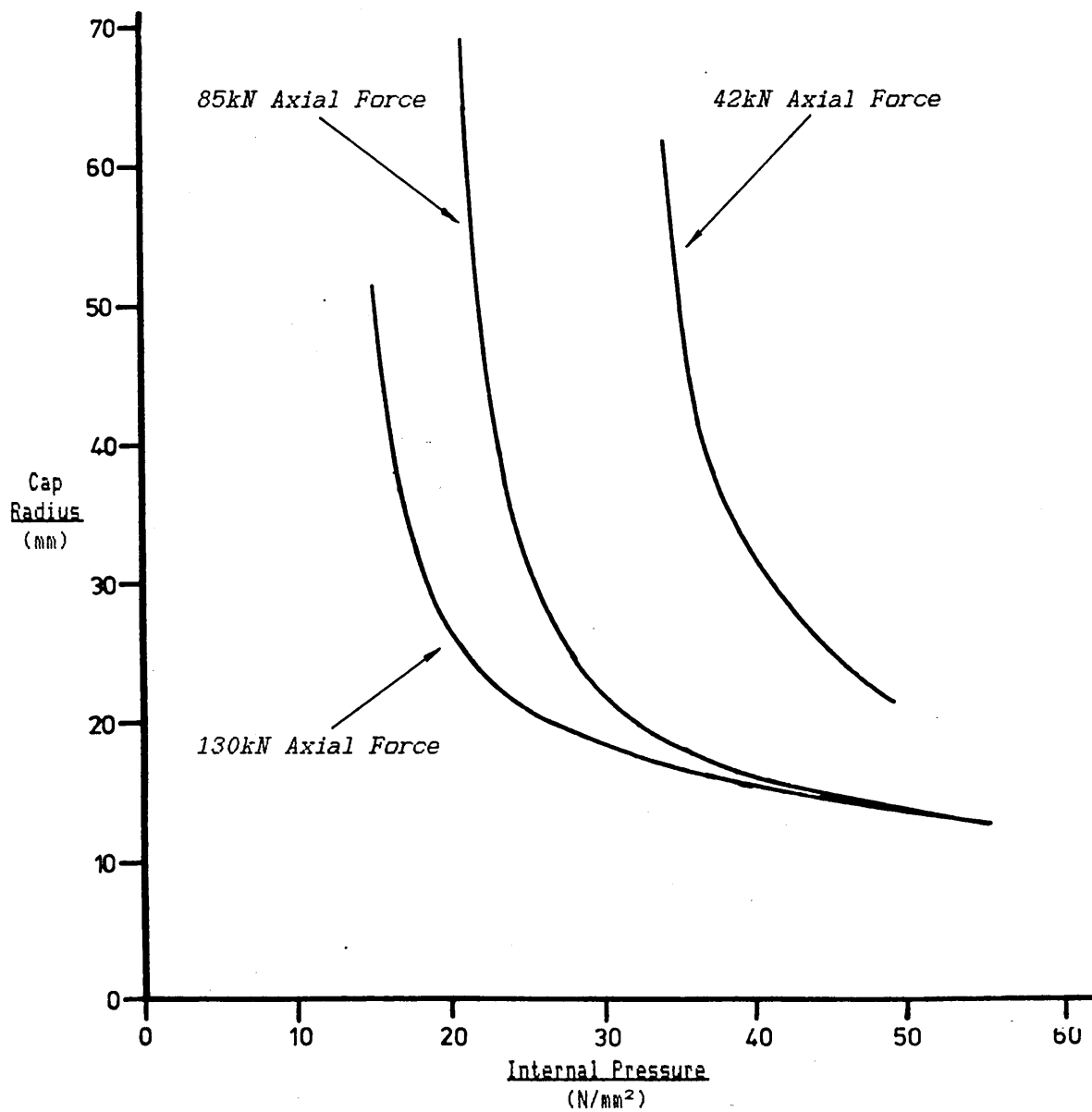


Fig. 41.
The Effect of Internal Pressure on the Cap Radius
of a Tee Piece.

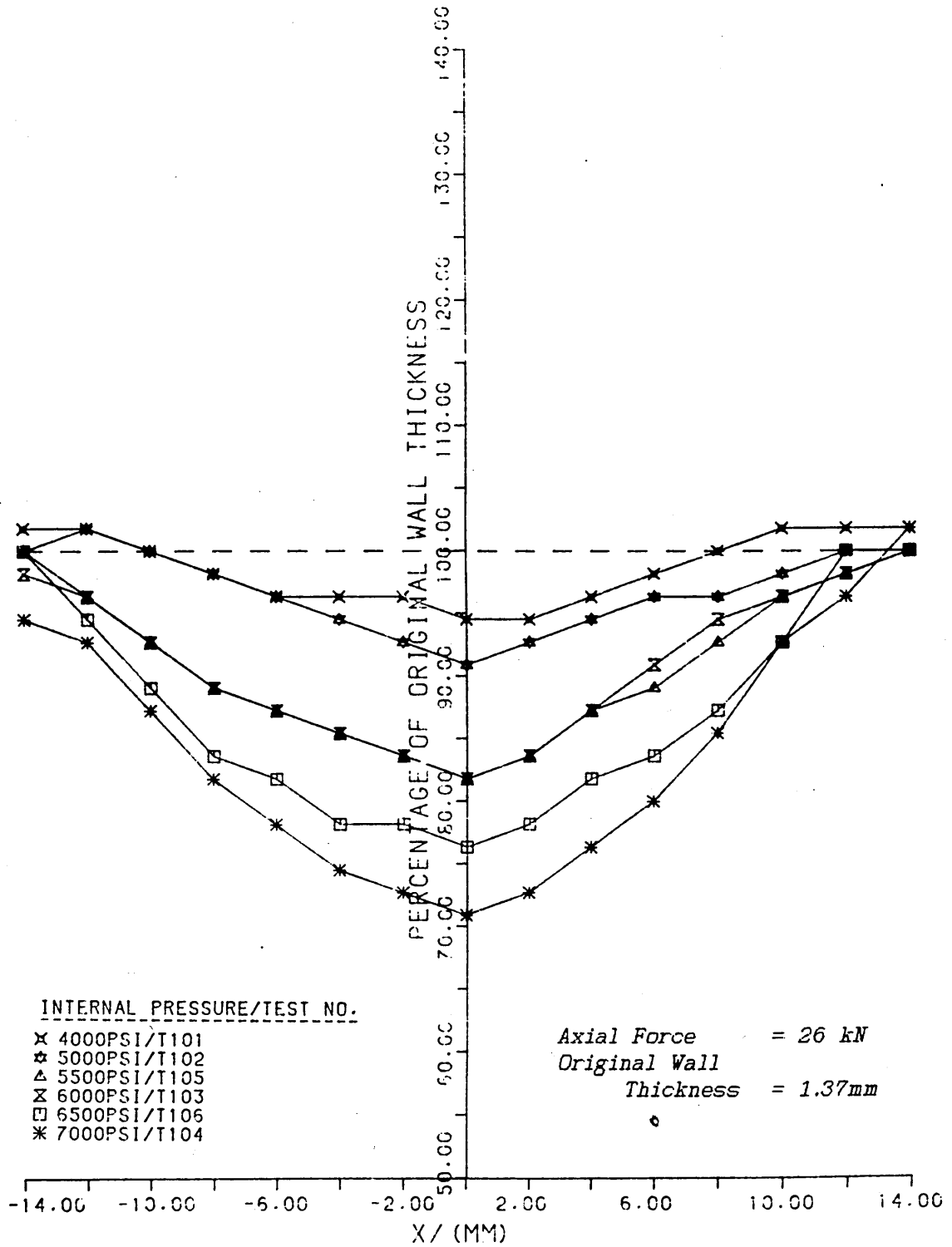


Fig. 42.

The wall thickness distributions across the bulges of tee pieces formed at various internal pressures, with a constant axial compressive force.

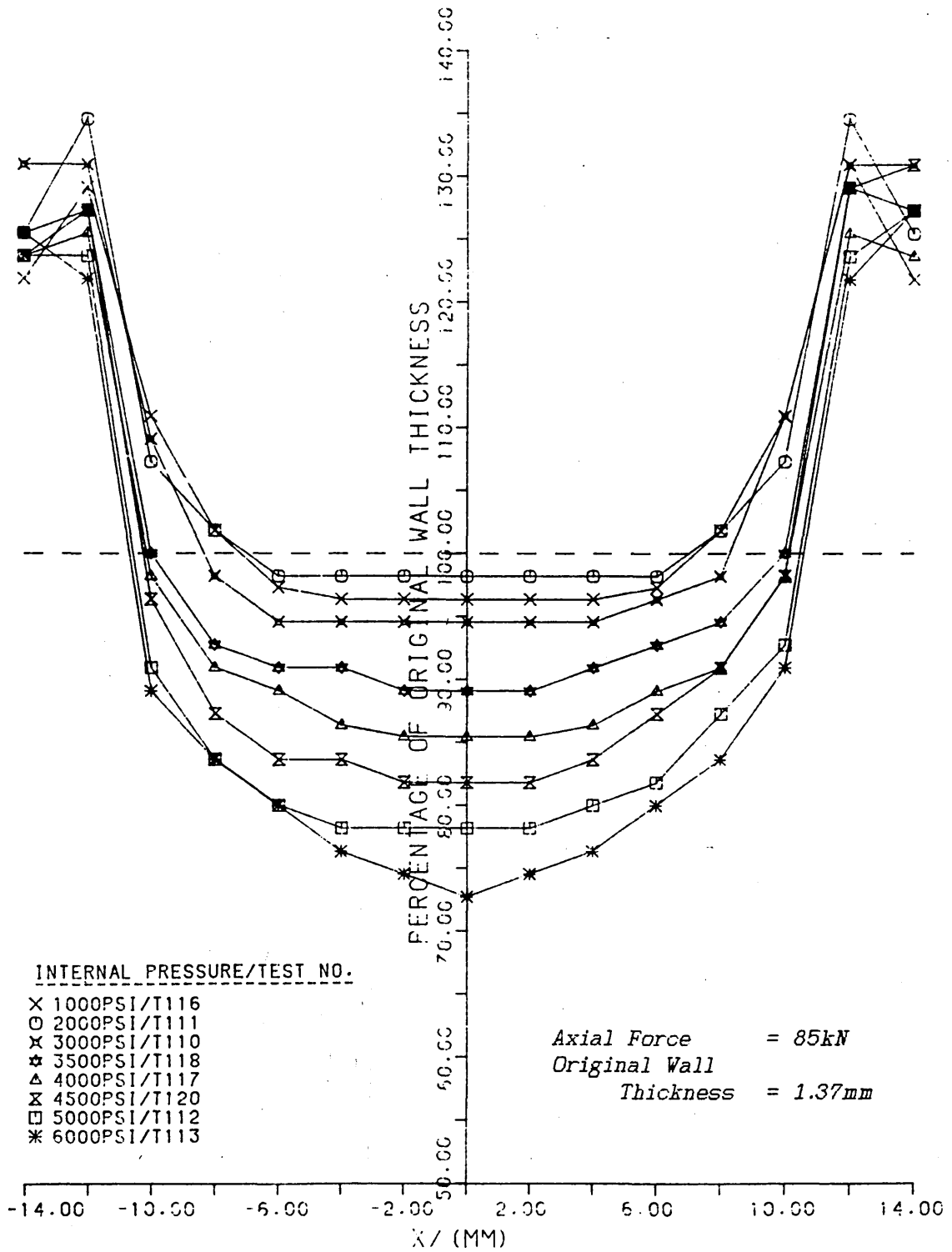


Fig. 43.
The wall thickness distributions across the bulges of tee pieces formed at various internal pressures, with a constant axial compressive force.

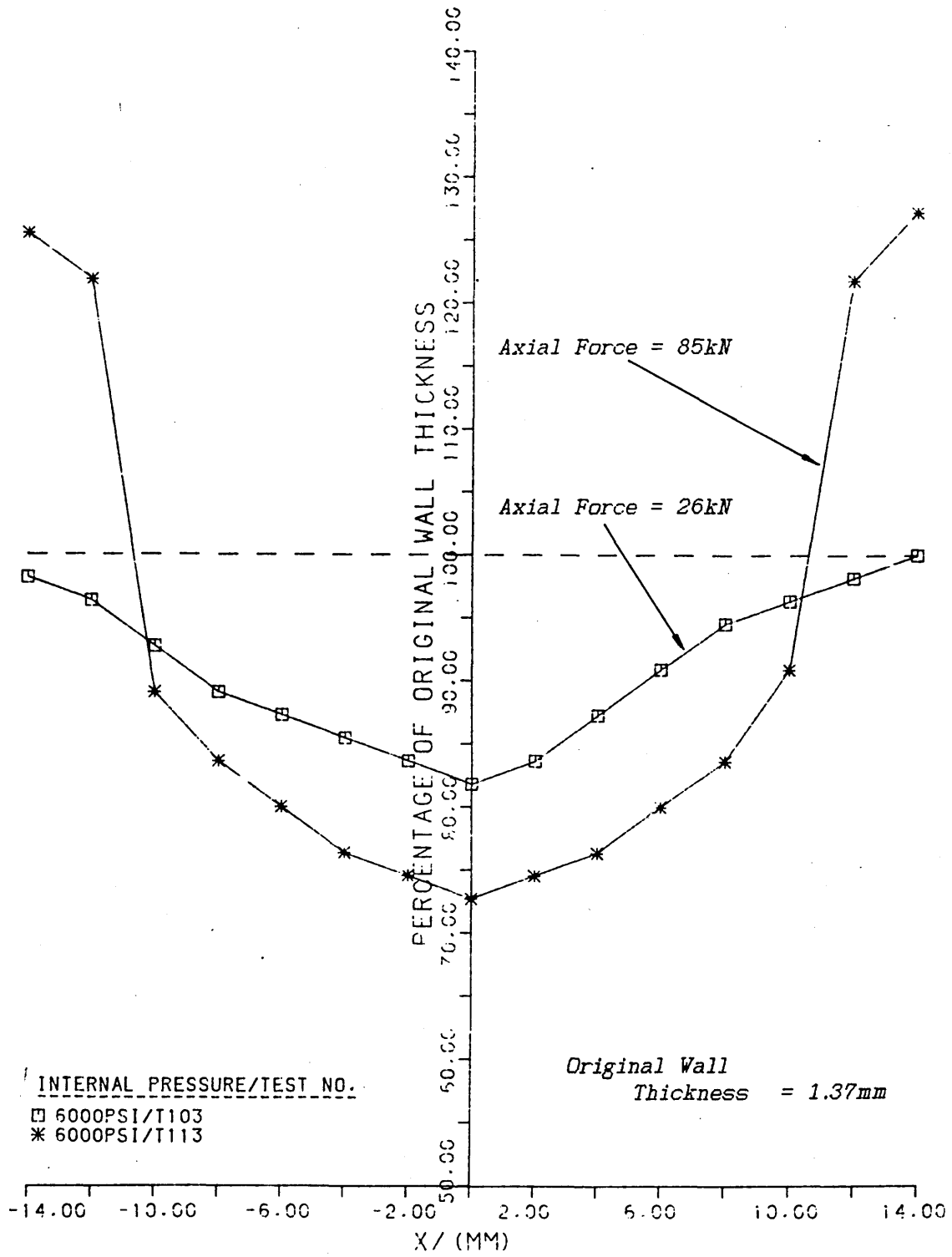


Fig. 44.
The wall thickness distributions across the bulges of tee pieces formed at a constant internal pressure, with various axial compressive forces.

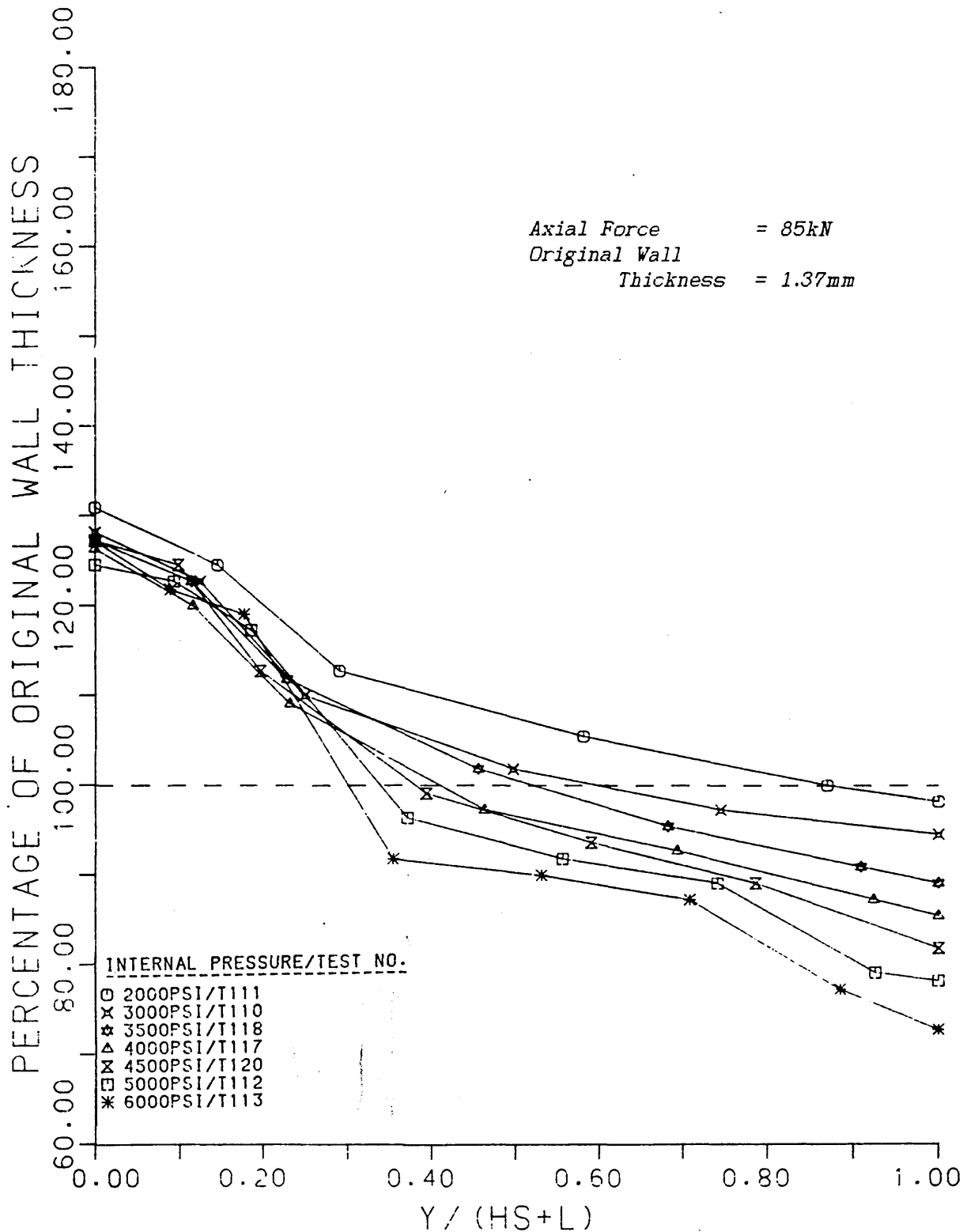


Fig. 45.a.
 The wall thickness distributions along the side branches
 of tee pieces formed at various internal pressures,
 with a constant axial compressive force.

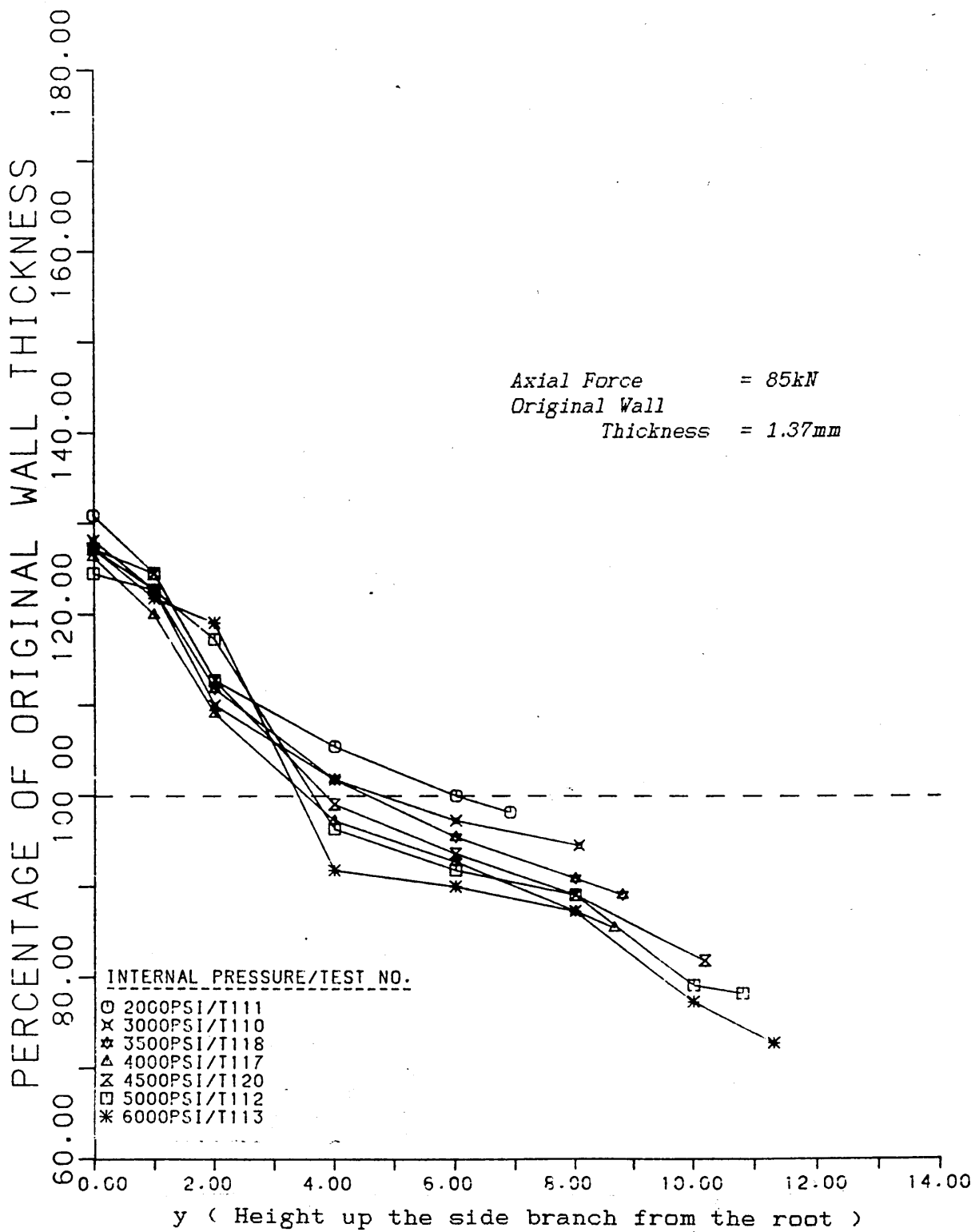


Fig. 45. b.
The wall thickness distributions along the side branches of tee pieces formed at various internal pressures, with a constant axial compressive force.

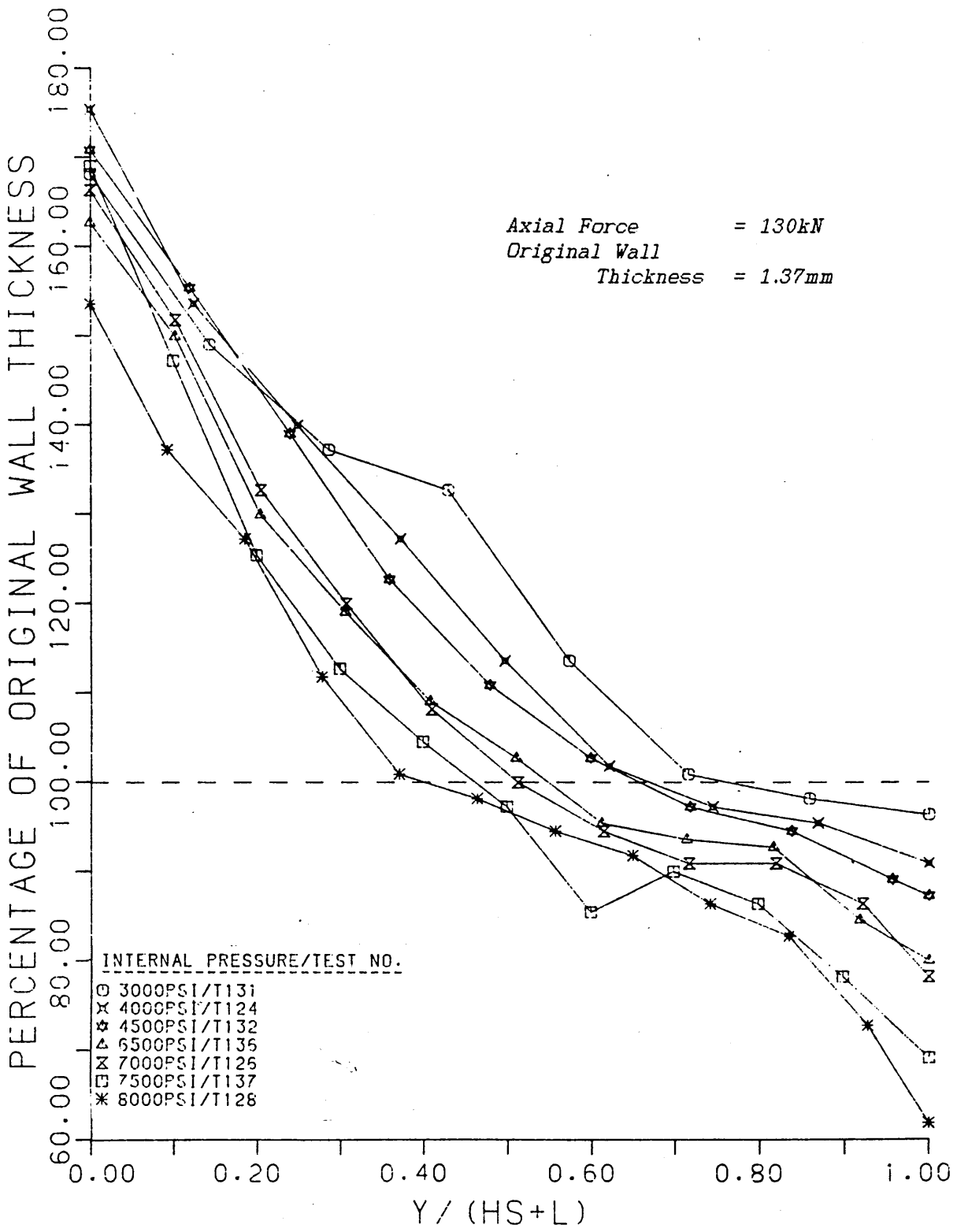


Fig. 46.a.
The wall thickness distributions along the side branches of tee pieces formed at various internal pressures, with a constant axial compressive force.

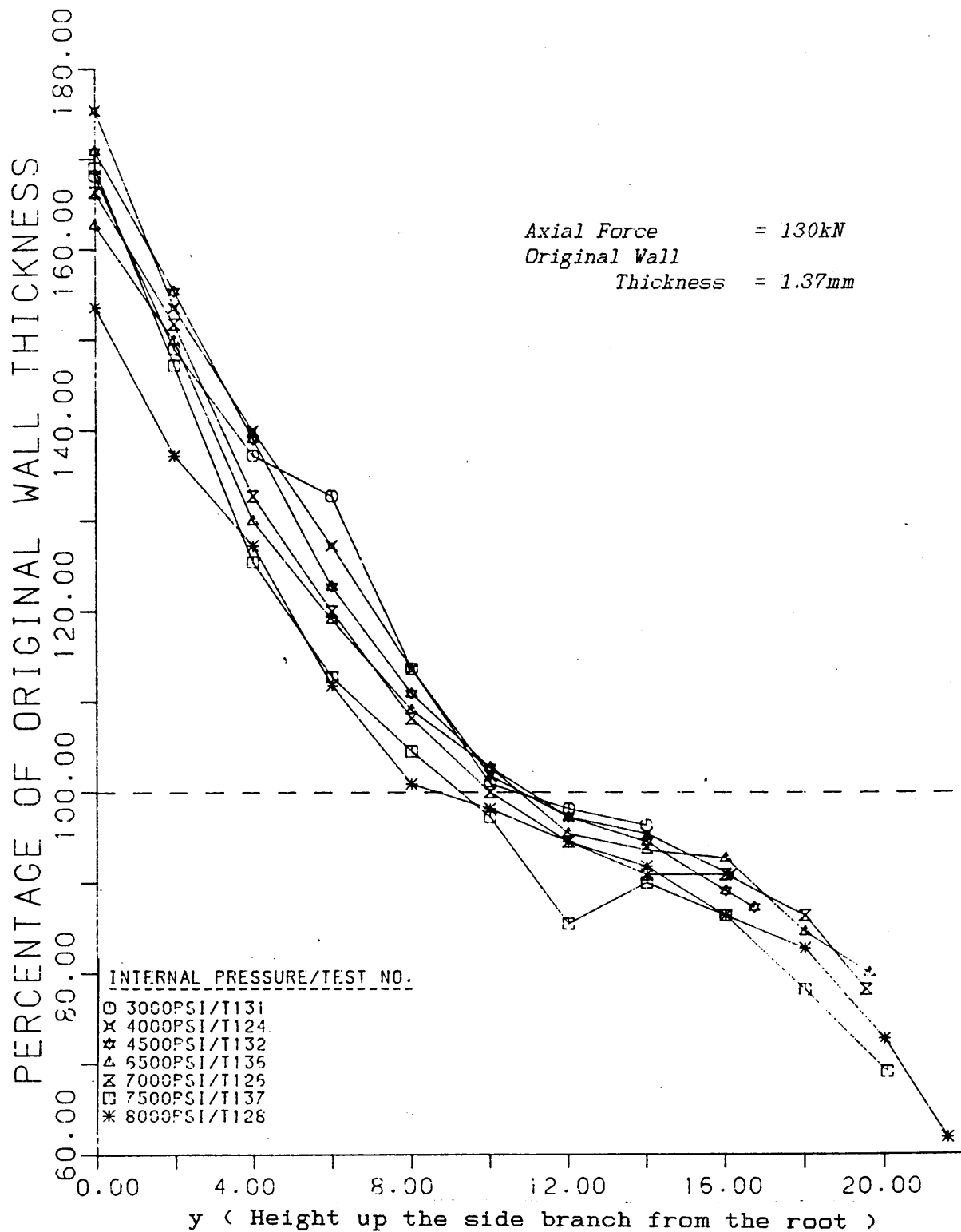


Fig. 46. b.
The wall thickness distributions along the side branches of tee pieces formed at various internal pressures, with a constant axial compressive force.

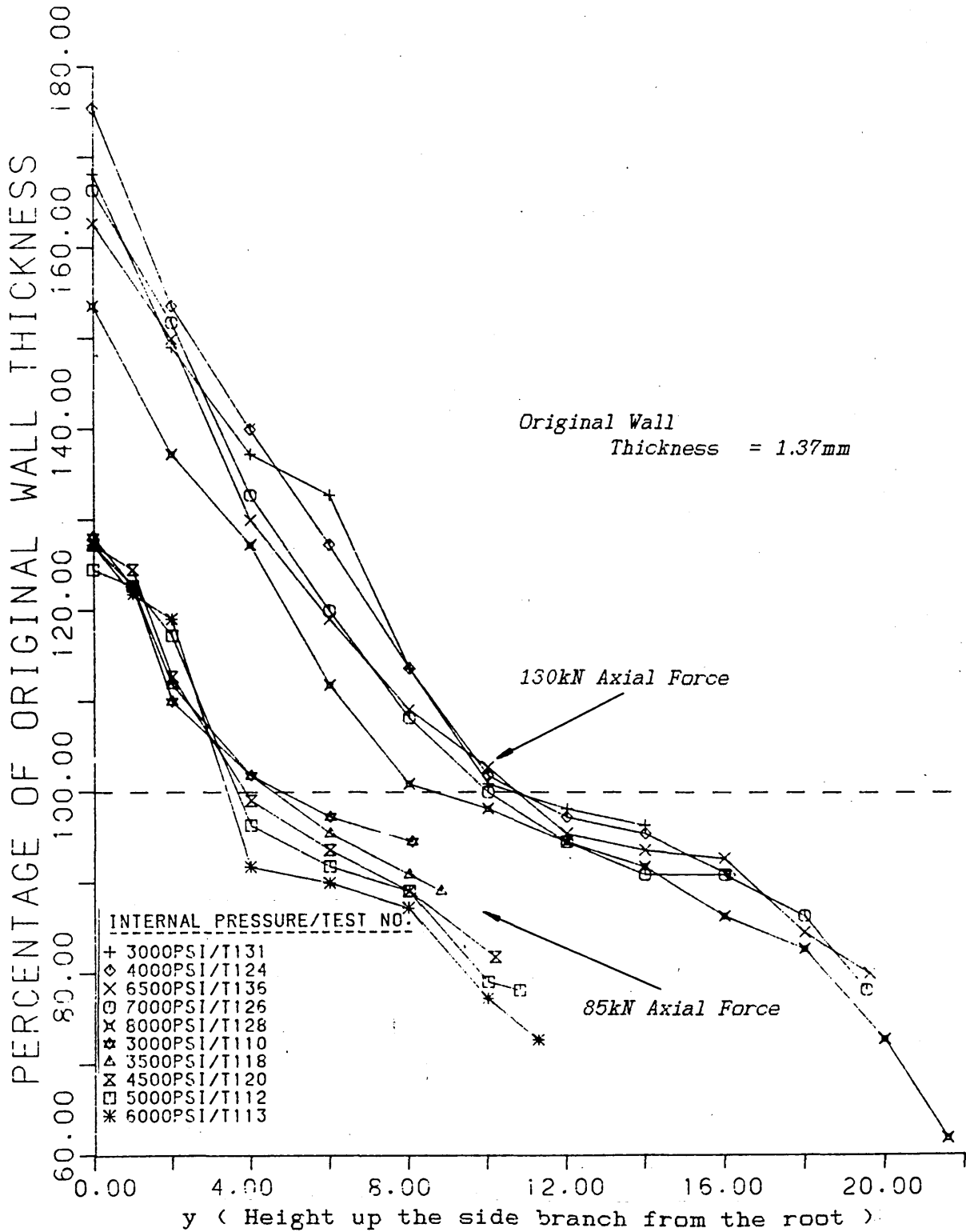


Fig. 47.
The wall thickness distributions along the side branches of tee pieces formed at various internal pressures, and with various axial compressive forces.

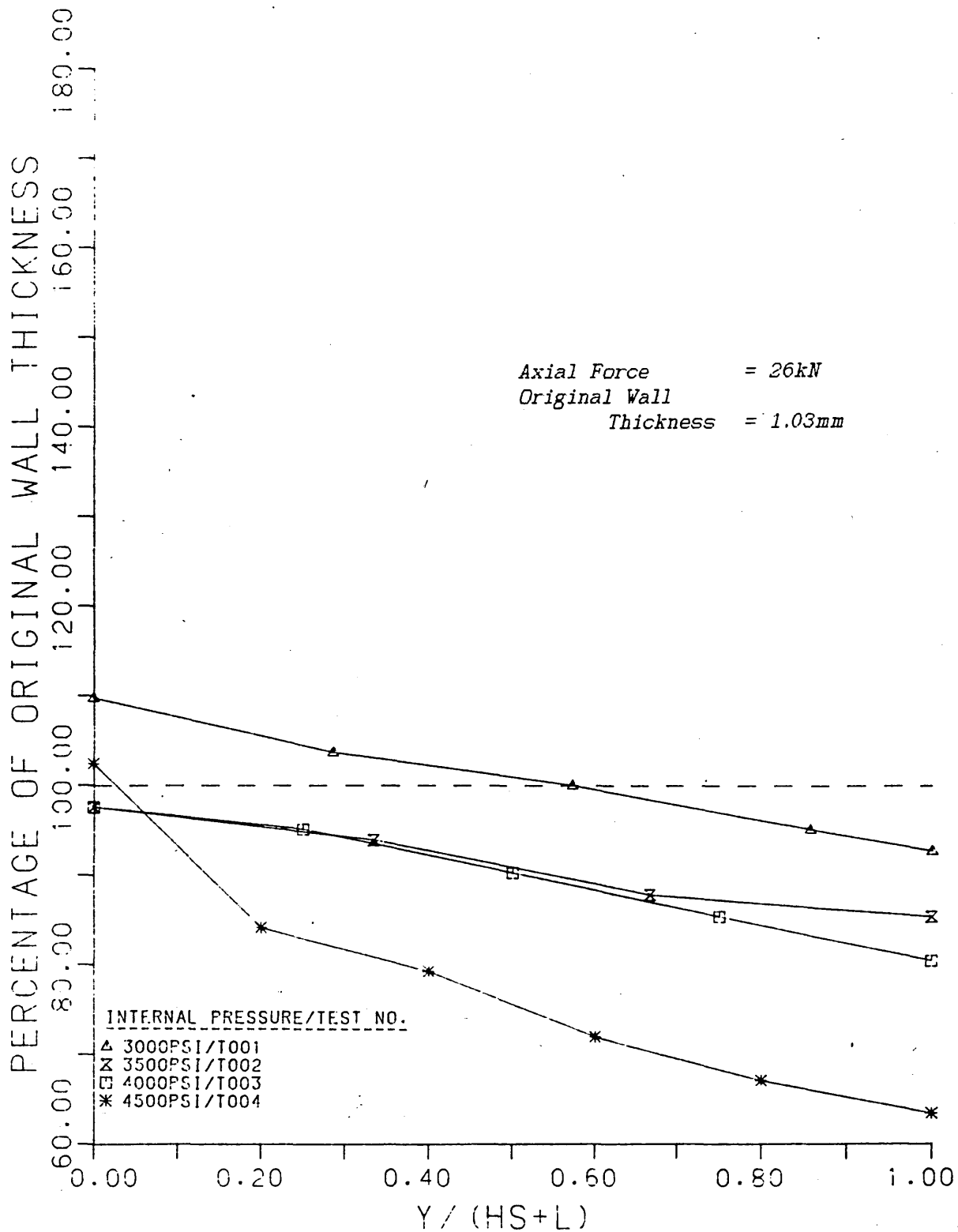


Fig. 48.a.
 The wall thickness distributions along the side branches of tee pieces formed at various internal pressures, with a constant axial compressive force.

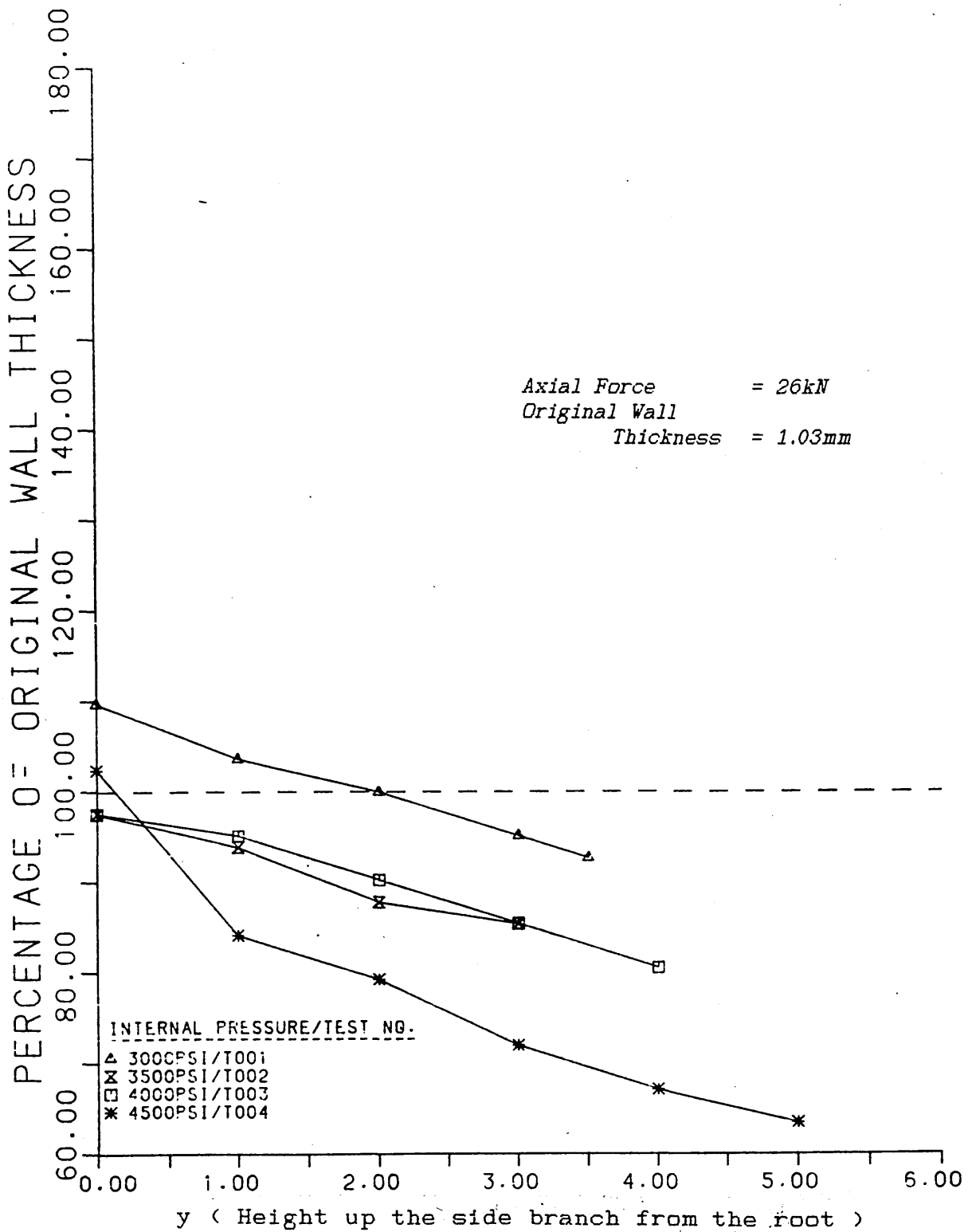


Fig. 48. b.
The wall thickness distributions along the side branches of tee pieces formed at various internal pressures, with a constant axial compressive force.

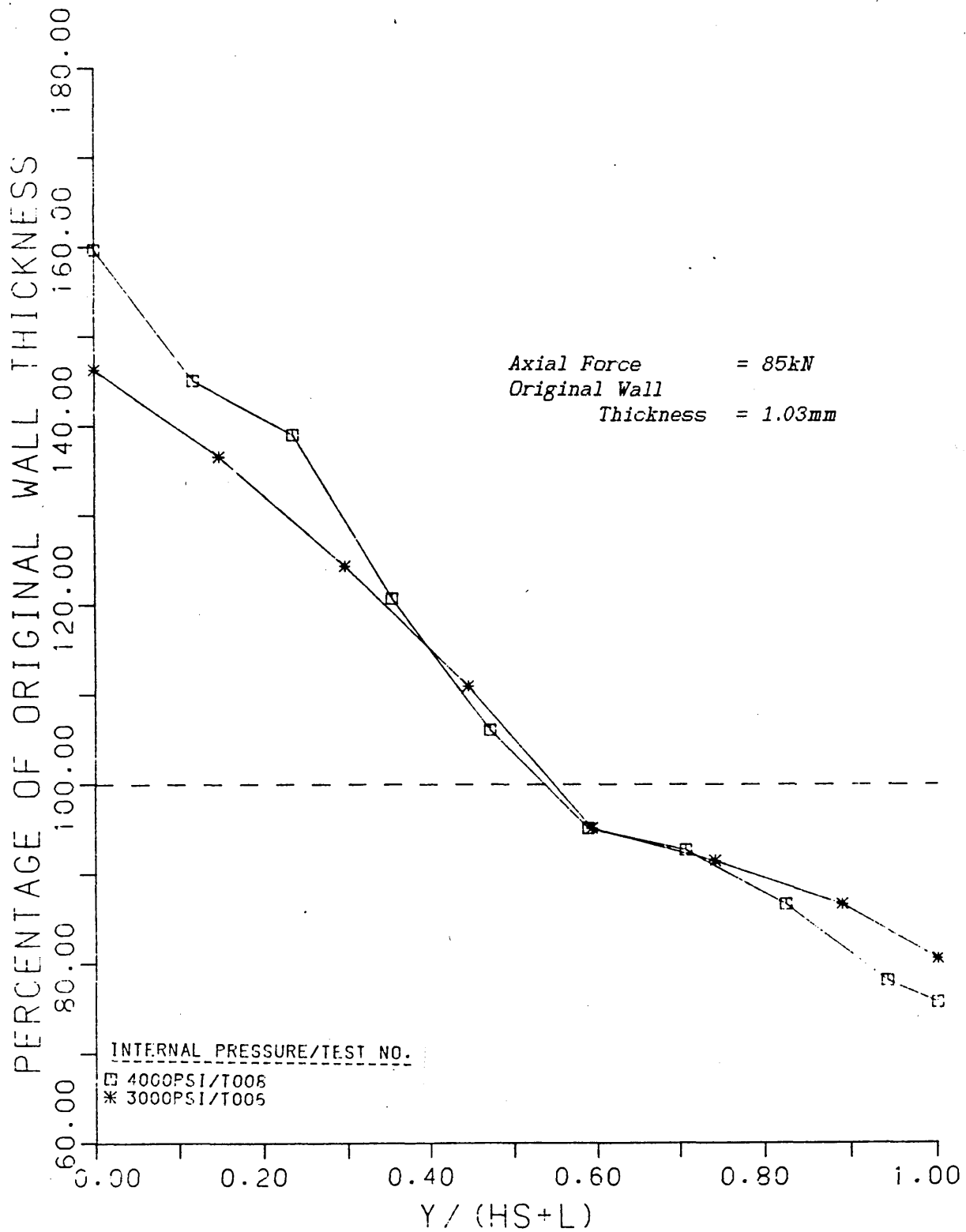


Fig. 49.a.

The wall thickness distributions along the side branches of tee pieces formed at various internal pressures, with a constant axial compressive force.

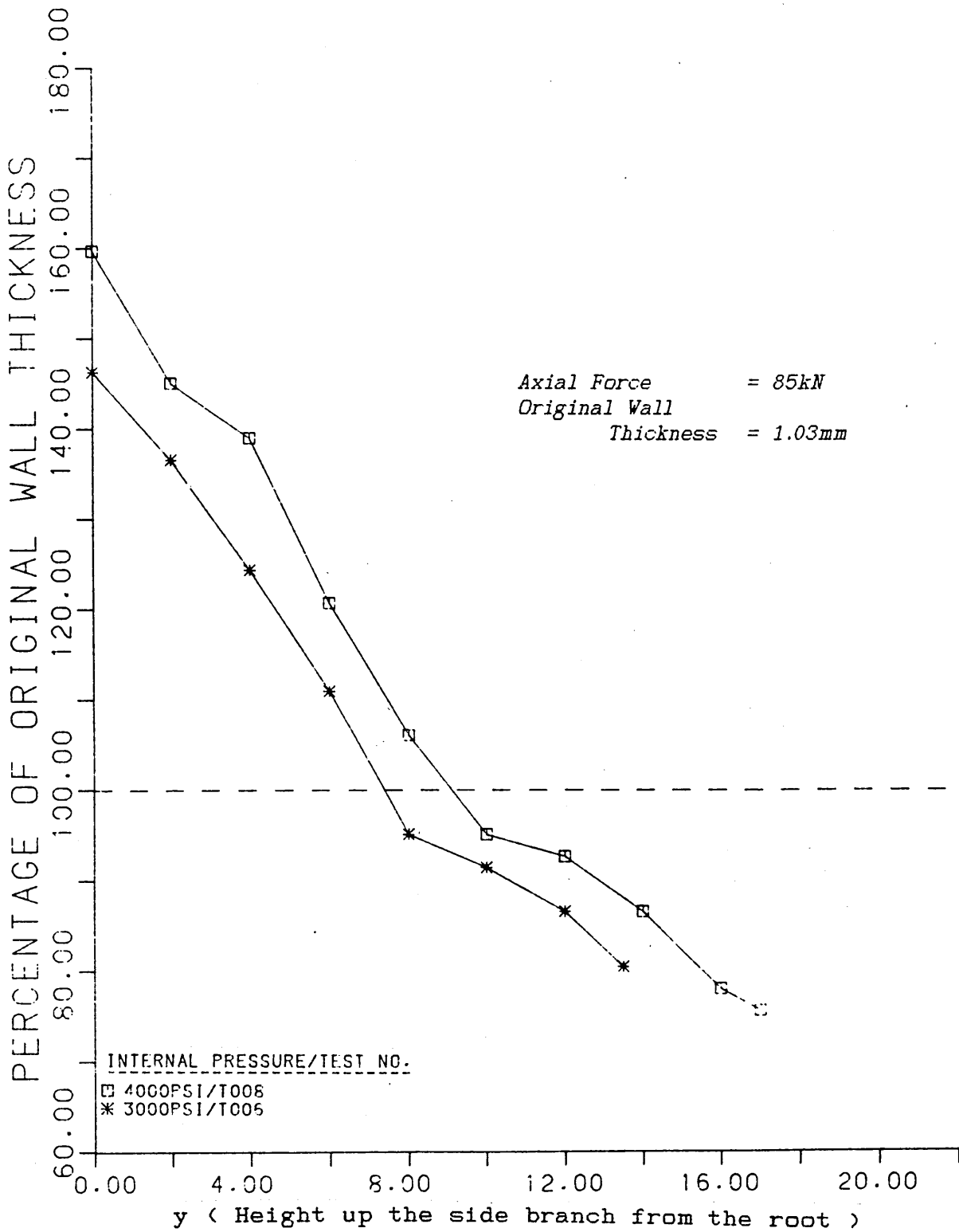


Fig. 49. b.
The wall thickness distributions along the side branches of tee pieces formed at various internal pressures, with a constant axial compressive force.

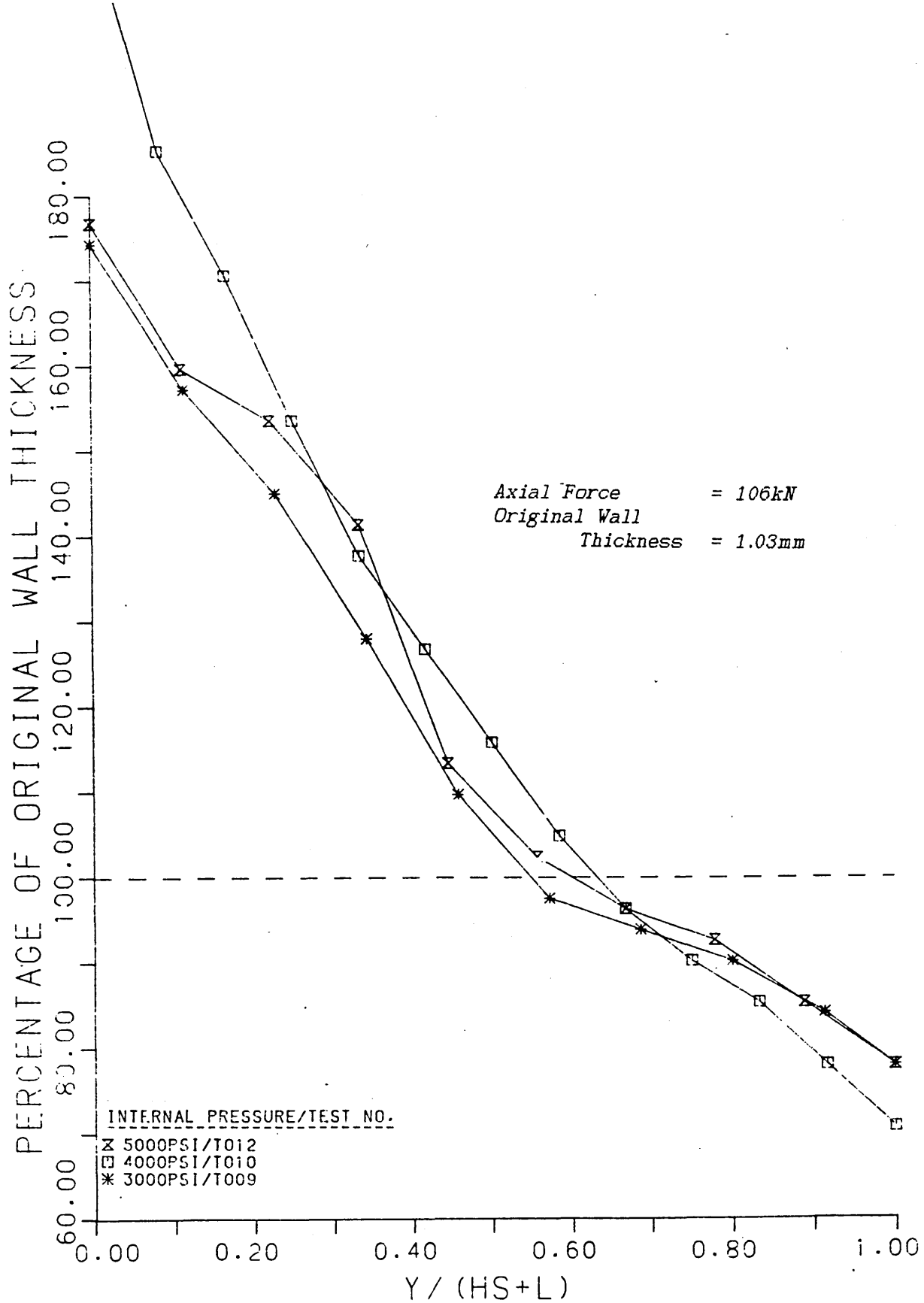


Fig. 50.a.

The wall thickness distributions along the side branches of tee pieces formed at various internal pressures, with a constant axial compressive force.

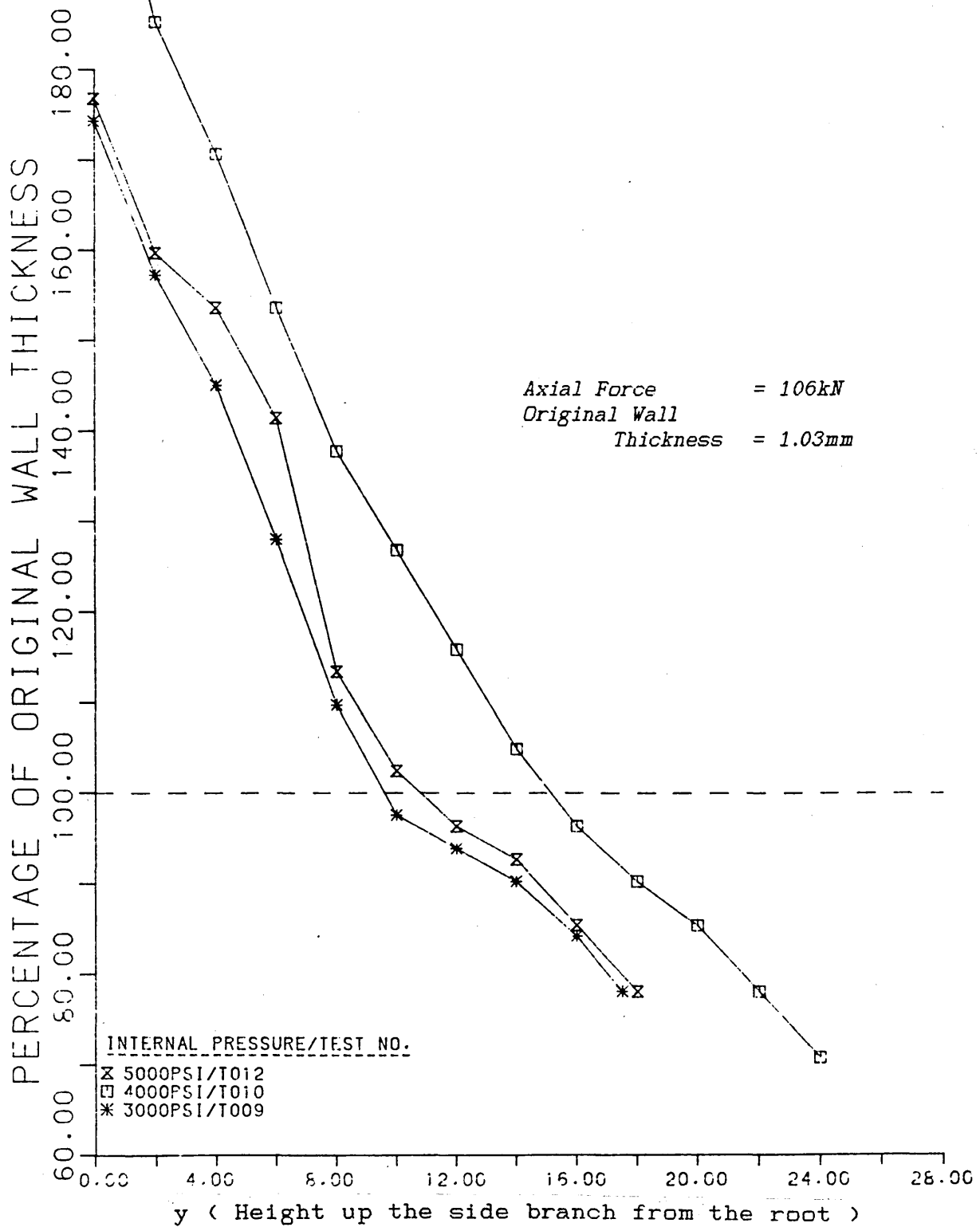


Fig. 50. b.
 The wall thickness distributions along the side branches of tee pieces formed at various internal pressures, with a constant axial compressive force.

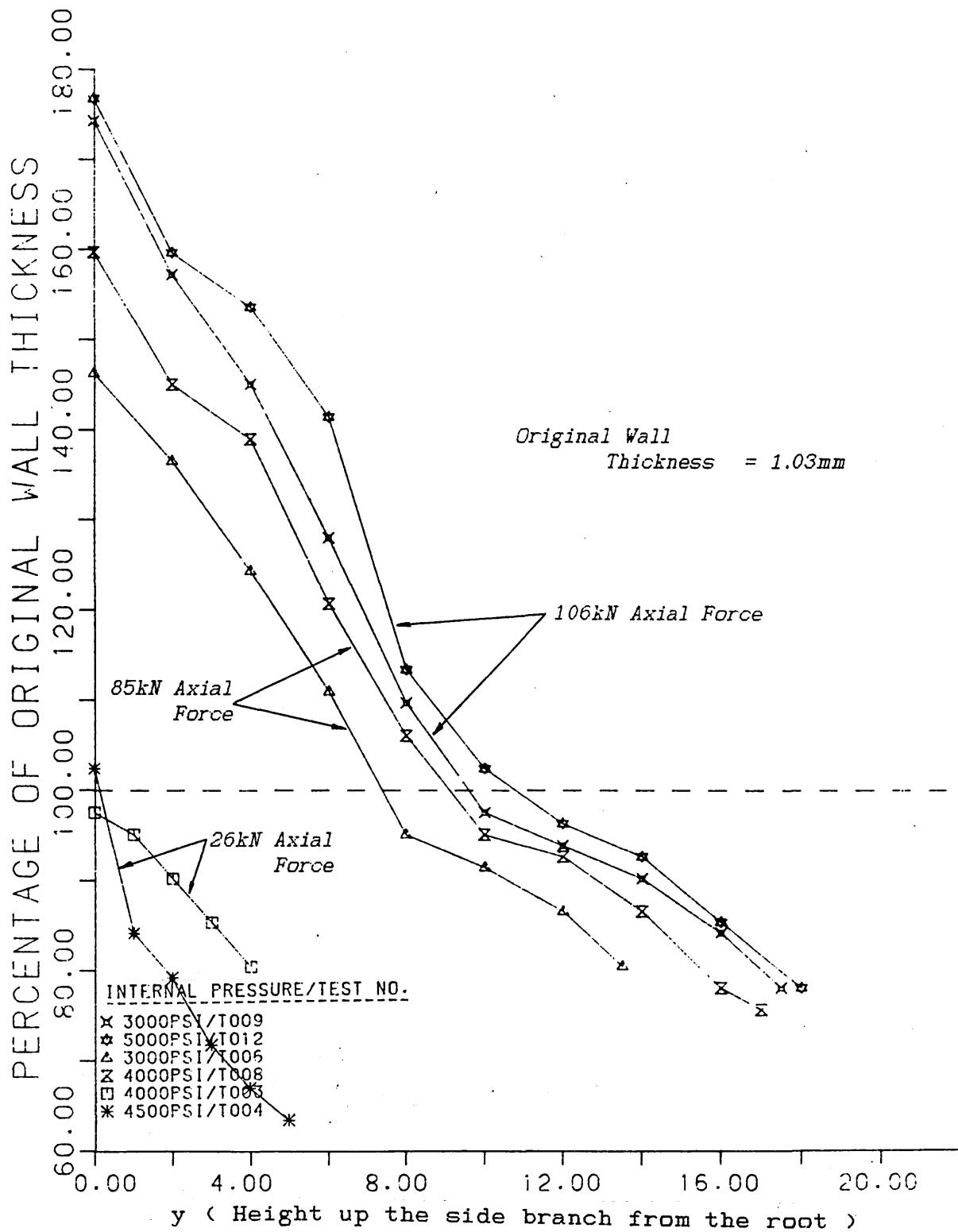


Fig. 51.
The wall thickness distributions along the side branches of tee pieces formed at various internal pressures, and with various axial compressive forces.

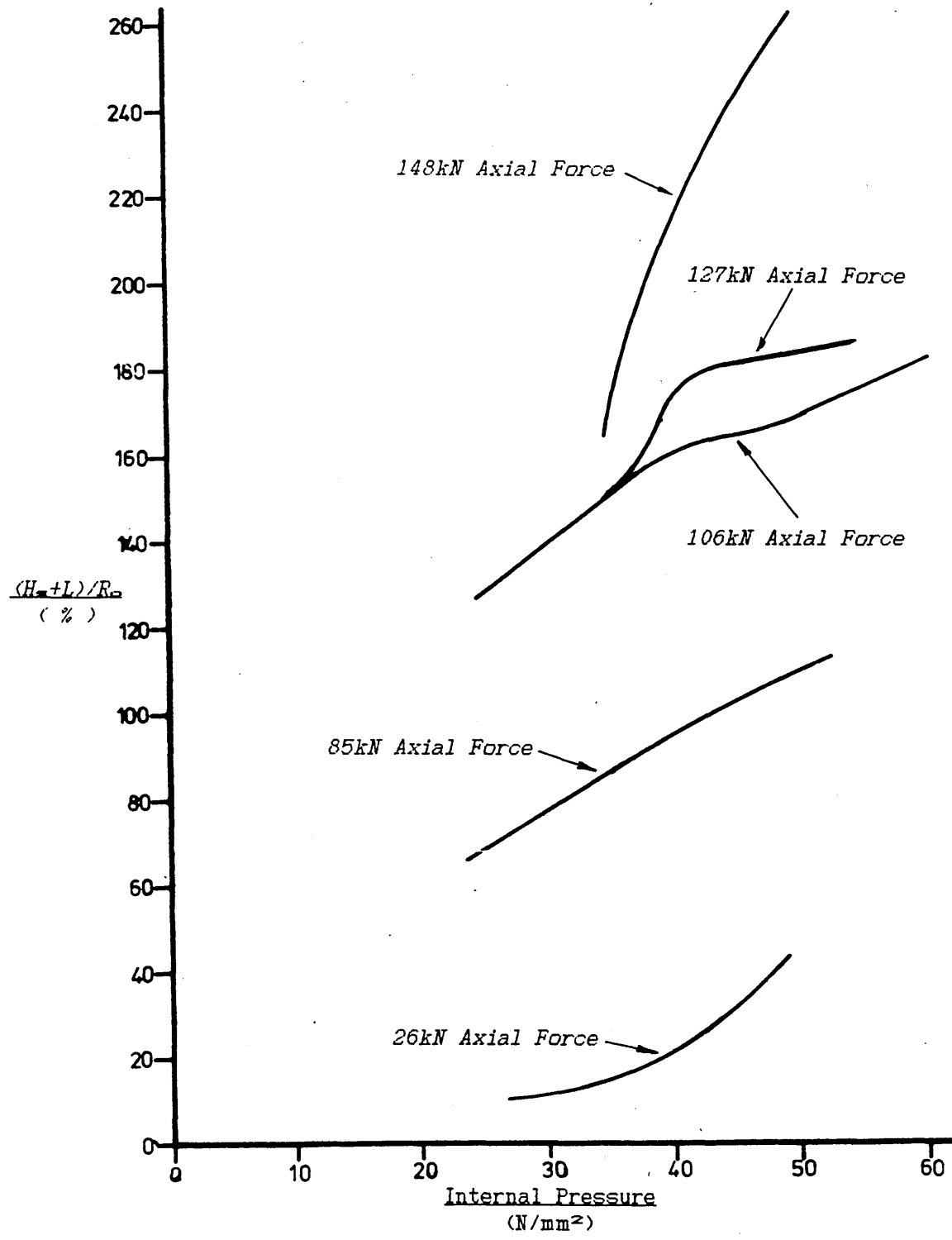


Fig. 52.
*The Effect of Internal Pressure on the Branch Length
of a Cross Piece.*

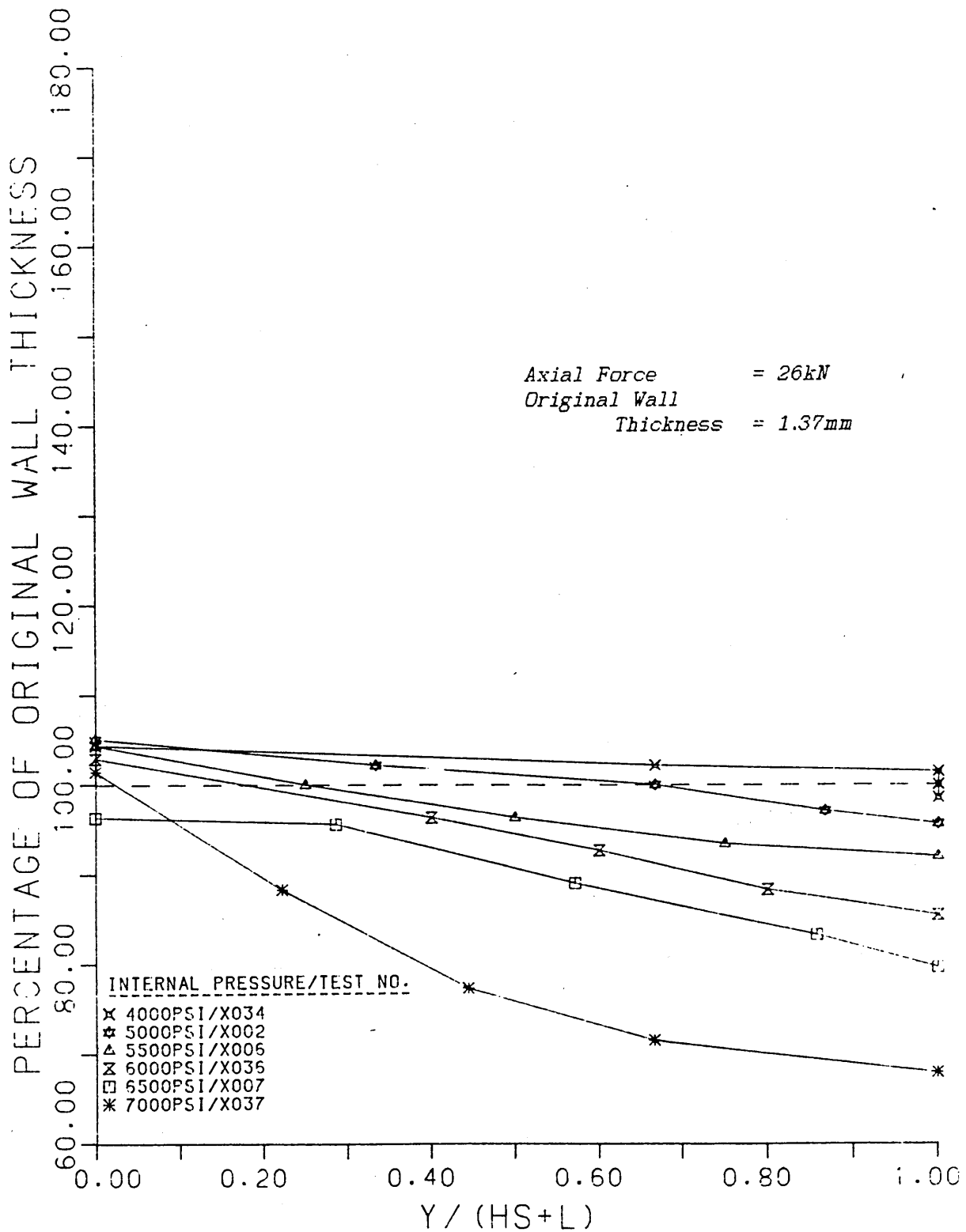


Fig. 53.a.

The wall thickness distributions along the side branches of cross pieces formed at various internal pressures, with a constant axial compressive force.

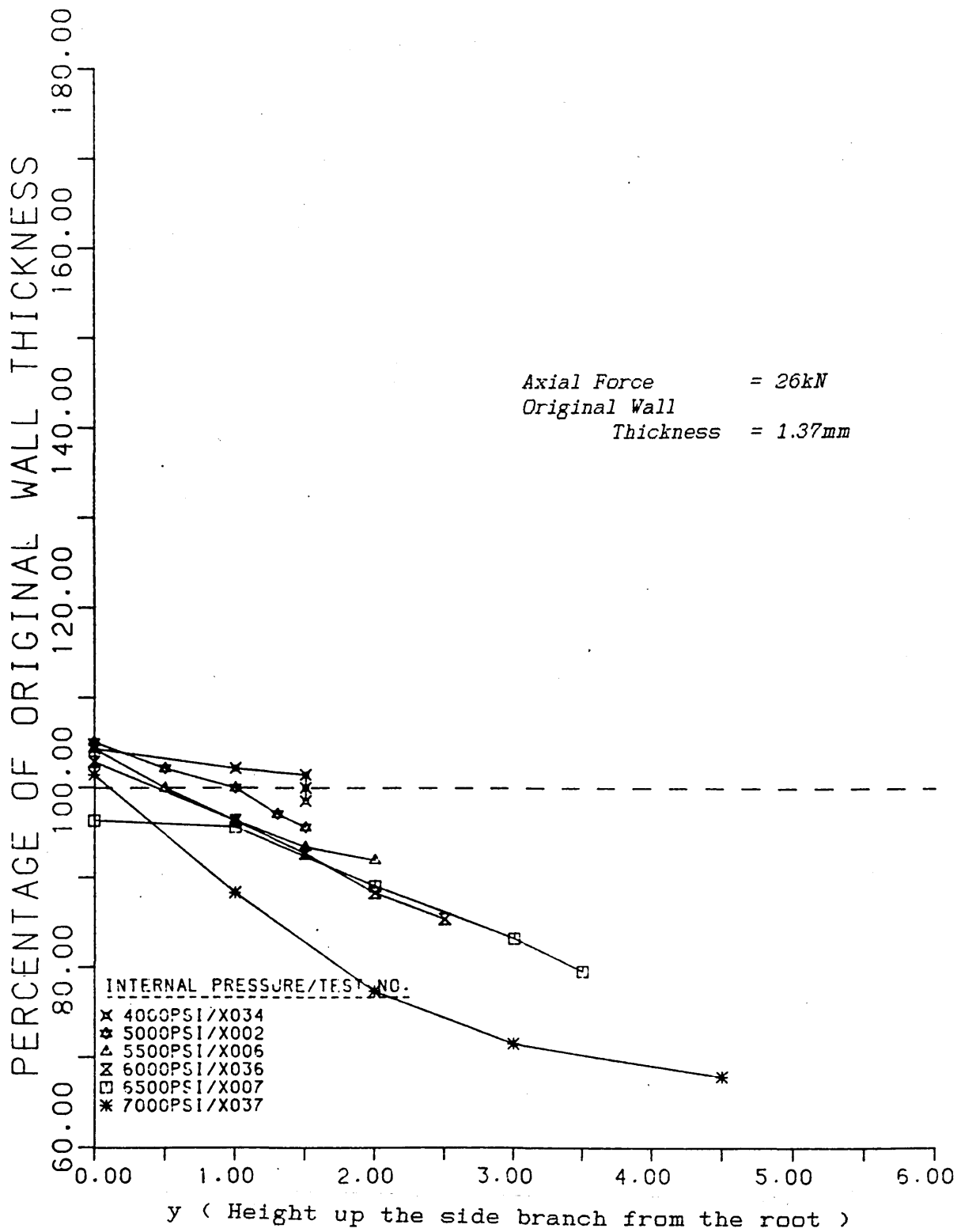


Fig. 53.b.
The wall thickness distributions along the side branches of cross pieces formed at various internal pressures, with a constant axial compressive force.

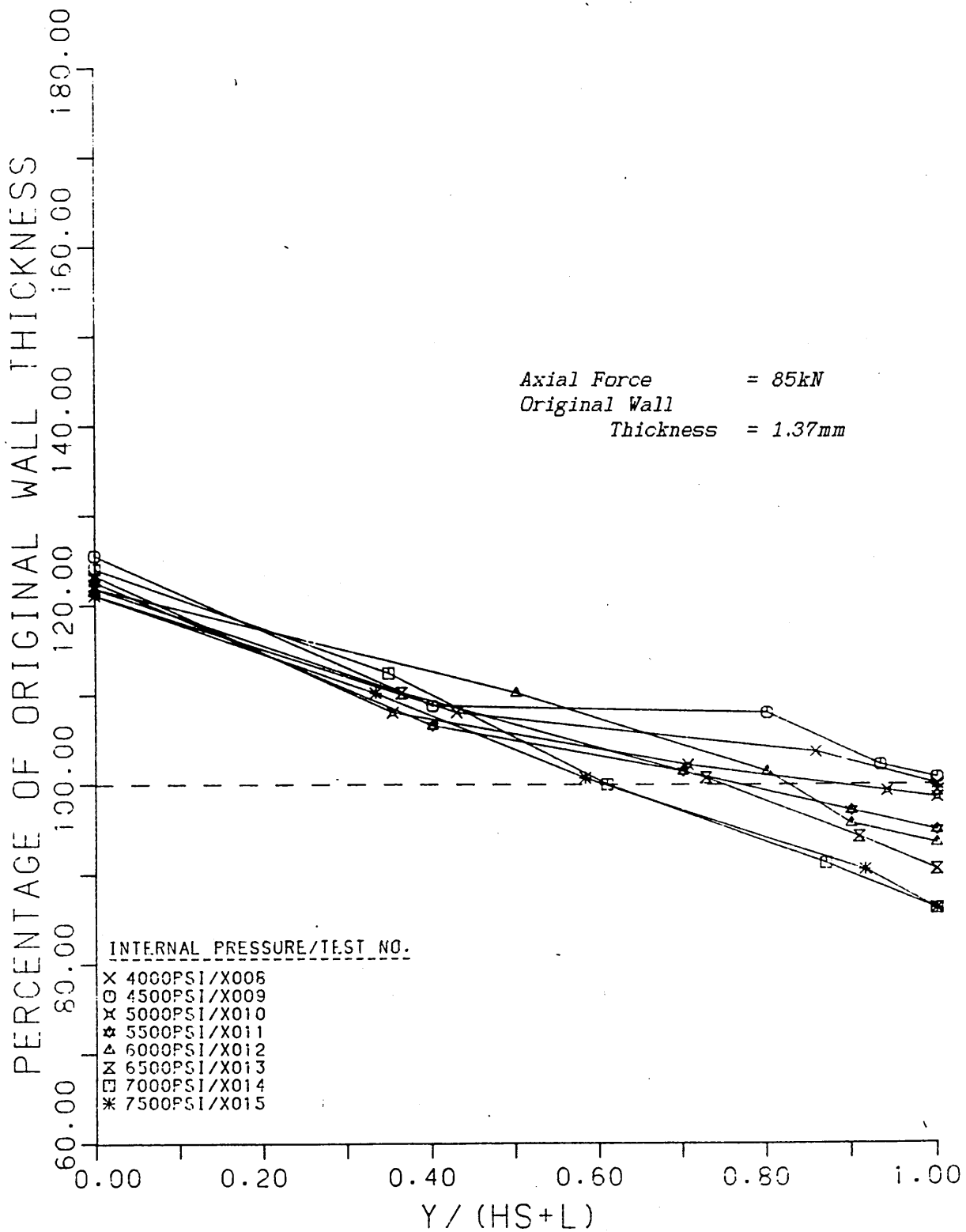


Fig. 54.a.

The wall thickness distributions along the side branches of cross pieces formed at various internal pressures, with a constant axial compressive force.

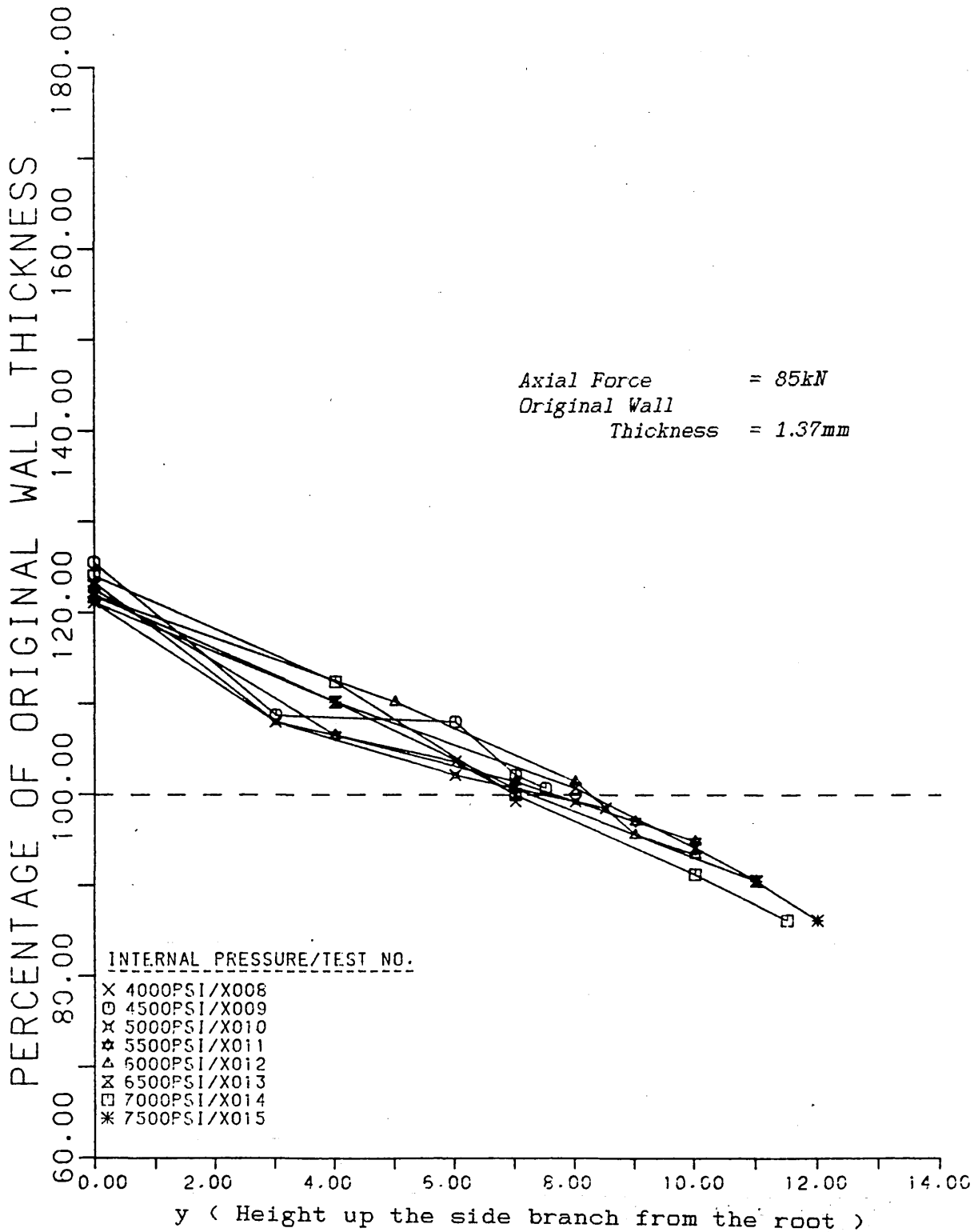


Fig. 54.b.
The wall thickness distributions along the side branches of cross pieces formed at various internal pressures, with a constant axial compressive force.

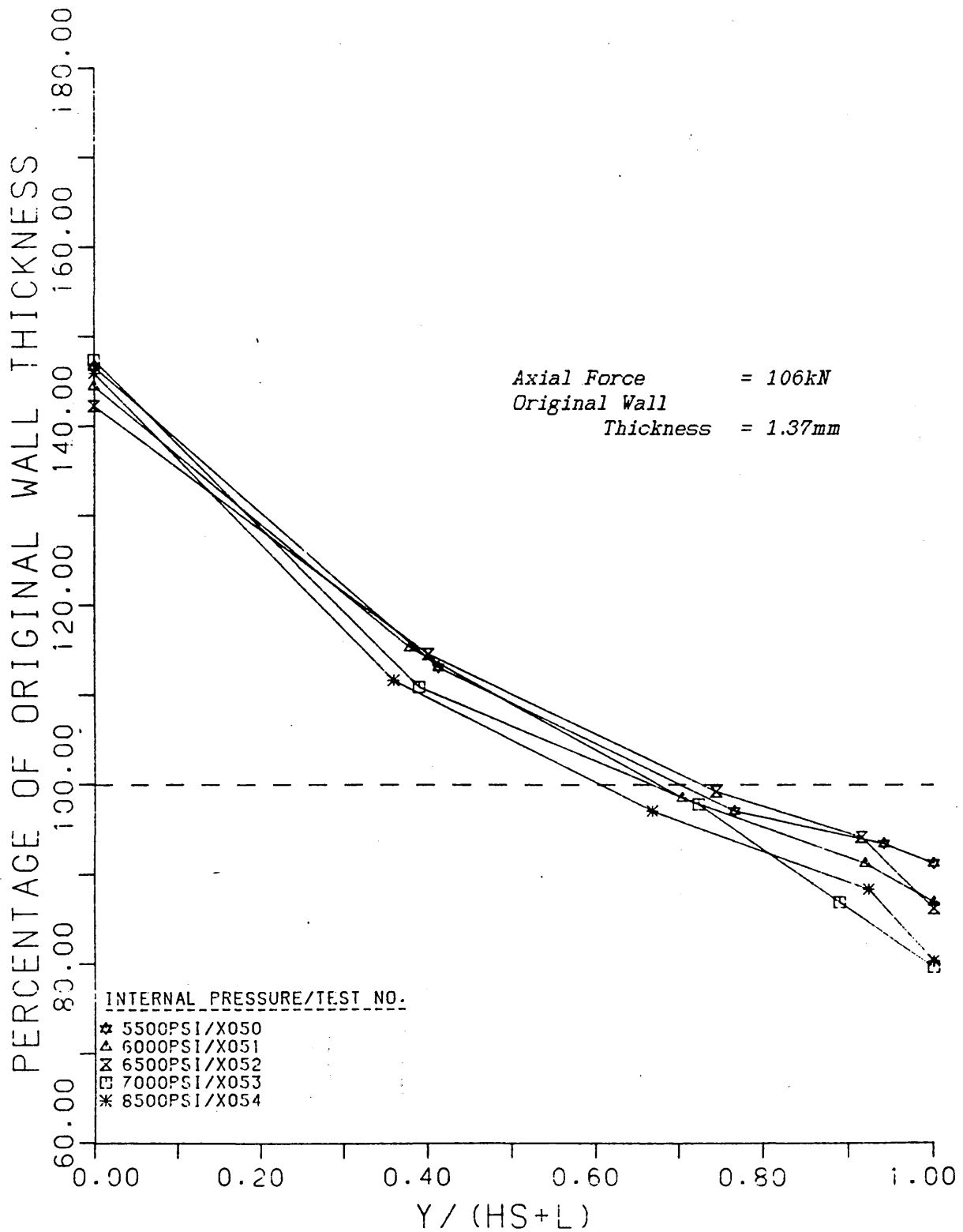


Fig. 55.a.
 The wall thickness distributions along the side branches
 of cross pieces formed at various internal pressures,
 with a constant axial compressive force.

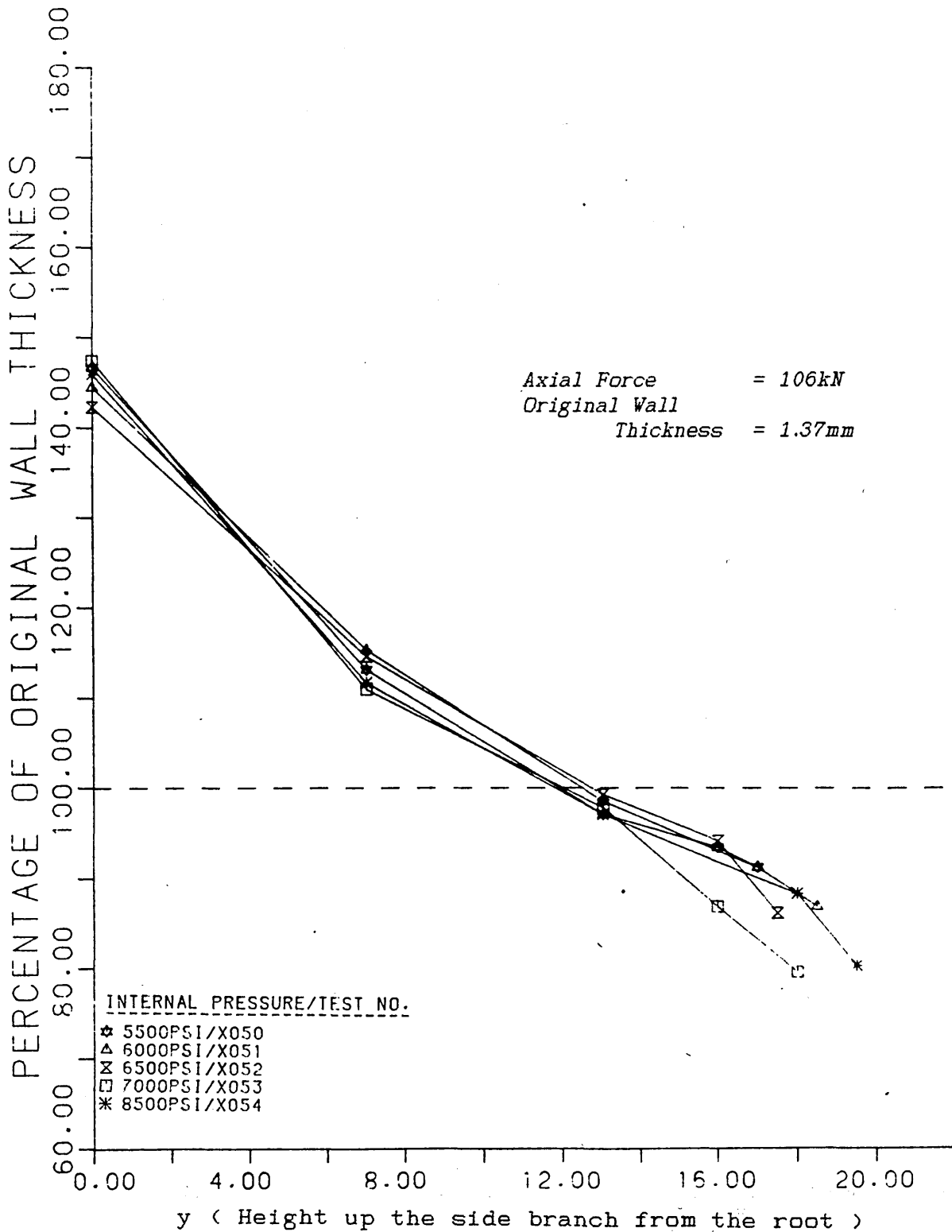


Fig. 55. b.
The wall thickness distributions along the side branches of cross pieces formed at various internal pressures, with a constant axial compressive force.

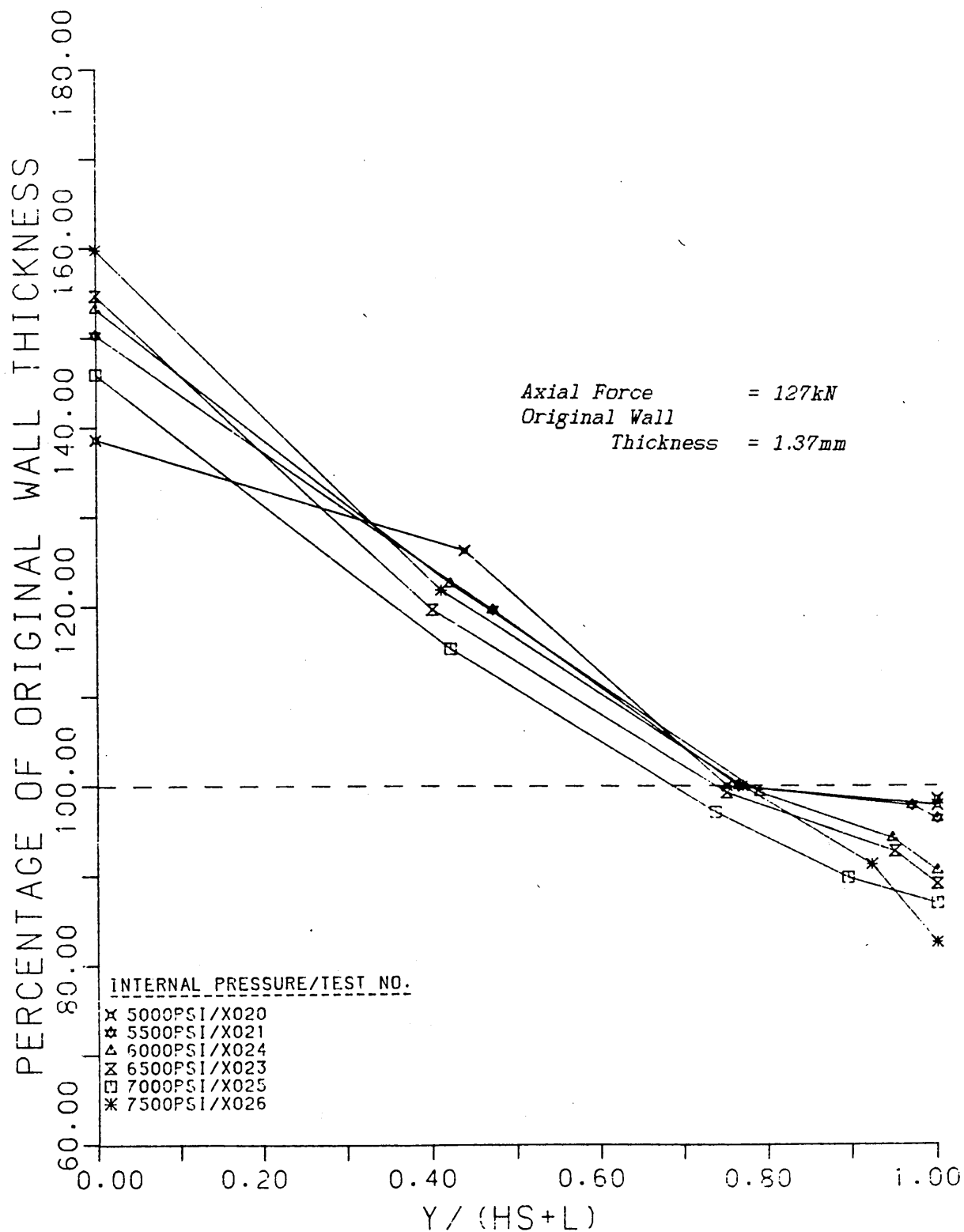


Fig. 56.a.
The wall thickness distributions along the side branches of cross pieces formed at various internal pressures, with a constant axial compressive force.

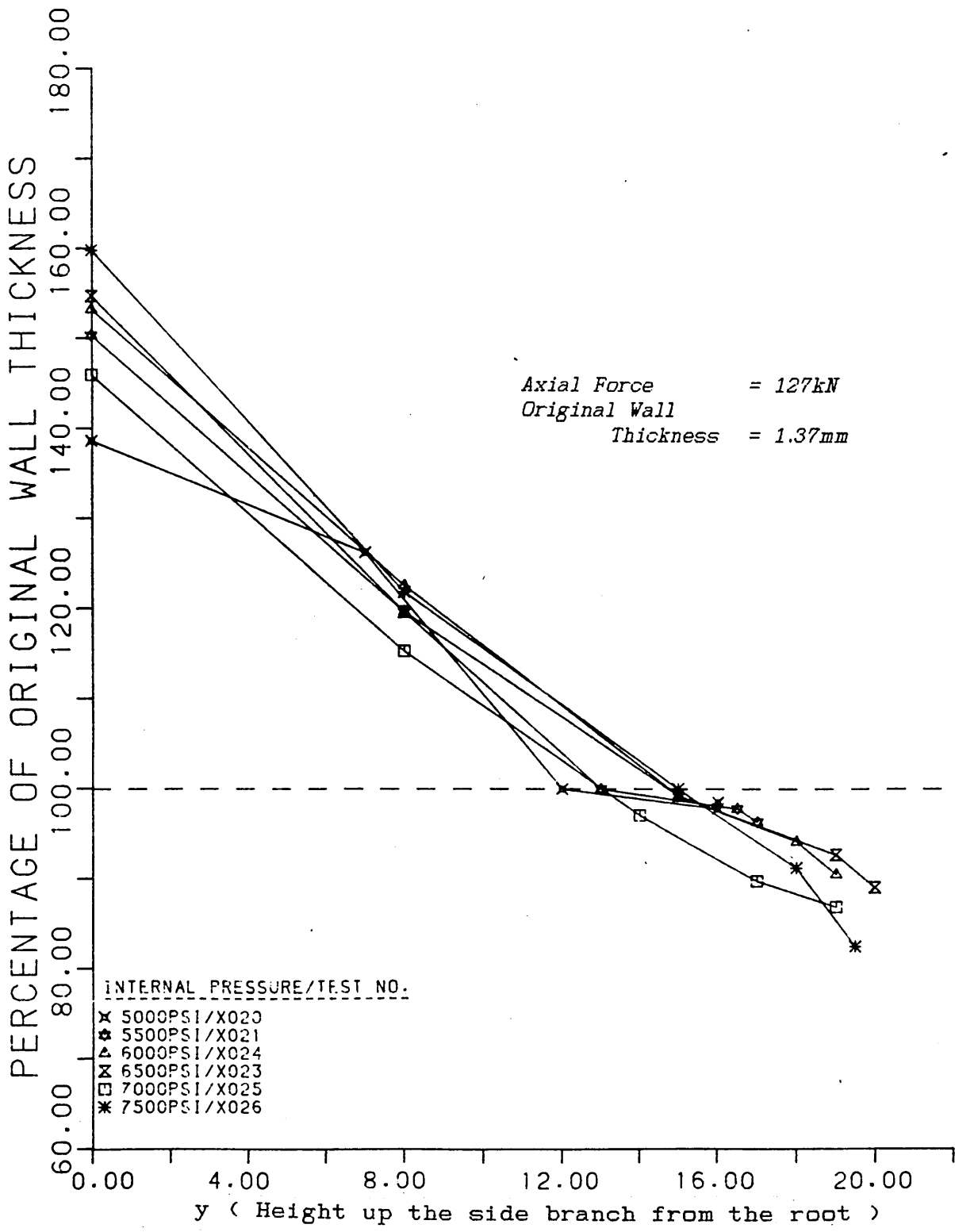


Fig. 56.b.
 The wall thickness distributions along the side branches of cross pieces formed at various internal pressures, with a constant axial compressive force.

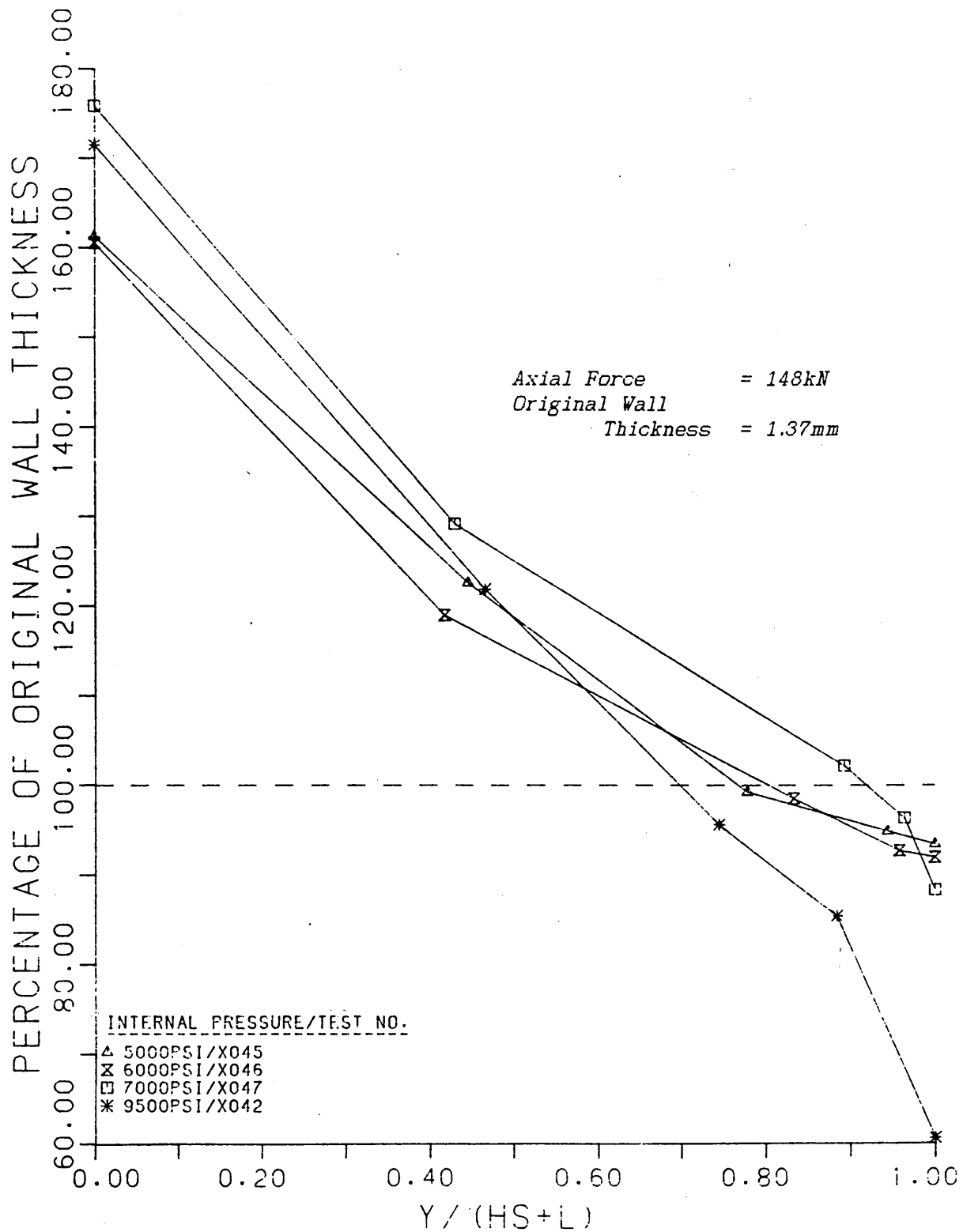


Fig. 57.a.

The wall thickness distributions along the side branches of cross pieces formed at various internal pressures, with a constant axial compressive force.

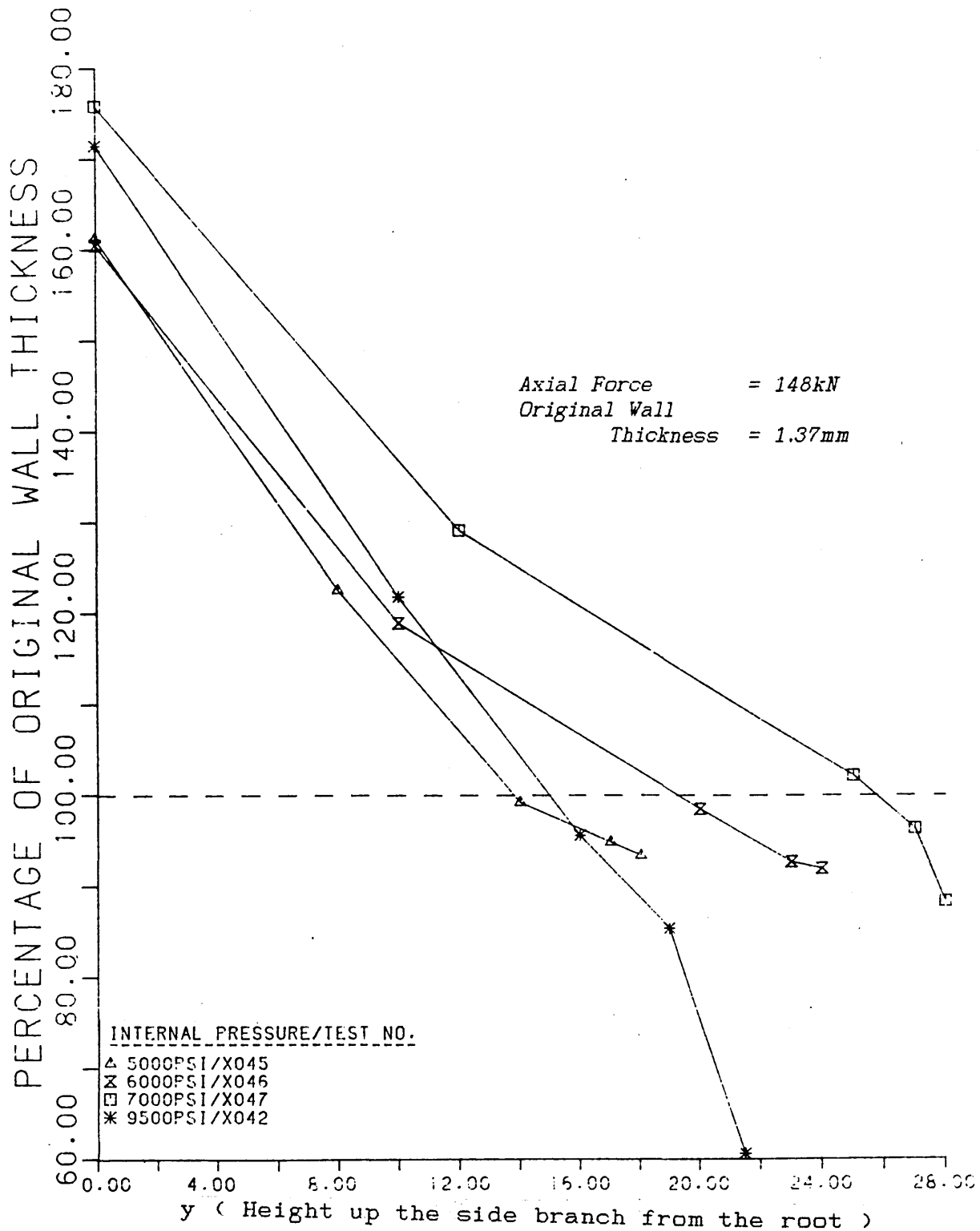


Fig. 57. b.
 The wall thickness distributions along the side branches of cross pieces formed at various internal pressures, with a constant axial compressive force.

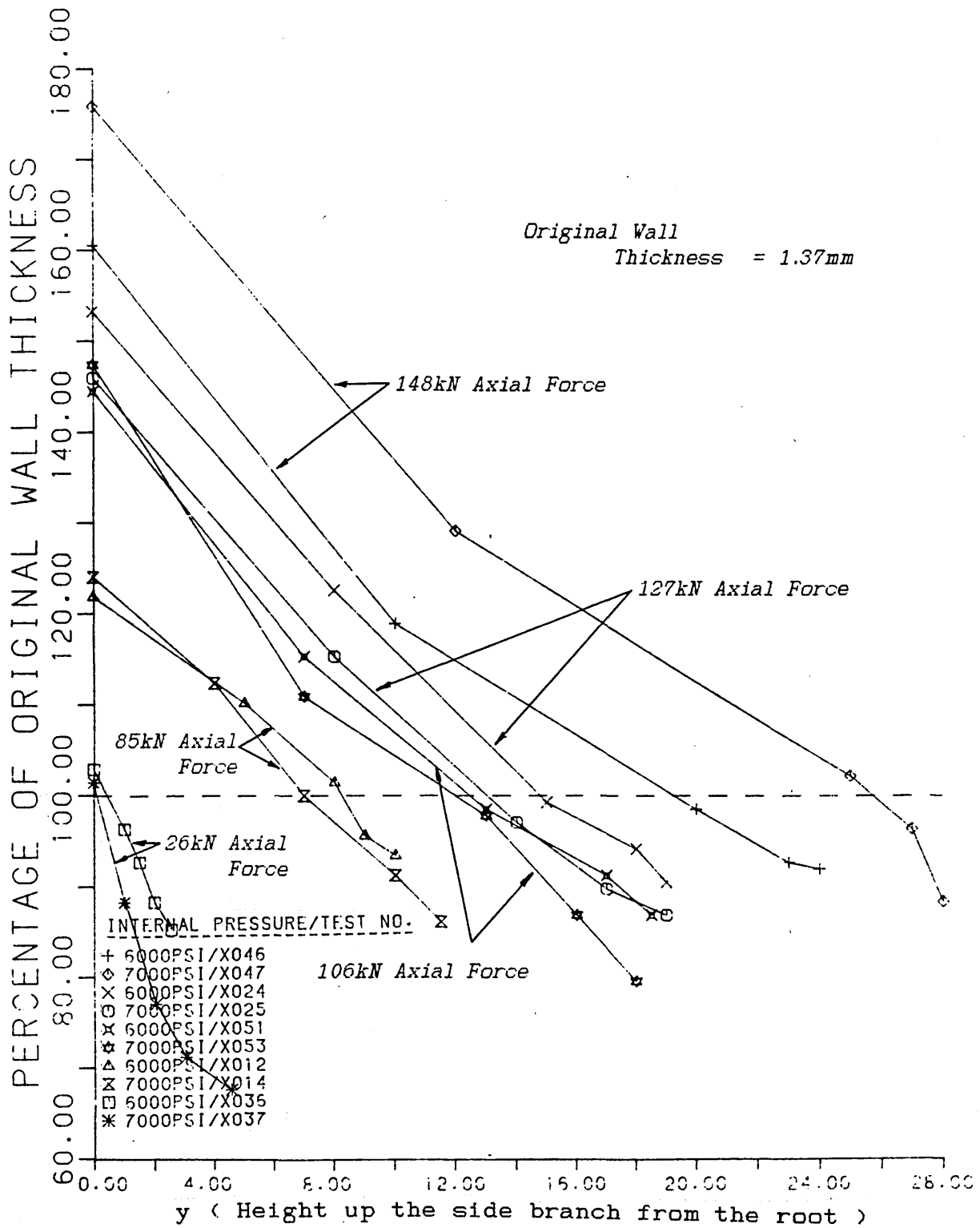


Fig. 58.
The wall thickness distributions along the side branches of cross pieces formed at various internal pressures, and with various axial compressive forces.

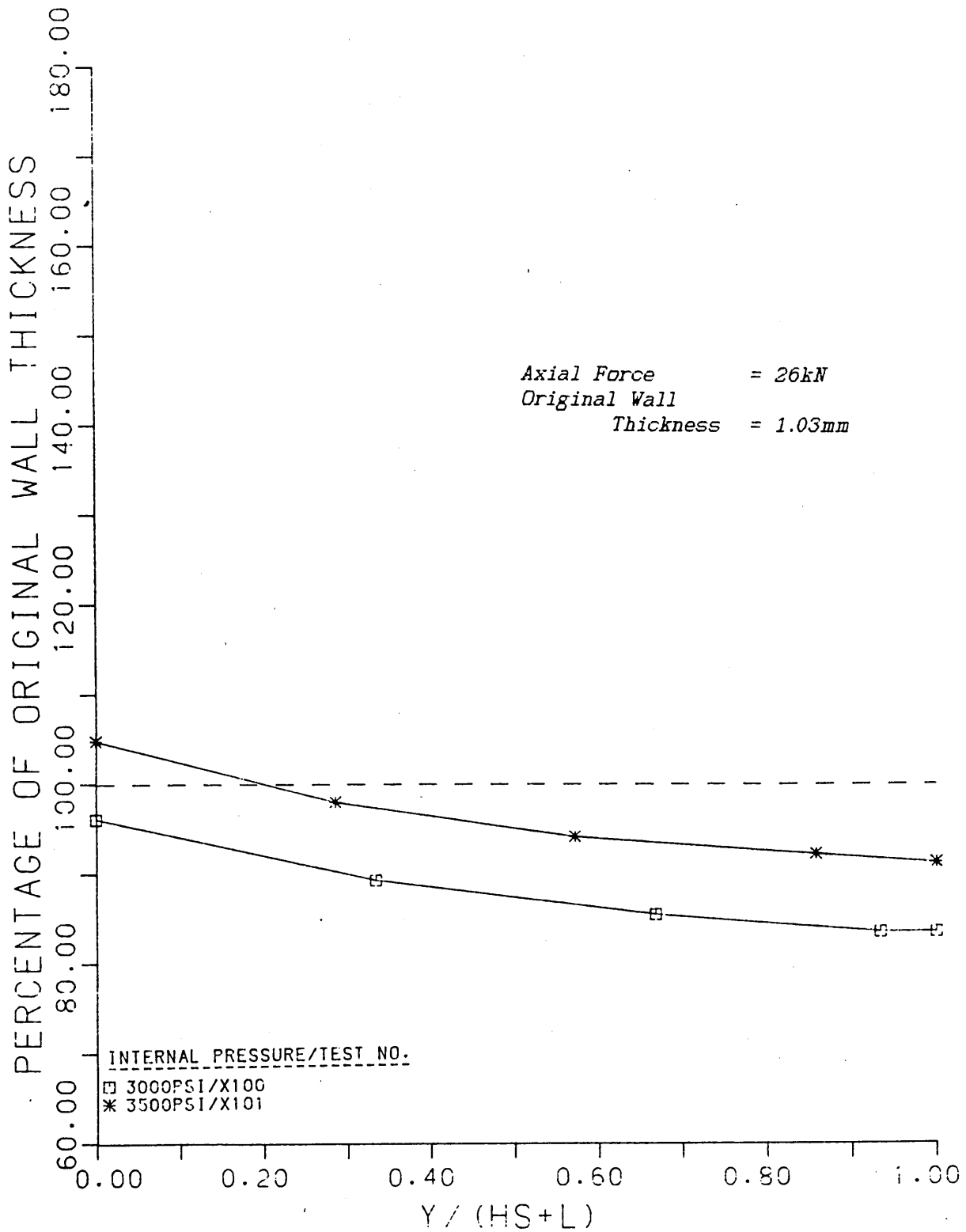


Fig. 59.a.
 The wall thickness distributions along the side branches of cross pieces formed at various internal pressures, with a constant axial compressive force.

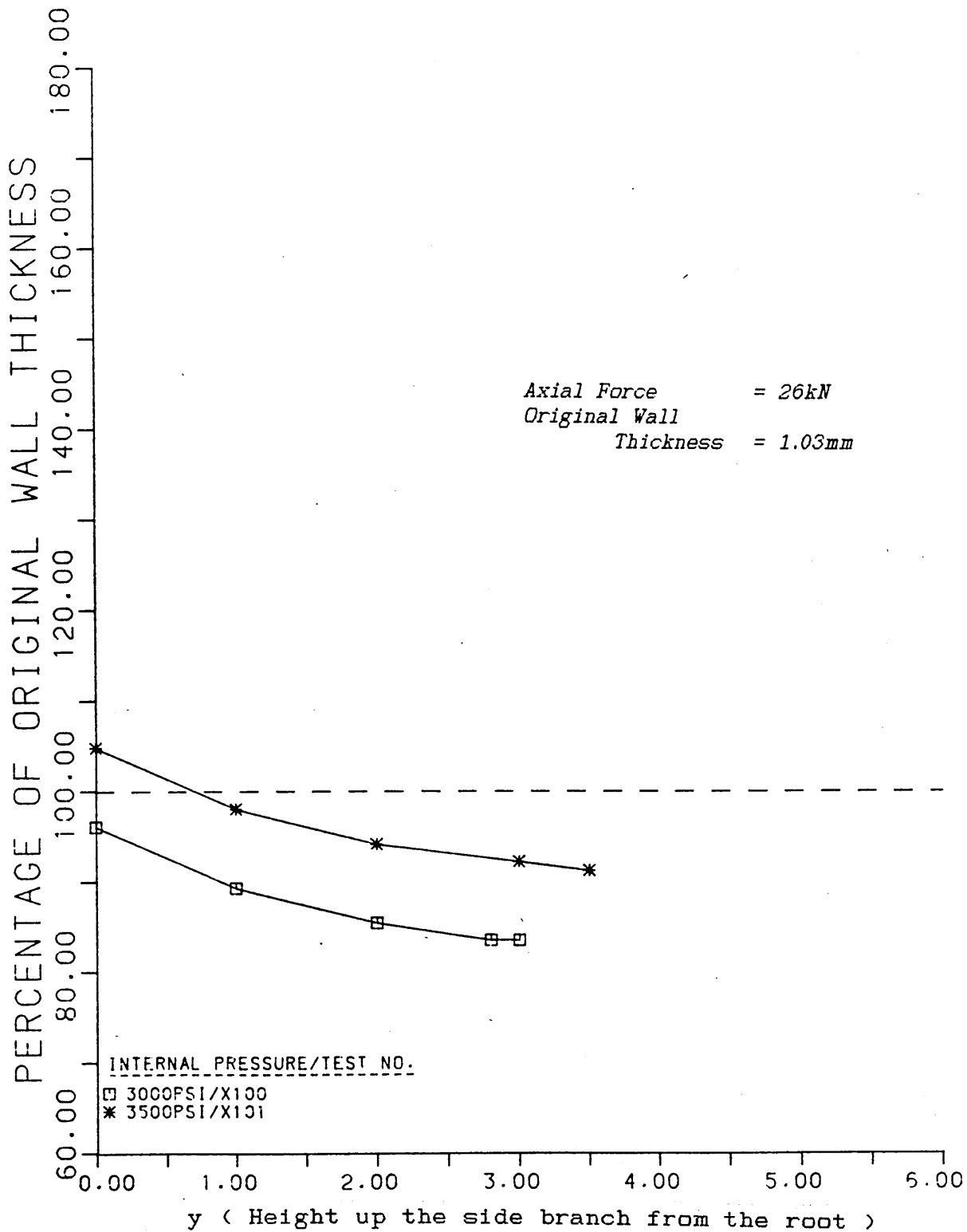


Fig. 59. b.
The wall thickness distributions along the side branches of cross pieces formed at various internal pressures, with a constant axial compressive force.

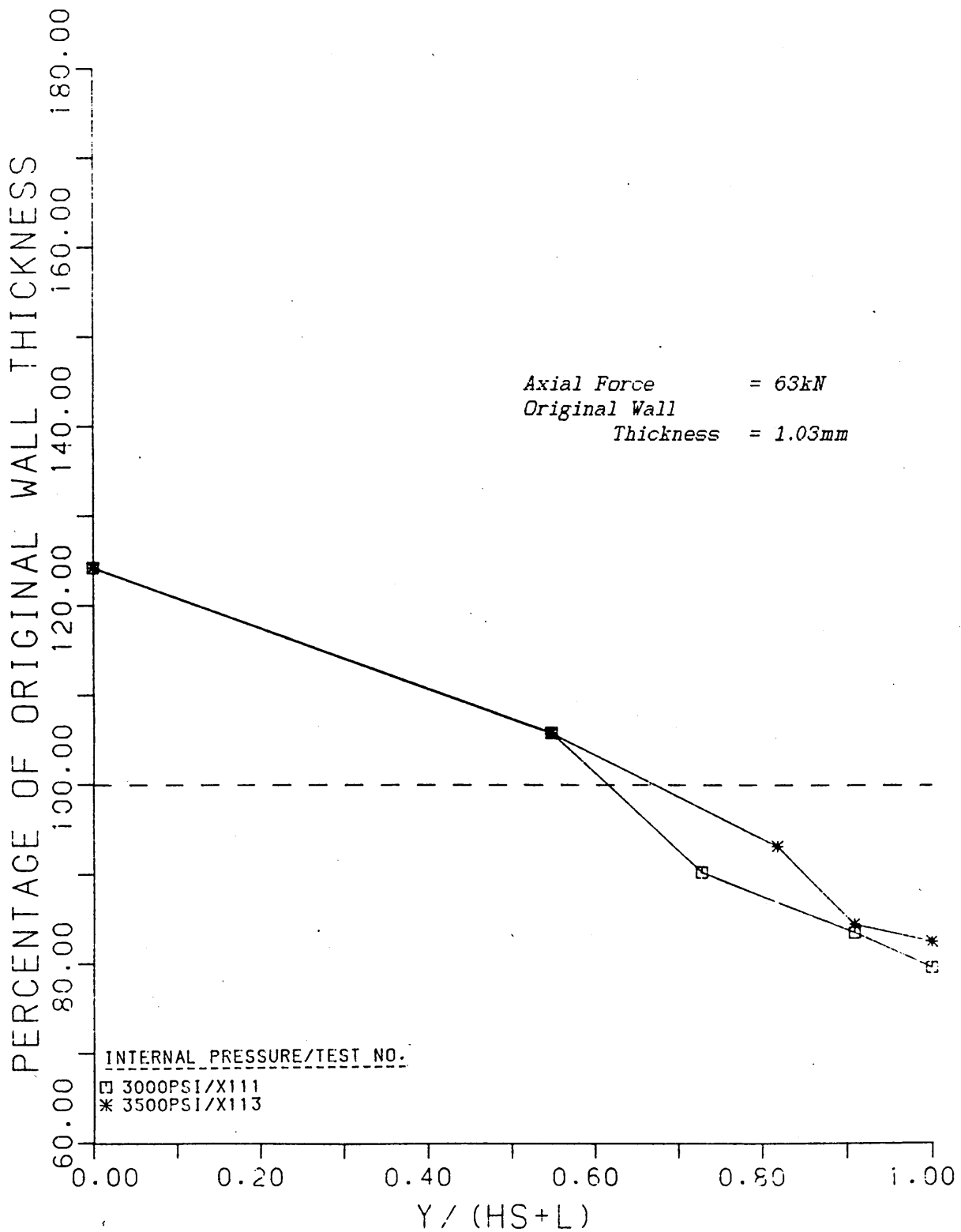


Fig. 60.a.
The wall thickness distributions along the side branches of cross pieces formed at various internal pressures, with a constant axial compressive force.

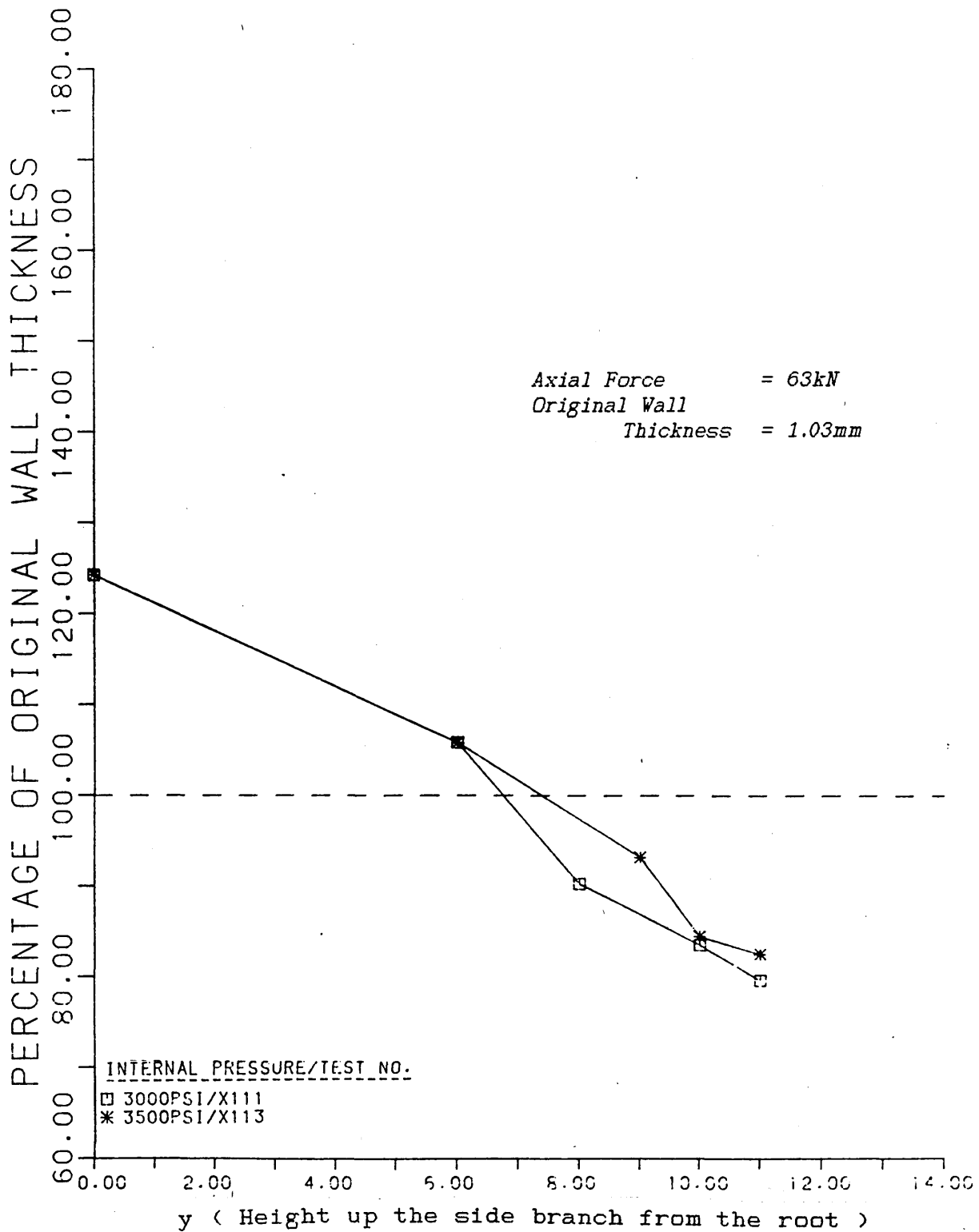


Fig. 60. b.
The wall thickness distributions along the side branches of cross pieces formed at various internal pressures, with a constant axial compressive force.

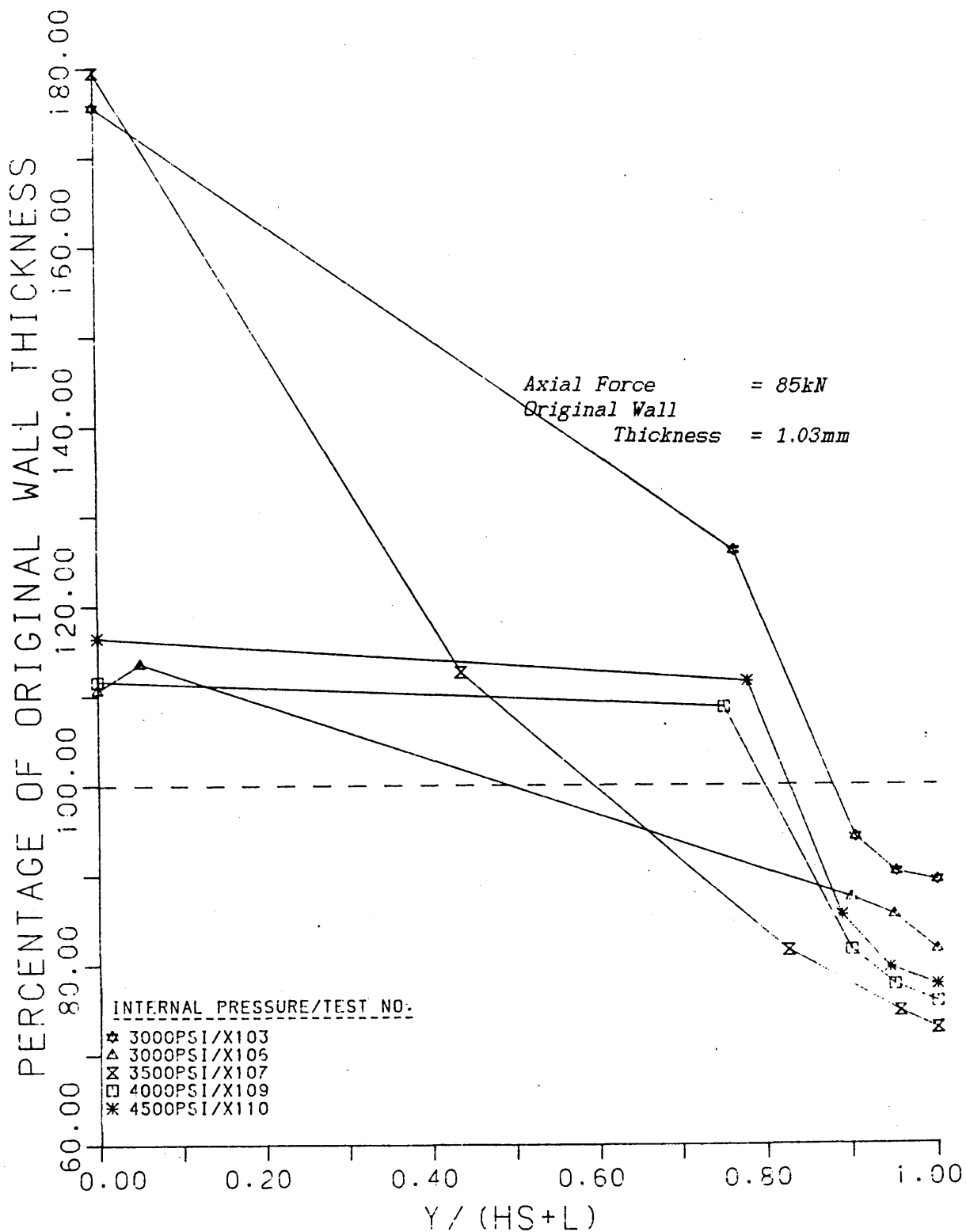


Fig. 61.a.
 The wall thickness distributions along the side branches of cross pieces formed at various internal pressures, with a constant axial compressive force.

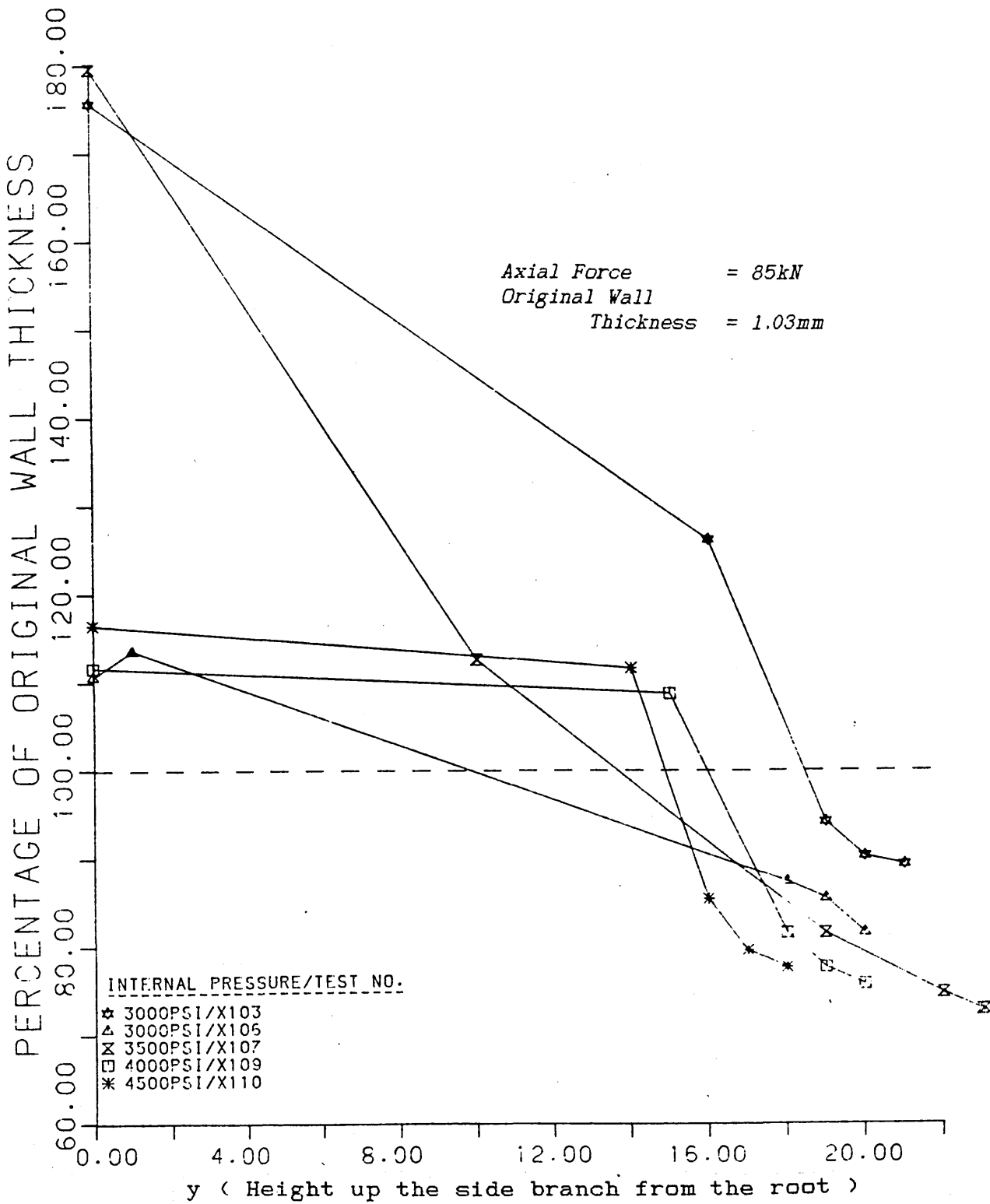


Fig. 61.b.
The wall thickness distributions along the side branches of cross pieces formed at various internal pressures, with a constant axial compressive force.

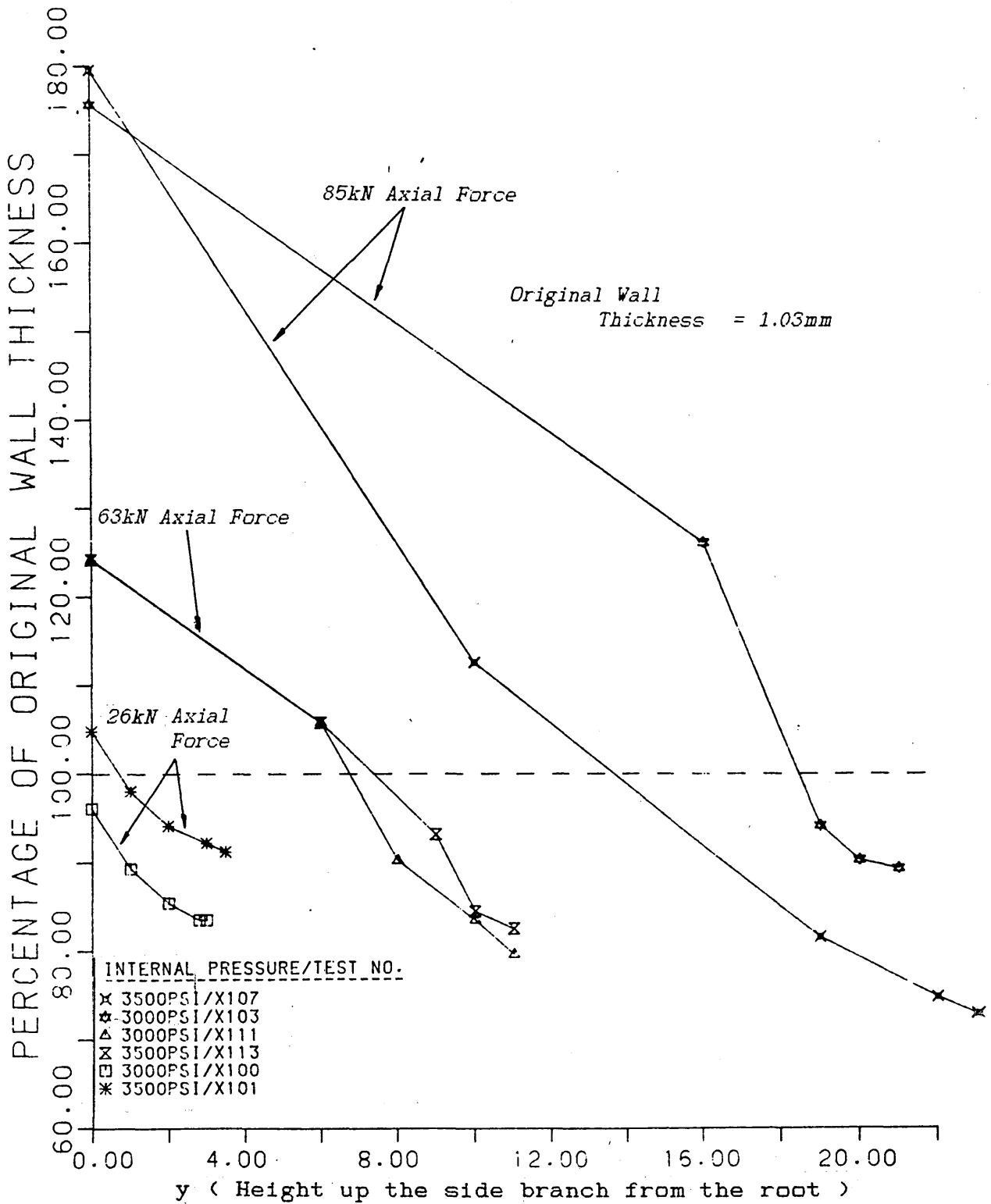


Fig. 62.
The wall thickness distributions along the side branches of cross pieces formed at various internal pressures, and with various axial compressive forces.

5. THEORETICAL WALL THICKNESS DISTRIBUTION

5.1. THEORETICAL ANALYSIS

The following is an extension of the analysis to predict the variation in the wall thickness around the bulge profile presented in references 25 & 26. The theory deals with the expansion of a tubular blank into an axisymmetric component ie. one having the same expansion all around the axis, as well as forming into a side branch. In order to analyse these two cases of bulge forming, the following assumptions are made:

1. the deformation profile at any instant can be described by a circular arc,
2. and the effect of additional material fed into the deformation zone may be taken into account by introducing an apparent strain factor (ASF).

5.1.1. Expansion of a Curved Surface

Referring to Fig. 63.a, the arc ABC of initial uniform thickness t_1 , polar height H_1 and radius of curvature ρ_1 , expands to an arc AB'C of polar height H_2 and radius of curvature ρ_2 . Consider an element with an axial position x_1 and a height of h_1 from the chord AC, on the undeformed arc ABC. On the expanded arc AB'C, this same element has an axial position of x_2 and a height of h_2 from the chord AC.

From geometry:

$$\frac{x_2}{x_0} = \frac{(h_2 + y_2)}{y_2}$$

and

$$\frac{x_1}{x_0} = \frac{(h_1 + y_1)}{y_1}$$

Combining these two equations gives:

$$\frac{x_2}{x_1} = \frac{y_1(h_2 + y_2)}{y_2(h_1 + y_1)} \dots\dots\dots(1)$$

but from geometry, $y_2H_2 = a^2$ and $y_1H_1 = a^2$

Combining these two equations gives:

$$y_2/y_1 = H_1/H_2 \dots\dots\dots(2)$$

Substituting for y_1 and y_2 into equation (1) gives:

$$\frac{x_2}{x_1} = \frac{a^2H_2(h_2 + a^2/H_2)}{H_1a^2(h_1 + a^2/H_1)}$$

$$\frac{x_2}{x_1} = \frac{(H_2h_2 + a^2)}{(H_1h_1 + a^2)} \dots\dots\dots(3)$$

Also from geometry

$$y_1 + h_1 = \frac{x_1^2}{(H_1 - h_1)} \dots\dots\dots(4)$$

and

$$y_2 + h_2 = \frac{x_2^2}{(H_2 - h_2)} \dots\dots\dots(5)$$

Combining equations (4) and (5) with equation (1) gives:

$$\frac{x_2}{x_1} = \frac{y_1(x_2^2/(H_2 - h_2))}{y_2(x_1^2/(H_1 - h_1))}$$

$$= \frac{y_1x_2^2(H_1 - h_1)}{y_2x_1^2(H_2 - h_2)}$$

$$\frac{x_2}{x_1} = \frac{y_2(H_2 - h_2)}{y_1(H_1 - h_1)}$$

But from equation (2) $y_2/y_1 = H_1/H_2$, thus:

$$\frac{x_2}{x_1} = \frac{H_1(H_2 - h_2)}{H_2(H_1 - h_1)} \dots\dots\dots(6)$$

Combining equations (3) and (6) gives:

$$\frac{(H_2h_2 + a^2)}{(H_1h_1 + a^2)} = \frac{H_1(H_2 - h_2)}{H_2(H_1 - h_1)}$$

$$(H_2h_2 + a^2)(H_1 - h_1) = (H_1h_1 + a^2)(H_2 - h_2)H_1/H_2$$

$$H_1H_2h_2 + a^2H_1 - H_2h_1h_2 - a^2h_1 =$$

$$(H_1H_2h_1 - H_1h_1h_2 + a^2H_2 - a^2h_2)H_1/H_2$$

$$-H_1^2 h_1 + H_1^2 h_1 h_2 / H_2 - H_2 h_1 h_2 - a^2 h_1 = -a^2 H_1 h_2 / H_2 - H_1 H_2 h_2$$

$$h_1 (-H_1^2 + H_1^2 h_2 / H_2 - H_2 h_2 - a^2) = -H_1 h_2 (a^2 + H_2^2) / H_2$$

$$h_1 [H_2 (H_1^2 + a^2) + h_2 (H_2^2 - H_1^2)] = H_1 h_2 (a^2 + H_2^2)$$

$$h_1 = \frac{H_1 h_2 (H_2^2 + a^2)}{H_2 (H_1^2 + a^2) + h_2 (H_2^2 - H_1^2)} \quad \dots (7)$$

Substituting for h_1 into equation (3)

$$\begin{aligned} \frac{x_2}{x_1} &= \frac{H_2 h_2 + a^2}{H_1 \frac{H_1 h_2 (H_2^2 + a^2)}{H_2 (H_1^2 + a^2) + h_2 (H_2^2 - H_1^2)} + a^2} \\ &= \frac{H_2 h_2 + a^2}{\frac{H_1^2 h_2 (H_2^2 + a^2) + a^2 H_2 (H_1^2 + a^2) + a^2 h_2 (H_2^2 - H_1^2)}{H_2 (H_1^2 + a^2) + h_2 (H_2^2 - H_1^2)}} \\ &= \frac{(H_2 h_2 + a^2) (H_2 (H_1^2 + a^2) + h_2 (H_2^2 - H_1^2))}{H_1^2 H_2^2 h_2 + a^2 H_1^2 h_2 + a^2 H_1^2 H_2 + a^4 H_2 + a^2 H_2^2 h_2 - a^2 h_2 H_1^2} \\ &= \frac{(H_2 h_2 + a^2) (H_2 (H_1^2 + a^2) + h_2 (H_2^2 - H_1^2))}{(H_2 h_2 + a^2) (H_1^2 H_2 + H_2 a^2)} \\ &= \frac{H_2 (H_1^2 + a^2) + h_2 (H_2^2 - H_1^2)}{H_2 (H_1^2 + a^2)} \\ \frac{x_2}{x_1} &= 1 + \frac{h_2 (H_2^2 - H_1^2)}{H_2 (H_1^2 + a^2)} \quad \dots (8) \end{aligned}$$

5.1.2. Axisymmetric Expansion of a Tubular Blank

Referring to Fig. 63.b, the force equilibrium in the normal direction is given by:

$$\frac{p}{t} = \frac{\sigma_e}{\rho_e} + \frac{\sigma_L}{\rho_L} \quad \dots (9)$$

At this point it is assumed that during the entire deformation process σ_e and σ_L will be connected by:

$$\sigma_e = K \sigma_L \quad \dots (10)$$

$$\text{where } K = (2 - \rho_e / \rho_L)$$

Substituting for σ_e in equation (9) gives:

$$\frac{p}{t} = \frac{K \sigma_L}{\rho_e} + \frac{\sigma_L}{\rho_L}$$

$$\begin{aligned}
\frac{p}{t} &= \frac{K\sigma_L \rho_L + \sigma_L \rho_e}{\rho_e \rho_L} \\
&= \frac{(2 - \rho_e/\rho_L)\sigma_L \rho_L + \sigma_L \rho_e}{\rho_e \rho_L} \\
&= \frac{2\sigma_L \rho_L - \sigma_L \rho_e + \sigma_L \rho_e}{\rho_e \rho_L} \\
&= \frac{2\sigma_L}{\rho_e} \dots\dots\dots(11)
\end{aligned}$$

Now the Levy-Mises plastic flow rule may be written as:

$$\frac{\epsilon_1}{\sigma_1'} = \frac{\epsilon_2}{\sigma_2'} = \frac{\epsilon_3}{\sigma_3'} = \lambda \dots\dots\dots(12)$$

where $\epsilon_1 = \ln \frac{x_2}{x_1}$, $\epsilon_2 = \ln \frac{r}{r_0}$ and $\epsilon_3 = \frac{t}{t_0}$

and σ_1' , σ_2' and σ_3' are the deviatoric components of the principal stresses $\sigma_1 = \sigma_L$, $\sigma_2 = \sigma_e$, and $\sigma_3 = -p$ respectively. The hydrostatic components of the principal stresses is given by $(\sigma_1 + \sigma_2)/3$ where $\sigma_3 = -p$ has been considered negligibly small in comparison to σ_1 and σ_2 .

Thus:

$$\begin{aligned}
\sigma_1' &= \sigma_L - (\sigma_L + \sigma_e)/3 \\
\sigma_2' &= \sigma_e - (\sigma_L + \sigma_e)/3
\end{aligned}$$

Substituting for σ_1' and σ_2' in equation (12) we obtain:

$$\begin{aligned}
\frac{\epsilon_2}{\epsilon_1} &= \frac{\sigma_e - (\sigma_L + \sigma_e)/3}{\sigma_L - (\sigma_L + \sigma_e)/3} \\
&= \frac{3\sigma_e - \sigma_L - \sigma_e}{3\sigma_L - \sigma_L - \sigma_e} \\
&= \frac{2\sigma_e - \sigma_L}{2\sigma_L - \sigma_e} \dots\dots\dots(13)
\end{aligned}$$

Substituting for σ_e from equation (10) gives:

$$\begin{aligned}
\frac{\epsilon_2}{\epsilon_1} &= \frac{2K\sigma_L - \sigma_L}{2\sigma_L - K\sigma_L} \\
&= \frac{2K - 1}{2 - K}
\end{aligned}$$

but $K = (2 - \rho_e/\rho_L)$, so:

$$\begin{aligned} \frac{\epsilon_2}{\epsilon_1} &= \frac{2(2 - \rho_0/\rho_L) - 1}{2 - (2 - \rho_0/\rho_L)} \\ &= \frac{4 - 2\rho_0/\rho_L - 1}{\rho_0/\rho_L} \\ &= \frac{3 - 2\rho_0/\rho_L}{\rho_0/\rho_L} \end{aligned}$$

or $\epsilon_2 = m\epsilon_1$ (14)

where $m = (3 - 2\rho_0/\rho_L)/(\rho_0/\rho_L)$ (15)

From the principle of volume constancy:

$$\epsilon_1 + \epsilon_2 + \epsilon_3 = 0$$

Substituting for ϵ_2 from equation (14) and rearranging gives:

$$\epsilon_3 = -(1+m)\epsilon_1 \quad \text{.....(16)}$$

but $\epsilon_3 = \ln \frac{t}{t_0}$ and $\epsilon_1 = \ln \frac{x_2}{x_1}$

Hence, equation (16) becomes:

$$\begin{aligned} \ln \frac{t}{t_0} &= -(1+m) \ln \frac{x_2}{x_1} \\ &= \ln \left(\frac{x_1}{x_2} \right)^{(1+m)} \end{aligned}$$

so that $t = t_0 \left(\frac{x_1}{x_2} \right)^{(1+m)}$ (17)

Substituting for (x_1/x_2) from equation (8), the current thickness at any point $h_2 = (r - r_0)$ on the bulged profile can be expressed as :

$$t = \frac{t_0}{\left[1 + \frac{h_2(H_2^2 - H_1^2)}{H_2(H_1^2 + a^2)} \right]^{(1+m)}} \quad \text{.....(18)}$$

5.1.3. Asymmetric Bulging of a Tube into a Side Cavity

The theory considers the bulging of a tubular blank such that a side branch is formed having a diameter equal to that of the blank. The successive deformation mode is illustrated schematically in Fig. 64.

during the initial process, the chord length DEF in the axial direction starts to deform from a radius of $\rho_L = \infty$ to ρ_m . In the transverse direction the curved length starts to deform from $\rho_e = r_o$ to ρ_m . ρ_m is the radius of curvature of the common spherical dome that is formed, with a height of H_m . This radius remains constant for the rest of the expansion process.

Referring to Fig. 64.a, and considering the geometry in the axial direction:

$$\begin{aligned} r_o^2 &= (2\rho_m - H_m) H_m \\ \rho_m &= \frac{1}{2}(r_o^2/H_m + H_m) \\ &= \frac{r_o^2 + H_m^2}{2H_m} \end{aligned} \quad \dots\dots\dots(19)$$

In the circumferential direction:

$$\rho_m = r_o + H_m \quad \dots\dots\dots(20)$$

where H_m is the polar height of the dome when $\rho_L = \rho_e = \rho_m$. Hence, combining equations (19) and (20):

$$r_o + H_m = \frac{r_o^2 + H_m^2}{2H_m}$$

$$2H_m r_o + 2H_m^2 - H_m^2 - r_o^2 = 0$$

$$H_m^2 + 2H_m r_o - r_o^2 = 0$$

Solving this quadratic equation for H_m :

$$H_m = \frac{-2r_o \pm \sqrt{4r_o^2 - 4(-r_o^2)}}{2}$$

$$= \frac{-2r_o \pm \sqrt{8r_o^2}}{2}$$

$$H_m = (\sqrt{2} - 1)r_o$$

$$\text{OR } H_m = (-\sqrt{2} - 1)r_o$$

As H_m must be positive:

$$H_m = (\sqrt{2} - 1)r_o \quad \dots\dots\dots(21)$$

Substituting into equation (20):

$$\begin{aligned} \rho_m &= r_o + (\sqrt{2} - 1)r_o \\ \rho_m &= \sqrt{2}r_o \end{aligned} \quad \dots\dots\dots(22)$$

During the initial stages of bulging, until the polar height becomes H_m ,

the thickness distribution along the profile in the axial direction is given by equation (18). At any intermediate stage the value of m is calculated from equation (15) using the prevailing values of ρ_L and ρ_e . When the spherical dome of height H_m has formed, with a radius of curvature ρ_m , then $\rho_L = \rho_e = \rho_m$ and therefore $m = 1$

Hence, equation (18) becomes:

$$t = \frac{t_o}{\left[1 + \frac{h_2(H_m^2 - H_1^2)}{H_m(H_1^2 + r_o^2)}\right]^2} \quad \dots\dots\dots(23)$$

This gives the thickness distribution along the deformed profile on the spherical cap.

5.1.4. Bulging after $\rho = \rho_m$

Once a spherical cap is formed, further expansion takes place as depicted in Fig. 64.b. This newly expanded bulge consists of two parts - a tubular branch with radius r_o , and a new spherical cap with radius of curvature ρ_m - both being formed from the original spherical cap. An element dl on the original cap expands to form the ring element dL on the tubular branch. Applying the principle of volume constancy:

$$2\pi x.dl.t = 2\pi r_o.dL.t_1$$

where t_1 is the wall thickness of the ring element on the tubular branch.

Rearranging and taking logs. gives:

$$\ln(r_o/x) + \ln(t_1/t) + \ln(dL/dl) = 0 \quad \dots\dots\dots(24)$$

But for this type of deformation

$$\ln(r_o/x) = \ln(dL/dl)$$

at any point and hence:

$$\begin{aligned} \ln(t/t_1) &= 2.\ln(r_o/x) \\ &= \ln(r_o/x)^2 \end{aligned}$$

so that $t_1 = t(x/r_o)^2$ (25)

Also since $\ln(r_o/x) = \ln(dL/dl)$

we have $r_o/x = dL/dl$

But from geometry:

$$x = \rho_s.\sin\theta$$

and $dl = \rho_s.d\theta$

hence: $\frac{r_o}{x} = \frac{r_o}{\rho_s.\sin\theta} = \frac{dL}{\rho_s.d\theta}$

so that:

$$r_o.\operatorname{cosec}\theta.d\theta = dL$$
(26)

Integrating equation (26) gives:

$$\begin{aligned} L &= \int r_o.\operatorname{cosec}\theta.d\theta \\ &= r_o.\ln(\tan(\theta/2)) + C \end{aligned}$$

where C is the constant of integration, and can be evaluated by considering the boundary conditions. Referring to Fig. 64.c, points D and F at the base of the original cap form the same points on the expanded branch. These points lie at an angle of θ_o , and on the expanded cap have a height on the tubular branch of $L = 0$. Substituting these values into the equation gives:

$$0 = r_o.\ln(\tan(\theta_o/2)) + C$$

$$C = -r_o.\ln(\tan(\theta_o/2))$$

Therefore $L = r_o.\ln(\tan(\theta/2)) - r_o.\ln(\tan(\theta_o/2))$

Now considering points G and H on the original cap, at an angle of θ_L . On the expanded branch these points lie on the junction between the tubular branch and the spherical cap. The height of these points on the expanded branch is $L = -L_o$ (negative because θ_L is less than θ_o). Substituting in these values gives

$$-L_o = r_o \cdot \ln(\tan(\theta_L/2)) - r_o \cdot \ln(\tan(\theta_o/2))$$

$$\frac{-L_o}{r_o} = \ln \frac{\tan(\theta_L/2)}{\tan(\theta_o/2)}$$

Rearranging gives:

$$\theta_L = 2 \cdot \tan^{-1}[\tan(\theta_o/2) \cdot \exp(-L_o/r_o)] \quad \dots(27)$$

Now substituting $(x/r_o) = (\rho_m \cdot \sin\theta_L/r_o)$ into equation (25), the wall thickness at the junction of the tubular branch of length L_o , and the spherical dome of radius of curvature ρ_m is found to be:

$$t_L = (t \cdot \rho_m^2 \cdot \sin^2\theta_L) / r_o^2 \quad \dots\dots\dots(28)$$

where t , which is the thickness on the original spherical cap at $\theta = \theta_L$ is given by equation (23) where $h_2 = h_{\theta_L} = H_m - \rho_m(1 - \cos\theta_L)$.

Once the value of the wall thickness at the junction of the tubular branch and the spherical cap is found, the thickness distribution along the spherical cap can be determined in the same manner as described above i.e:

$$t' = \frac{t_L}{\left[1 + \frac{h_o(H_m^2 - H_1^2)}{H_m(H_1^2 + a^2)}\right]^2} \quad \dots\dots\dots(29)$$

where t' is the wall thickness of the expanded spherical cap at a height of h_o from the junction of the tubular branch and the spherical dome - see Fig. 64.c. h_o varies from 0 at the junction, to H_m at the tip of the dome.

5.1.5. The Effect of Axial Deformation

Feeding new material into the deformation zone has two effects on the resulting bulge. The deformation causes thickening of the wall along the whole length of the blank. During initial bulging, until the spherical dome is formed, this causes thickening along the cap. Once the spherical dome of height H_m and radius of curvature ρ_m is formed, any increase in the amount of axial deformation has no effect on the cap, but is simply used to form the tubular branch. The amount of deformation that effects the thickness of the spherical cap, can be evaluated by equating the displaced volume to the volume of the bulges:

$$\text{Volume due to displacement } dx_1 = \pi r_o^2 dx_1$$

The volume of the spherical cap can be obtained by integrating the area of a semi-circle ($x^2 + y^2 = r^2$) about its diameter, between the limits $(\rho_m - H_m)$ and ρ_m . ie.

$$dV/dx = \pi y^2 = \pi(r^2 - x^2)$$

$$\begin{aligned} \text{Volume of spherical cap} &= \int_{\rho_m - H_m}^{\rho_m} \pi(r^2 - x^2) dx \\ &= \left[\pi(r^2 x - x^3/3) \right]_{\rho_m - H_m}^{\rho_m} \\ &= \pi(\rho_m^2 \rho_m - \rho_m^3/3) - \pi(\rho_m^2(\rho_m - H_m) - (\rho_m - H_m)^3/3) \\ &= \pi(2\rho_m^3/3 - \rho_m^2(\rho_m - H_m) + (\rho_m - H_m)^3/3) \end{aligned}$$

Equating the two volumes and substituting $\rho_m = 2.r_o$ and

$H_m = (\sqrt{2} - 1)r_o$ gives:

$$\begin{aligned} dx_1 &= 4\sqrt{2}.r_o/3 - 2r_o + r_o/3 \\ &= 0.219 r_o \dots\dots\dots(30) \end{aligned}$$

Therefore, the axial deformation will cause an increase in the wall thickness of the cap from the start of the deformation until the axial displacement of each end of the tube equals $0.219 r_o$. After this further

axial deformation will contribute towards forming the wall of the tubular branch. The thickness distribution on the spherical cap along the longitudinal axis previously obtained is multiplied by the apparent strain factor to allow for the thickening that occurs. This apparent strain factor is given by the ratio of the original length to the compressed length of the blank.

Note that this applies for the forming of both tee pieces and cross pieces. In the case of forming cross pieces the deformation occurring at each end of the tube is equated to the volumes of the two spherical caps formed. For tee pieces, half the deformation at the end of the tube is equated to the volume of the one spherical cap formed. The other half of the deformation contributes to the thickening of the main branch opposite the side branch.

Axial deformation in excess of dx_1 will contribute towards forming the wall of the tubular part of the branch. The wall thickness at the root of the branch will be governed by the apparent strain factor prevailing at that stage. As each plunger moves inwards by dx_2 , the wall of the blank thickens, and hence, the resulting height, L_0 , of the branch formed from the deformation, becomes smaller than the axial displacement, dx_2 . The relationship between dx_2 and L_0 may be obtained by equating the displaced volume of the blank due to dx_2 , to the volume of the tubular branch formed, of height L_0 and thickness varying from t_0 at the junction with the previously formed cap, to t' at the root. Thus:

$$dx_2 \cdot t_0 = L_0(t' + t_0)/2$$

but $t' = f \cdot t_0$ so that:

$$dx_2 \cdot t_0 = L_0 \cdot t_0(1 + f)/2$$

By rearranging, the length of the tubular branch formed, L_0 , can be obtained from the apparent strain factor, f :

$$L_0 = \frac{2 \cdot dx_2}{(1+f)} \dots\dots\dots(31)$$

where $f = \frac{\text{original length of the blank}}{\text{deformed length of the blank}}$

The effect of axial deformation is shown diagrammatically in Fig. 65. This illustrates a blank, with a spherical cap and tubular branch already formed due to internal pressure, subjected to various degrees of deformation.

5.2. APPLICATION OF THE THEORY

For different stages in the bulging process, different equations have to be used to determine the thickness distribution around the bulge. To illustrate this the bulge profiles will be determined for three different examples. These are the three different cases that can be obtained which are:

1. The formation of a dome of height H_2 , which is less than H_m , and of radius of curvature, in the longitudinal direction, ρ_L which is greater than ρ_m .
2. The formation of a spherical dome of height H_m , and radius of curvature ρ_m .
3. The formation of a spherical dome of height H_m , and radius of curvature ρ_m , and a tubular branch of length L_0 .

These are illustrated in Fig. 66, which shows the various bulges formed from the effect of internal pressure alone and also from the added effect of axial deformation. For these three cases the analysis will be based on the following dimensions:

$$\text{Original Length} = 107 \text{ mm}$$

$$\text{Original Radius} = 12.06 \text{ mm}$$

5.2.1. For Case 1

the equation that applies in this case is equation (18):

$$t = \frac{t_0}{\left[\frac{1 + h_2(H_2^2 - H_1^2)}{H_2(H_1^2 + a^2)} \right]^{(1+m)}} \dots\dots\dots(18)$$

$$\text{where } m = \frac{(3 - 2\rho_e/\rho_L)}{\rho_e/\rho_L} \dots\dots\dots(15)$$

$$\text{and } a = r_0$$

When considering the thickness distribution in the longitudinal direction, $H_1=0$. Therefore equation (18) can be simplified to:

$$t = \frac{t_0}{\left[\frac{1 + h_2(H_2^2)}{H_2(r_0^2)} \right]^{(1+m)}}$$

Now considering a bulge height, H_2 , equal to 3mm.

$$\rho_e = r_0 + H_2$$

$$= 15.06 \text{ mm}$$

$$\rho_L = (r_0^2 + H_2^2)/2H_2$$

$$= 25.7 \text{ mm}$$

$$\rho_e/\rho_L = 15.06/25.7$$

$$= 0.586$$

$$\text{From equation (15)} \quad m = (3 - 2 \times 0.586)/0.586$$

$$= 3.12$$

$$(H_2/r_0)^2 = (3/12.06)^2$$

$$= 0.062$$

Hence the wall thickness ratio is given by:

$$\frac{t}{t_0} = \frac{1.0}{[1 + 0.062(h_2/H_2)]^{4.12}}$$

This can be evaluated for various values of (h_2/H_2) ranging from 0 to 1.0. The wall thickness ratios thus obtained are shown in Table 2.

h_2/mm	0.0	0.6	1.2	1.8	2.4	3.0
h_2/H_2	0.0	0.2	0.4	0.6	0.8	1.0
t/t_0	1.0	0.950	0.904	0.860	0.819	0.780

TABLE 2

5.2.1. For Case 2

For this case, when $\rho_L = \rho_0 = \rho_*$, equation (23) applies:

$$t = \frac{t_0}{\left[1 + \frac{h_2(H_*^2 - H_1^2)}{H_* (H_1^2 + r_0^2)} \right]^2} \dots\dots\dots(23)$$

where $H_* = (\sqrt{2} - 1)r_0$
 $= 5.0 \text{ mm}$

Again, considering the wall thickness in the longitudinal direction,

$H_1 = 0$, so that:

$$\frac{t}{t_0} = \frac{1.0}{\left[1 + \frac{h_2}{H_* (r_0)} \right]^2}$$

$$\frac{H_2^2}{r_0^2} = \frac{((\sqrt{2} - 1)r_0)^2}{r_0^2}$$

$$= 0.172$$

Therefore, for this case, the thickness distribution around the spherical cap is given by:

$$\frac{t}{t_0} = \frac{1.0}{[1 + 0.172 (h_2/H_*)]^2}$$

The values of the wall thickness ratios are shown in TABLE 3 for values of (h_z/H_m) ranging from 0.0, at the root of the bulge, to 1.0, at the tip of the spherical cap.

h_z/mm	0.0	1.0	2.0	3.0	4.0	5.0
h_z/H_m	0.0	0.2	0.4	0.6	0.8	1.0
t/t_o	1.0	0.935	0.875	0.822	0.773	0.728

TABLE 3

5.2.3. For Case 3

This case involves rather more calculation than the previous two cases. The original cap has been further expanded to form a new cap and a tubular branch. Now considering an element that forms part of the junction between the spherical cap and the tubular branch. On the original cap this element would have been at an angle of θ_L . This angle can be evaluated from equation (27), considering, for this example, that a branch length, L_o , of 3mm is formed.

$$\theta_L = 2 \cdot \tan^{-1} [\tan(\theta_o/2) \cdot \exp(-L_o/r_o)] \quad \dots(27)$$

$$\text{where } \theta_o = \sin^{-1}(r_o/\rho_m)$$

$$= \sin^{-1}(r_o/2 \cdot r_o) = 45^\circ$$

$$\theta_L = 2 \cdot \tan^{-1} [\tan(45^\circ/2) \cdot \exp(-3/12.06)]$$

$$= 35^\circ 48'$$

This angle corresponds to a polar height, h_{eL} , on the original spherical cap of:

$$h_{eL} = H_m - \rho_m(1 - \cos\theta_L)$$

$$\text{where } \rho_m = \sqrt{2} \cdot r_o = 17.06 \text{ mm}$$

$$\text{and } H_m = 5.0 \text{ mm}$$

$$\begin{aligned}
 h_{eL} &= 5.0 - 17.06(1 - \cos(35^\circ 48')) \\
 &= 1.78 \text{ mm}
 \end{aligned}$$

the wall thickness of this element on the original cap can now be obtained, using the equation used for Case 2, and substituting $h_2 = h_{eL}$ ie:

$$\begin{aligned}
 \frac{t}{t_o} &= \frac{1.0}{\left[1 + \frac{h_{eL}}{H_m} \left(\frac{H_m}{r_o} \right)^2 \right]^2} \\
 &= \frac{1.0}{[1 + (1.78/5)0.172]^2} \\
 &= 0.888
 \end{aligned}$$

This is the wall thickness of the element on the original spherical cap. As the cap is expanded to form a tubular branch, of length 3mm, and a new cap, this element expands to form part of the junction. The new thickness of this element on the expanded cap can be found from equation (28):

$$t_L = (t \cdot \rho_s^2 \cdot \sin^2 \theta_L) / r_o^2$$

substituting for $\rho_s = \sqrt{2} \cdot r_o$

gives $t_L = 2 \cdot t \cdot \sin^2 \theta_L$

Thus $t_L = 2 \times 0.888 t_o \times \sin^2(35^\circ 48')$

$$t_L = 0.608 t_o$$

The thickness around the new cap can be found using a similar method as Case 2

$$\begin{aligned}
 \frac{t'}{t_o} &= \frac{t_L}{\left[1 + \frac{h_{eL}}{H_m} \left(\frac{H_m}{r_o} \right)^2 \right]^2} \\
 \frac{t'}{t_o} &= \frac{0.608}{[1 + 0.172(h_{eL}/H_m)]^2}
 \end{aligned}$$

Values for the wall thickness ratio around the new cap are shown in TABLE 4, for h_0/H_0 ranging from 0 to 1.0. Note that these values are the same as the values in TABLE 3 multiplied by t_L/t_0 (0.608).

h_0/mm	0.0	1.0	2.0	3.0	4.0	5.0
h_0/H_0	0.0	0.2	0.4	0.6	0.8	1.0
t'/t_0	0.608	0.568	0.532	0.500	0.470	0.443

TABLE 4

To evaluate the wall thickness along the tubular branch, the process to find t_L must be repeated. TABLE 5 shows values obtained at a polar height of L , where L varies from 0.0 at the root, to L_0 at the junction.

L	θ_L	$h_{\theta L}$	t/t_0	t_L/t_0
0.0	45.0	0.0	1.0	1.0
1.0	41.74	0.66	0.956	0.847
2.0	38.67	1.25	0.919	0.717

TABLE 5

The wall thickness distribution around the bulge profile is shown graphically in Fig. 67, for all three cases. The graph is generally labelled t/t_0 against y which corresponds to:

FOR CASE 1 $t/t_0 = t/t_0$ from TABLE 2

$y = h_2$ from TABLE 2

FOR CASE 2 $t/t_o = t'/t_o$ from TABLE 3
 $y = h_z$ from TABLE 3

FOR CASE 3 $t/t_o = t'/t_o$ from TABLE 4
 $y = (h_e \text{ from TABLE 4}) + L_o$
 $= h_e + 3\text{mm}$

{ for the
spherical
cap

also $t/t_o = t_L/t_o$ from TABLE 5
 $y = L$ from TABLE 5

{ for the
tubular branch

Note that for Case 3, the graph is made up of two parts, one for the spherical cap, and another for the tubular branch

5.2.4 The Effect of Axial Deformation

From the theory - see Section 5.1.5. - the initial effect of the axial deformation is to cause thickening of the cap. This continues until:

$$\begin{aligned} dx_1 &= 0.219r_o \\ &= 2.64 \text{ mm} \end{aligned}$$

At this stage the deformed length of the blank will be:

$$\begin{aligned} \text{Deformed Length} &= 107 - 2 \cdot dx_1 \\ &= 101.72 \text{ mm} \end{aligned}$$

The modified values for the wall thickness are obtained by multiplying the values previously obtained by the **Apparent Strain Factor (f)**. This is given by the ratio of the original length over the deformed length of the blank.

$$\begin{aligned} f &= 107/101.72 \\ &= 1.052 \end{aligned}$$

FOR CASE 1

h_2/mm	0.0	0.6	1.2	1.8	2.4	3.0
Orig. t/t_0	1.0	0.950	0.904	0.860	0.819	0.780
Mod. t/t_0	1.052	0.999	0.951	0.905	0.862	0.821

FOR CASE 2

h_2/mm	0.0	1.0	2.0	3.0	4.0	5.0
Orig. t/t_0	1.0	0.935	0.875	0.822	0.773	0.728
Mod. t/t_0	1.052	0.984	0.921	0.865	0.813	0.766

FOR CASE 3

h_2/mm	0.0	1.0	2.0	3.0	4.0	5.0
Orig. t'/t_0	0.608	0.568	0.532	0.500	0.470	0.443
Mod. t'/t_0	0.640	0.598	0.560	0.526	0.494	0.466

L	Orig. t_L/t_0	Mod. t_L/t_0
0.0	1.0	1.052
1.0	0.847	0.891
2.0	0.717	0.754

TABLE 6

*The wall thickness distribution around the bulge profile
for the three different cases with (Mod.) and without (Orig.)
the added effect of axial deformation*

The modified wall thicknesses are shown in TABLE 6 for all three cases. The original values have simply been multiplied by 1.052 to obtain the modified values.

Any additional deformation will cause a tubular branch to be formed. The theoretical length of this tubular branch can be calculated from the amount of deformation using equation (31). Considering a final deformed length of the blank of 70mm:

$$\begin{aligned}
 \text{Then} \quad f &= 107/70 \\
 &= 1.529 \\
 dx_1 &= 2.64 \text{ mm} \\
 \text{Therefore} \quad dx_2 &= (107 - 70)/2 - 2.64 \text{ mm} \\
 &= 15.86 \text{ mm} \\
 L_D &= \frac{2 \cdot dx_2}{(1 + f)} \dots\dots\dots(31) \\
 &= \frac{2 \times 15.86}{(1 + 1.529)} \text{ mm} \\
 &= 12.5 \text{ mm}
 \end{aligned}$$

Therefore, a tubular branch of length 12.5 mm. will be formed. The thickness at the root will be $1.529t_0$, and at the top it will be $1.052t_0$. For all three cases the tubular branch will be the same, and on top of it will be the cap previously determined for each case. Note that for Case 3, the bulge consists of a tubular branch formed from the axial deformation and another tubular branch formed from the expansion of the spherical cap.

The thickness distribution for the three cases after axial deformation are shown graphically in Fig. 68. Again the graph is labelled t/t_0 against y , as in Fig. 67. t/t_0 corresponds to the modified values of t/t_0 , t/t_0 and t'/t_0 from TABLE 6, for Cases 1, 2 and 3

respectively. y corresponds to h_2 from TABLE 6 plus the length of the tubular branch, L_0 , ie h_2 plus 12.5 mm, for Cases 1 and 2. The value of y for Case 3 is equal to the value of h_2 plus L_0 and L_0 . For Case 3, t/t_0 also equals the modified values of t_L/t_0 , and the value of y corresponds to L plus L_0 .

From the graph it can be seen that all three cases share the same tubular branch, ie. from $y = 0\text{mm}$ to $y = 12.5\text{mm}$. On this part of the bulge, thickening of the tube wall occurs. After this point the three graphs separate. Case 1, which has the smallest bulge, has the least wall thinning occurring at the bulge tip, although the graph is steeper than for Case 2. When a spherical cap is formed, as in Case 2, greater thinning occurs at the tip. However, severe thinning of the tube wall occurs in Case 3, when the spherical cap is further expanded to form a tubular wall. Along this tubular section, the rate of thinning of the tube wall is greatest. In practise it would be unlikely to be able to produce this example with such severe wall thinning occurring. Rupture of the tube wall would occur before the bulge could be fully formed. It would be possible, however, to produce a bulge of the Case 3 type, with a smaller tubular branch formed from the cap.

5.3. COMPARISON OF THEORETICAL AND EXPERIMENTAL RESULTS

As has been previously illustrated, the bulge can be formed in three ways - Case 1, 2 and 3. It is possible that each case could produce a branch of the same length, eg. suppose a branch length of 15mm is produced. This could be made up of:

CASE 1. a cap of height 3mm, and a tubular branch formed from axial deformation 12mm long.

CASE 2. a cap of height 5mm, and a tubular branch formed from axial deformation 10mm long.

CASE 3: a cap of height 5mm, a tubular branch formed from the cap of length 3mm and a tubular branch formed from axial deformation 7mm long.

In order to decide on how the branch has been formed, the theoretical predictions are based on the amount of axial deformation occurring. Knowing the original and final lengths of the tube blank, the theoretical length of the tubular branch formed from the deformation can be obtained from equation (31). Also the theoretical height of the spherical cap, H_s , is known (5.0mm for the tube radius 12.06mm being used). Therefore, subtracting the theoretical branch length from the actual length of the branch will leave the height of the cap or the height of the cap and the tubular branch formed from it. Comparison of this height with the H_s will determine which case the example falls into. ie.

If the height of the cap is less than H_s then Case 1 is used.

If the height of the cap equals H_s then Case 2 is used.

If the height of the cap is greater than H_c , then Case 3 is used, where the length of the tubular branch expanded from the cap, L_o , is the difference between the height of the cap and H_c .

With this information it is then possible to predict the wall thickness distributions around the bulge. The theoretical predictions are shown in graphical form in Figs. 69 to 107, plotted with the actual values of the component. A computer program has been used to evaluate the theory and produce the graph - see Appendix 2. For each component, this program initially evaluates the Theory as a Case 2 example. It then compares the heights of the branch as previously mentioned, and evaluates a second time as a Case 1 or Case 3 example. The graphical output shows a plot of the actual values - in solid line marked with the symbol '*' - and the two theoretical plots - shown as dashed lines. The theory has been applied to both the tee pieces and the cross pieces.

5.3.1. Tee Pieces

Figs. 69 to 75 show the wall thickness variation for tee pieces formed with an axial compressive force of 85kN. All the components have been subjected to a similar amount of axial deformation, with a final blank length of 83-85 mm. The internal pressures used to form these components range from 2000psi (14N/mm²) in Fig. 69 to 6000psi (41N/mm²) in Fig. 75. In all the Figs, the theoretical prediction, based on a Case 2 example, produces a plot much longer than the actual length of the side branch. In Fig. 66 the actual length of the branch is shorter than the length of just the tubular branch. For this reason, there is only one line plotted for the theory. Increasing the internal pressure increases the length of the branch. The theory shows this by an increase in the

height of the cap. Note that as the internal pressure increases the theoretical branch length remains almost constant - shown by the single straight dashed line. This line then splits into two - Case 1 and 2. Case 1 is the steeper, shorter dashed line, and Case 2 is the longer one. Increasing the internal pressure causes an increase in the length of the plot for Case 1 and a decrease in the wall thickness at the tip of the bulge. Comparison of theoretical and experimental values shows good agreement at the root of the bulge, $y = 0$, but there is a discrepancy with increasing y . For the Case 1 plot there is as much as a 10% difference towards the tip of the bulge. For the components formed at higher pressure, with a more pronounced cap, the theoretical predictions are in better agreement.

Figs. 76 to 82 show the results of components formed with an axial force of 130 kN. Again, an increase in the internal pressure causes an increase in the branch length. Figs. 76, 77 and 78 are similar to those previous, showing the theoretical predictions for Case 1 and 2. As the branch length increases, the length of the Case 1 branch also increases in length. In Fig. 80 a spherical cap has almost been formed, and the plot of Case 1 and 2 are almost identical - there are two dashed lines plotted, almost on top of each other. Figs. 79, 81 and 82 are of components with even longer branches. For these, the theory for Case 3 examples has been evaluated. The Case 3 plot is the lower one with the step in it. This step represents where a tubular branch has been formed from the spherical cap. The theory compares fairly well with the actual results, at the root and at the tip of the bulge, although there is some discrepancy between the two between these two points.

Similar graphs are plotted for tee pieces formed from the thinner tube. Figs. 83, 84 and 85 shows the comparison for components formed with an axial compressive force of 85kN. In these graphs, the actual length of the branch is shorter than just the tubular branch length predicted by the theory. Hence, only one theoretical line is plotted - the Case 2 one. However, the theoretical prediction for the wall thickness at the tip of the bulge is fairly close to the actual value, although the theory predicts greater wall thickening at the root of the bulge than actually occurs.

Figs. 86 and 87 are for components formed with an axial compressive force of 106kN. Fig. 87 is similar to the three previous figs, with the theory predicting greater wall thickening at the root, and a longer branch length. However, the component in Fig. 86 has a much longer branch length, and has greater wall thickening occurring at the root. For this component, the theory is able to produce a Case 1 and a Case 2 plot. Comparison of the theoretical and actual values show better agreement at the root. At the tip there is also fairly good agreement with the Case 1 and Case 2 values, although Case 2 predicts a longer branch.

5.3.2. Cross Pieces

Similar graphs have been produced for the cross pieces. Figs. 88 to 92 show the wall thickness variation around the bulge zone for cross pieces formed with an axial compressive force of 106kN. The theory predicts a greater amount of wall thickening at the root of the bulge than actually occurs. However, there is better agreement at the tip of the bulge. In Figs. 88 and 89, the theory predicts much greater wall

thinning occurring at the tip than the actual values. With larger internal pressures, and longer branches being formed - Figs. 90 to 92, this discrepancy decreases to produce a good agreement between the theory and the actual values at the tip.

An axial compressive force of 127kN has been used in Figs. 93 to 98 to produce the cross pieces. Comparison of the theoretical and actual values is similar to before, with greater wall thickening predicted at the root than actually occurring. Again there is a discrepancy between the two at the tip of the bulge at low internal pressures - small bulge heights - which decreases with increasing internal pressure.

Figs. 99 and 100 are for components formed with an axial force of 148kN. The theoretical prediction in Fig. 99 are similar to the previous graphs. In Fig. 100, longer side branches have been produced than previously. and on this graph the theory is shown for a Case 2 and 3 example. Again there is good agreement at the tip of the bulge, this time with the Case 3 theory, although there is some discrepancy for the rest.

For cross pieces formed from the thinner tube with a low axial force, the comparison of theoretical and actual results are similar to the results with tee pieces. Figs. 101 and 102 are for cross pieces formed with an axial force of 63kN. For these the theory predicts a tubular branch length longer than the total length of one of the side branches, resulting in only the Case 2 theory being plotted. Again the theory predicts greater wall thickening occurring at the root of the bulge, and fairly good agreement at the tip of it, although a longer branch length is predicted.

With a greater axial compressive force, there are still discrepancies between the theory and the actual wall thickness values. Figs. 103 to 106 show the results for cross pieces formed with an axial force of 85kN. In Figs. 104 and 105 the theory and actual values follow similar trends, but with discrepancies throughout. The components formed in Figs. 105 and 106 show very little wall thickening occurring at the root, unlike other components formed with similar axial deformation. Hence, there is a large error between the theoretical and actual values at this point. At the tip, however, there is good agreement in the wall thickness with the Case 2 theory, although it predicts a longer branch length.

5.4. DISCREPANCIES IN THE THEORY

The theory, when compared to the results of components that have been formed on the bulge forming machine, gives an approximate prediction of the wall thickness distribution. There are, however, a lot of discrepancies between the two. Considering, initially, the theoretical value of the wall thickness at the root of the bulge, for components formed from the tube of wall thickness 1.37mm. The tee pieces showed good agreement, whereas the cross pieces were not as thick as that predicted. This may be due to the radius in the die between the main branch and the side branch. This radius is to allow the metal to flow smoothly when forming the side branch. For the tee pieces, the die, the first one to be made, had only a small radius. In some cases it was found that the metal had difficulty in getting around this, resulting in a gap between the tube wall and the die at the bottom of the side branch.

When the cross piece die was made, a larger radius was chosen to try to overcome this problem. The theory calculates the root value for a branch radius of r_0 . The actual radius at the root of the bulge will in fact be a little larger than this, due to radius between the branches, especially for the cross pieces. Hence, for the cross pieces the actual wall thickness at the root is likely to be thinner than if they were formed from a die with only a small radius between the branches.

Another place of error with the theory seems to be the determination of the tubular branch length. Generally it predicted a tubular branch length longer than the actual value. Although it is difficult to distinguish the tubular branch from the cap on the formed component, examination of the graphs give an idea of where the tubular branch ends and where the cap begins. On most of the graphs it is possible to approximate the plot by two straight lines - a steep one for the tubular branch and a flatter one for the cap. As an example, Fig. 107 shows this done to the original graph in Fig. 77. Note that the line for the tubular branch is a lot steeper and finishes shorter than the theory. This leaves a much longer cap, which, if considered separately by the theory, would be predicted to undergo severe thinning. Hence, the effect of axial deformation must have greater effect on the cap formed than the theory predicts, and less of an effect on the length of the tubular branch. This may be in some way due to the theory assuming a constant volume during the process. On the bulge forming machine a relief valve allows out excess oil to prevent a high internal pressure being reached. If this occurs then the volume of the formed component will be smaller than the original blank. Another assumption the theory makes is that the cap forms the arc of a circle. Examination of the

radius of curvatures of the actual caps - done in order to produce Fig. 41 - showed that the radius decreases towards the edge of the cap in order to join onto the tubular branch.

Apart from the discrepancies, the theory will provide a fairly good idea of the thickness distribution around the branch of a tee or cross piece. This may be useful when considering the amount of axial deformation to subject a blank to, to produce a side branch of sufficient length without severe wall thinning occurring at the cap.

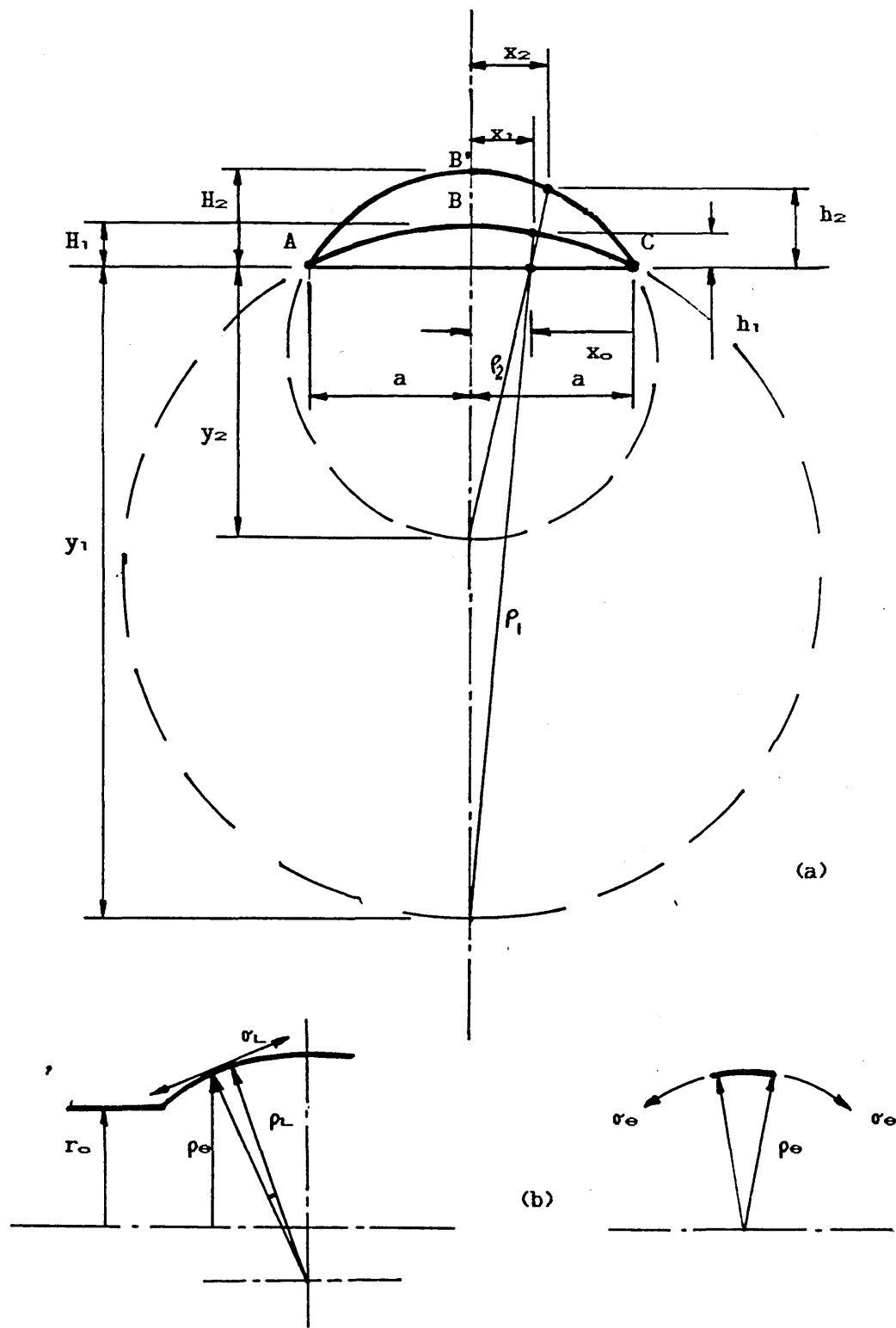


Fig. 63.
 (a). The Geometric Expansion Mode of a Circular Arc.
 (b). The Force Equilibrium.

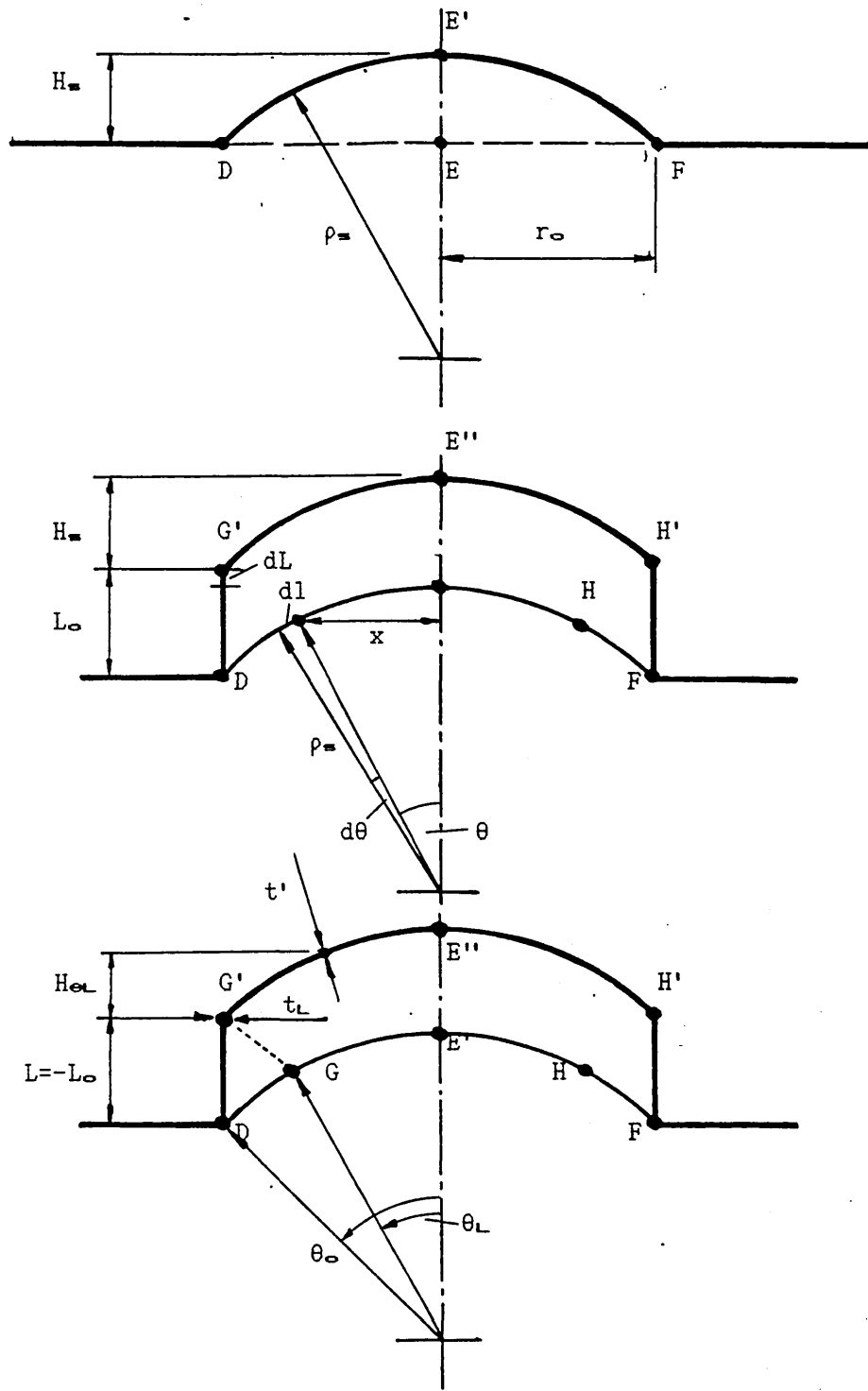


Fig. 64.
The Formation of a Tubular Branch.

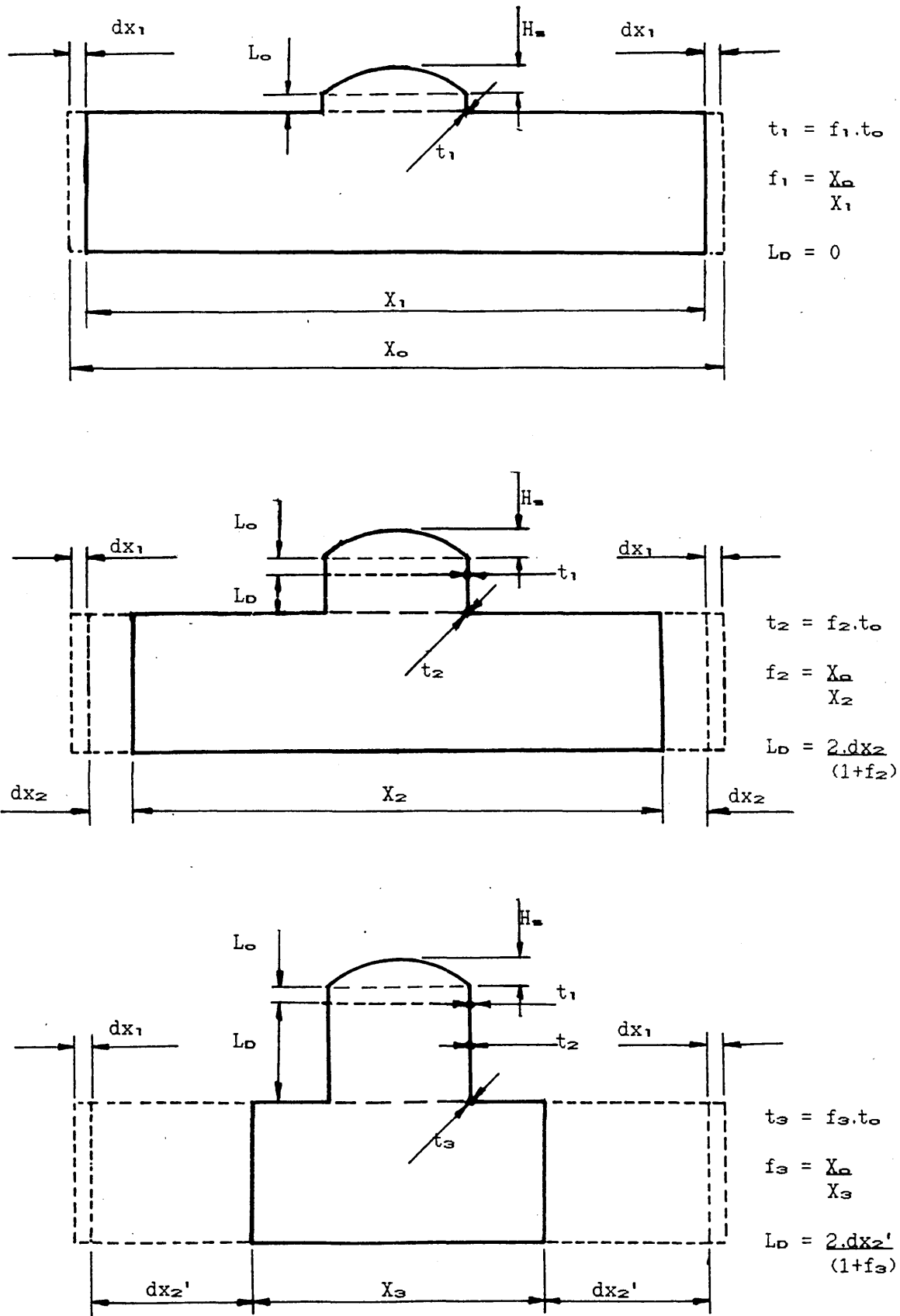
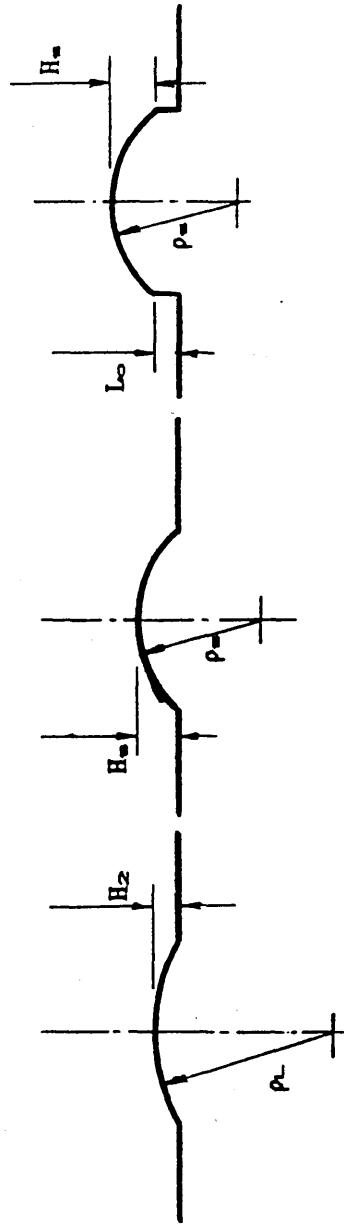


Fig. 65.
The Effect of Axial Deformation During Forming.

THE EFFECT
OF INTERNAL
PRESSURE



CASE 1

Low internal pressure
causing a small cap
to be formed.

Radius $> \rho_i$
Height $< H_i$

CASE 2

Sufficient internal
pressure to cause a
spherical cap to
be formed.

Radius = ρ_i
Height = H_i

CASE 3

High internal pressure
causing a tubular cap
to be formed out of
the spherical cap.

THE ADDED
EFFECT OF
AXIAL
DEFORMATION

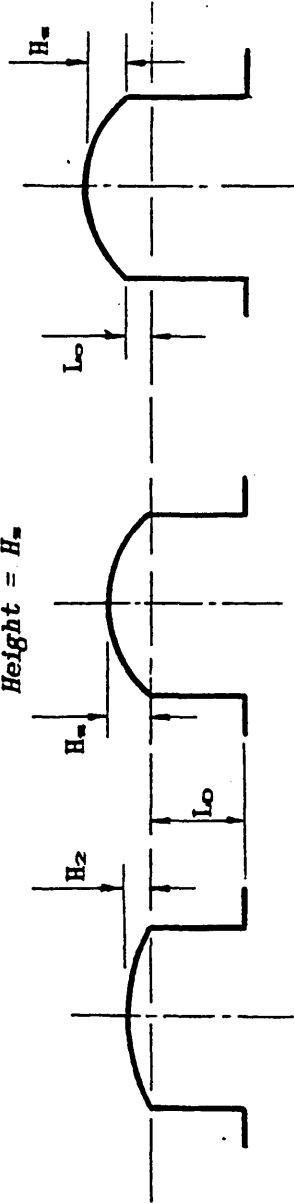


Fig. 66.
The Various Bulge Formations.

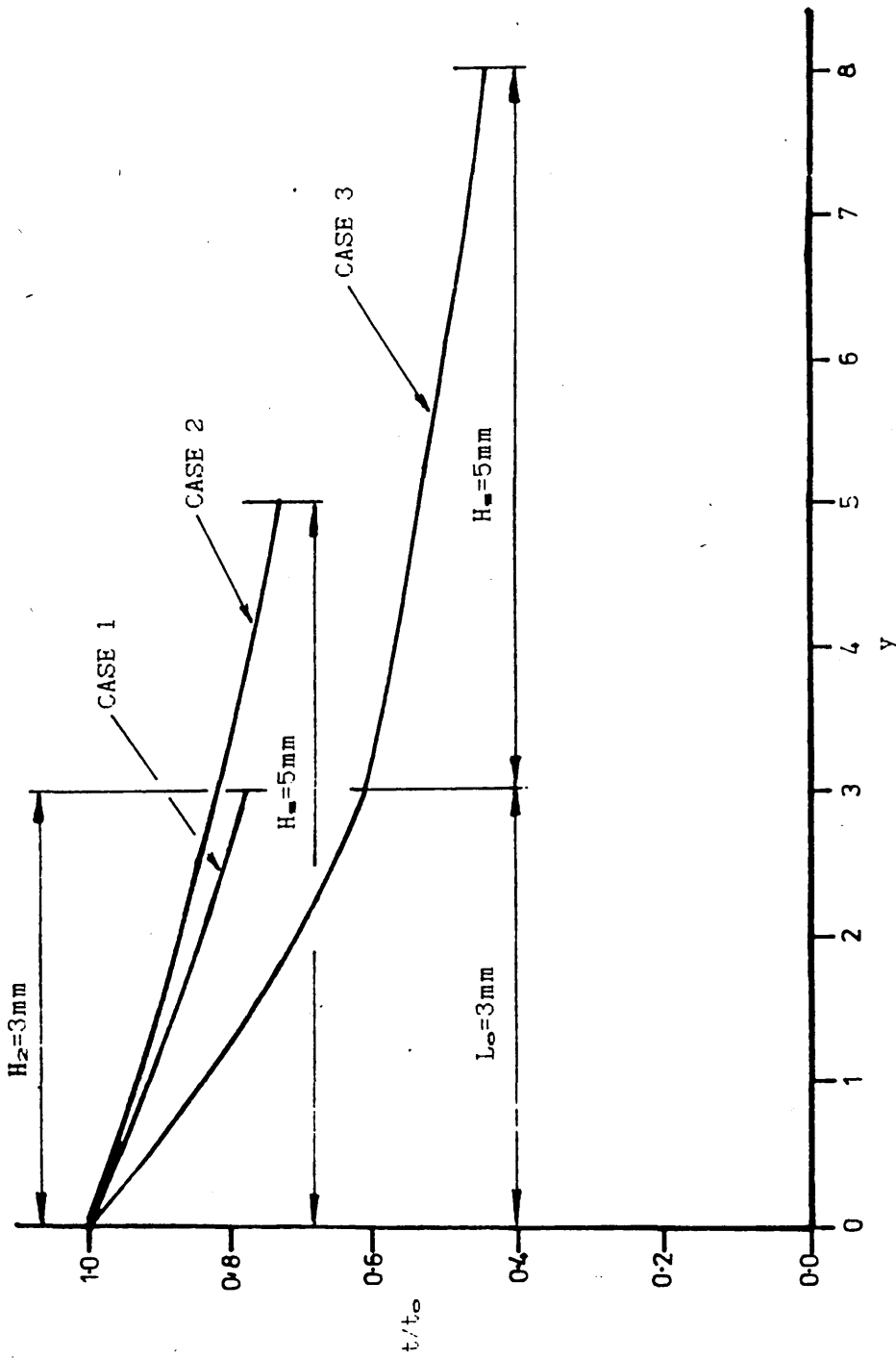


Fig. 67.
The Theoretical Wall Thickness Distribution along the Bulge Profile
Without Axial Deformation.

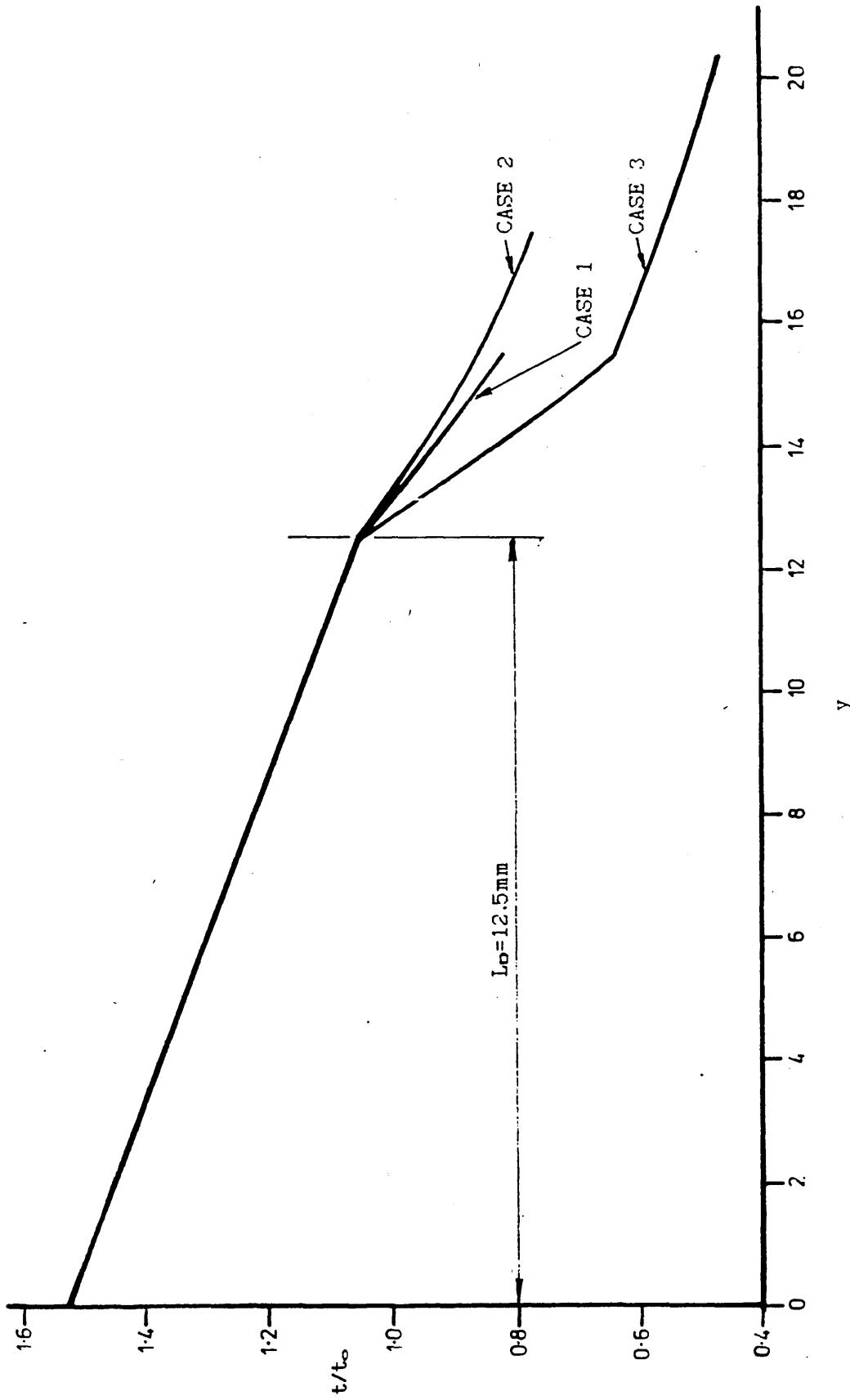


Fig. 68.
The Theoretical Wall Thickness Distribution along the Bulge Profile-
With Axial Deformation.

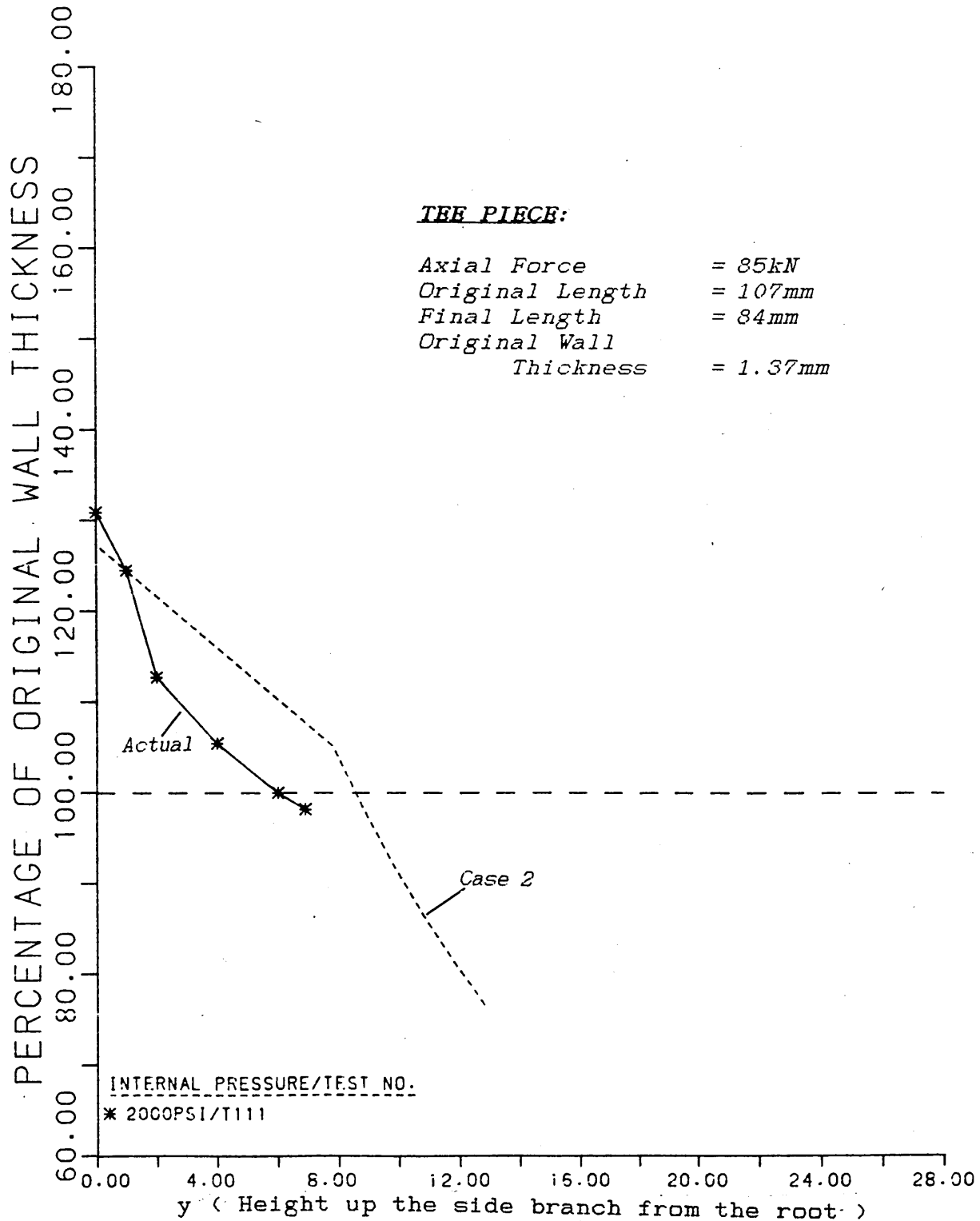


Fig. 69.
 Comparison of the Experimental Wall Thickness Distribution
 with Theoretical Predictions.

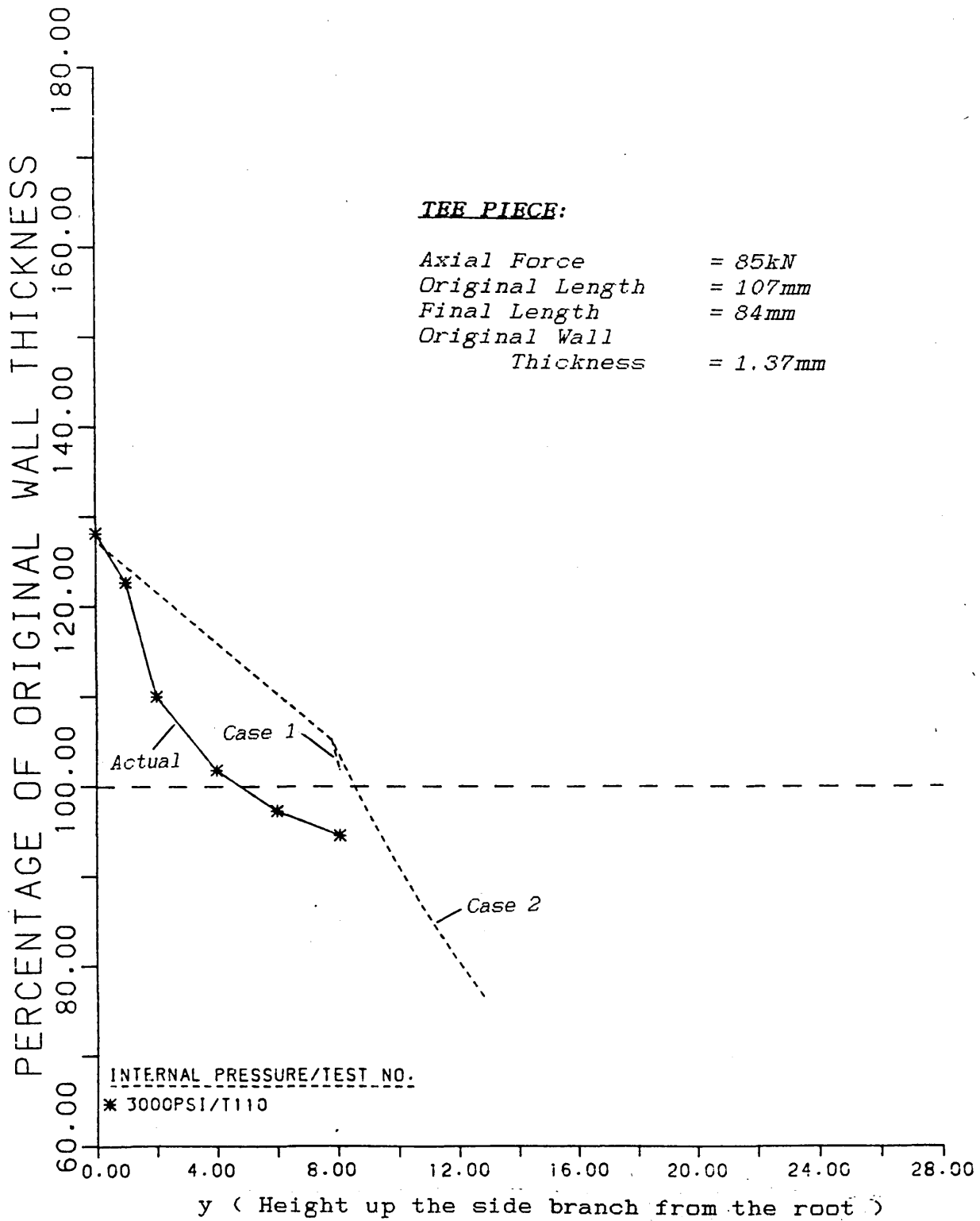


Fig. 70.
 Comparison of the Experimental Wall Thickness Distribution
 with Theoretical Predictions.

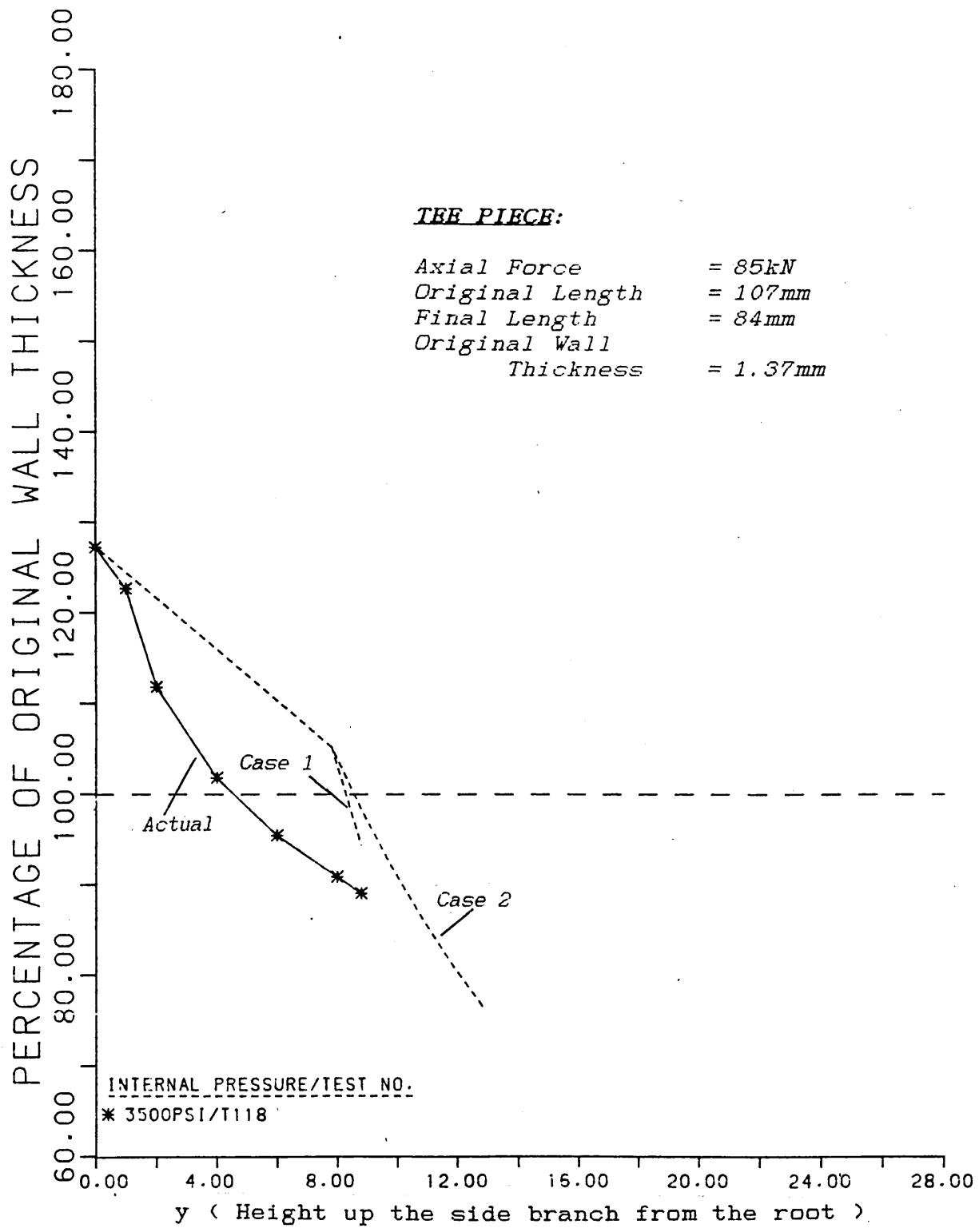


Fig. 71.
 Comparison of the Experimental Wall Thickness Distribution
 with Theoretical Predictions.

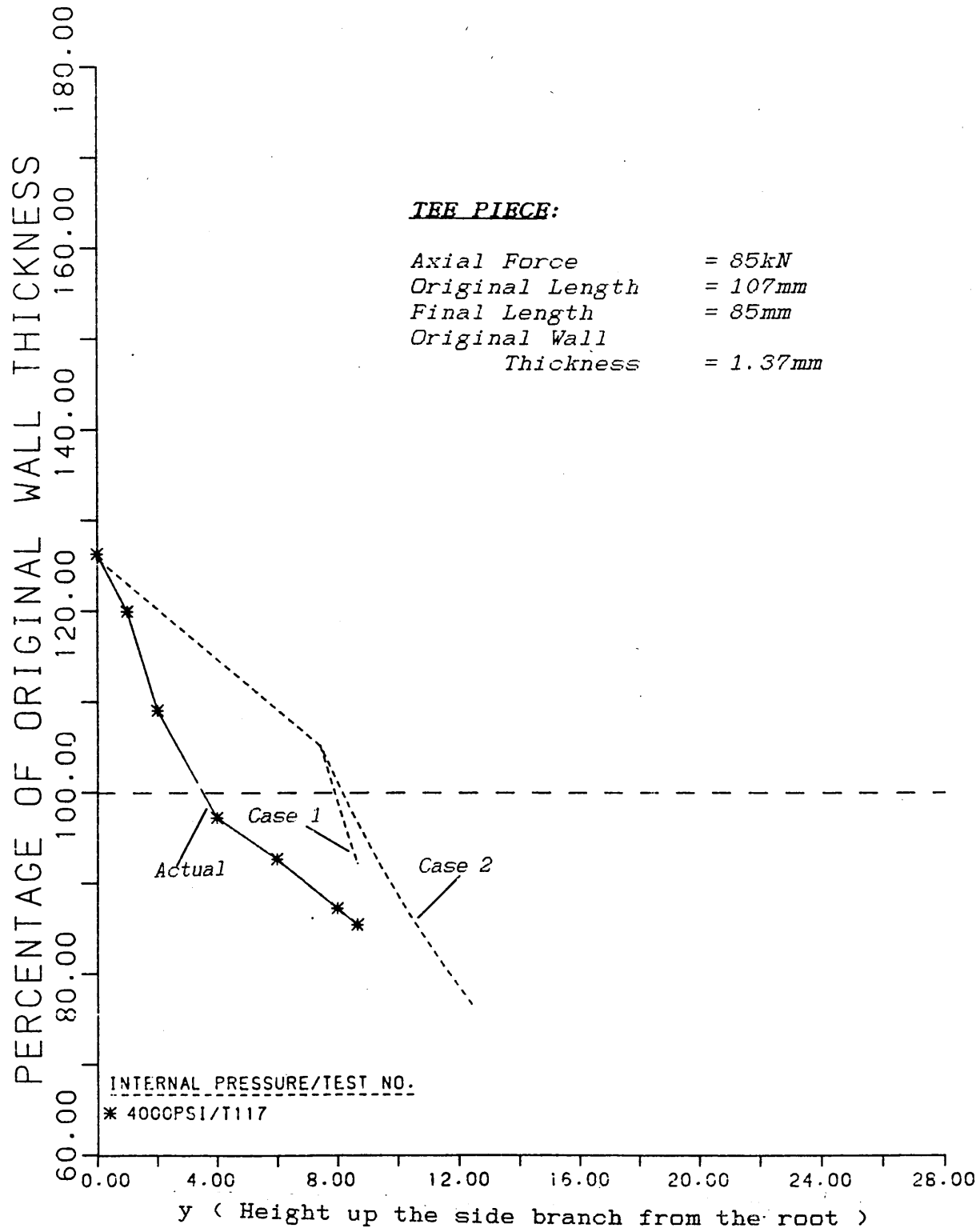


Fig. 72.
Comparison of the Experimental Wall Thickness Distribution
with Theoretical Predictions.

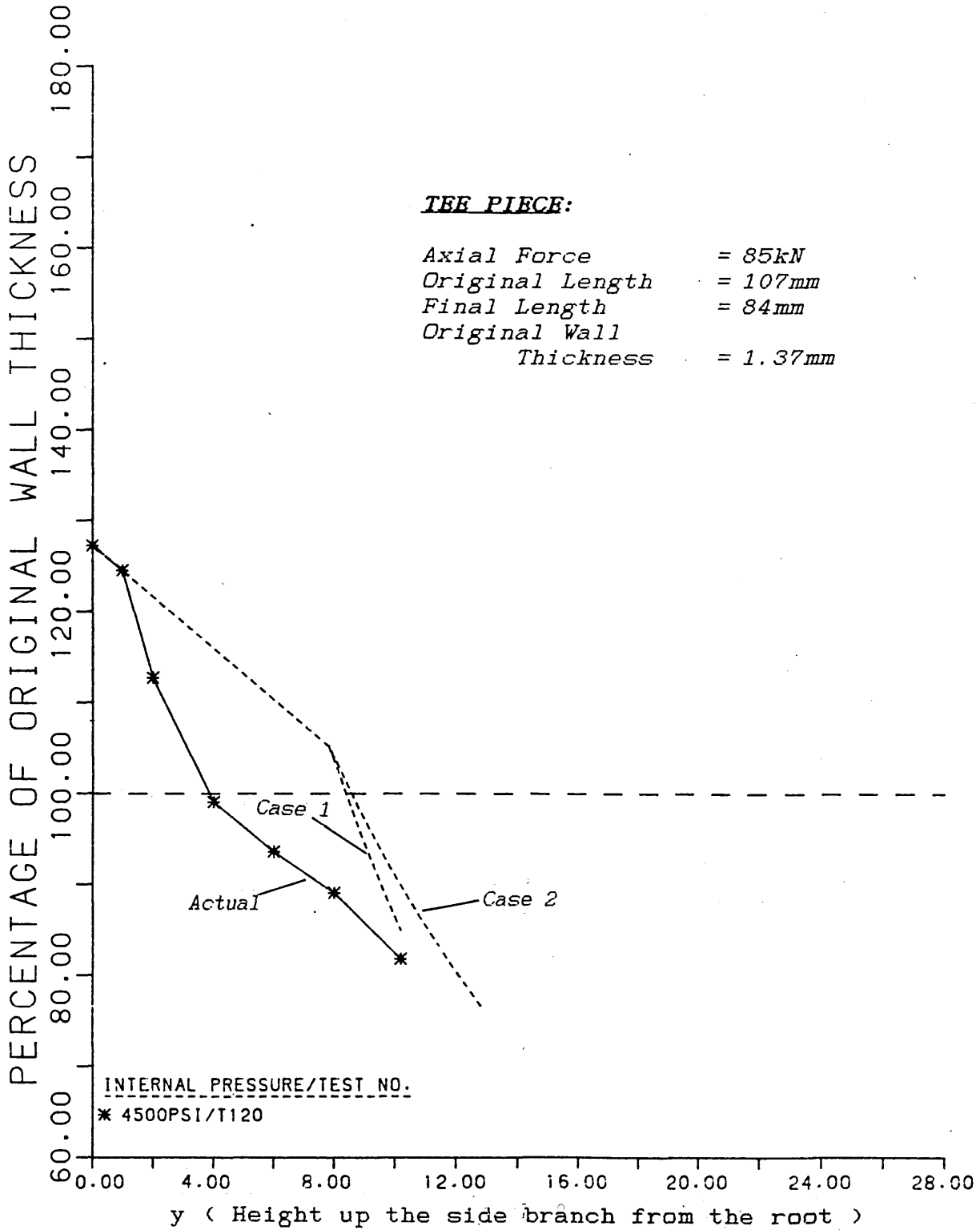


Fig. 73.
 Comparison of the Experimental Wall Thickness Distribution
 with Theoretical Predictions.

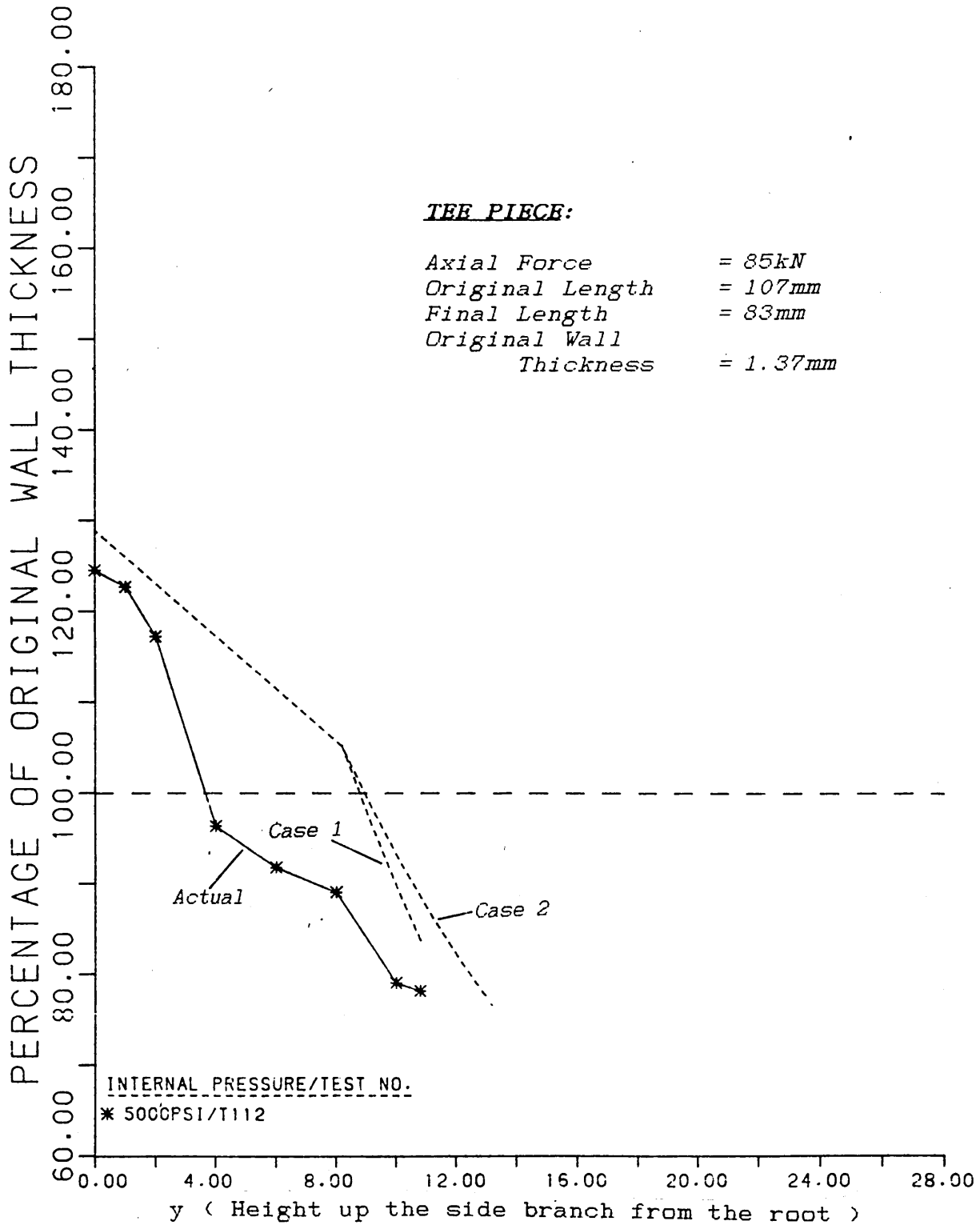


Fig. 74.
**Comparison of the Experimental Wall Thickness Distribution
with Theoretical Predictions.**

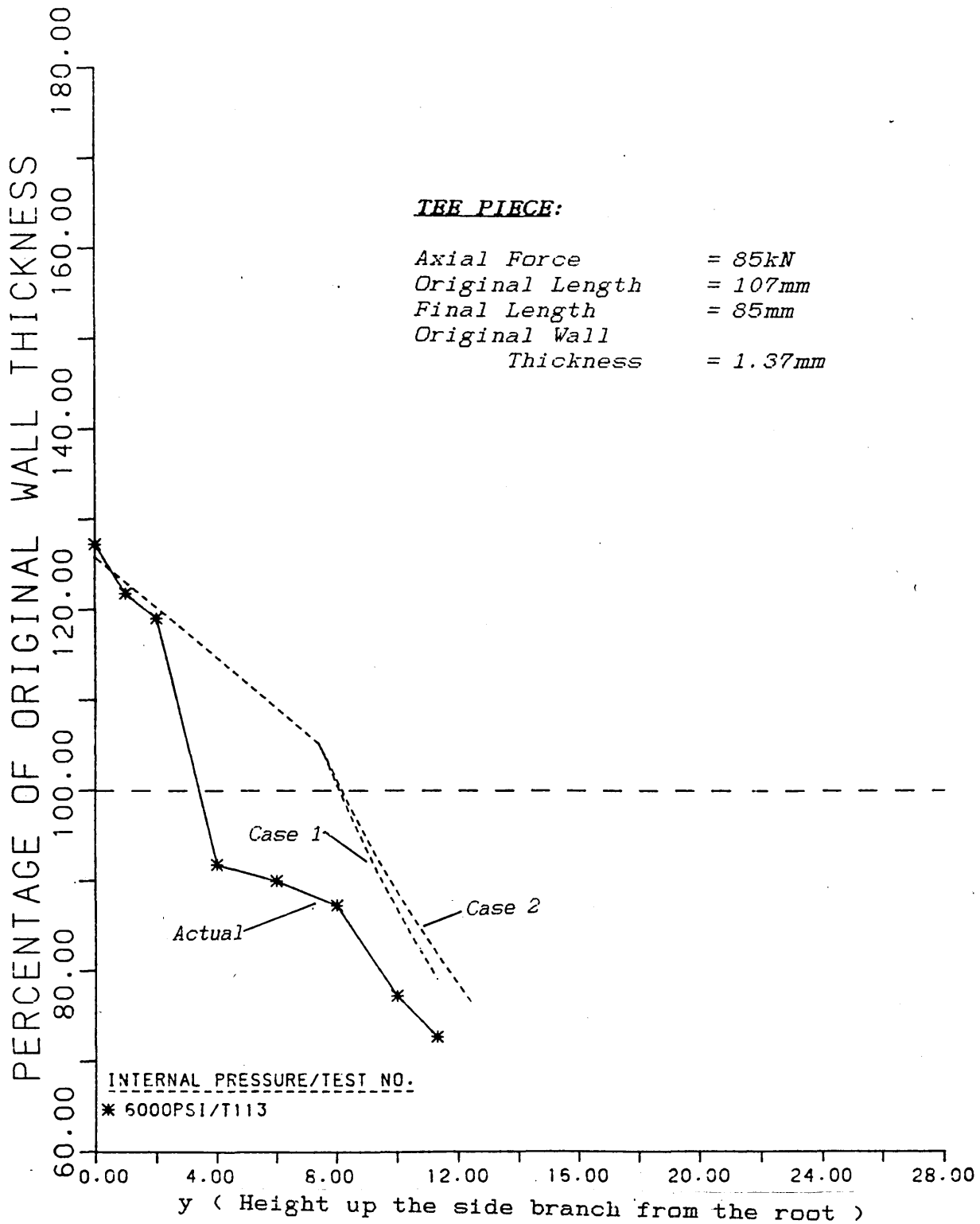


Fig. 75.
**Comparison of the Experimental Wall Thickness Distribution
with Theoretical Predictions.**

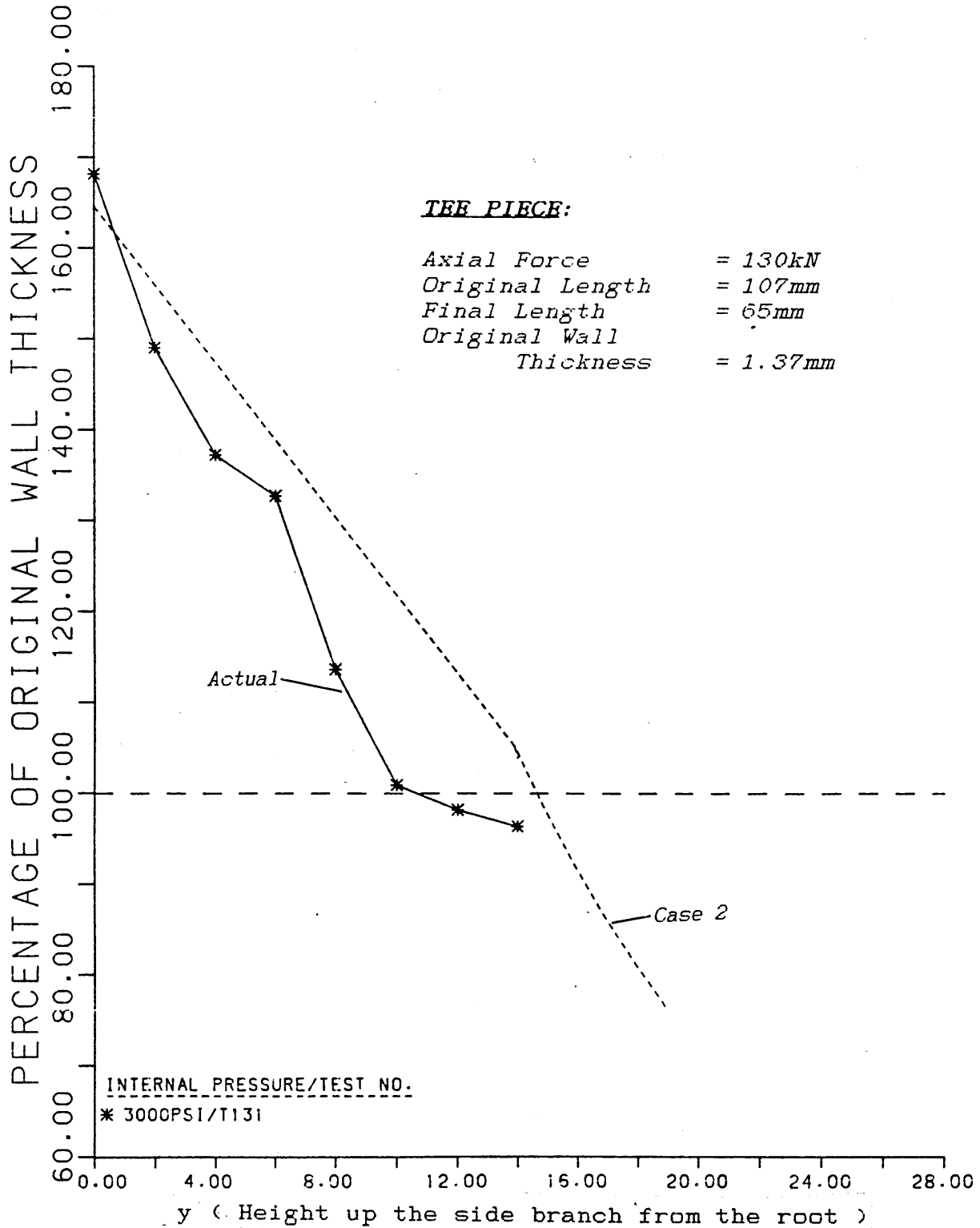


Fig. 76.
Comparison of the Experimental Wall Thickness Distribution with Theoretical Predictions.

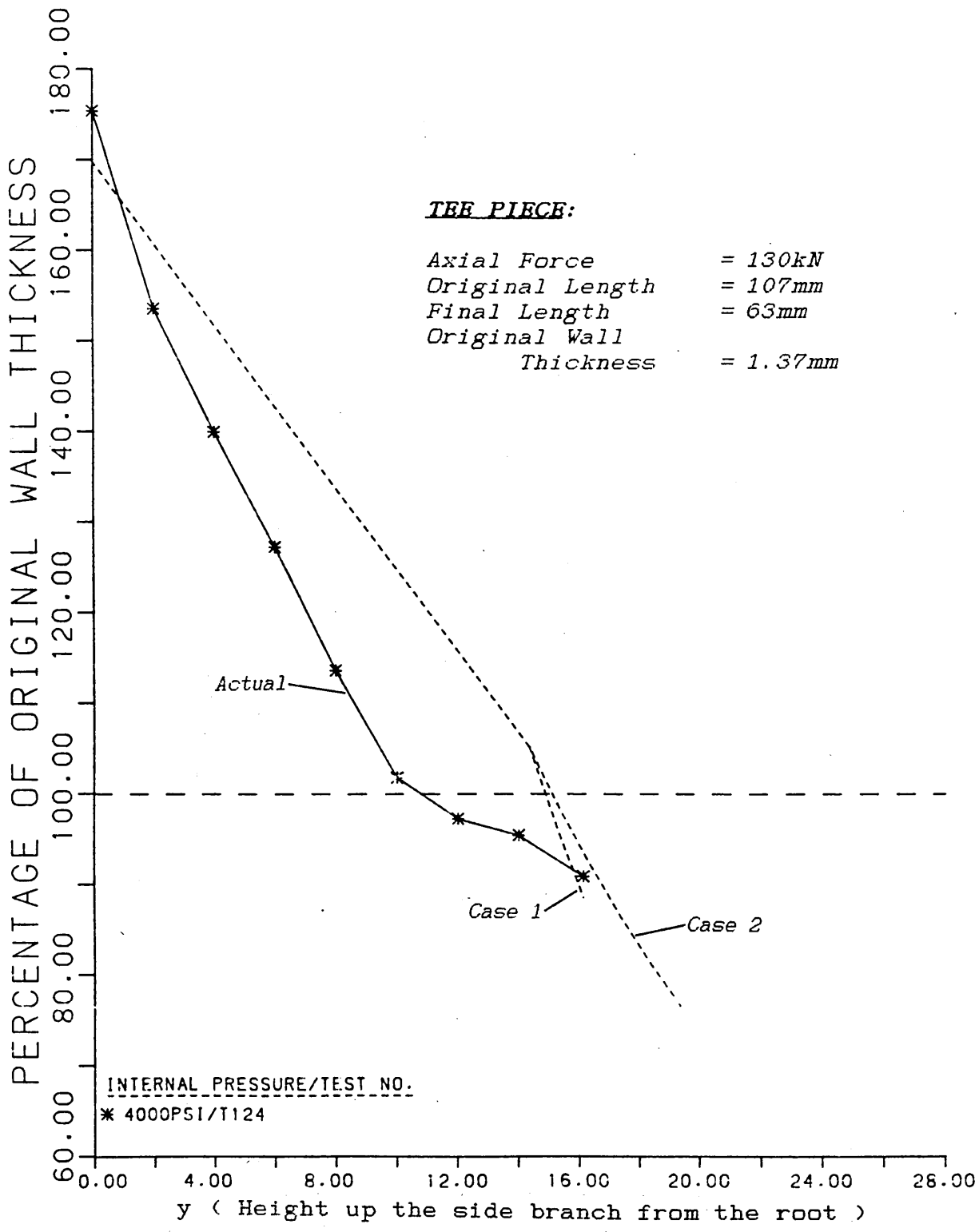


Fig. 77.
Comparison of the Experimental Wall Thickness Distribution with Theoretical Predictions.

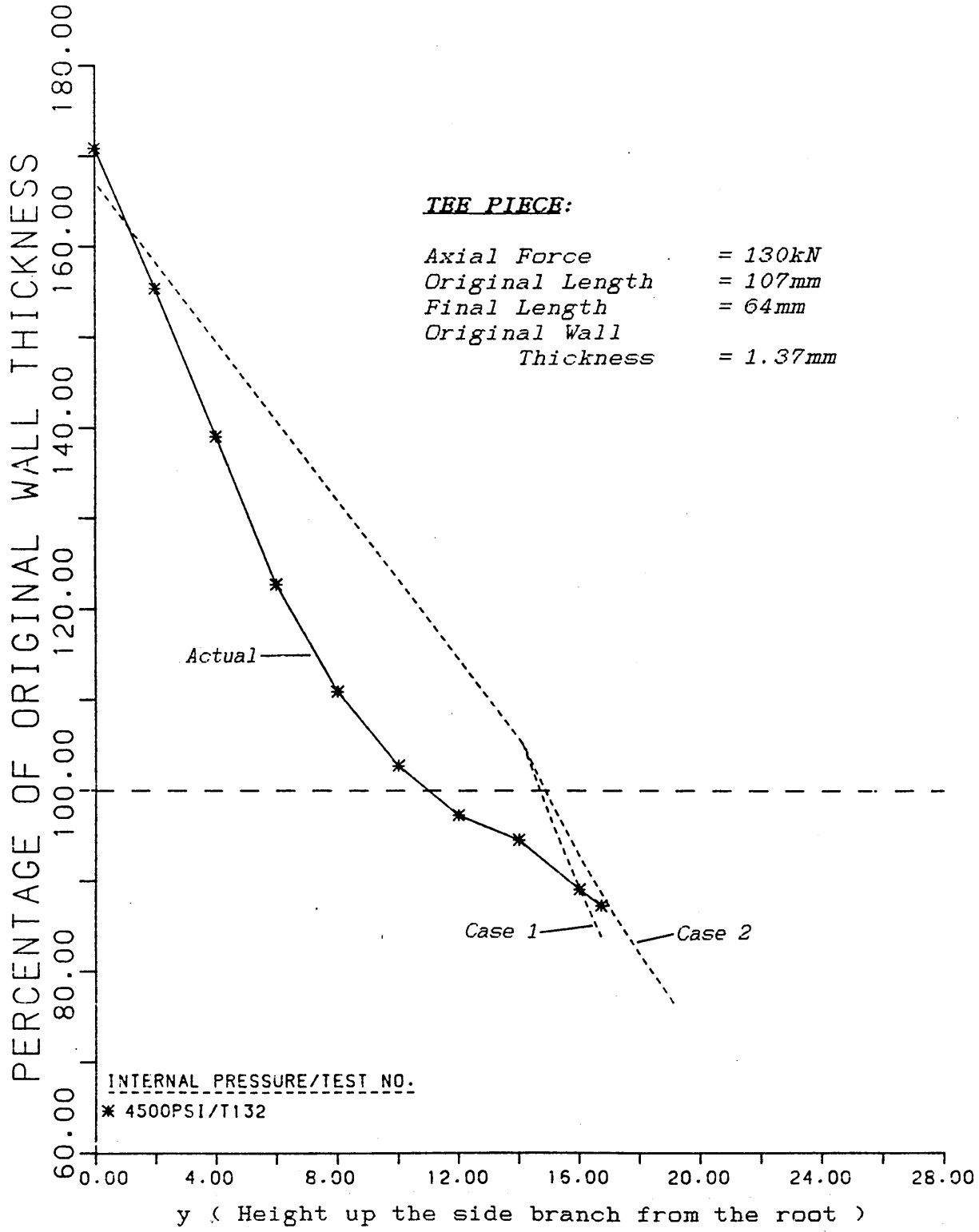


Fig. 78.
 Comparison of the Experimental Wall Thickness Distribution with Theoretical Predictions.

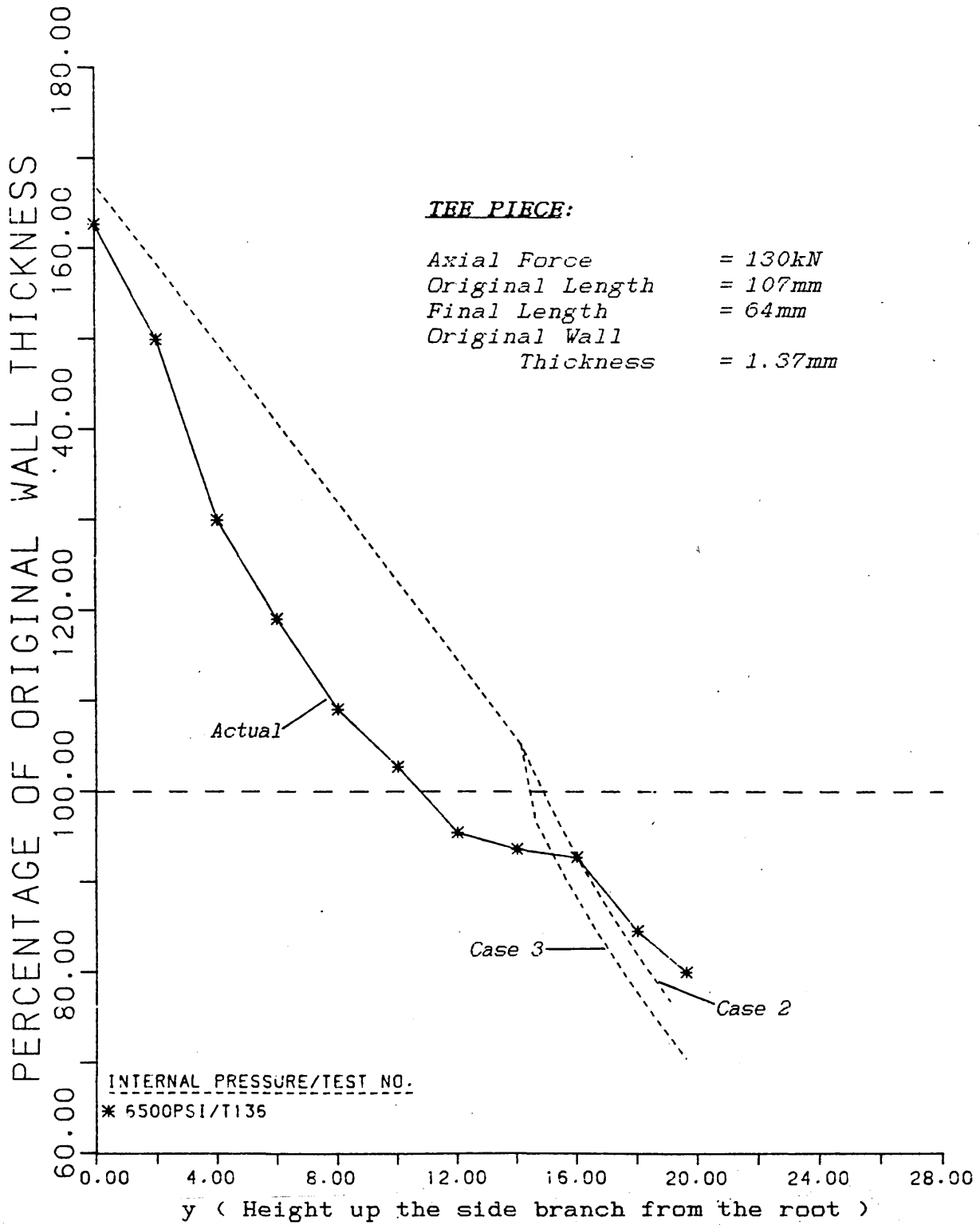


Fig. 79.
 Comparison of the Experimental Wall Thickness Distribution
 with Theoretical Predictions.

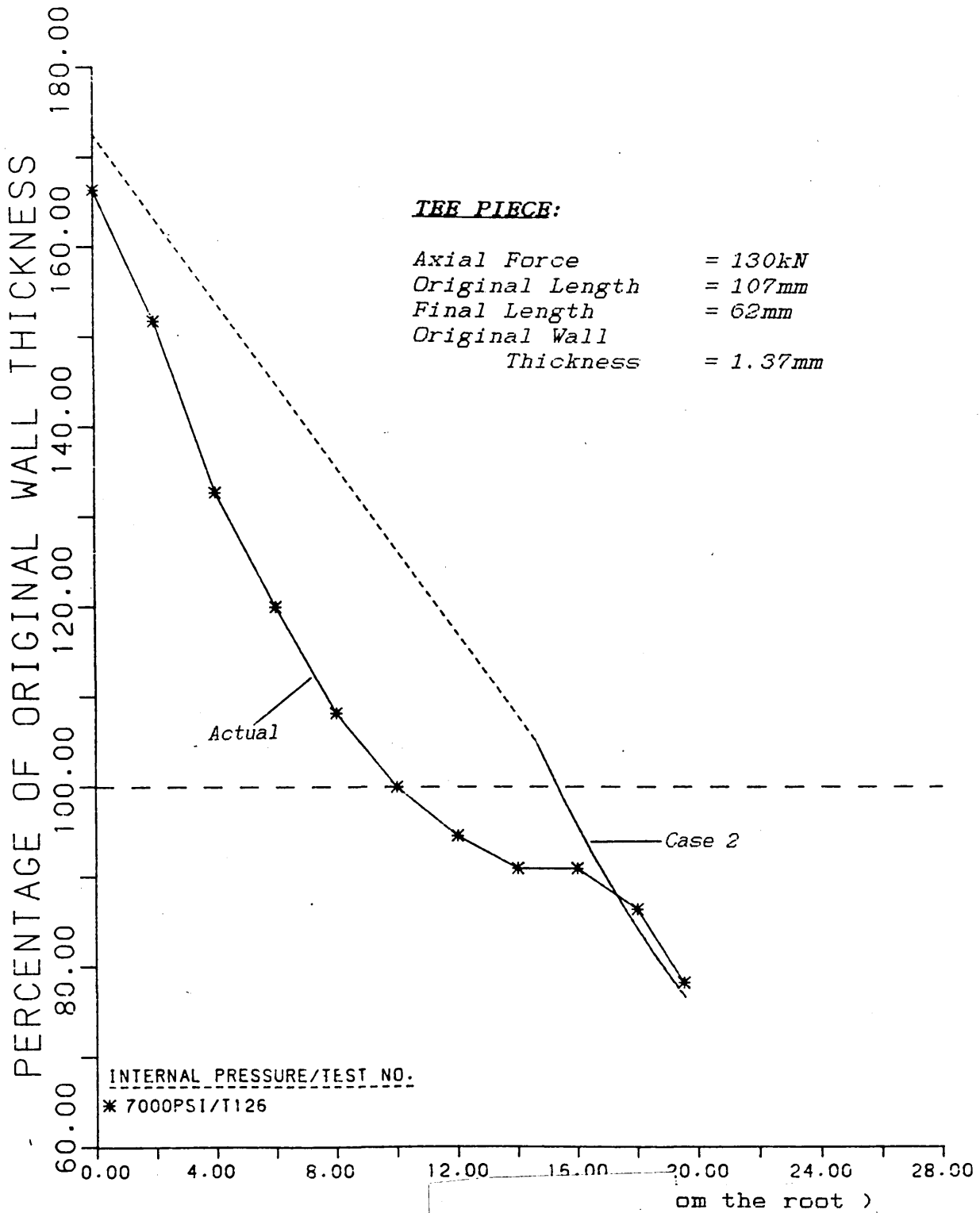


Fig. 80.
Comparison of the Experimental Wall Thickness Distribution with Theoretical Predictions.

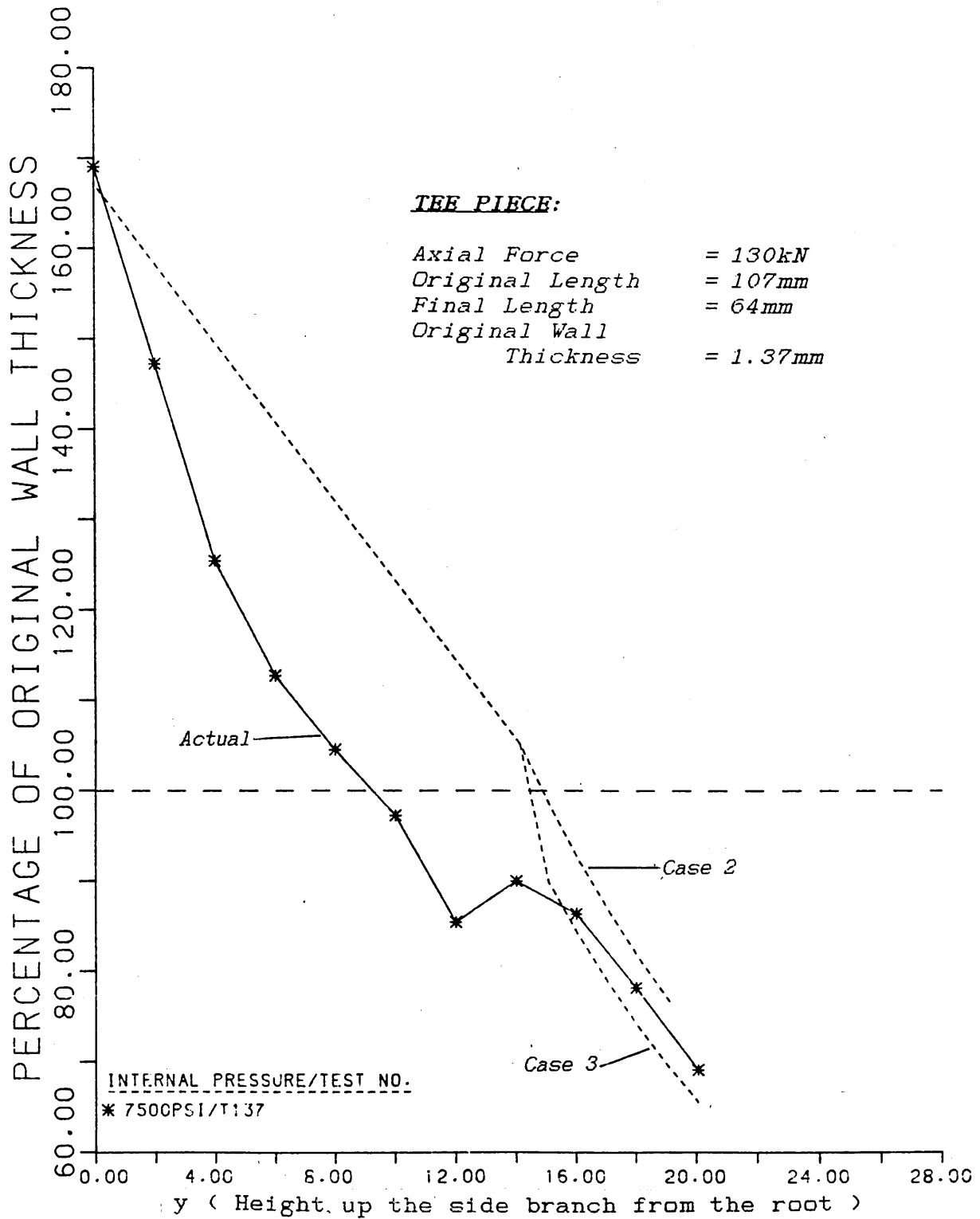


Fig. 81.
Comparison of the Experimental Wall Thickness Distribution with Theoretical Predictions.

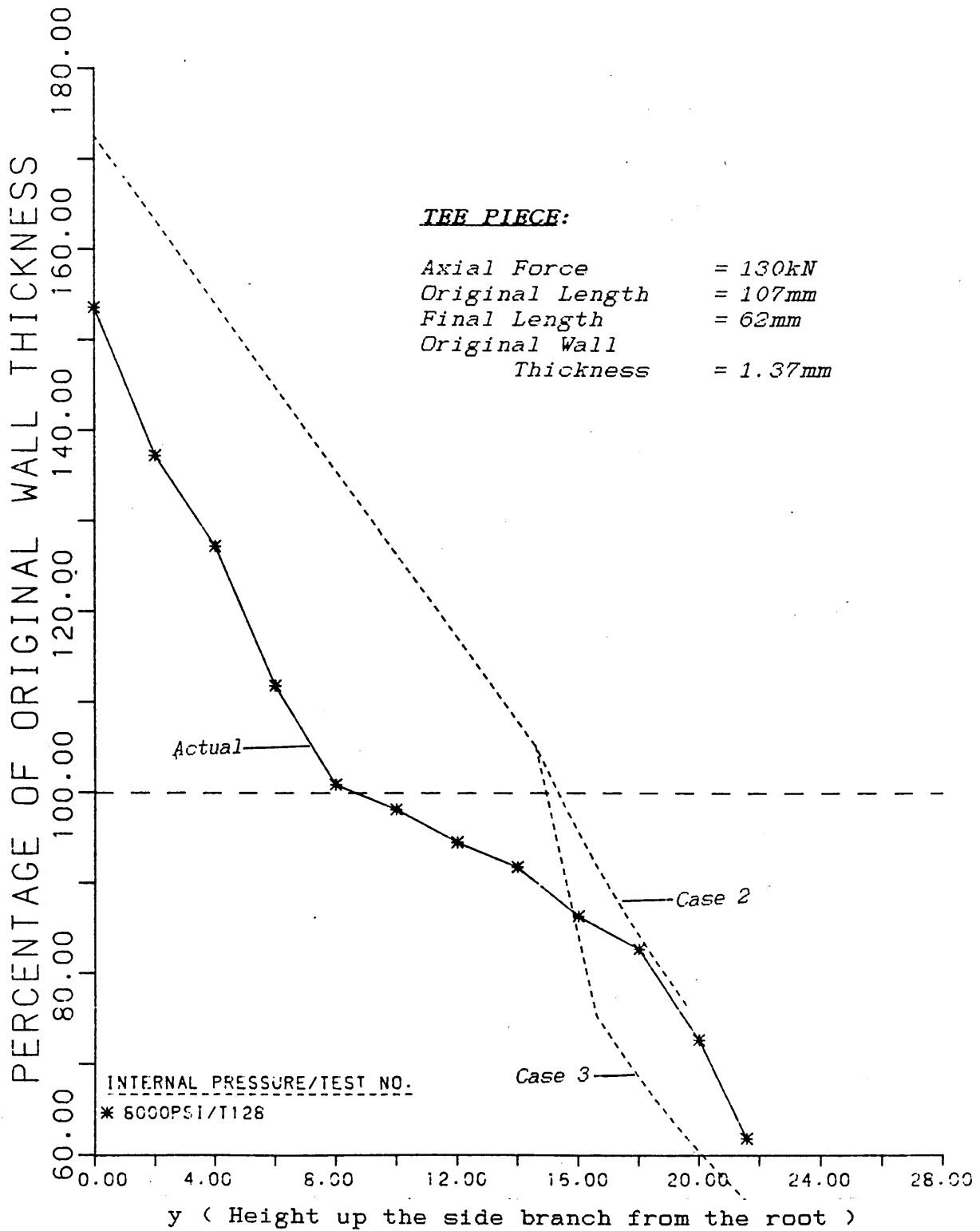


Fig. 82.
Comparison of the Experimental Wall Thickness Distribution
with Theoretical Predictions.

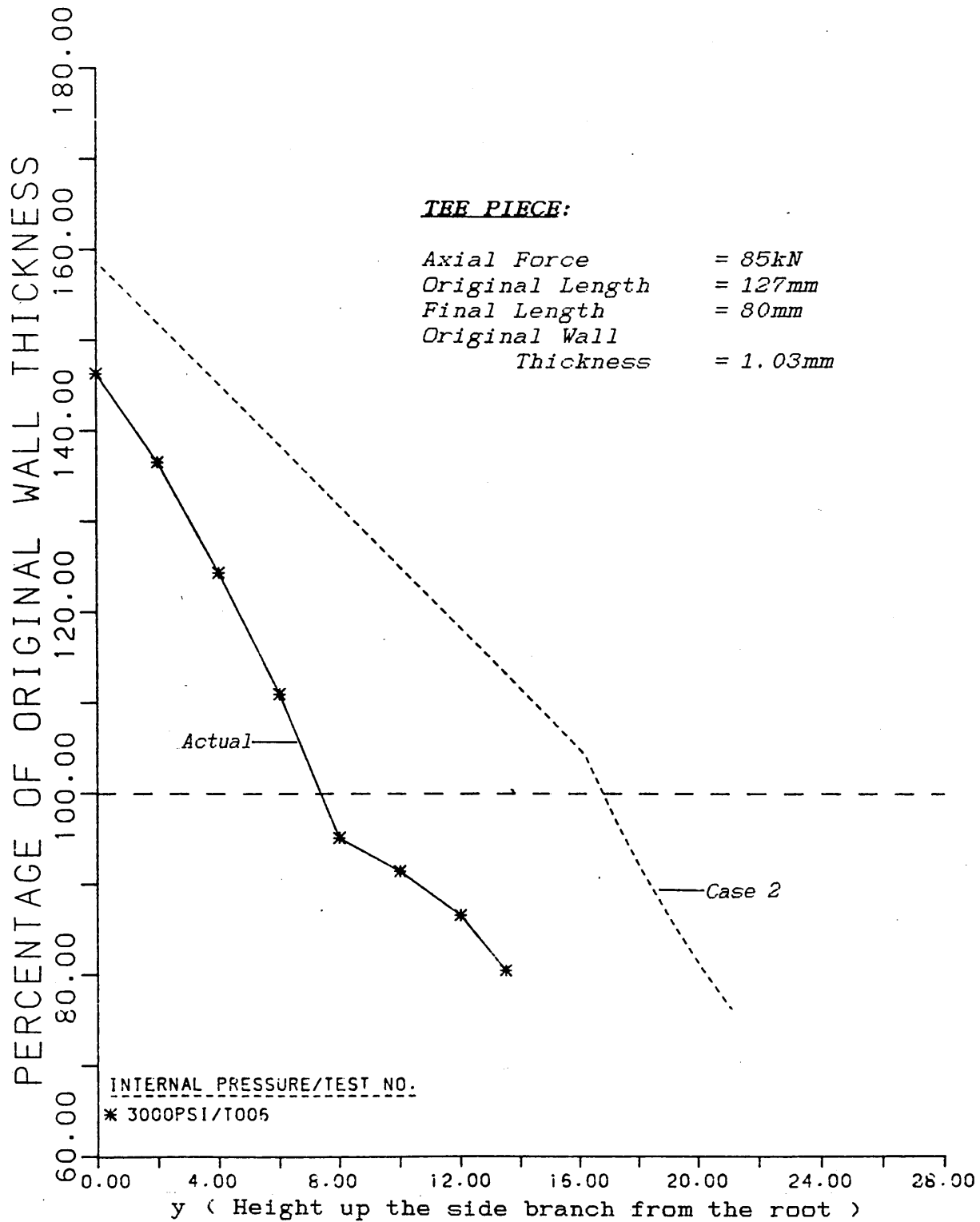


Fig. 83.
 Comparison of the Experimental Wall Thickness Distribution
 with Theoretical Predictions.

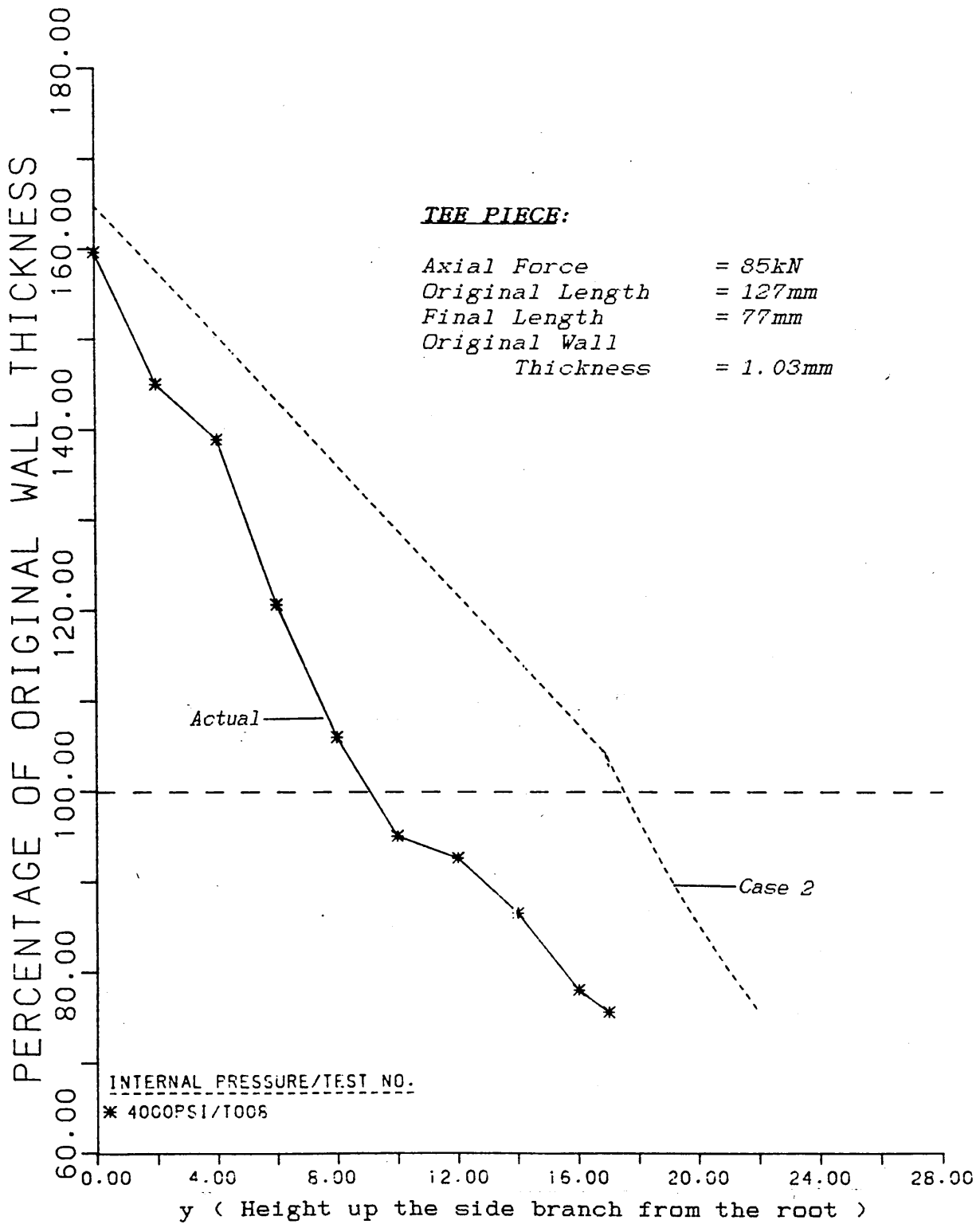


Fig. 84.
Comparison of the Experimental Wall Thickness Distribution with Theoretical Predictions.

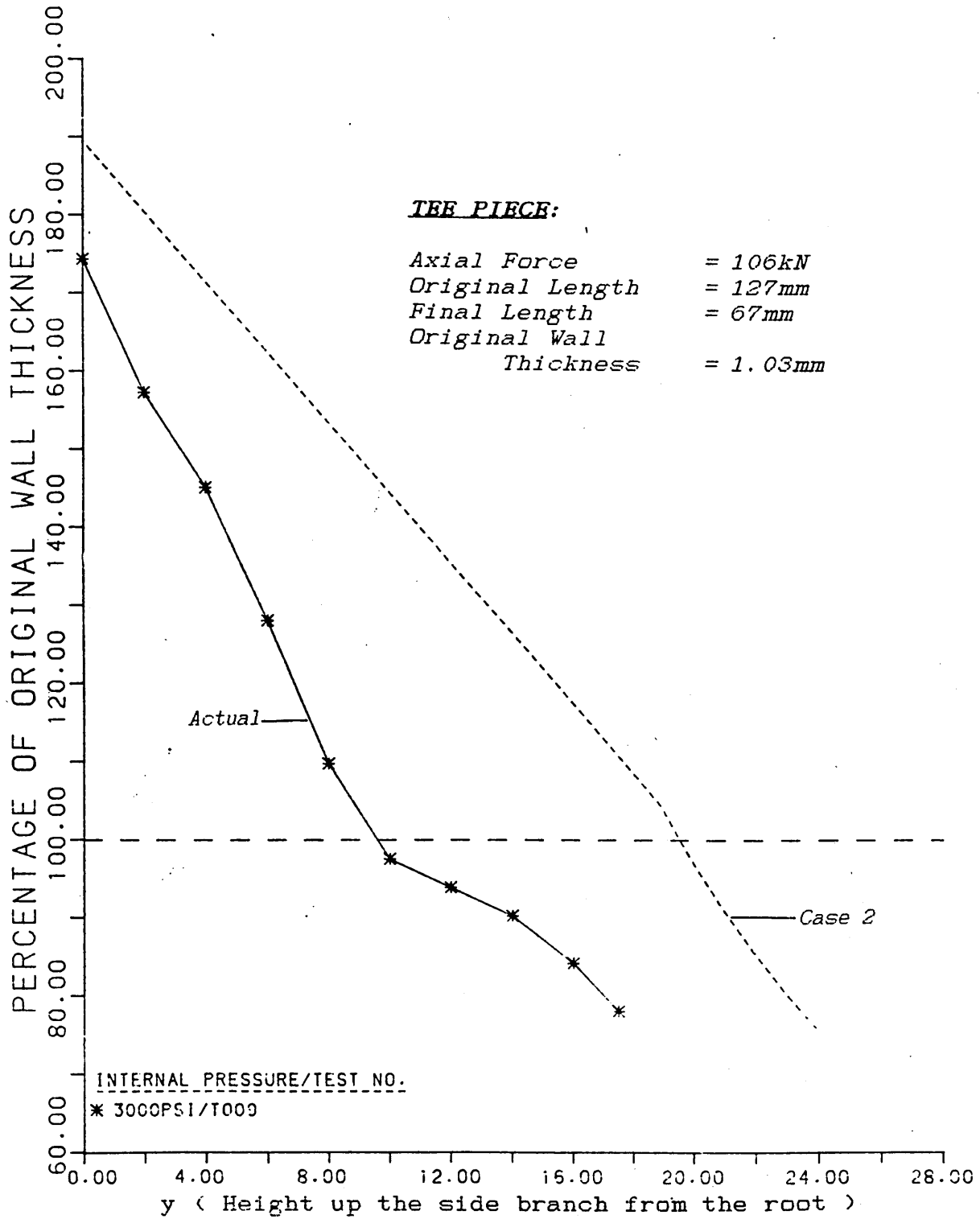


Fig. 85.
Comparison of the Experimental Wall Thickness Distribution with Theoretical Predictions.

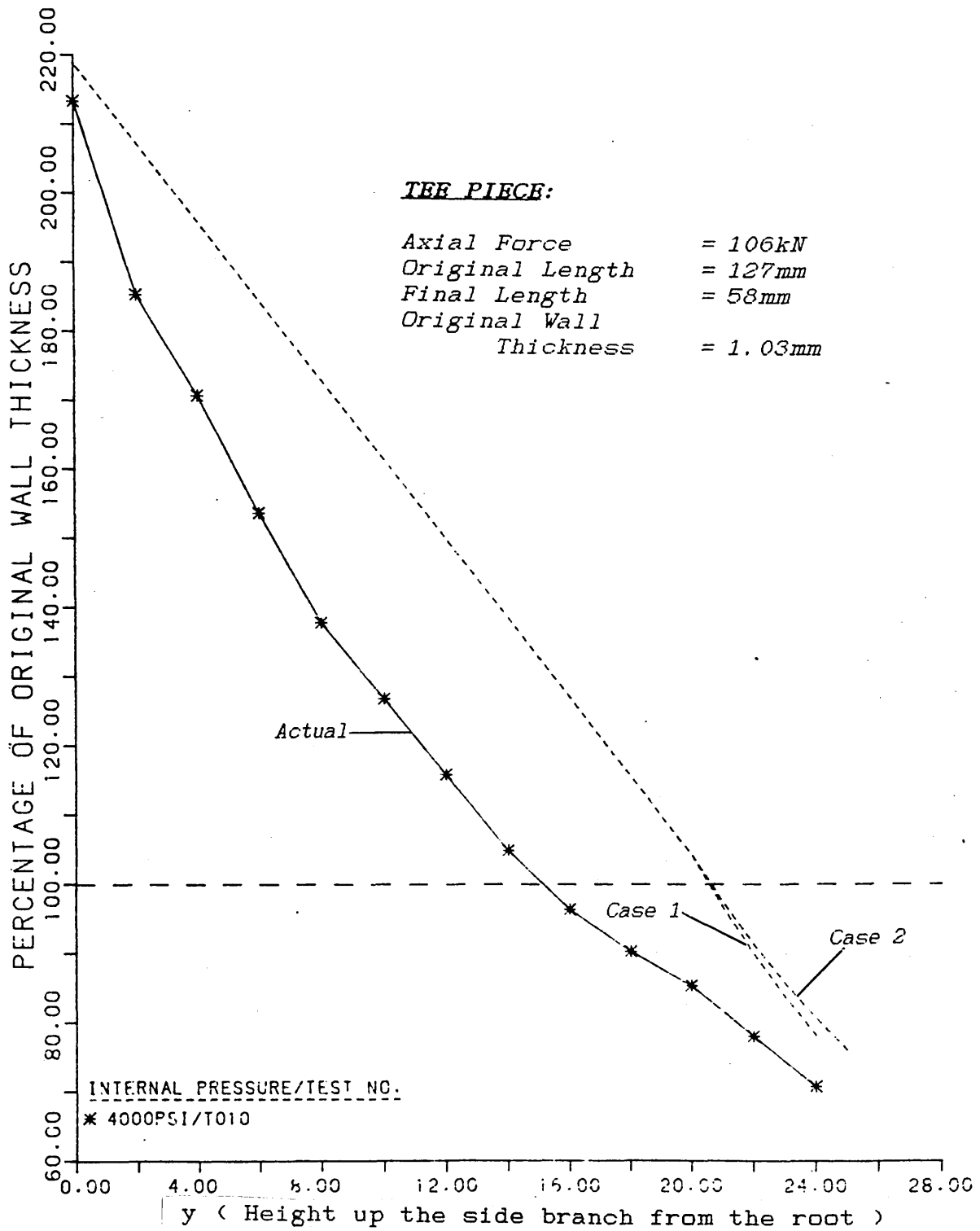


Fig. 86.
Comparison of the Experimental Wall Thickness Distribution with Theoretical Predictions.

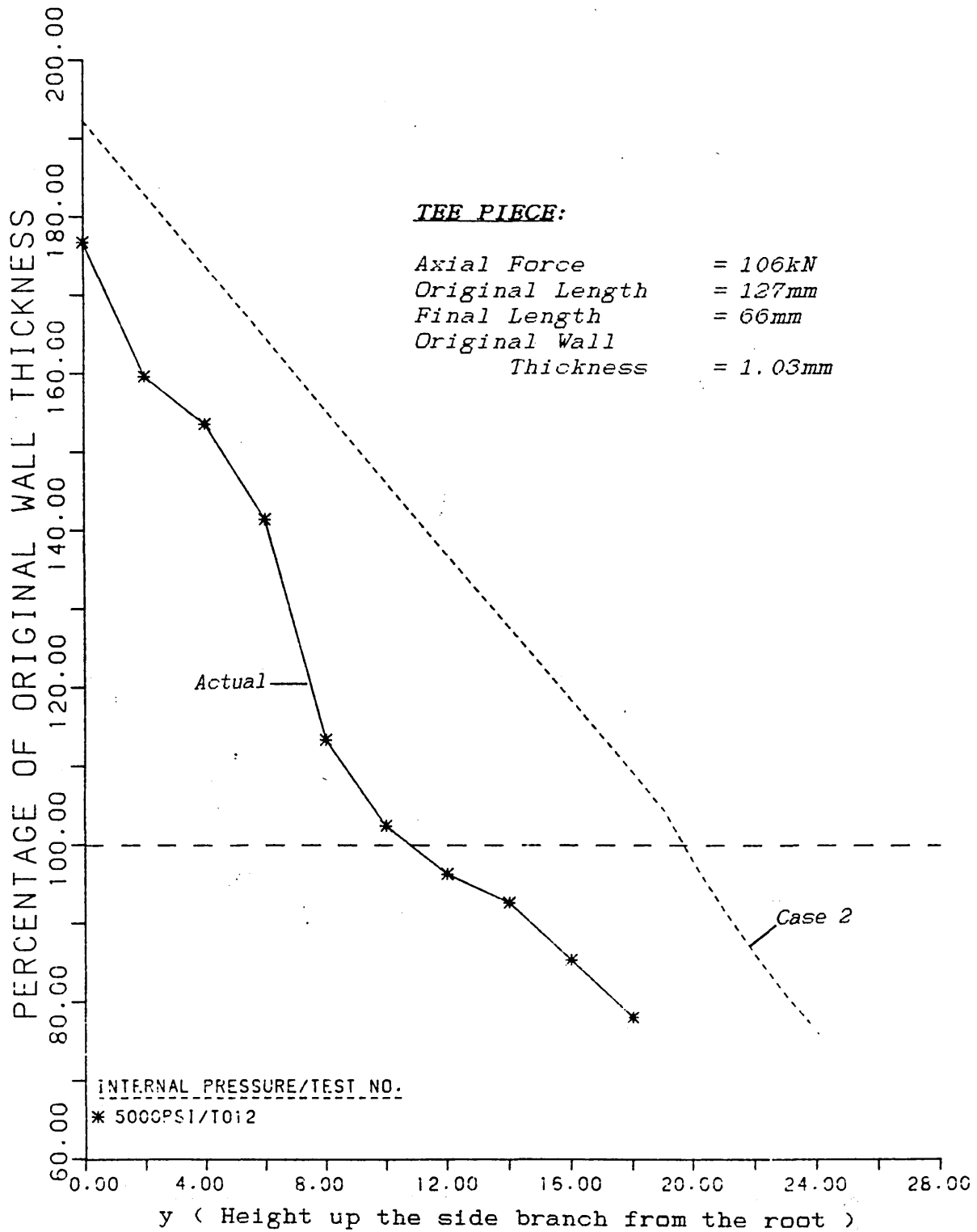


Fig. 87.
Comparison of the Experimental Wall Thickness Distribution with Theoretical Predictions.

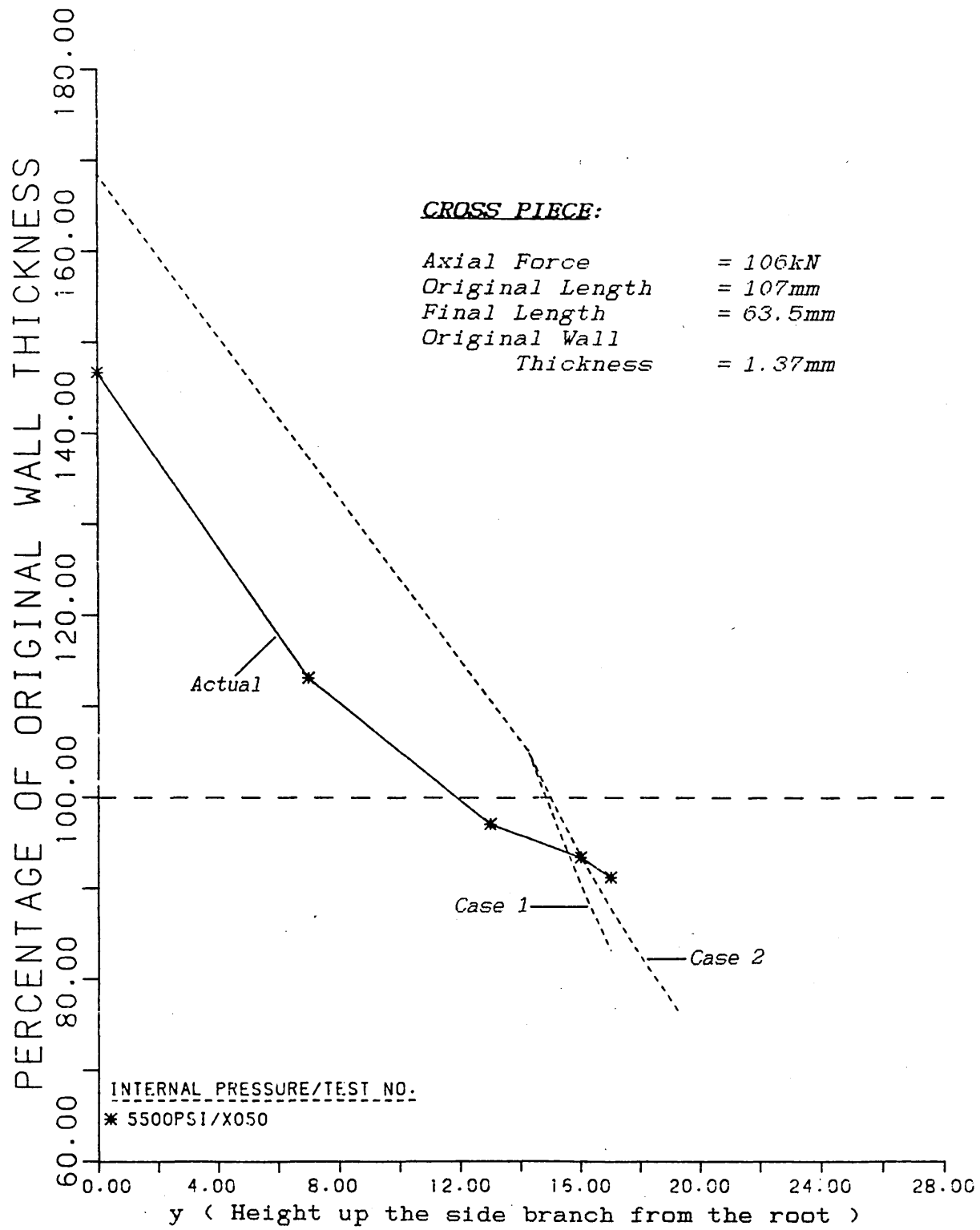


Fig. 88.
Comparison of the Experimental Wall Thickness Distribution with Theoretical Predictions.

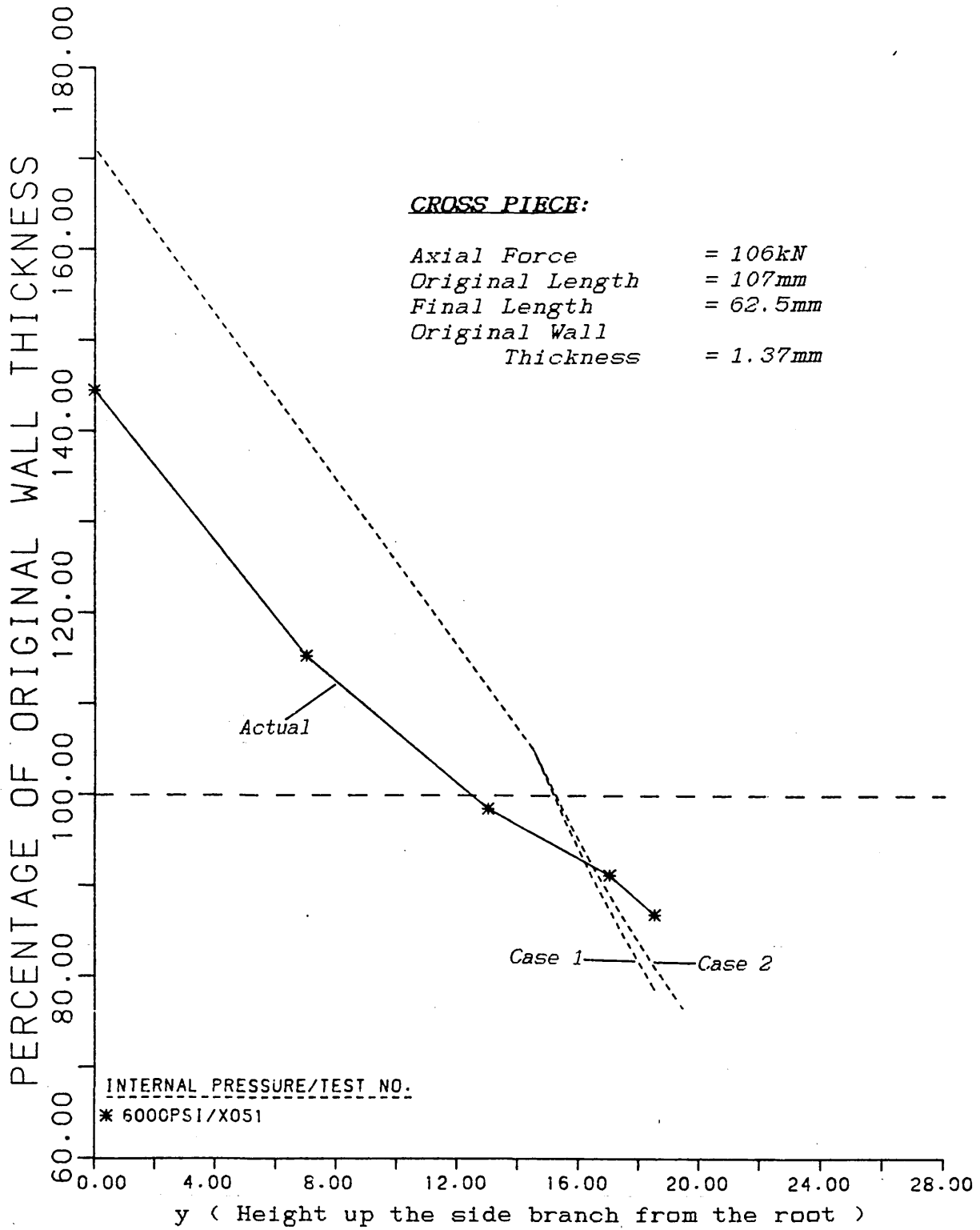


Fig. 89.
Comparison of the Experimental Wall Thickness Distribution with Theoretical Predictions.

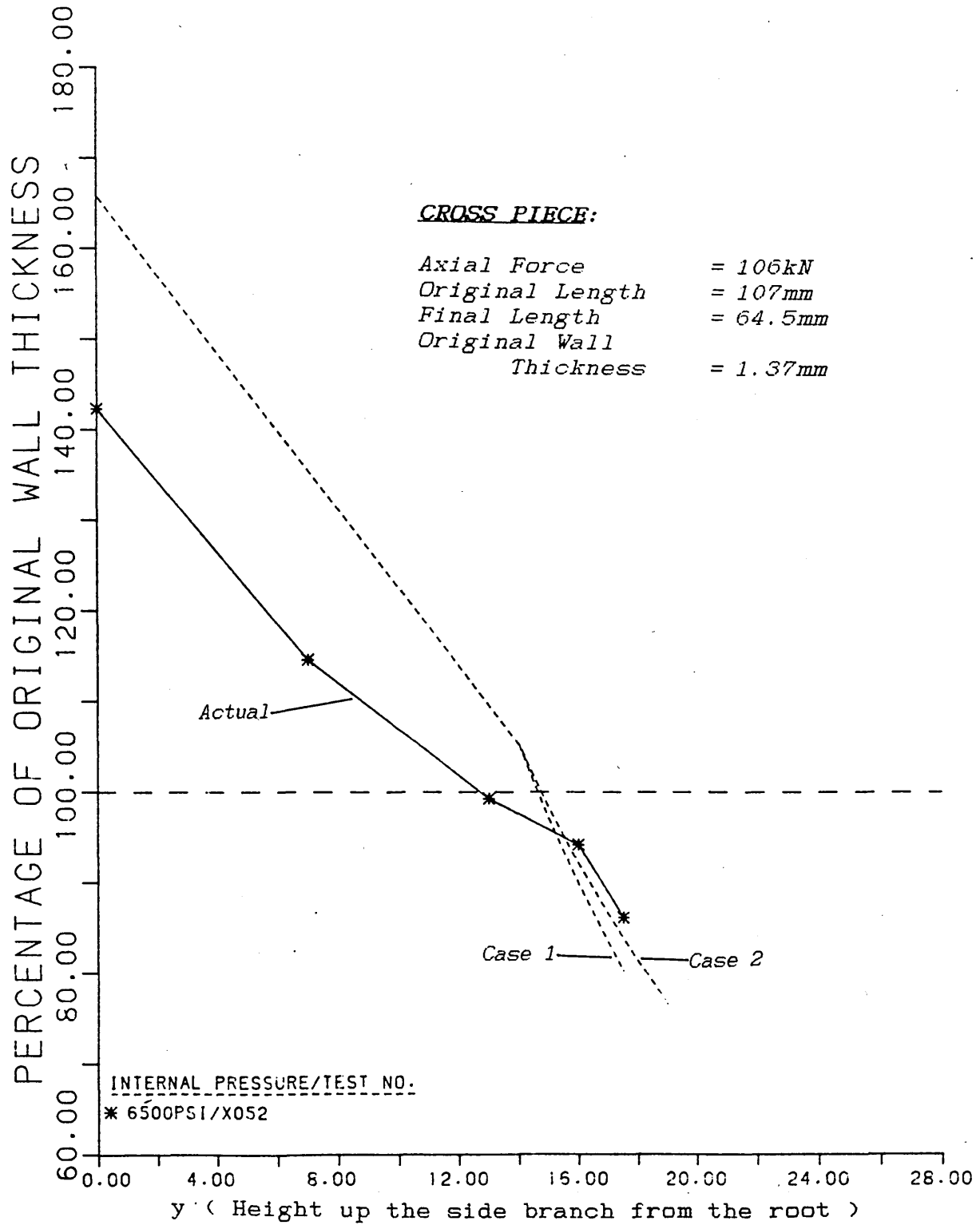


Fig. 90.
Comparison of the Experimental Wall Thickness Distribution with Theoretical Predictions.

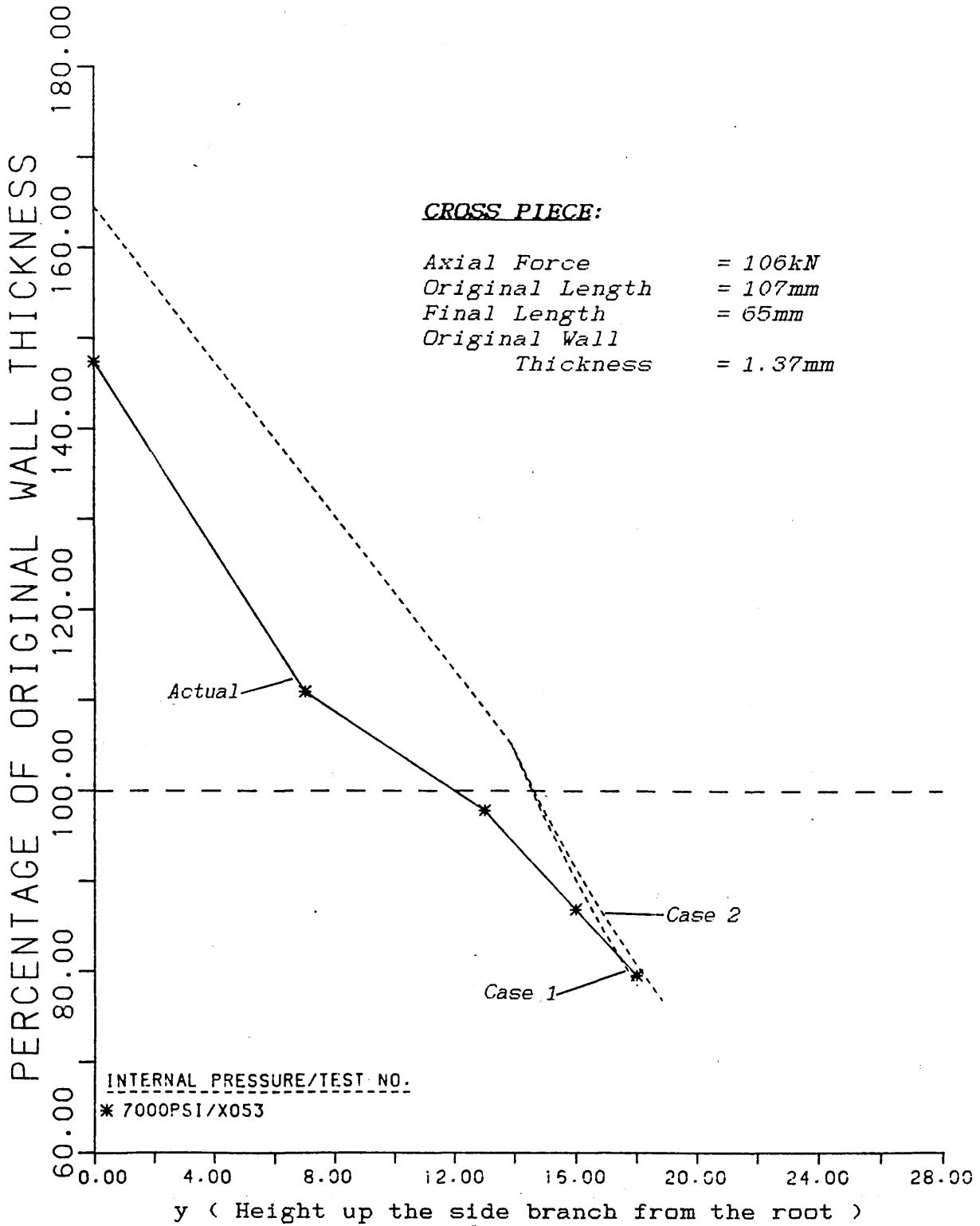


Fig. 91.
Comparison of the Experimental Wall Thickness Distribution with Theoretical Predictions.

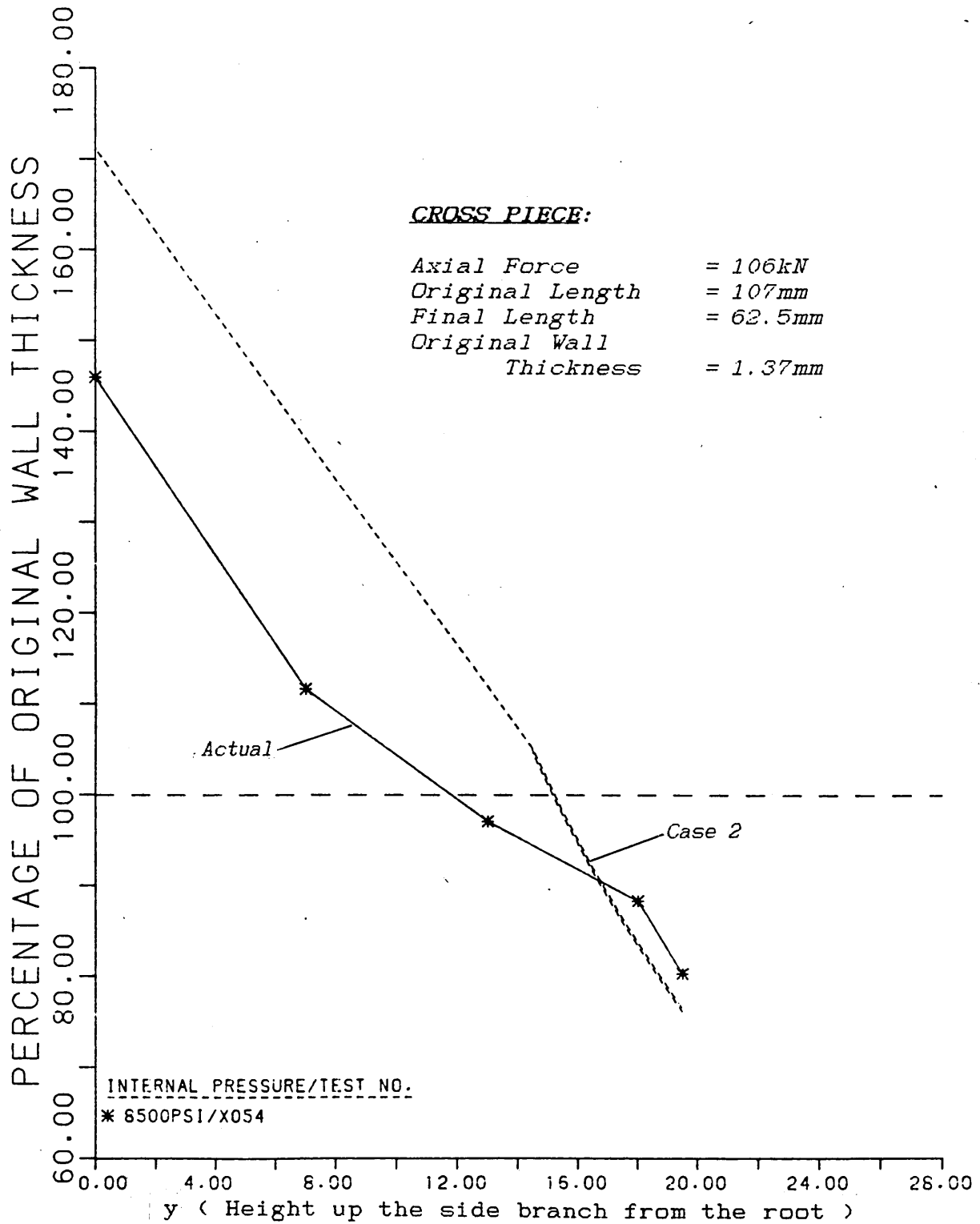


Fig. 92.
Comparison of the Experimental Wall Thickness Distribution with Theoretical Predictions.

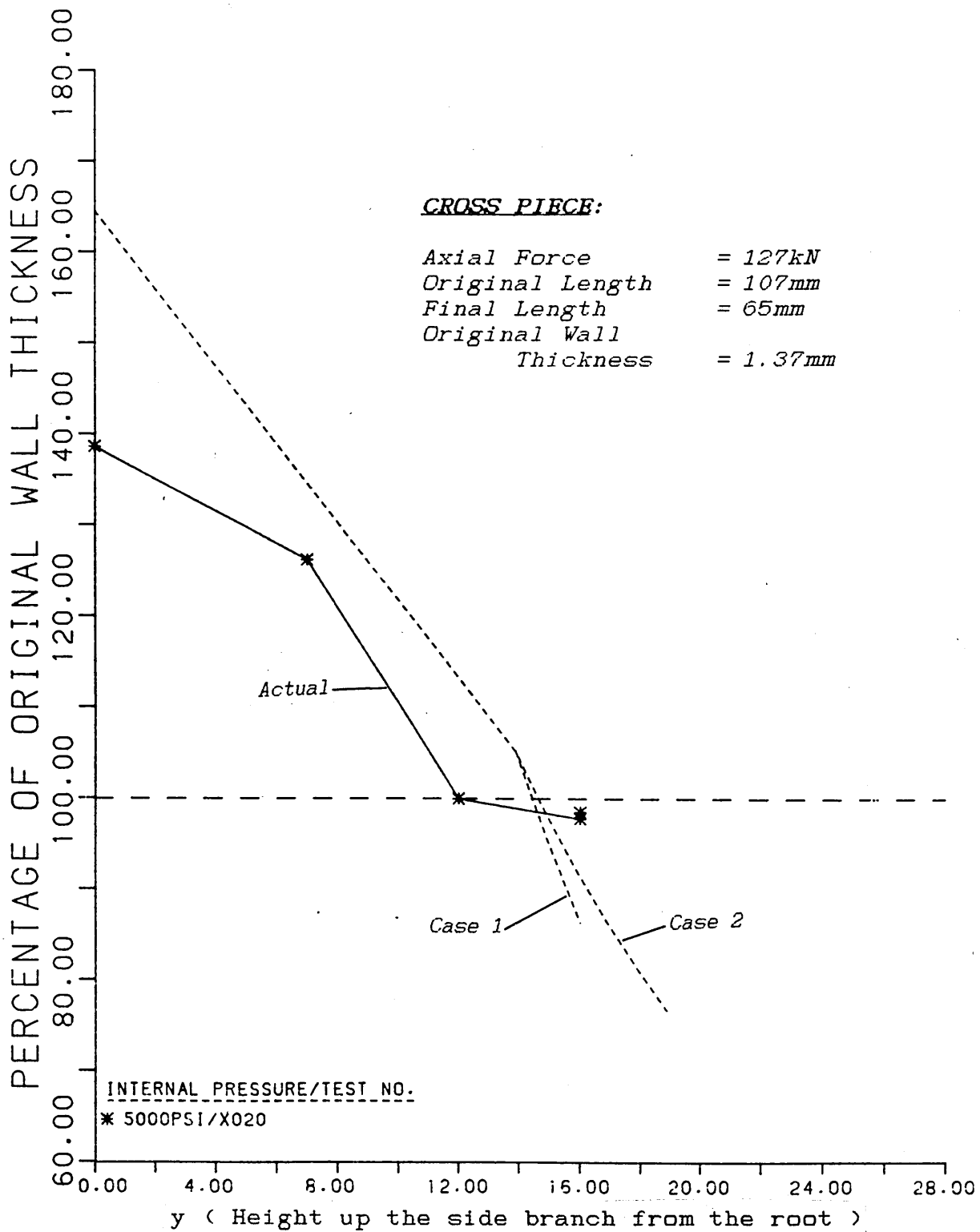


Fig. 93.
Comparison of the Experimental Wall Thickness Distribution with Theoretical Predictions.

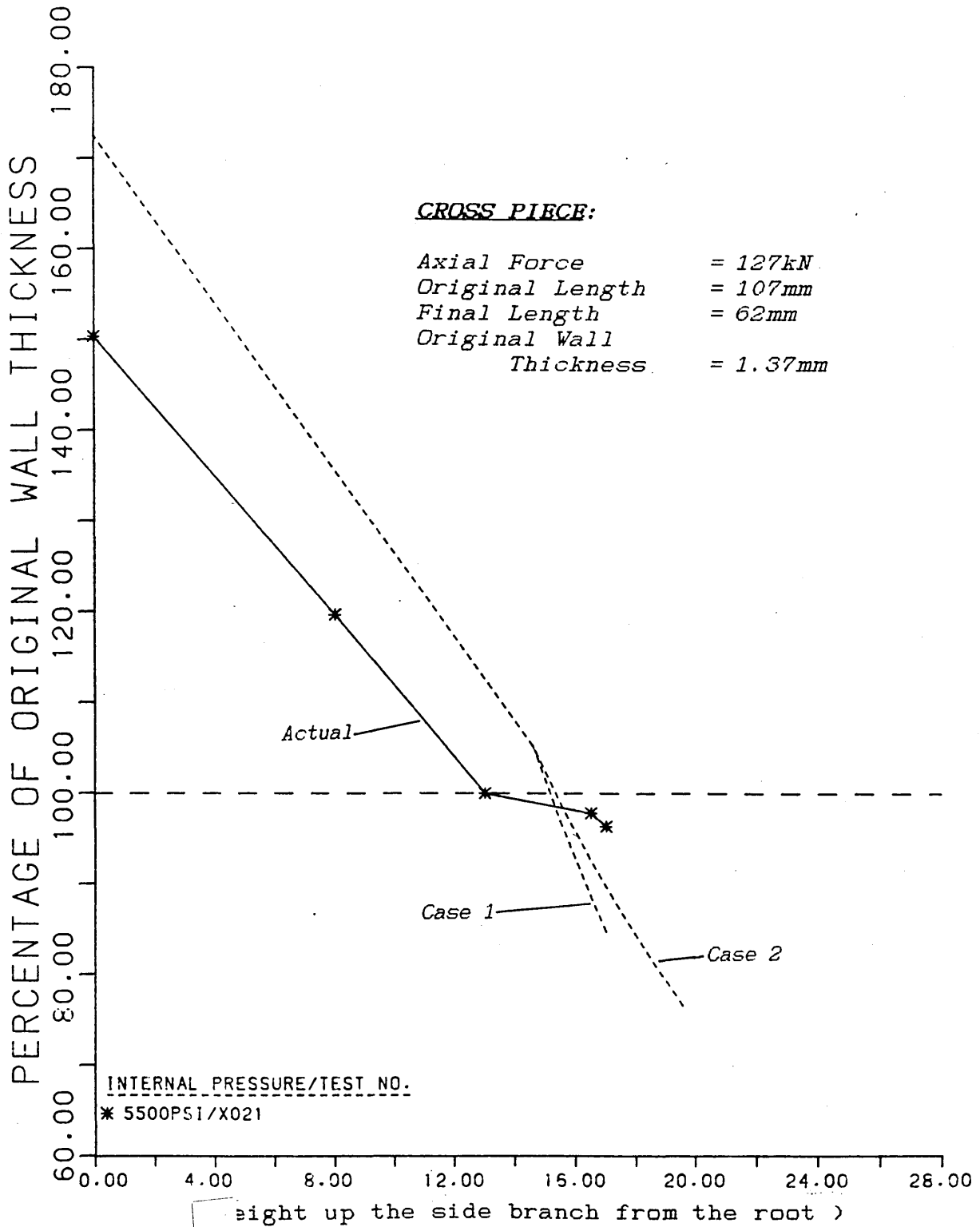


Fig. 94.
Comparison of the Experimental Wall Thickness Distribution with Theoretical Predictions.

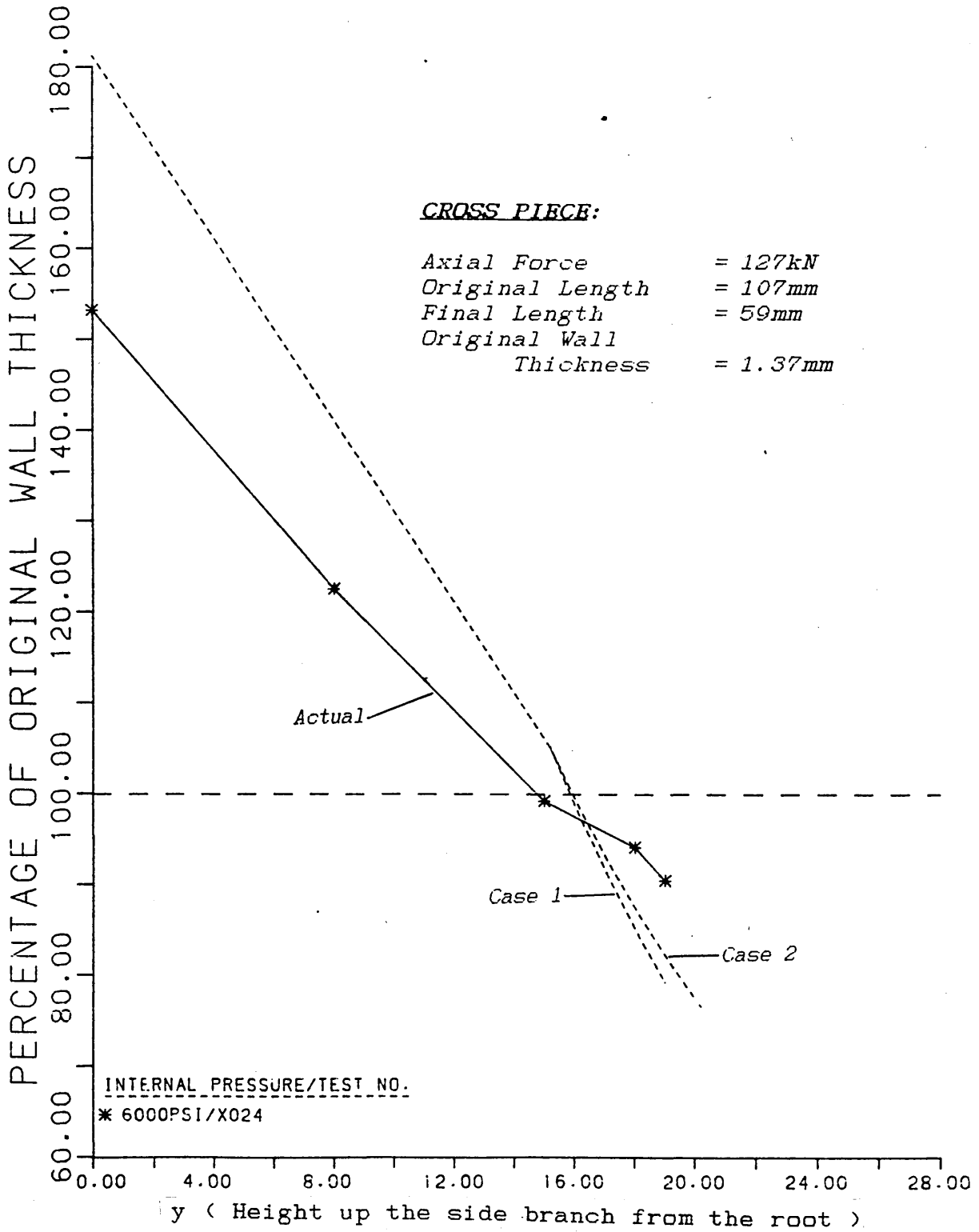


Fig. 95.
Comparison of the Experimental Wall Thickness Distribution with Theoretical Predictions.

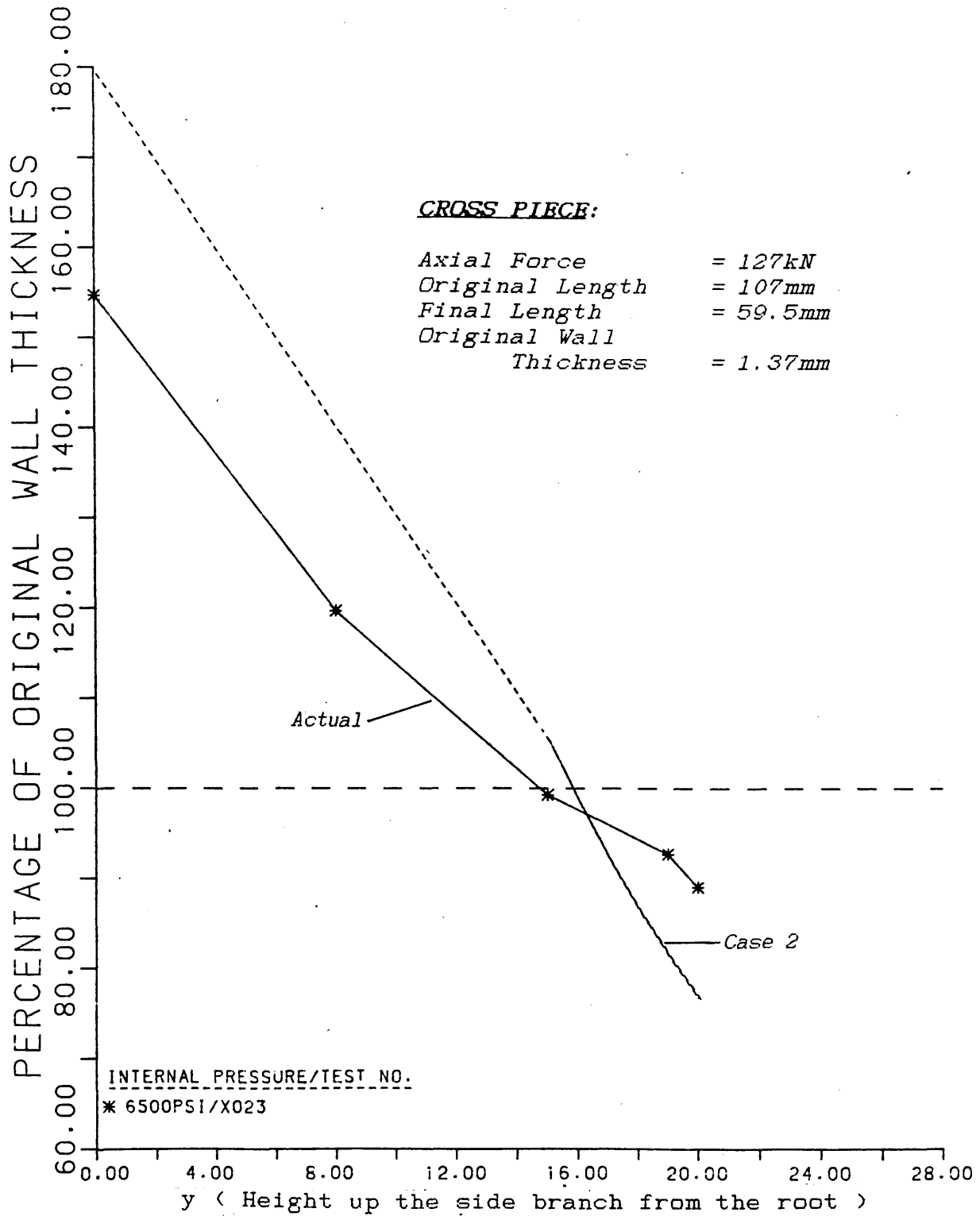


Fig. 96.
Comparison of the Experimental Wall Thickness Distribution with Theoretical Predictions.

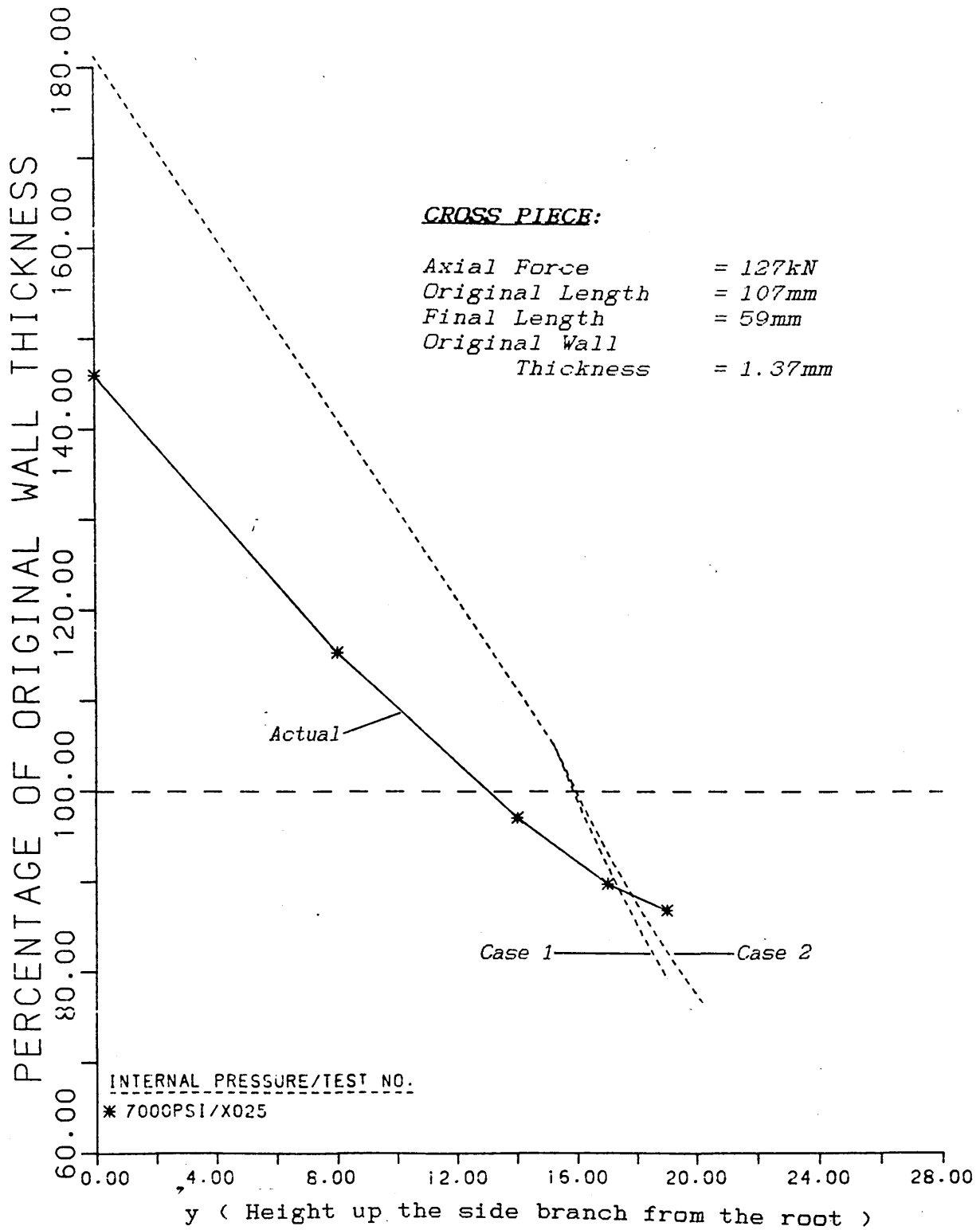


Fig. 97.
Comparison of the Experimental Wall Thickness Distribution with Theoretical Predictions.

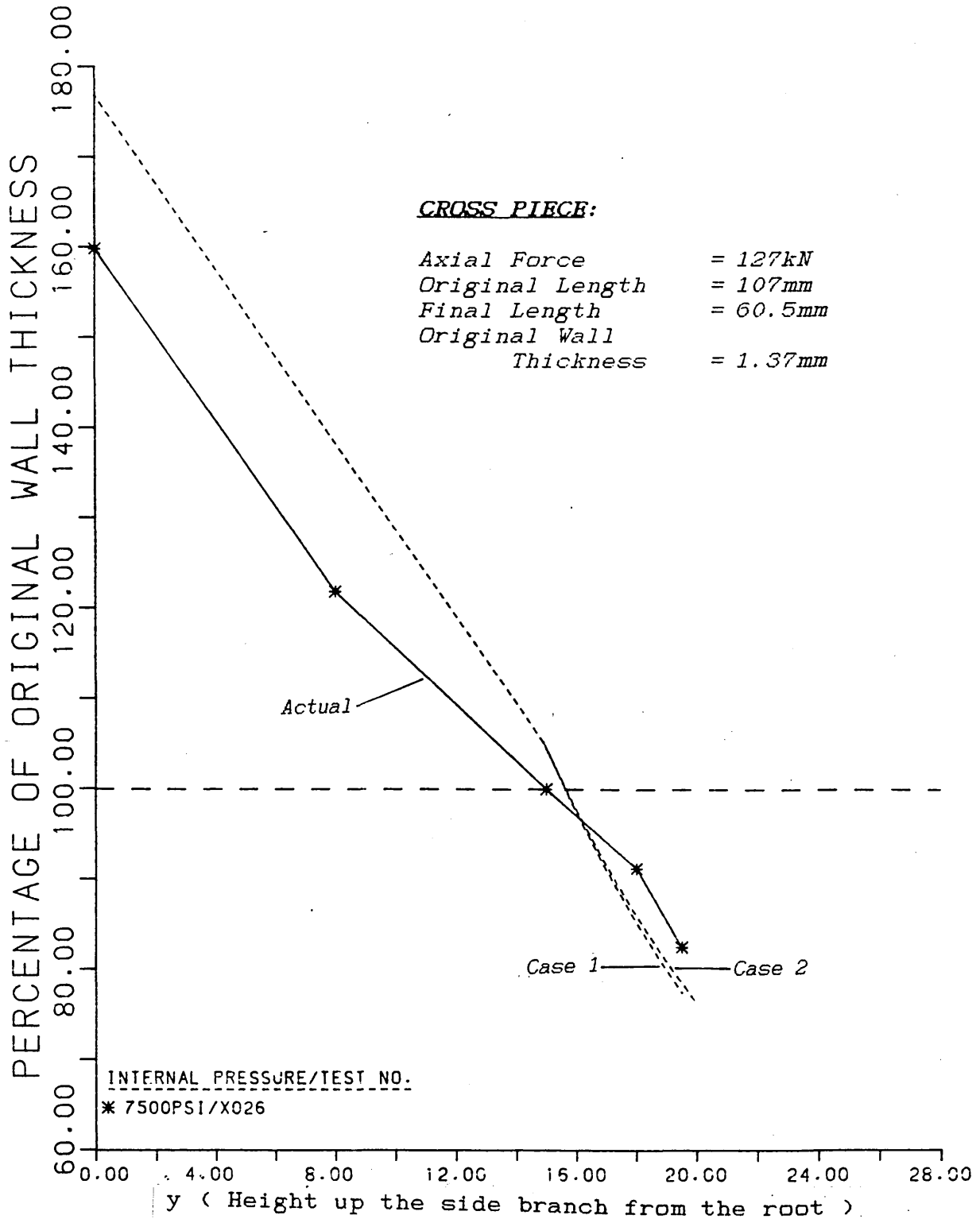


Fig. 98.
Comparison of the Experimental Wall Thickness Distribution with Theoretical Predictions.

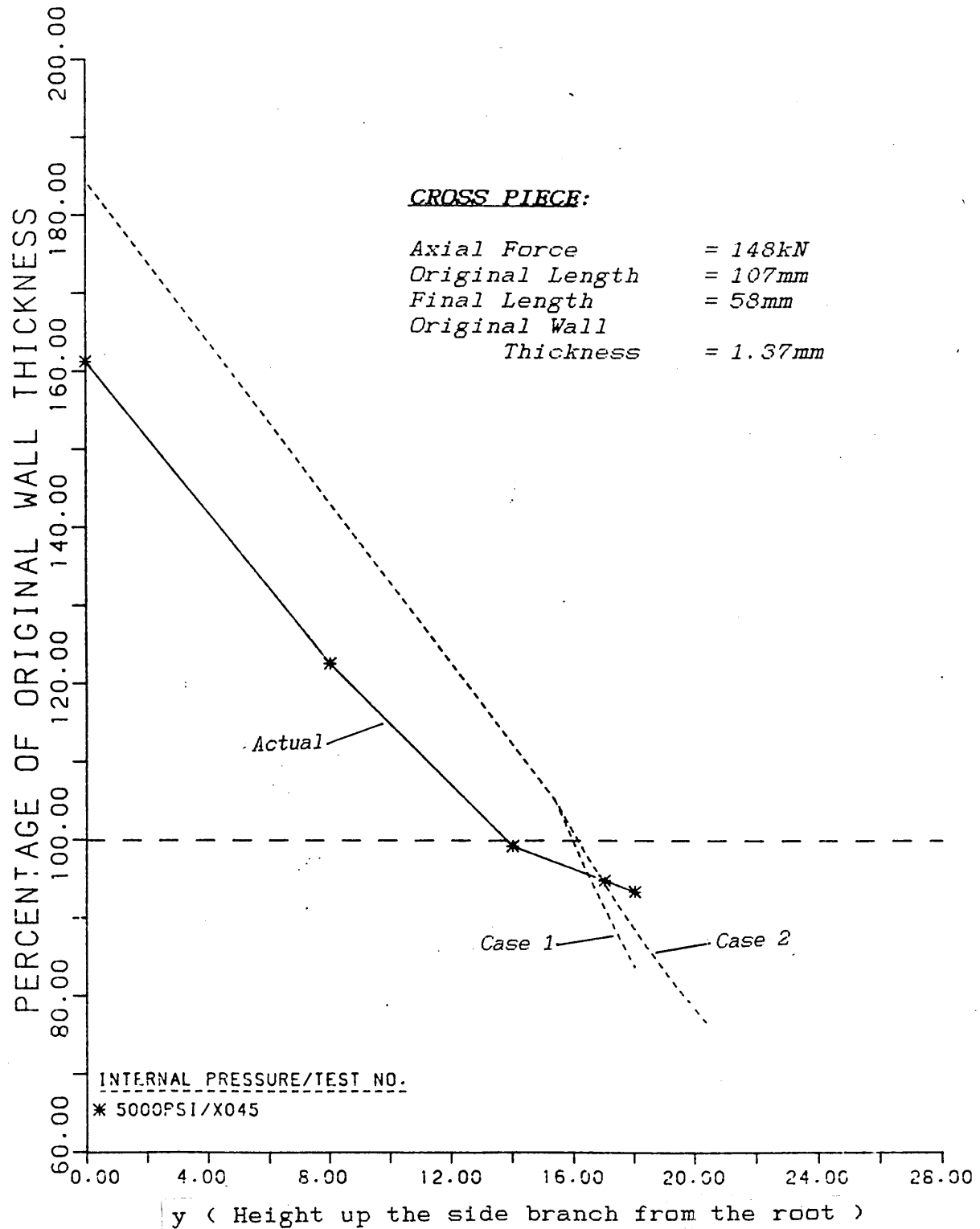


Fig. 99.
Comparison of the Experimental Wall Thickness Distribution with Theoretical Predictions.

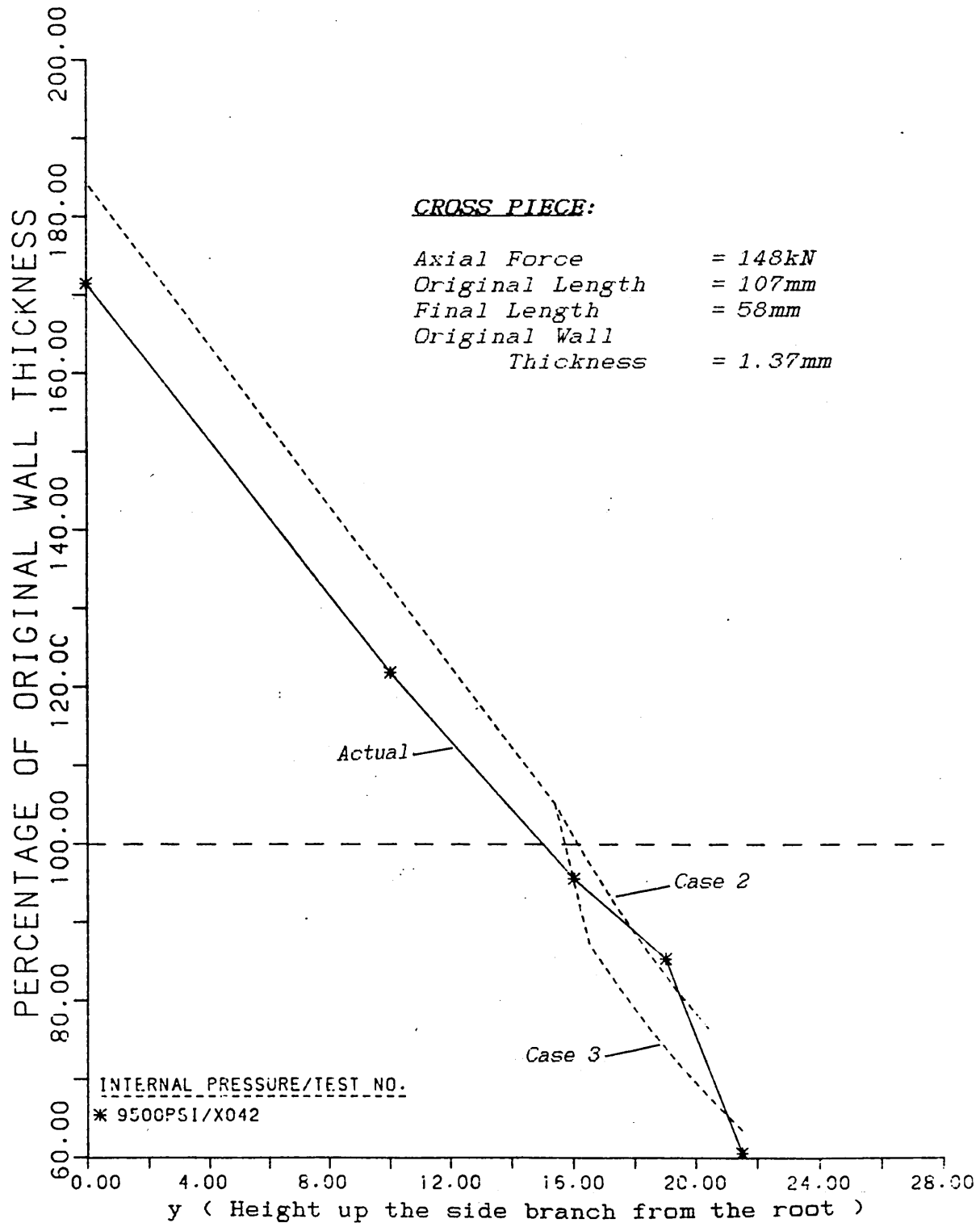


Fig. 100.
Comparison of the Experimental Wall Thickness Distribution with Theoretical Predictions.

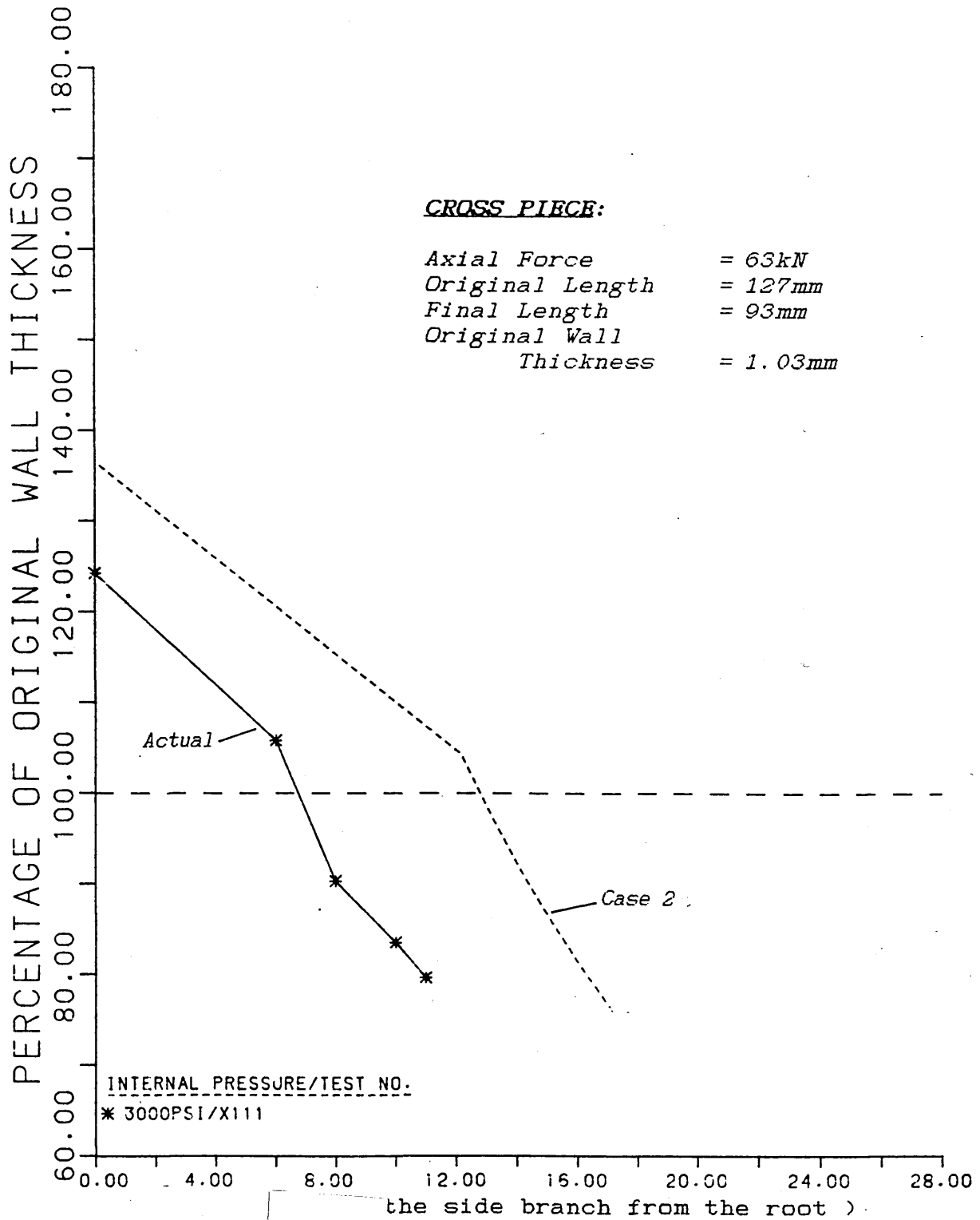


Fig. 101.
Comparison of the Experimental Wall Thickness Distribution
with Theoretical Predictions.

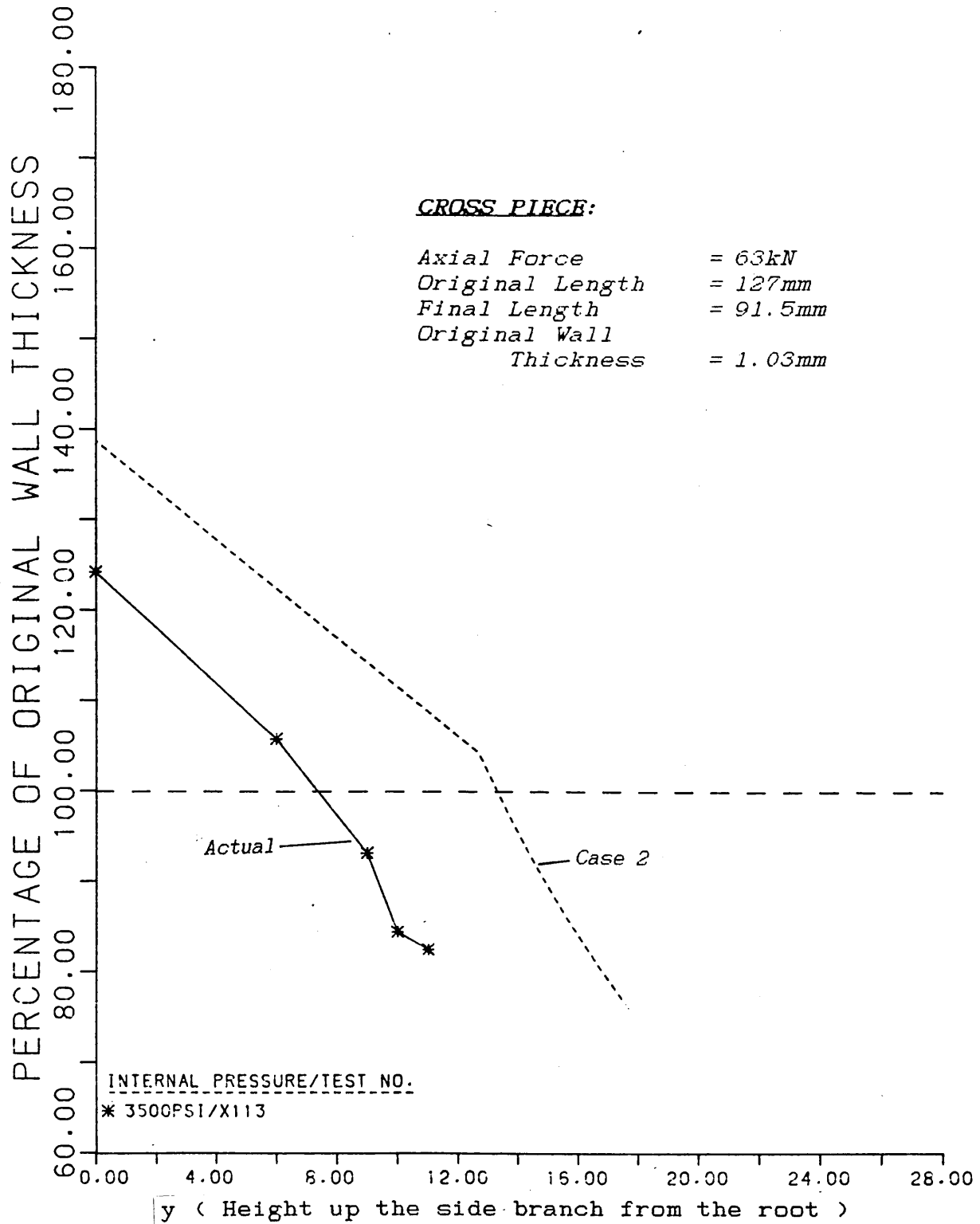


Fig. 102.
Comparison of the Experimental Wall Thickness Distribution with Theoretical Predictions.

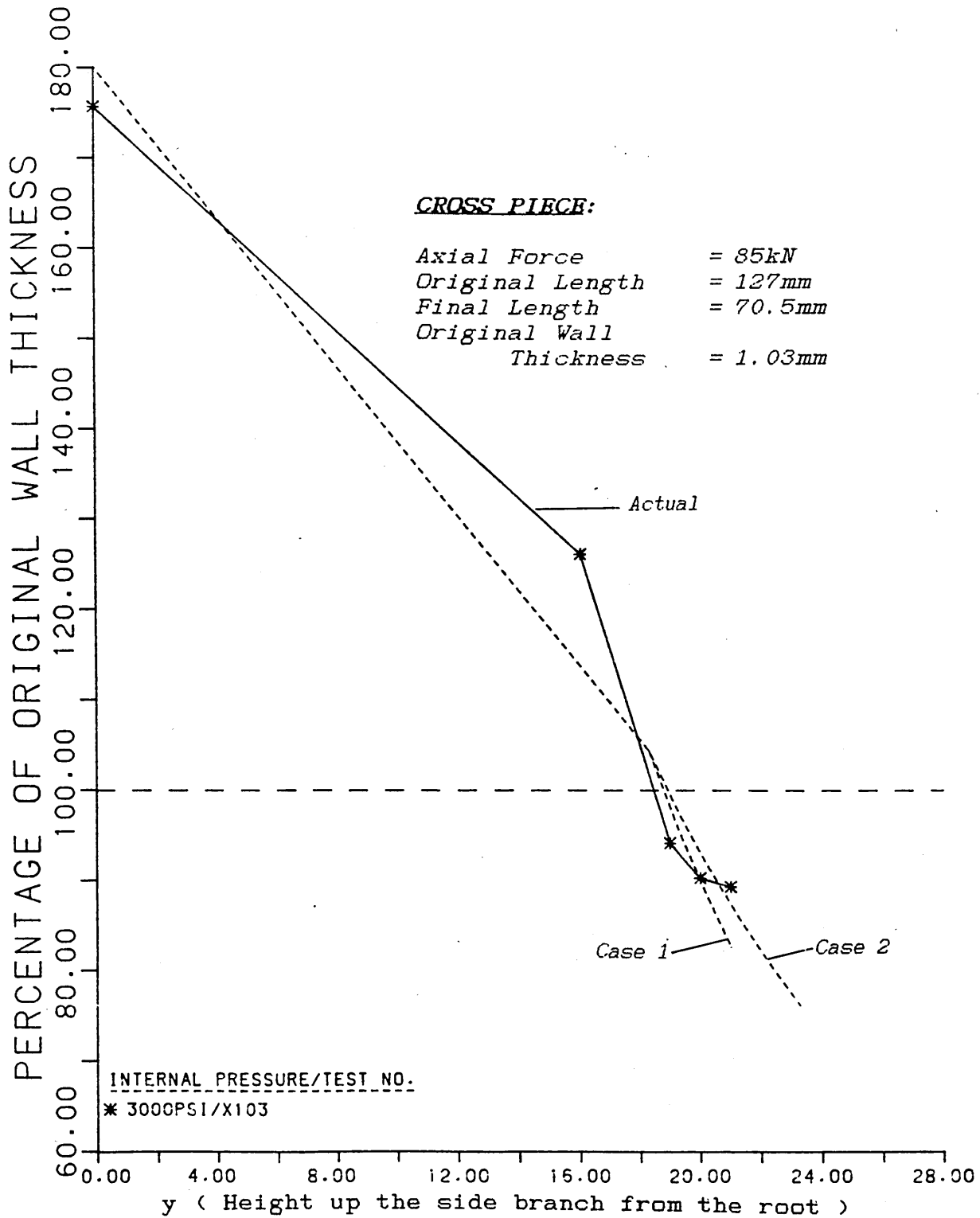


Fig. 103.
Comparison of the Experimental Wall Thickness Distribution with Theoretical Predictions.

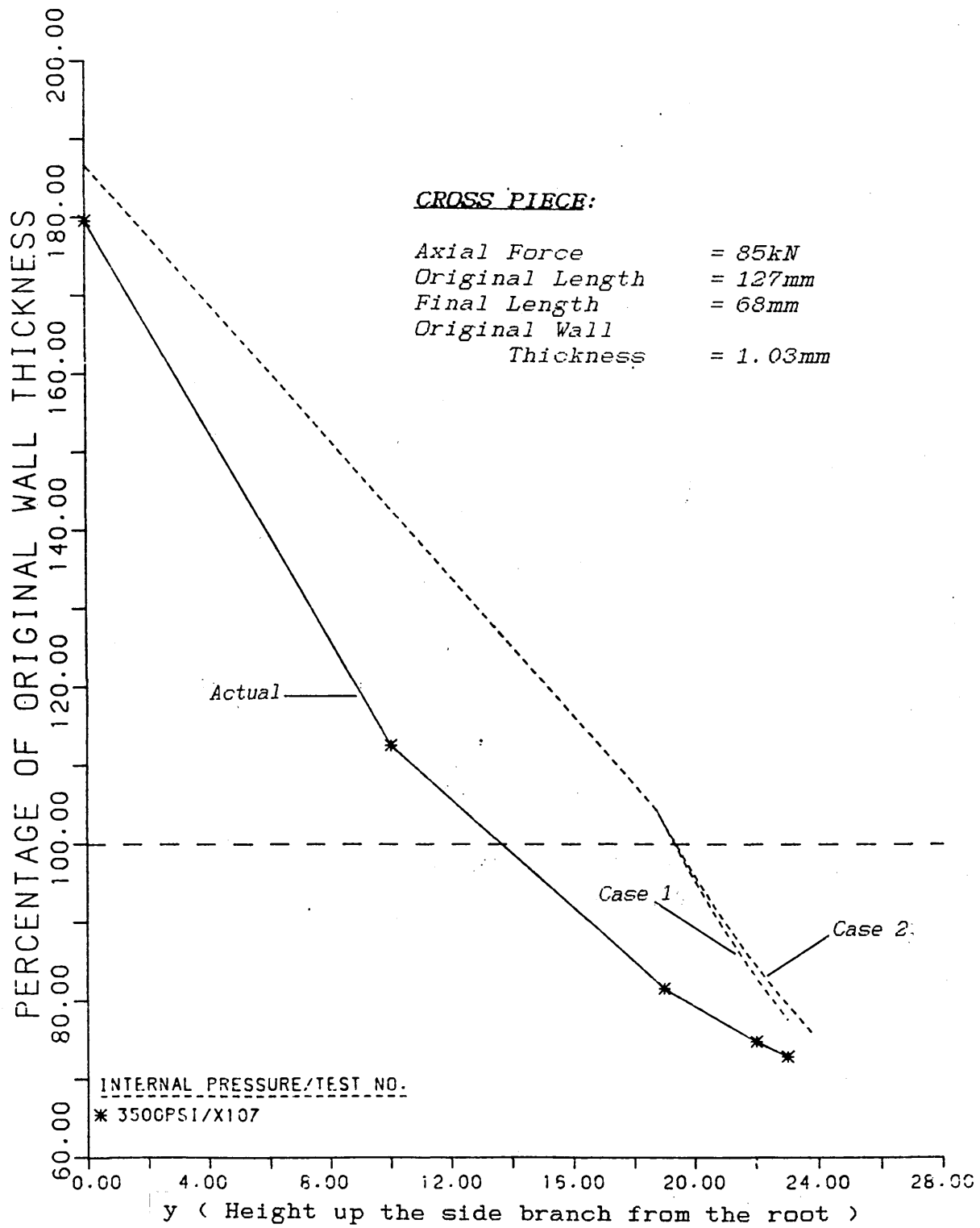


Fig. 104.
**Comparison of the Experimental Wall Thickness Distribution
with Theoretical Predictions.**

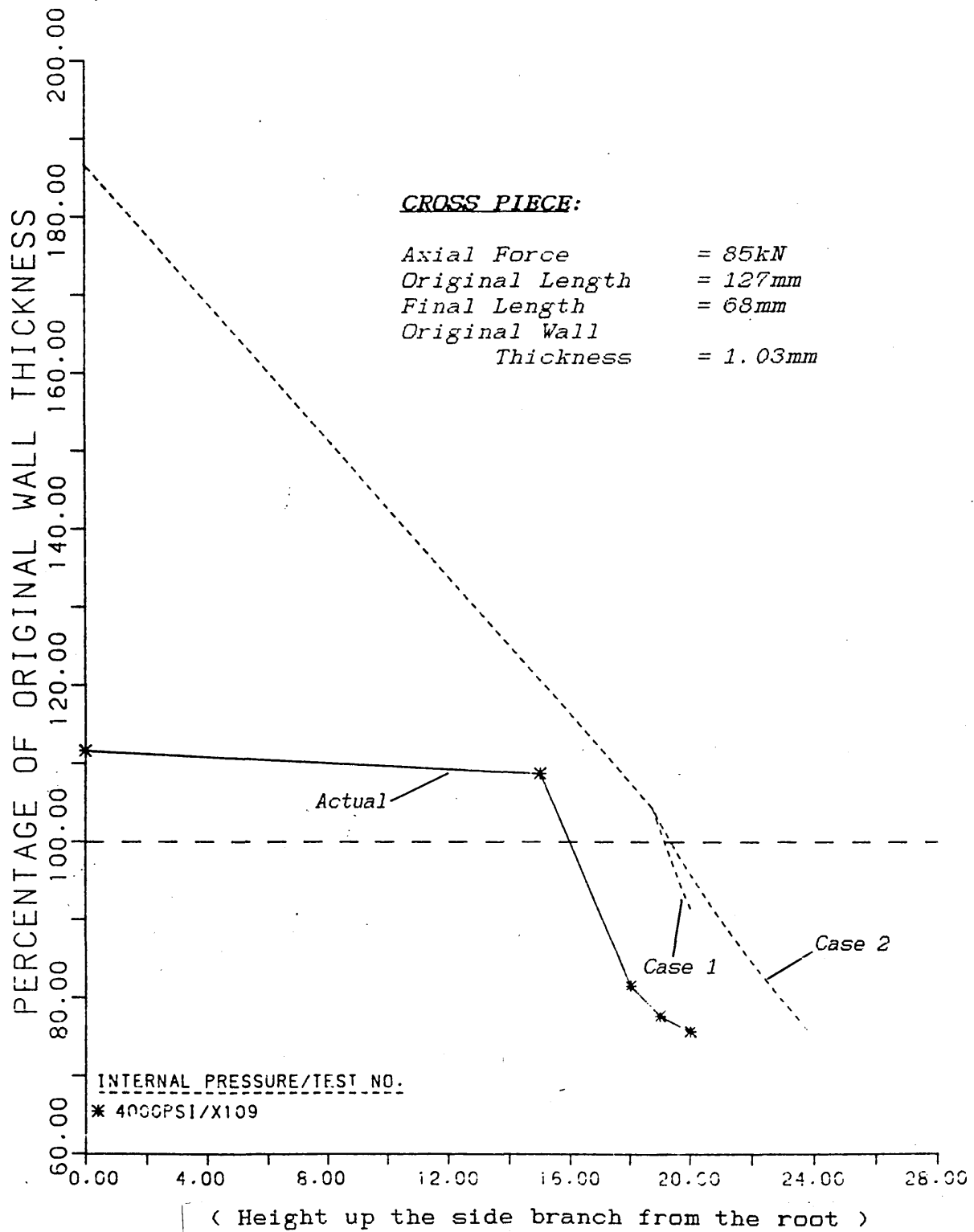


Fig. 105.
Comparison of the Experimental Wall Thickness Distribution
with Theoretical Predictions.

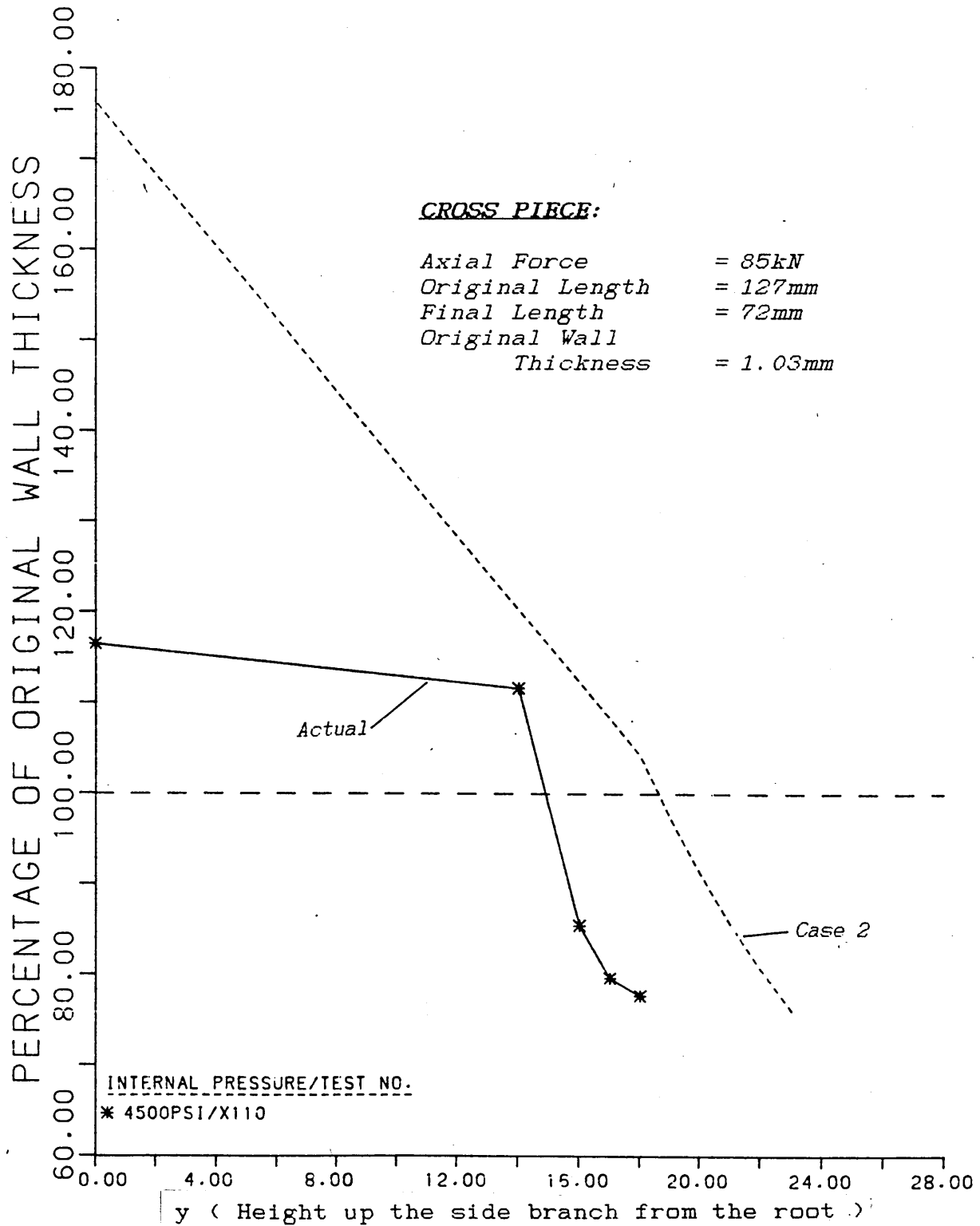


Fig. 106.
Comparison of the Experimental Wall Thickness Distribution
with Theoretical Predictions.

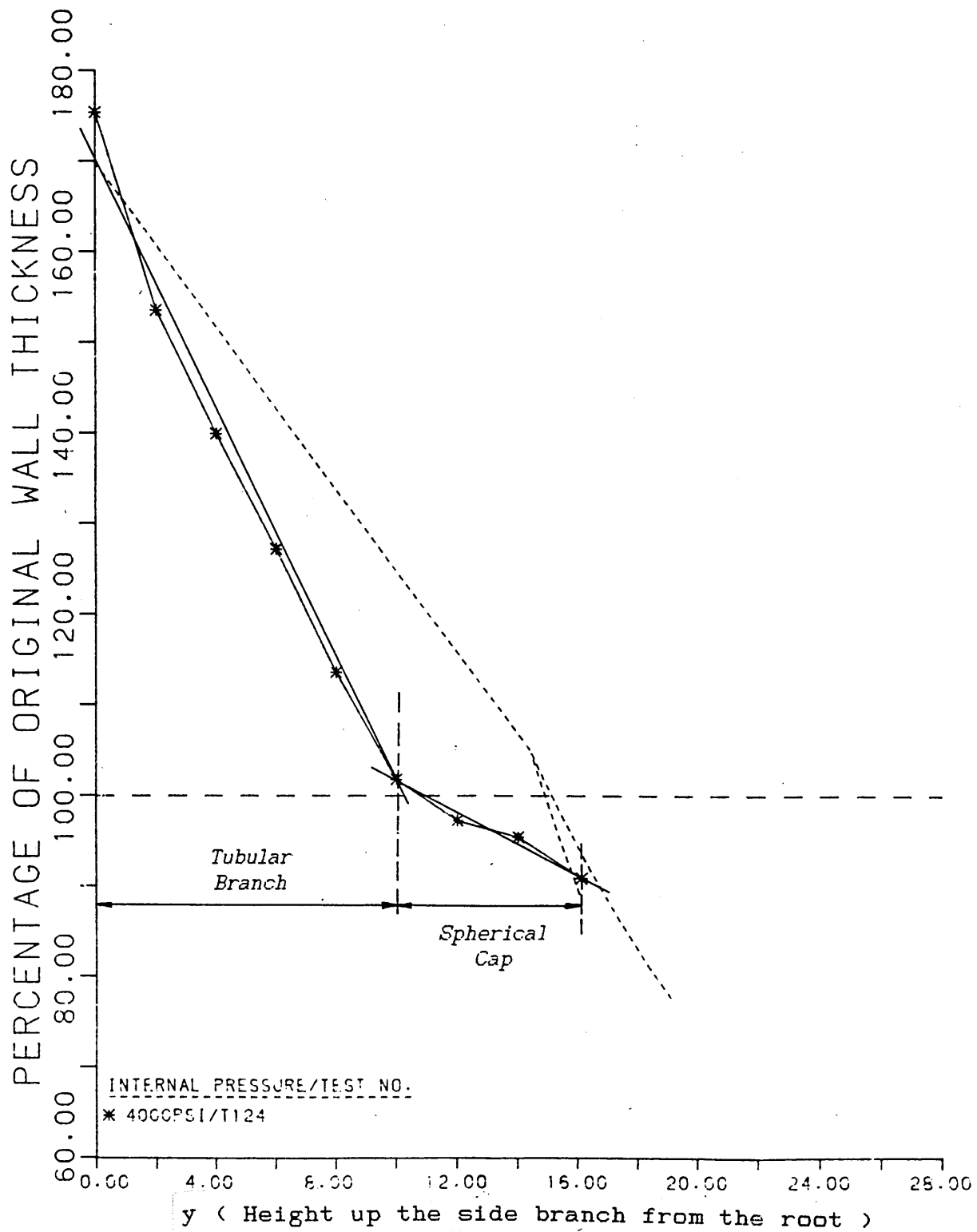


Fig. 107.
Distinguishing the Tubular Branch and Spherical Cap by
Linear Interpretation of the Wall Thickness Distribution.

6. DISCUSSION

6.1. THE DESIGN AND COMMISSIONING OF THE MACHINE

6.1.1. Operating Parameters and Design Considerations

The operating parameters and design considerations were based on tests carried out using a prototype bulge forming rig, and on an assessment of a literature survey that was carried out. The main problems encountered when using the prototype rig were the length of time it took to carry out each test and an inconsistency in the applied forces (it was impossible to carry out two tests in which all of the forming conditions were identical).

The first consideration in the design of the new bulge forming machine was that it should be free standing and self contained. The prototype rig required assembling on a Denison compression testing machine before each test and had to be dismantled afterwards. This considerably lengthened the time required for each test, and involved moving heavy lumps of metal around. The next consideration concerned the problems previously encountered trying to extract the formed component from the dies. These were split laterally in relation to the tube in the prototype. During forming the tube would expand along the entire length, and where restricted the tube wall would be forced against the wall of the die. This prevented the two halves of the die from being separated.

Therefore, to allow the easy separation of the two die halves and removal of the formed component, it was decided that the dies should split axially. However, this meant that the two die halves would have to be clamped together during forming in order to resist the internal pressure trying to force the two halves apart. This could have been done

with bolts or clamps, but a hydraulic cylinder was chosen as this would actually open and close the dies and would be quicker to use. Another reason for using a hydraulic cylinder was that the design of the machine had to incorporate facilities for subsequent automatic control using a micro-processor or computer.

6.1.2. Hydraulic System

Hydraulic cylinders were also selected for applying the axial compressive forces to the ends of the tube. In the prototype this was done by the compression testing machine, which provided the deformation of both ends of the tube. However, this did not produce equal deformation of each end, sometimes resulting in a mishaped component being formed. To avoid this it was decided to use two cylinders, one located at each end of the tube, hydraulically coupled together through a flow divider. Using this system would mean that the two cylinders would act approximately in unison, providing equal deformation of each end of the tube.

From the analysis of tests previously carried out on the prototype rig, an axial compressive force of 200kN and an internal pressure of 10000psi (69 N/mm²) was considered necessary. This was so that tubes of copper and possibly some stronger material could be formed on the new machine. Using this value of internal pressure and assuming a tube blank with dimensions 25mm diameter and 150mm long, a clamping force of 300kN was required to resist the the forces separating the dies.

In order to provide the internal pressure of 10000psi (69 N/mm²) a pressure intensifier to increase the pressure from a hydraulic pressure supply of 2500psi (17 N/mm²) was used. This was because of the expense

that would be involved operating the whole system at 10000psi (69 N/mm²). Running the system at 2500psi (17 N/mm²) would mean that the system would be less costly, but the pressure was sufficiently high as to make the hydraulic cylinders of a manageable size. This led to the choice of two cylinders, , with a diameter of 125mm and a stroke of 100mm, for applying the axial compressive force. To clamp the die together a cylinder, with a diameter of 160mm and a stroke of 150mm was chosen. These were to be powered by a variable displacement piston pump driven by a 7.5kW electric motor.

Having decided on cylinders required for the machine, the next stage in the design was to consider the hydraulic circuit. This was required to control three operations:

1. Opening and closing (clamping) the dies.
2. Applying the axial force to the ends of the tube.
3. Pressurising the internal region of the tube.

The circuit allows independent control of these operations and is in three parts, the simplest part being that supplying the clamping cylinder. This contains a directional control valve to select to open or close the dies, and flow control valves to control the speed of the opening and closing. Also included in this part of the circuit is a pilot operated non-return valve, to prevent the dies from accidentally closing when the supply is turned off.

The part of the circuit supplying the two cylinders applying the axial force contains two parts, each with its own directional control valve, pressure reducing valve, and flow control valve. This is to allow two different forces to be applied to the ends of the tube. The first one being small so as to bring the plungers into contact with the tubes

and seal them, but without deforming them. The second force is required to actually deform the tube and therefore is set to a larger force. The flow from both these two halves pass through a flow divider, as previously mentioned, before reaching the cylinders.

The final part of the circuit supplies hydraulic fluid to the internal region of the tube. As previously mentioned the supply pressure requires boosting through a pressure intensifier to provide the high internal pressure. Also included in this part of the circuit are a pressure reducing valve, a flow control valve and a directional control valve. The directional control valve can either activate the pressure intensifier, or bypass it. Bypassing it is useful when the tube is being filled at the start of the test, as this produces a faster flow rate than the intensifier. In addition, the circuit also contains a valve which allows the air to be bled from the tube when it is being filled with oil.

The circuit has safety features, including pressure relief valves and check valves, to prevent damage to the circuit from too high a pressures and filters to keep the hydraulic fluid free from contamination. All of the operations, apart from opening the valve to bleed the air from the tube, are activated by solenoid operated directional control valves. The pressures and forces being applied can be preset using the pressure reducing valves and the pressure relief valves. It would, therefore, be quite possible to apply automatic control to sequence the operation, using a micro computer or a micro processor, although at the moment operation is by manual control.

6.1.3. Structural Design

Once the size and shape of the hydraulic cylinders had been ascertained the structural design was undertaken. The central and most important part of the machine is the die block in which the actual forming process occurs. As previously mentioned the die block is split axially to allow access to the formed component. When the two halves are brought together it is important that they mate up with each other. This is achieved by mounting them on a "Desoutter" die set, consisting of two plates aligned by pins and bushes. To allow different components to be produced each die block half consists of an outer die holder and an inner die which can be removed and replaced with differently shaped dies.

Around this die block are mounted the three hydraulic cylinders. The two cylinders applying the axial compressive force are mounted horizontally at opposite ends of the die block acting inwards. The clamping force is achieved by mounting the third cylinder vertically, above the die block, acting downwards. To restrain this clamping force, the plate to which the cylinder is bolted is connected to a similar plate beneath the die block by four tie bars. The axial compressive force is restrained by mounting the cylinders on a pair of sturdy channel section beams. In the centre of these beams is positioned the die block and clamping cylinder. Originally it had been intended to weld the assembly together. However, equipment was not available to machine the mounting surfaces square to one another. Instead the assembly was bolted together to avoid any distortion which might have occurred during welding.

To transmit the axial force from the horizontal cylinders to the ends of the tube, plungers are used which enter the ends of the die block through guides. These plungers are also used to deliver the oil to the

internal pressurised region of the tube. Thus, they contain oil passages down their length. Another important job of the plungers is to seal the ends of the tube so that an internal pressure can build up. In the prototype, this was achieved using O-rings which were invariably damaged by the ends of the tube. This resulted in leakage, causing a loss of the internal pressure. On the new forming machine, the use of O-rings has been discarded and instead, the part of the plunger entering the tube is tapered. This produces a tight fit when fully inserted into the tube. Like the prototype rig the tube butts up against a step on the plunger and sealing is also achieved by the application of an axial compressive force.

To provide a reasonable working height and to support the assembly, the machine is mounted in a framework made up of angle iron. This allows easy access to the die blocks in order to position a tube blank prior to forming, and to remove the formed component afterwards. Onto this framework is also mounted all the hydraulic valves and pipework, with the hydraulic power supply unit positioned behind the machine on the floor, connected by flexible hoses.

6.1.4. Commissioning

The initial problem encountered after completion of the machine was the misalignment of the two horizontal hydraulic cylinders. These cylinders apply the axial compressive force to the ends of the tube. This force is transmitted to the tube via plungers which enter the ends of the die blocks through guides. In the initial design, the plungers were attached to the cylinders by bolts passing through them into a plunger mount attached to the end of the cylinder rod. As has been previously mentioned, machinery was not available to machine the mounting faces square. Although great care was taken in the building of the machine to keep everything in line, slight misalignment was present. This prevented the original mounting method being used. Instead a floating connection allowing movement of the plunger was required. This was achieved by fitting an oversized collar over the end of the plunger and bolting it to the original plunger mount. Now when extending the cylinders, the plungers are pushed directly by the plunger mount, but are allowed to move sideways within the collar. On retracting the cylinders, the plungers are pulled back by the collars.

At the same time a second problem was solved, which also concerned the horizontal cylinders. On the extension and retraction of the cylinders, rotation of the cylinder rods occurred. This had to be prevented because of the hydraulic pipes and hoses connected to the plungers to provide the internal pressure. Rotation of the rods could have caused rupture of these pipes if they snagged on anything during movement. The rotation of the rods was prevented by machining a flat onto the plunger mounting collars, and mounting a piece of angle iron

along side each one. This sliding contact between the flat on the collar and the angle iron during extension and retraction prevents any excessive rotation occurring.

Problems in the hydraulic circuit were then identified. The first was the inability to create a high internal pressure using the pressure intensifier. This was corrected simply by shortening one of the pipe fittings screwed into the body of the pressure intensifier. However, having solved that problem, when the axial compressive force was applied to deform the tube, an excessive internal pressure was generated, which caused rupture of the tube. When forming tee and cross pieces there is a decrease in the internal volume - the axial deformation causes an increase in the wall thickness along the main branch. This decrease in volume causes an increase in the internal pressure, which should be released by the pressure relief valve once it reaches the level set by the valve. Therefore, the generation of an excessively high internal pressure indicated a fault in the operation of the high pressure relief valve. This was removed from the machine and another valve fitted. However, this did not remedy the fault, and the original pressure relief valve was found to work perfectly when set up on a test bench. The cause of the fault was eventually traced to the drain pipe from the valve. On its way back to the tank, the drain from the relief valve joined the drain pipe from the pressure intensifier and then the return pipe from the rest of the circuit. Apparently a large back pressure was being generated in the drain pipes, which prevented the pressure relief valve from operating properly. Providing the pressure relief valve with its own separate drain pipe all the way back to the tank prevented this problem and allowed the valve to function correctly.

With these problems corrected, it was then possible to form tee pieces. After several tests, it was noted that the side branch was not being formed centrally on the tube. In the design of the machine, the use of a flow divider had been incorporated in order to synchronize the movement of the two horizontal hydraulic cylinders. Therefore, the components should be formed with the side branch approximately central on the tube. Obviously the two cylinders were not moving in unison, which indicated a fault in the flow divider. This was cured by simply removing the flow divider temporarily from the machine, and cleaning it out. The fault was due to a small amount of dirt inside the flow divider, causing the spool to stick. On replacement, the tee pieces were formed with the side branch central on the tube.

Once these problems had been sorted out, no further difficulties were encountered with the machine. The only work that needed doing to it during a long series of tests was the replacement of an oil filter and topping the main tank up with oil.

A large amount of oil is allowed out of the hydraulic system during the forming operation. Some of it is allowed to escape when bleeding the air out of the tube prior to forming. The remainder is contained within the cavity in the bottom die when the formed component is removed. This oil is allowed to drain into a large drip tray mounted underneath the machine. The drip tray is periodically drained and the dirty oil is cleaned by passing it through a filter. The oil is then returned back to the tank. If the forming machine was required for long runs, eg. running for 8 hours a day, this oil recycling operation may be a frequent requirement. In this case, the operation could be simplified, by

attaching a small pump and filter unit to the drain in the drip tray, to automatically return cleaned oil to the main tank.

6.2. EXPERIMENTAL RESULTS

Having overcome all the problems encountered in the commissioning of the machine, the forming of tee pieces and cross pieces was attempted. These were found to be quite easy to produce from copper tube, especially the thicker walled tube (1.37mm original wall thickness). Components were formed with an internal pressure ranging from 3000psi - 8000psi (21N/mm^2 - 55N/mm^2) and an axial compressive force of 26, 63, 85, 106, 127 or 148 kN. From the resulting components formed it was possible to predict the forming limits required for the successful production of a component. These limits are illustrated graphically in Figs. 38.a and 38.b for both the thick walled (1.37mm) and the thin walled (1.03mm) tube. The amount of internal pressure that is required to avoid rupture or buckling is dependant on the axial compressive force being applied. For example, forming the thicker walled tube with an axial compressive force of 50kN requires an internal pressure of between 13 and 48 N/mm^2 . After initial deformation, this pressure can be increased up to a maximum of 55N/mm^2 . If a larger axial compressive force of 150kN was used, the internal pressure would have to be in the range 35 - 48 N/mm^2 , which may be increased to a maximum of 65N/mm^2 during the deformation. Hence, with a higher axial compressive force, a higher internal pressure range is required to prevent the tube from buckling due to the axial deformation.

The bulge forming machine allowed three different ways of controlling the internal pressure during the forming process. The choice

of control depended on the pressures required and the wall thickness of the tube. A constant internal pressure could be used during the process, set by the pressure relief valve. This was used when only a low internal pressure was required - below 6000psi (41N/mm²). When using a high internal pressure - above 6000psi (41 N/mm²) - it was found that this would initially cause rupture of the tube. However, after partial deformation, a tube would be able to contain this pressure. Therefore, in these cases, a low internal pressure, in the range 4000 - 6000 psi (28 - 41 N/mm²) would be applied initially (governed by the pressure reducing valve controlling the pressure intensifier). During forming, this pressure would increase, due to the axial deformation of the tube, to a high internal pressure of between 6000 and 8000 psi (41 - 55 N/mm²), set by the pressure relief valve.

The thin walled tube (1.03mm original wall thickness) was found to be much more difficult to form into a good component, especially with axial compressive forces of 106kN and over. A side branch would form, but this was sometimes squashed in the axial direction, or buckling would occur. To prevent this from occurring a high internal pressure - above 5000psi (35N/mm²) - was required, but this would lead to rupture of the tube. Components were found to be more successfully produced when the process was taken in stages. The tube would be partly deformed with a low internal pressure of about 3000psi (21N/mm²). After this, the internal pressure would be increased to about 6000psi (41N/mm²) and the axial deformation allowed to continue by increasing the axial compressive force. This produced components that were better shaped, although they still suffered from slight buckling.

This method of forming the tube could have been performed using several stages, increasing the internal pressure at the end of each stage, and illustrates the need of control during the process. This could be achieved by a micro-processor, monitoring the axial compressive force and axial deformation, and adjusting the internal pressure as the deformation progresses.

From the components formed, it was noted that the axial compressive force had the greatest effect on the length of the side branch produced. Increasing the internal pressure had only a small effect, resulting in a small expansion of the cap and a decrease in its radius. However, its presence is very important to prevent buckling.

After forming the components, they were cut into half, and the wall thickness around the bulge was measured. The graphs produced from these measurements, shown in Figs. 42-62, show the variation of the wall thickness from the root of the bulge to the tip. At the root, thickening occurs due to the axial deformation - the greater the deformation the greater the wall thickening. With the largest axial compressive force used - 148kN - the root wall thickness was approximately 180% of the original wall thickness. Up the side of the branch, towards the tip, the amount of wall thickening got less, until at one point near the cap, the wall thickness is the same as the original thickness. Above this point the wall gets thinner until it reaches its maximum value at the tip. It was at the tip that rupture would occur, if the wall thinning was too severe. In general, wall thicknesses of approximately 65% of the original thickness could be obtained at the tip before rupture occurred.

Comparison of the thickness distributions of components formed with the same axial compressive force, illustrated in graphical form, shows

that they follow the same trends. The effect of increasing the internal pressure is to extend the graph slightly, producing a slightly longer side branch with a thinner wall at the tip. Increasing the axial compressive force causes an increase in the wall thickness at the root, as well as an increase in the length of the side branch, although there is little change in the wall thickness of the cap at the top of the bulge.

One problem encountered, in some of the tee pieces produced, was 'shrinkage' occurring at the base of the side branch - see Section 1.3. and Fig. 4. This was due to the small radius between the main branch and the side branch (radius of draw) forcing the tube wall away from the die wall as it flowed around the radius to form the side branch. This effect was more obvious on the tee pieces formed with a large side branch and with a small internal pressure. Increasing the internal pressure helped to reduce this shrinkage, but the main reason for it occurring appeared to be that the radius of draw was too small. When the dies were made for forming the cross pieces, a larger radius of draw was used to try to overcome this problem. This produced better results, although it did not completely overcome the problem. Redesigning the dies, with a more complicated geometry between the main branch and the side branch(es) to provide a smoother flow, is needed to try to eliminate this problem completely. However, the problem was not too severe and fairly good results were obtained using these two dies.

6.3. THEORETICAL PREDICTIONS

Although there are discrepancies between the actual wall thickness distributions and the theoretical predictions, the two do follow the same trends. The best comparisons were obtained with components which had a large side branch and were formed with a fairly high internal pressure. Tee pieces thus formed, showed good agreement at the root and at the tip of the bulge with the theoretical predictions. For the cross pieces, however, the agreement was not as good at the root of the bulge.

Components formed with only a little axial deformation seemed to have branch lengths much shorter than the theory predicted. This seems to indicate that the axial deformation has a greater effect on the formation of the cap than predicted by the analysis. For components with well formed branch lengths the theory gave good results. However, estimating the tubular branch length from the graphs of wall thickness distribution for the actual results, showed that the theory predicted a longer tubular branch length, with a smaller cap on top of it. Again this shows that the axial deformation has less of an effect on the length of the tubular branch formed than the theory predicts, and a greater effect on the spherical cap. This may be due to the geometry of the cap being more complicated than the arc of a circle the theory assumes. Some of the axial deformation may contribute to the forming of the junction between the tubular branch and the spherical cap.

Other reasons for this discrepancy could be due to an initial axial deformation occurring before the application of an internal pressure. The tube blank is subjected to a small axial compressive force to seal the ends of the tube prior to filling with oil. Although only a small force

is used, some deformation could occur, causing wall thickening along the entire length of the blank and shortening of the initial tube blank length. However, this effect would only be small, as no significant deformation was noticed when applying the sealing force.

At the root of the bulge the theory gave good predictions of the wall thickness for the tee pieces. However, for the cross pieces the theory generally predicted greater wall thickening than actually occurred. In the analysis, a sharp radius is assumed between the tube and the side branch. In practice, however, the large radius between the tube and the side branches on the cross piece dies may result in less thickening of the tube occurring at the root, than if they were formed in dies with a small radius. Alternatively, the more uniform flow encountered with the cross pieces may reduce the amount of wall thickening that occurs on the main branch during forming.

Although the theory had some discrepancies in its predictions, it could be used to give a fairly good idea of what wall thickness distribution may be expected for a tee or cross piece. For components formed with a fairly prominent spherical cap, the thicknesses at the tip of the bulge were in good agreement. This is a critical point of the component, as it is at this point that rupture may occur. Therefore, the theory may be useful in evaluating the amount of axial deformation the blank should be subjected to, in order to produce a side branch of sufficient length without causing rupture of the cap.

6.4. FURTHER WORK

The dies used produced fairly good results, however, further work is required into the design of the dies in the area of the joint between the tube and the side branch(es). At present the tube wall has to flow around a fairly sharp radius which resulted in shrinkage occurring in some of the components. Making this radius much larger would correct this, but this is not a desirable feature on the finished component. An alternative solution may be to modify the geometry of the die in the region around the junction between the side branch and the tube along the centre plane. Considering the centre line through the tee pieces and cross pieces (the centre line through which the components were sectioned, as in Figs. 35 and 36), a sharp radius is required in this area on the formed component. However, moving away from the central plane and down the side of the tube, the radius is not so critical. Hence, in this region the radius could be increased to provide a smoother flow path.

As well as modifications in the design of the dies, varying the shape of the ends of the plungers may help in forming some components. When tee pieces were formed, most of the metal flow to form the branch came from the top half of the blank (the half that the side branch projects from). On the opposite side, thickening of the tube wall occurred, and on a commercial product this would have to be machined away. With a different plunger end shape it may be possible to direct this metal to the bulge area, and prevent this excessive wall thickening from occurring. This might be done with plungers that are pointed at the bottom, to stretch the wall out sideways as they advance along the tube wall opposite the side branch.

In the tests carried out only tee pieces and cross pieces were formed. It should be possible to produce a large variety of components once the appropriately shaped die inserts have been made. Some examples of the shapes, both asymmetric and axisymmetric, that should be possible to bulge form are illustrated in Figs. 2.a and 2.b. At the moment the only limitation on the component is the diameter of the tube blank to be used, currently 24.12mm diameter. If a tube blank of a different diameter were to be used, new die inserts, die blocks and plungers would have to be made. Once made up it would be fairly simple to set up the machine for the new tube blanks, which need not necessarily be made of copper. Other materials could be used, such as mild steel or brass.

Other important work that can be done using this machine is the application of a micro processor/computer to sequence the operations and also to control the internal pressure and axial compressive force during the process. The sequencing of the process should be fairly simple, as the directional valves are all solenoid operated. These could be operated by relays controlled by the output port of a micro processor/computer. The only process that can not be automated at the moment is bleeding the air out of the tube prior to forming. The valve fitted is manually operated, but this could be replaced with a valve that will automatically bleed the air out and seal itself afterwards.

Controlling the process is a more complex problem, and would have to be based on a relationship between the axial compressive force or the axial displacement and the internal pressure. The internal pressure on the machine is controlled by two valves - a pressure reducing valve controlling the pressure reaching the pressure intensifier and a pressure relief valve allowing excessive pressure to escape. At the moment these

can only be manually adjusted, although the pressure supply to the intensifier can be turned on and off by a solenoid valve. Some extra equipment, therefore, may have to be fitted to vary the setting of one of these valves during the process.

The control needs to maintain a sufficiently high internal pressure to prevent buckling of the component, whilst preventing excessive pressure from being generated that would burst the tube. In the test procedure, the best components were formed by increasing the internal pressure during the process to a pressure that would have caused rupture to the initial blank. This could be incorporated into the control of the process, using either a linear relationship between the internal pressure and the axial displacement or a step function. This could be evaluated from the forming limits, and ideally should incorporate as high an internal pressure as possible without causing rupture.

7. CONCLUSIONS

The bulge forming process is a useful method of shaping tubular components, by the use of a internal hydrostatic pressure and an axial compressive force. It can be used to form a variety of components, both axisymmetrical and asymmetrical. For some of the components it can form, eg tee pieces and cross pieces, the only alternative form of production is from castings or from welded designs, as they could not be formed with customary rigid tools.

The design of the bulge forming machine was based on a literature survey and experience gained using a prototype rig. Once initial commissioning problems had been corrected, the machine was found to be easy to use in producing tee pieces and cross pieces. The difficulties experienced when using the prototype rig had been avoided with the new machine, allowing components to be quickly and easily formed.

A series of tests were carried out in order to evaluate the machine and to establish the forming limits. These were carried out with various internal pressures and axial compressive forces, forming tee pieces and cross pieces from copper tube blanks of two different wall thicknesses. From the results obtained, it was found that the internal pressure required to prevent the tube from buckling became more critical with increasing axial compressive force,.

Analysis of the formed component showed that the size of the axial compressive force had the greatest effect on the formed component. Increasing this force caused an increase in the length of the side branch, and thickening of the tube wall at the root of the branch. The wall thickness at the tip of the branch remained almost unaffected.

Increasing the internal pressure had only a small effect on the length of the branch, but would cause a decrease in the wall thickness of the spherical cap at the end of the branch.

Comparison of the wall thickness distribution with theoretical predictions showed a fairly good agreement, especially at the root and the tip of the bulge. Between these two, however, there was a discrepancy, which seemed to be due to the theory predicting a longer tubular branch and a smaller cap than actually occurred.

8. REFERENCES

1. GRAY J.E., DEVEREAUX A.P., and PARKER W.M., "Apparatus for making wrought metal T's.", United states Patent Office, Patent N^o. 2203868, June 11, 1940.
2. CRAWFORD R.E., "Solder fittings.", Industrial Progress, May 1948, pp. 33-36, 62.
3. STALTER J.D., "Method of forming complex tubing shapes.", The Patent Office, London, Patent N^o. 1181611, 18 Feb, 1970.
4. AL-QURESHI H.A., "Comparison between the bulging of thin-walled tubes using rubber forming techniques and hydraulic forming process.", Sheet Metal Industries, July 1970, pp. 607-612.
5. LIMB M.E., CHAKRABARTY J. and GARBER S., "Hydraulic forming of tubes.", Sheet Metal Industries, November 1976, pp. 418-424.
6. LIMB M.E., CHAKRABARTY J. and GARBER S., "The forming of axisymmetric and asymmetric components from tube.", Proc. 14th. Int. M.T.D.R. Conf, 1973, pp. 799-805.
7. OGURA T., UEDA T. and TAKAGI R., "The use of an hydraulic hollowing out process.", Industrie-Anzeiger, 10 May & 17 June 1966, pp. 107-110 & pp. 84-89.

8. OGURA T. and UEDA T., "Liquid bulge forming.", Metalworking Production, April 1968, pp. 73-81.
9. "A liquid pressure bulge forming apparatus and process.", The Patent Office, London, Patent N^o. 1083354, Sept 1967.
10. "Hydrostatic cold forming of tubular products.", Metallurgia, June 1978, pp. 293-294.
11. SMITH J.A., "Hydrostatic forming of tubing produces complex parts.", Automation, June 1963, pp. 84-89.
12. "Improvements relating to the manufacture of elbow fittings from straight tubing.", The Patent Office, London, N^o. 1029892, May 1963.
13. "Device and method for manufacturing elbow fittings from straight tubing.", United States Patent Office, Patent N^o. 3328996, July 1967.
14. REMMERSWAAL J.L. and VERKAIK A., "Use of compensating forces and stresses in difficult metalforming operations.", Int. Conf. Manu. Tech, Am. Sc. Tool & Manu. Eng, Mich, 1967.
15. BOYD C. and TRAVIS F.W., "Bending of thin walled tubes by combined external mechanical forces and internal fluid pressure.", Proc. 12th. Int. M.T.D.R. Conf.,1971.

16. POWELL G. and AVITZUR B., "Forming of tubes by hydraulic pressure.", 1971.
17. WOO D.M., "Development of a bulge forming process.", Sheet Metal Industries, May 1978, pp. 623,624,628.
18. WOO D.M., "Tube bulging under internal pressure and axial force", Journal of Engineering Materials and Technology, October 1973, pp. 219-223.
19. WOO D.M. and LUA A.C., "Plastic deformation of anisotropic tubes in hydraulic bulging", Journal of Engineering Materials and Technology, October 1978, pp. 421-425.
20. BANERJEE J.K., "Limiting deformations in bulge forming of thin cylinders of fixed length.", Int. J. Mech. Sci., Vol. 17, 1975, pp. 650-662.
21. KANDIL S.E.A.E., "Hydrostatic metal tube bulging as a basic process.", Metallurgia and Metal Forming, May 1976, pp. 152-155.
22. BADRAN F.M.F. and EMARA K.M., "Axially uniform tube bulging.", Sheet Metal Industries, November 1978, pp. 1192-1196.
23. SAVER W.J., GOTERA A., ROBB F. and HUANG P., "Free bulge forming of tubes under internal pressure and axial compression.", Proc. 6th. North American Metalwork Research Conf., 1978, pp. 228-235.

24. LUKANOV V.L., KLECKKOV V.V., SHATEEV V.P. and ORLOV L.V., "Hydromechanical stamping of tees with regulated liquid pressure.", Forging and Stamping Industry, No. 3, 1980, pp. 5-7.
25. HASHMI M.S.J., "Radial thickness distribution around a hydraulically bulged formed annealed copper T-joint: experimental and theoretical predictions.", Proc. 22nd. Int. M.T.D.R. Conf., 1981, pp. 507-516.
26. HASHMI M.S.J., "Forming of tubular components from straight tubing using combined axial load and internal pressure: theory and experiment.", Proc. Int. Conf. on Developments on Drawing of Metals, Metals Society, 1983, pp. 146-155.
27. BS 4, Part 1, 1980, "Specifications for hot rolled sections."
28. BS 449, Part 2, 1969, "The use of structural steel in building."
29. BS 4168, 1981, "Specification for hexagon socket head cap screws."
30. BS 4186, 1967, "Specification for clearance holes for metric bolts and screws."
31. BS 4190, 1967, "ISO metric black hexagon bolts, screws and nuts."
32. BS 4500, 1969, "ISO limits and fits."

APPENDIX 1

THE HYDRAULIC COMPONENTS

The following is a list of the hydraulic components fitted to the bulge forming machine. The reference numbers refer to Fig. 12.

CYLINDERS:

A Mecman Series 206,160mm dia,150mm stroke
B Mecman Series 203,125mm dia,100mm stroke

PUMP:

Sperry Vickers PVB 10

PRESSURE INTENSIFIER:

PI Fluids Control Inc. 1T11-2W-66

FLOW DIVIDER:

FD Fluids Control Inc. 2V13-4-3-6-S

DIRECTIONAL CONTROL VALVES:

V1 Sperry Vickers DG4V-3-OC-M-U-H7-30
V2 Sperry Vickers DG4V-3-2A-M-U-H7-30
V3 Sperry Vickers DG4V-3-2BL-M-U-H7-30
V4 Sperry Vickers DG4V-3-2C-M-U-H7-30

PRESSURE REDUCING VALVES:

PR1	Sun	PBDB-FBN-EBP
PR2	Sun	PEDB-KAN-EBP
PR3	Sun	PEDB-KBN-EBP

RELIEF VALVES:

RV1	Sun	RPEC-FAN-FBP
RV2	Hawe	MV-41-AP

FLOW CONTROL VALVES:

FC1	Sperry Vickers	DGMFN-3-Z-P2W-20
FC2	Sperry Vickers	DGMFN-3-Z-P2W-20
FC3	Sperry Vickers	DGMFN-3-Z-P2W-20
FC4	Sperry Vickers	DGMFN-3-Y-A2W-B2N-20

CHECK VALVES:

CV1	Sun	CKCA-XAN-EBA
CV2	Sun	CKCA-XAN-EBA
CV3	Hawe	RC-1-F
CV4	Hawe	RC-1-F

SUBPLATE

Sperry Vickers	DGMS-3-4E-10R
----------------	---------------

APPENDIX 2

THEORETICAL ANALYSIS COMPUTER PROGRAM

The following computer program was used to evaluate the theoretical predictions of the wall thickness distributions around the side branch of tee pieces and cross pieces. The output is in graphical form, showing the theoretical wall thickness distribution together with experimentally obtained results, which can be seen in Figs. 69-106.

```

REAL*8 FNAME(10)
DIMENSION TITL(3),THICK(15),XPLOT(17),YPLOT(17)
*,MARK(10),YDIS(15)
*,RATTH(10),DISY(10)
DATA MARK/11,0,12,2,14,10,1,4,5,3/,Y/0.4/
*,RADIN/12.06/,PI/3.1415926/
WRITE(6,10)
10  FORMAT(' NUMBER OF TESTS TO ENTER - ')
    READ(5,*)N
    DO 50 M=1,N
    WRITE(6,20)M
20  FORMAT(' ENTER TEST NUMBER FOR TEST - ',I2)
    READ(5,30)FNAME(M)
30  FORMAT(A8)
50  CONTINUE
    XSTART=0.0
    XSCALE=28.0/14.0
    YSTART=60.0
    YSCALE=140.0/18.0
    CALL PLOTS(0,0,1)
    CALL PLOT(1.5,6.0,-3)
    CALL FACTOR(18.0/14.0)
    CALL AXIS(0.0,0.0,'PERCENTAGE OF ORIGINAL WALL THICKNESS',37,14.0
*,90.0,60.0,10.0)
    CALL FACTOR(1.0)
    CALL AXIS(0.0,0.0,'Y',-1,14.0,0.0,0.0,2.0)
    CALL PLOT(0.0,6.0,3)
    CALL DASHP(14.0,6.0,0.3)
    DO 600 I=1,N
    CALL FILEDF(I,RET,3,'DISK',FNAME(I),'DATA','B')
    WRITE(6,60)IRET
60  FORMAT(I6)
    REWIND 3
    WRITE(6,70)FNAME(I)
70  FORMAT(' LOADING TEST - ',A8)
    READ(3,80)ORGTH,TITL
80  FORMAT(F6.2,4X,3A4)
    READ(3,90)BULHT,TOPTH,NUM
90  FORMAT(F6.2,4X,F6.2,4X,I4)
    READ(3,100)(YDIS(M),THICK(M),M=1,NUM)
100 FORMAT(4(F6.2,2X,F6.2,2X))
    DO 150 J=1,NUM
    XPLOT(J)=YDIS(J)
    YPLOT(J)=THICK(J)/ORGTH*100
150 CONTINUE
    XPLOT(NUM+1)=BULHT
    YPLOT(NUM+1)=TOPTH/ORGTH*100
    THICK(NUM+1)=TOPTH
    XPLOT(NUM+2)=XSTART
    YPLOT(NUM+2)=YSTART
    XPLOT(NUM+3)=XSCALE
    YPLOT(NUM+3)=YSCALE
    NUM=NUM+1
    WRITE(6,200)(XPLOT(M),THICK(M),YPLOT(M),M=1,NUM)
200 FORMAT(' Y = ',F6.2,2X,' THICKNESS = ',F6.2,2X,' THICKNESS RATIO = '
*,F6.2)
    CALL LINE(XPLOT,YPLOT,NUM,1,1,MARK(I))
    Y=Y+0.3
    CALL SYMBOL(0.2,Y,0.2,MARK(I),0.0,-1)
    CALL SYMBOL(0.5,Y-0.1,0.2,TITL,0,0,12)
600 CONTINUE

```

C*****THEORY*****

```
WRITE(6,220)
220  FORMAT(' ENTER THE INITIAL AND FINAL LENGTHS OF THE BLANK')
      READ(5,*)BLENIN,BLNFIN
      F=BLENIN/BLNFIN
      DX1=0.219*RADIN
      DX2=(BLENIN-BLNFIN)/2-DX1
      BRALEN=2*DX2/(F+1.0)
      HS=(2.0**0.5-1.0)*RADIN
      WRITE(6,230)F,DX1,DX2,BRALEN,HS
230  FORMAT(5F10.4)
      RATTH(1)=F*100
      DISY(1)=0.0
      RATTH(2)=100*BLENIN/(BLENIN-2*DX1)
      DISY(2)=BRALEN
      DISY(8)=XSTART
      RATTH(8)=YSTART
      DISY(9)=XSCALE
      RATTH(9)=YSCALE
```

C*****CASE 2*****

```
SHRAT =3-2*2**0.5
DO 300 I=1,5
H=I
IF(H.GT.HS)THEN H=HS
DISY(I+2)=BRALEN +H
RATTH(I+2)=RATTH(2)/((1.0+SHRAT*H/HS)**2.0)
300  CONTINUE
      CALL DASHS(ARRAY,1)
      CALL LINE(DISY,RATTH,7,1,0,3)
      CALL DASHS(ARRAY,0)
      WRITE(6,320)(DISY(I),RATTH(I),I=1,7)
320  FORMAT(' Y = ',F10.6,' THICKNESS RATIO = ',F10.6)
```

C*****CASE 1*****

```
H2=BULHT-BRALEN
IF(H2.LT.0.0)GOTO 610
IF(H2.GT.HS)GOTO 450
ROEH=RADIN+H2
ROEL=(RADIN**2+H2**2)/(2.0*H2)
ROERAT=ROEH/ROEL
C  PM=ROERAT/(3.0-2.0*ROERAT)
  PM=(3.0-2.0*ROERAT)/ROERAT
  HTRAT=(H2/RADIN)**2
  WRITE(6,340)ROEH,ROEL,ROERAT,PM,HTRAT
340  FORMAT(5F10.4)
      DO 400 I=1,5
      H=I
      IF(H.GT.H2)H=H2
      DISY(I+2)=BRALEN +H
      RATTH(I+2)=RATTH(2)/((1+HTRAT*H/H2)**(PM+1.0))
400  CONTINUE
      RATTH(1)=RATTH(2)
      DISY(1)=DISY(2)
      CALL DASHS(ARRAY,1)
      CALL LINE(DISY,RATTH,7,1,0,5)
      CALL DASHS(ARRAY,0)
      WRITE(6,420)(DISY(I),RATTH(I),I=1,7)
420  FORMAT(' Y = ',F10.6,' THICKNESS RATIO = ',F10.6)
      GOTO 610
```

```

C*****CASE 3*****
450  WRITE(6,460)
460  FORMAT(' *****CASE 3*****
*****')
      BL1=BULHT-(BRALEN+HS)
      THEL=2*ATAN(TAN(PI/8)*EXP((0.0-BL1)/RADIN))
      HTHEL=HS-(2*0.5*RADIN*(1-COS(THEL)))
      SHRAT=3-2.0*2.0**0.5
      TRAT=1/((1.0+SHRAT*HTHEL/HS)**2)
      RATTH(3)=RATTH(2)*2.0*TRAT*(SIN(THEL)**2)
      DISY(3)=BRALEN+BL1
      DO 520 N=1,2
520  CONTINUE
      DO 530 I=1,5
      H=I
      IF(H.GT.HS)H=HS
      DISY(I+3)=DISY(3)+H
      RATTH(I+3)=RATTH(3)/((1.0+SHRAT*H/HS)**2)
530  CONTINUE
      RATTH(1)=RATTH(2)
      DISY(1)=DISY(2)
      CALL DASHS(ARRAY,1)
      CALL LINE(DISY,RATTH,8,1,0,5)
      CALL DASHS(ARRAY,0)
      WRITE(6,550)(DISY(I),RATTH(I),I=1,10)
550  FORMAT('  Y = ',F10.6,' THICKNESS RATIO = ',F10.6)
610  WRITE(6,620)
620  FORMAT(' NOW TYPE PLOT IF YOU REQUIRE A COPY ')
      CALL SYMBOL(0.2,Y+0.4,0.2,'INTERNAL PRESSURE/TEST NO.',0.0,26)
      CALL SYMBOL(0.2,Y+0.2,0.2,'-----',0.0,26)
      CALL PLOT(10.0,0.0,999)
      CALL EXIT
      STOP
      END

```

THE DESIGN OF AN EXPERIMENTAL HYDRAULIC BULGE FORMING MACHINE

T. J. BARLOW, R. CRAMPTON and M. S. J. HASHMI
Department of Mechanical and Production Engineering
Sheffield City Polytechnic

SUMMARY

Preliminary investigations into hydraulic bulge forming of tubular components on a prototype machine produced useful but limited results. The need for a dedicated experimental bulge forming machine, which would be capable of producing a wider variety of components more readily and with more comprehensive instrumentation, quickly became evident. A new machine was designed and built on the basis of the operating parameters determined from the prototype machine. Axial compressive forces of up to 200 kN and internal pressures of up to 69 N/mm² can be obtained. Facilities for future automation were incorporated early in the design stages. The machine is now in operation and results are promising. This paper describes the design of the machine and some of the problems overcome in commissioning. Initial experimental results achieved from the machine are presented.

INTRODUCTION

The bulge forming process is used for shaping tubular metal parts by subjecting a tubular blank to internal hydrostatic pressure whilst being contained within a die bearing the shape of the component to be formed. The pressure is transmitted via a medium which can be a liquid, a soft metal or an elastomer. Where the tube is unrestricted within the die, expansion occurs until the required shape is formed.

Bulge forming using internal pressure alone causes considerable thinning of the tube wall which can lead to rupture of the tube at only moderate expansions. To form larger expansions, metal has to be fed into the deformation zone during the forming process. This is achieved by the application of an axial compressive force to the ends of the tube. If this force is great enough to cause axial deformation of the tube blank, i.e. shortening of the tube length, much greater expansions can be obtained before rupture due to wall thinning can occur.

The technique of applying an axial force in conjunction with the internal pressure has been used industry and research institutions to produce tee pieces, cross pieces, reducer/expansion shapes and other axisymmetric and assymmetric components /1,2,3/. Results from preliminary investigations by the author have been published previously /4/. In those investigations, tests were carried out using a prototype bulge forming machine. This paper deals with the problems encountered in using the prototype machine and the resultant design and commissioning of a new forming machine.

PROTOTYPE BULGE FORMING MACHINE

The prototype machine consisted of two die halves each mounted in a robust die holder which was split laterally in relation to the tube (see Fig(1)). Each die half was drilled through to allow the insertion of a tube blank when the two halves were together. An axial compressive force could be applied to the ends of the tube by means of two plungers, one at each end, which entered the ends of the die to butt up against the tube. The plungers were turned down at the ends to allow them to locate inside the tube. This part of the plungers also housed an 'O' ring which sealed against the inside of the tube to prevent leakage of the pressure medium. Axial alignment was maintained by mounting the plungers onto guide plates with the die block suspended between the two on heavy duty springs. The plungers were drilled down their length to allow the tube blank to be filled with oil prior to forming. Axial compression was achieved by placing the whole assembly onto a 200kN Denison compression testing machine. The internal pressure was provided by a hydraulic hand pump connected to the bottom plunger via an adjustable pressure relief valve. A bleed screw in the upper plunger allowed air to escape before forming proceeded. The forming procedure involved increasing the internal pressure until some initial value was reached, followed by axial deformation using the compression testing machine. Once the required degree of deformation had been obtained, or the tube burst, the axial compression force and internal pressure were released. The plungers were then withdrawn from the die blocks and, after separation of the two halves of the die

blocks, the formed component was removed. During the forming procedure, note was made of the maximum deformation force and internal pressure.

PROBLEMS WITH THE PROTOTYPE RIG

As mentioned previously, the rig had to be assembled before each test and dismantled afterwards to remove the formed component. However, because the die blocks split laterally in relation to the tube, it was sometimes difficult to separate the two die halves and remove the component from them. This was due to the internal pressure forcing the walls of the tube against the die walls during forming. Because of this, each test could take over half an hour to complete from set-up to extraction of formed component. 'O' rings were located at the ends of the plungers to seal the ends of the tube. These invariably became damaged by the ends of the copper tube and had to be replaced after only one or two tests. On some of the tests carried out, the tube would not seal properly and the internal pressure had to be maintained by constant use of the hydraulic hand pump. Leakage was not so much of a problem, though, when large axial compressive forces were used to form tees and cross pieces, especially when using the thickest walled tube. Unfortunately, this large axial force sometimes allowed the ends of the tube to form into the recess containing the 'O' rings at the end of the plungers. This prevented the plungers from being withdrawn from the tube at the end of the test. Consequently, the removal of the plungers had to be achieved with the use of a hammer, but with caution since the springs between the die block and the guide plates were held in a compressed state. These springs were used to keep the two die halves together and also to keep them central between the two guide plates, so that the bulge would be formed centrally on the tube. Unfortunately, this did not always work, resulting in the bulge being formed off central due to one plunger meeting a greater resistance than the other.

In addition to the problems in assembling and dismantling the rig, there was also a lack of process control and instrumentation. These deficiencies caused large variations in the component formed and made accurate recording of the process difficult. The strain rate for the axial compression could be adjusted on the compression testing machine. However, there was little control over the internal pressure during the process apart from pumping it up to an initial value and setting its maximum value with the pressure relief valve. With the variations in the effectiveness of the tube sealing, it was difficult to carry out a series of tests with similar internal pressure conditions.

Because of the problems previously mentioned, a new, dedicated experimental bulge forming machine was designed, built and commissioned.

The new machine is free standing and self contained. The main part of the machine is the die block in which the actual forming takes place. In the prototype, this was split laterally in relation to the tube and resulted in problems extracting the formed component. Splitting the die blocks axially overcomes this problem, but the two halves have to be clamped together to resist the internal pressure forcing them apart. For this, a hydraulic ram is used which has the secondary purpose of opening and closing the dies allowing access for insertion and removal of the component. Two hydraulic rams are also used for applying the axial compressive force to the ends of the tube.

DESIGN OF NEW MACHINE

The operating parameters for the design of the machine were based on tests carried out using the prototype rig. Internal pressures of up to 38 N/mm^2 (5500 psi) together with axial compression forces of up to 110 kN were used to form axisymmetric and asymmetric components. A maximum pressure of 69 N/mm^2 (10000 psi) was chosen. This would provide sufficient internal pressure to form copper tubes and also tubes of harder material. A maximum axial force of 200 kN was considered suitable. The clamping force required to hold the die blocks together was calculated to be 300 kN.

The size of the cylinders necessary to generate the desired forces obviously depends upon the hydraulic circuit pressure chosen. There are other constraints to take into account. The hydraulic pressure was required to do two things - to operate the cylinders and also provide the internal forming pressure. Running the hydraulic system at the same pressure as the maximum internal pressure would prove to be very costly. Alternatively, a lower supply pressure could be chosen and this pressure increased through a pressure intensifier to provide the forming pressure. The second route was taken, with a main circuit pressure of 17 N/mm^2 (2500 psi) - sufficiently high as to reduce the size of the cylinders required to a manageable size, but not so high as to make the hydraulic circuit very expensive.

The sizes of the hydraulic cylinders needed were 125mm diameter to provide a 200kN axial compressive force and 160mm diameter to provide a 300kN clamping force. These were powered by a variable displacement piston pump driven by a 7.5kW electric motor. The pump can operate at pressures up to 21 N/mm^2 but was set at an

operating pressure of 17.5 N/mm which gives a delivery flow rate of approximately 25 litre/min. The maximum theoretical forces that can be applied by the hydraulic cylinders running under these conditions are an axial compressive force of 215kN and a clamping force of 350kN.

Design of hydraulic circuit.

The hydraulic circuit has three functions, namely to connect and control the supply to:-

- i) the hydraulic clamping cylinder,
- ii) the two cylinders providing axial force,
- iii) the internal pressurised region of the tube blank.

The first requirement was fairly simple and needed only the use of a directional control valve with three positions - one position to extend the ram, one to stop it and one to withdraw it. The second requirement needed some extra control. As previously mentioned, one of the considerations for the design of the new machine was that the two hydraulic cylinders applying the axial force should move in unison in order to form the bulge centrally on the tube. This was achieved by the use of a flow divider in the circuit between the pump and the two hydraulic cylinders. This divides the flow from the pump into two equal parts regardless of the forces acting on the cylinders, and so synchronises the movement of the two cylinders. A pressure reducing valve was also required to control the force that was being applied to the tube ends as was a directional control valve to extend and withdraw the rams as before. The third requirement was to provide the internal pressure for forming the component. The maximum required pressure of 69 N/mm² was achieved by the use of a pressure intensifier between the pump and the high pressure circuit. Again, a pressure reducing valve and directional control valve were required in this part of the circuit. The functions of the directional control valve in this case were:-

- i) to bypass the pressure intensifier (in order to fill the tube blank quickly at low pressure),
- ii) to stop the supply,
- iii) to supply the pressure intensifier.

Also needed in this part of the circuit was a valve to bleed the air while filling the tube with oil.

The full hydraulic circuit is illustrated in Fig (2).

Variable flow control valves were added in the circuit to the clamping cylinder so that the speed of opening and closing the dies could be adjusted. Also added was a pilot operated check valve to prevent closure of the dies when the supply is off.

The supply to the cylinders applying the axial compressive force was split into two, each with its own flow control and pressure reducing valve. These allowed two separate supply pressures and flow rates to be used - one to bring the plungers into contact with the tube blank at low pressure and the second to deform the tube at higher pressure.

The high pressure part of the circuit contains a pressure intensifier (6 - 1 ratio) with a by-pass, two non-return valves and a pressure relief valve to prevent excessive pressure being generated.

The directional control valves in the circuit are all solenoid operated, working on a 24V d.c. supply. This allows the application of a microcomputer or microprocessor to control the operation of the process, to be achieved with minimum modifications. Currently the operation of the process is by manual control.

The clamping cylinder is mounted on a top plate which is supported by four tie bars from a substantial base plate. The bottom half of the die block is positioned centrally on the base plate. The top half of the die block is connected directly to the clamping cylinder and guided down precisely by a 'Desoutter' die set.

Each die block contains a removable die insert. This enables the component shape to be changed with ease by simply replacing the die insert with the appropriate shaped die.

The two horizontal cylinders are mounted on brackets which are bolted to two channel section beams of size 305mm x 102mm. Above these is mounted the base plate referred to earlier. The axial compression force is transmitted from the hydraulic cylinders to the ends of the tube to be formed by plungers which enter the ends of the die block through guides. These plungers have axially drilled holes through which the internal pressurising fluid can pass. The seal on the ends of the tube was achieved by turning down the plungers as in the prototype, but the 'O' rings were discarded and a tapered portion used instead.

The whole assembly was then mounted onto a sturdy framework to give the correct working height as can be seen in photograph, Fig (3).

COMMISSIONING THE MACHINE

One problem encountered before any tests were carried out was the alignment of the plungers in the die blocks. It had been intended to bolt the plungers to the ends of the cylinder rods, but due to slight

misalignment, an alternative method of connection was used. This involved a floating connection using a collar fixed to the end of the cylinder rod and going around the end of the plunger, allowing movement of the plunger within it. A second problem encountered before testing could proceed was that the pressure intensifier failed to work. This was traced to a pipe fitting being screwed too far into the body of the intensifier and shutting off a port. This was rectified by shortening the pipe fitting and refitting. After these problems had been resolved, initial tests were carried out by forming tee pieces from copper tube. These tests highlighted two other problems, one being that the bulge was being formed off central indicating that the flow divider was not operating correctly. This was corrected by simply cleaning the flow divider. It was assumed that dirt had entered the system on assembly of the hydraulic circuit. The second problem was excessive pressure being generated in the tube blank, causing early rupture of the tube. This was due to the pressure relief valve on the high pressure circuit not operating correctly due to a large back pressure forming in the drain pipe. Originally, all the drain pipes from the various valves were piped together and led back to the oil reservoir. The relief valve was made to function correctly by providing it with a separate drain to tank.

INITIAL TEST RESULTS

After overcoming initial teething problems, a series of tests were carried out to produce both tee and cross pieces from copper tube. The results so far have been very promising and have highlighted the importance of the die geometry around the radius at the main and side branch. Figs (4) and (5) show a selection of tee and cross pieces that have been formed at various pressures and axial forces. These components have been sectioned to show the variations in wall thickness. Figures (6), (7) and (8) show some of the results obtained when varying internal pressure and axial force. Figure (6) shows the variation in wall thickness around the bulged portion of a tee piece when varying the internal pressure between 2000 psi and 6000 psi, but maintaining the end load constant at 85kN. It is evident that at the root of the bulge, thickening occurs to a value of approximately 30% with a gradual thinning to the tip of the bulged zone. The lower internal pressures cause less thinning at the tip of the bulged zone. Figure (7) shows the thickness distribution across the dome of the side branch for an axial force of 85kN. This is basically the same data as shown by Figure (6), but drawn in a different manner. The centre axis represents the centre of the bulged zone. The figure clearly illustrates the reduction in thickness towards the centre

of the domed portion with greater reduction as the internal pressure increases. Figure (8) illustrates the increase in bulged height with internal pressure for end loads of 85kN and 130kN. It is evident that greater bulge heights are attainable both with increased internal pressure and increased axial force. The results presented are as expected and do not represent new knowledge, but show that the bulge forming machine is capable of producing, experimentally, a sound component.

CONCLUSIONS

The paper has described the design of an experimental bulge forming machine which can be used to form a variety of components. The machine in its current state is manually controlled, but was designed with future application of microcomputer control in mind. Initial tests on the machine are very promising and show that both tee and cross pieces are easily formed. Extensive tests on these are now being conducted, together with tests on more complex shapes and the results from these investigations will be reported in a future paper.

REFERENCES

1. M.S.J.HASHMI 'Forming of tubular components from straight tubings using combined axial load and internal pressure: theory and experiment.' Proc. Int. Conf. on Developments on Drawing of Metals. Metals Soc, London, p146-155, 1983.
2. D.M.WOO 'Tube bulging under internal pressure and axial force.' Journal of Engineering Materials and Technology, p219-223, Oct 1973.
3. T. OGURA and T. UEDA 'Liquid bulge forming.' Metalworking Production, p73-81, April 1968.
4. M.S.J.HASHMI and R. CRAMPTON 'Hydraulic bulge forming of axisymmetric and assymmetric components: comparison of experimental results and theoretical predictions.' Proc. 25 Int. MTDR Conf. p541-549, 1985.

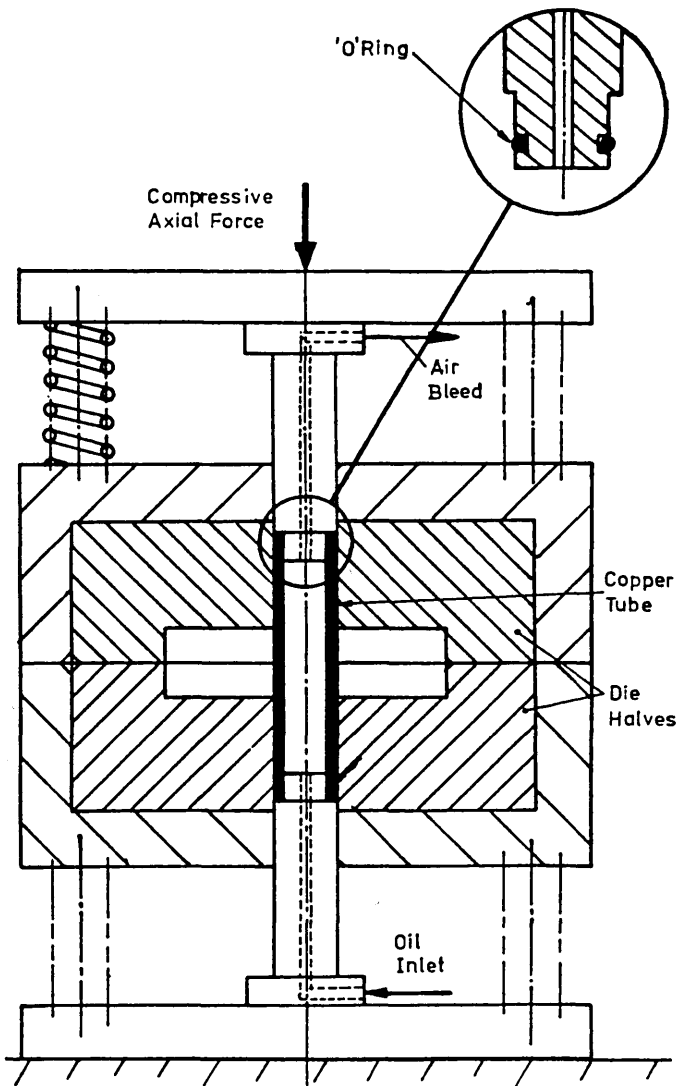


FIGURE 1. The prototype die and tool system for bulge forming. Insert - cross section through the end of one of the plungers.

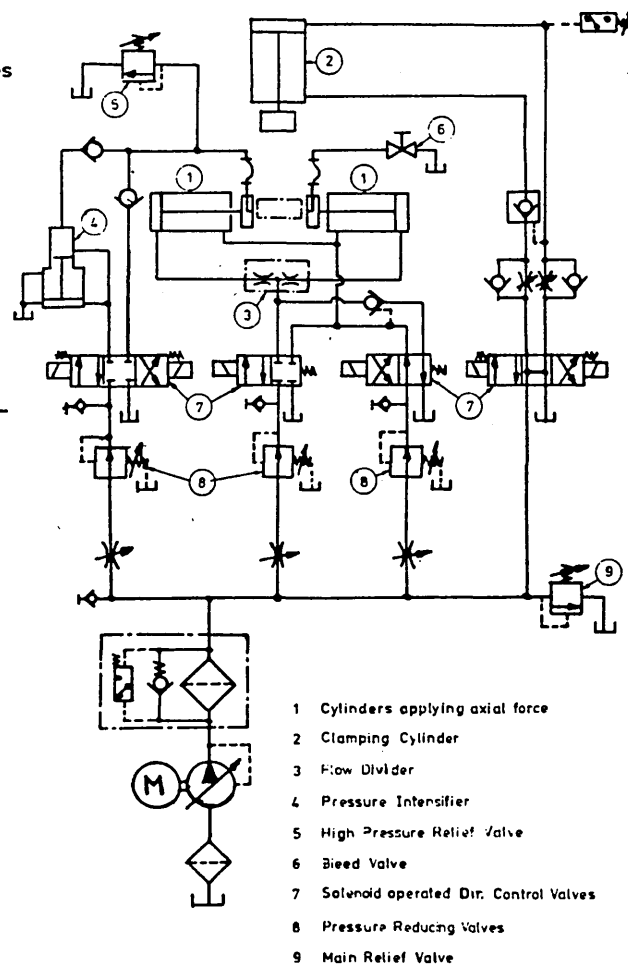


FIGURE 2. Hydraulic circuit diagram of bulge forming machine.

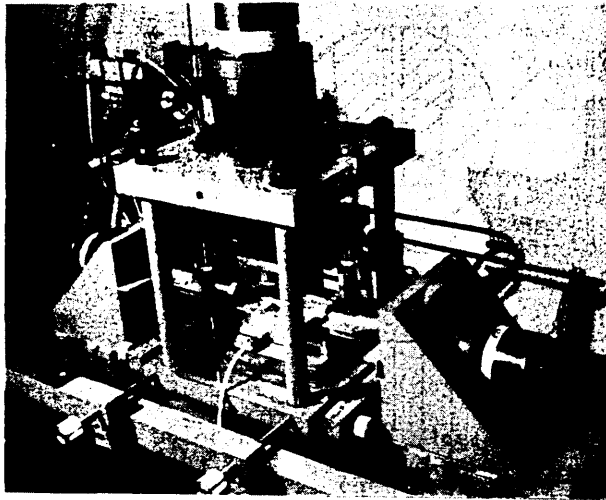


FIGURE 3. General view of bulge forming machine.

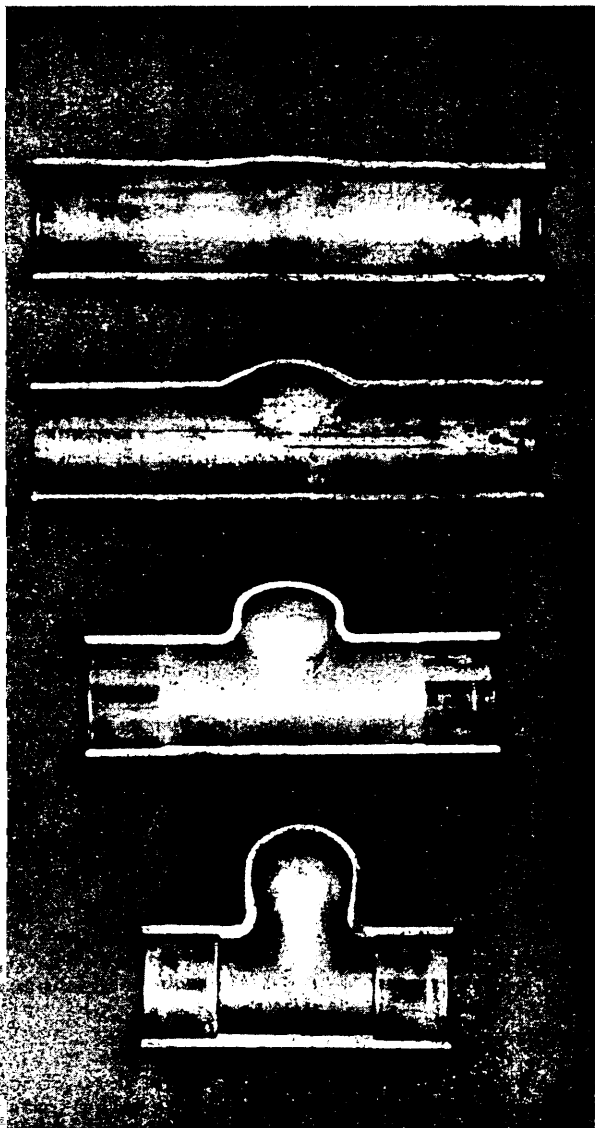


FIGURE 4. Photograph of sectioned tee pieces formed to various degrees.

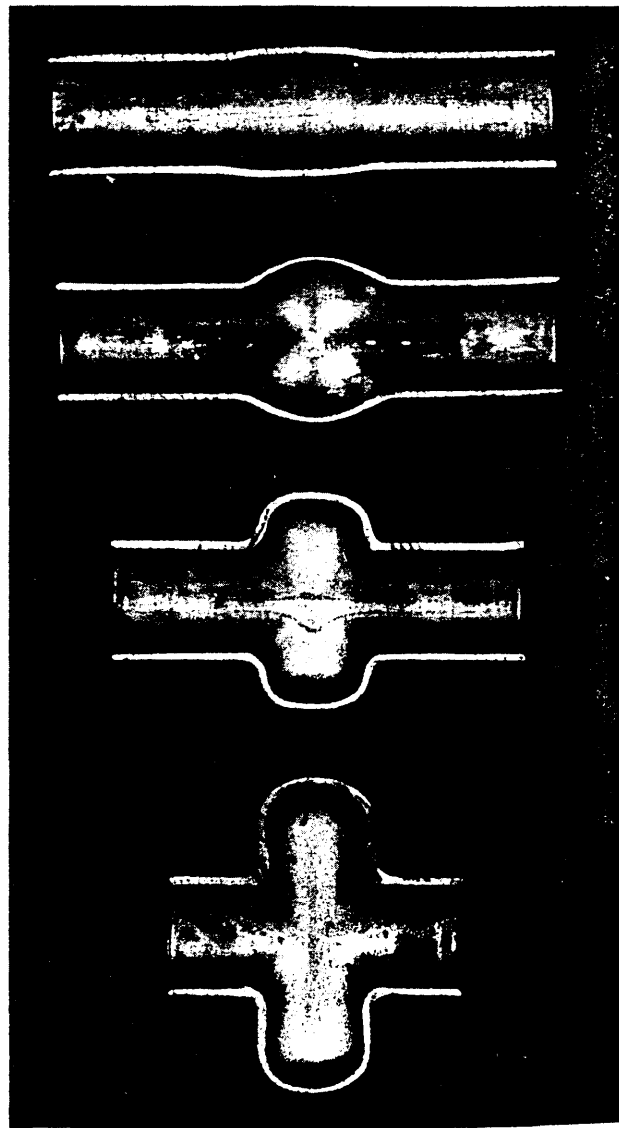


FIGURE 5. Photograph of sectioned cross pieces formed to various degrees.

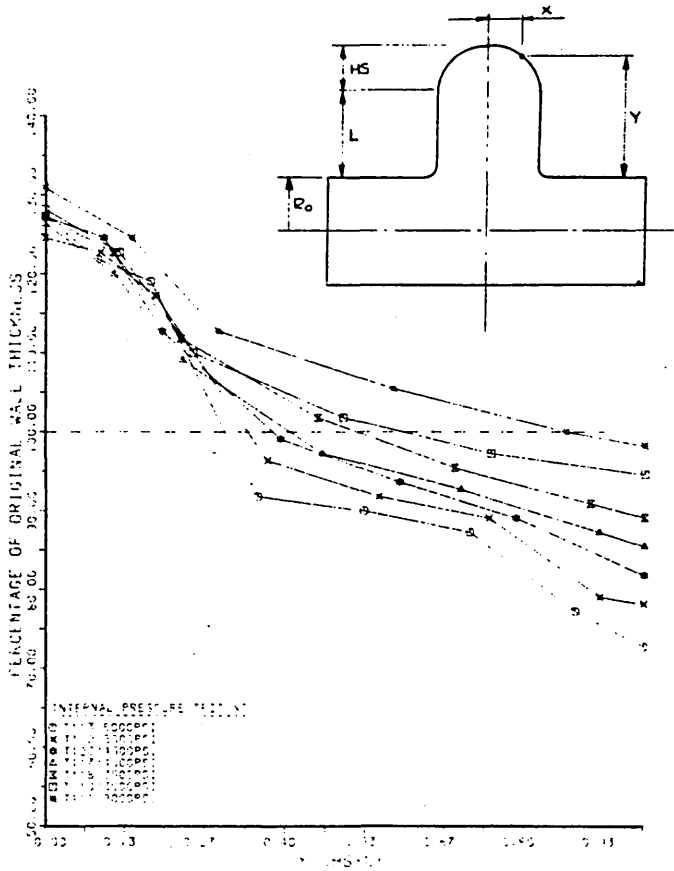


FIGURE 6. Thickness distribution along side branch of a tee piece (Axial force = 85kN).

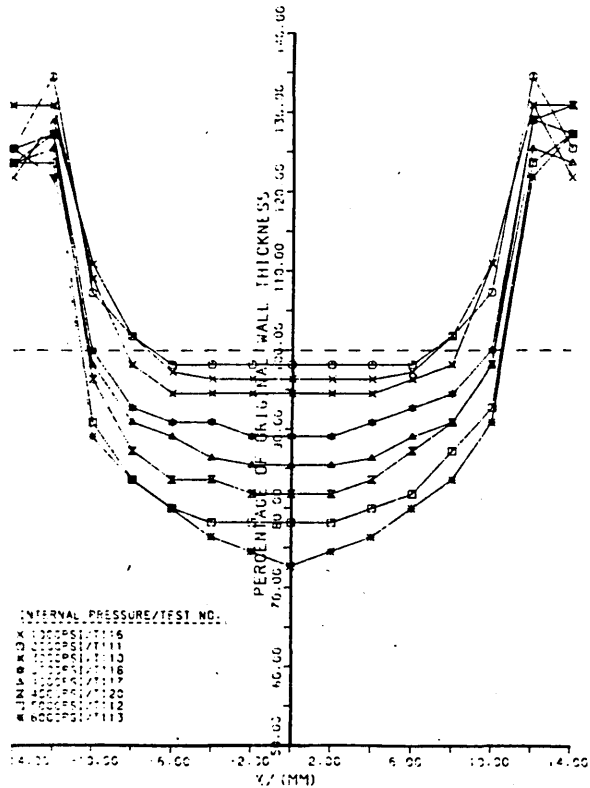


FIGURE 7. Thickness distribution across the dome of the side branch (Axial force = 85kN).

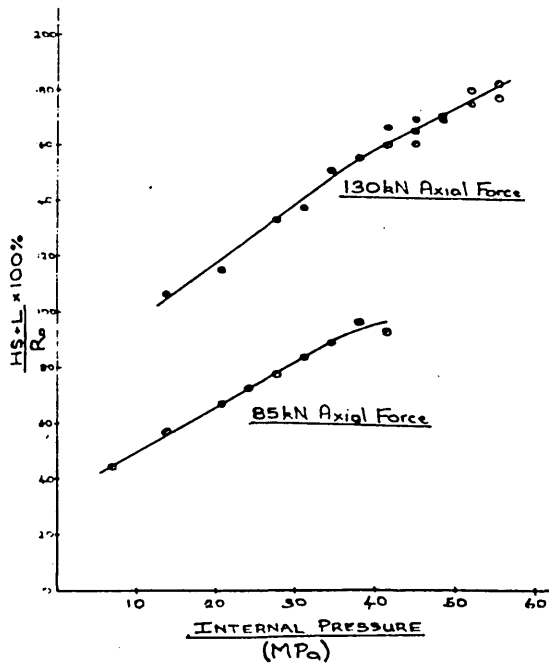


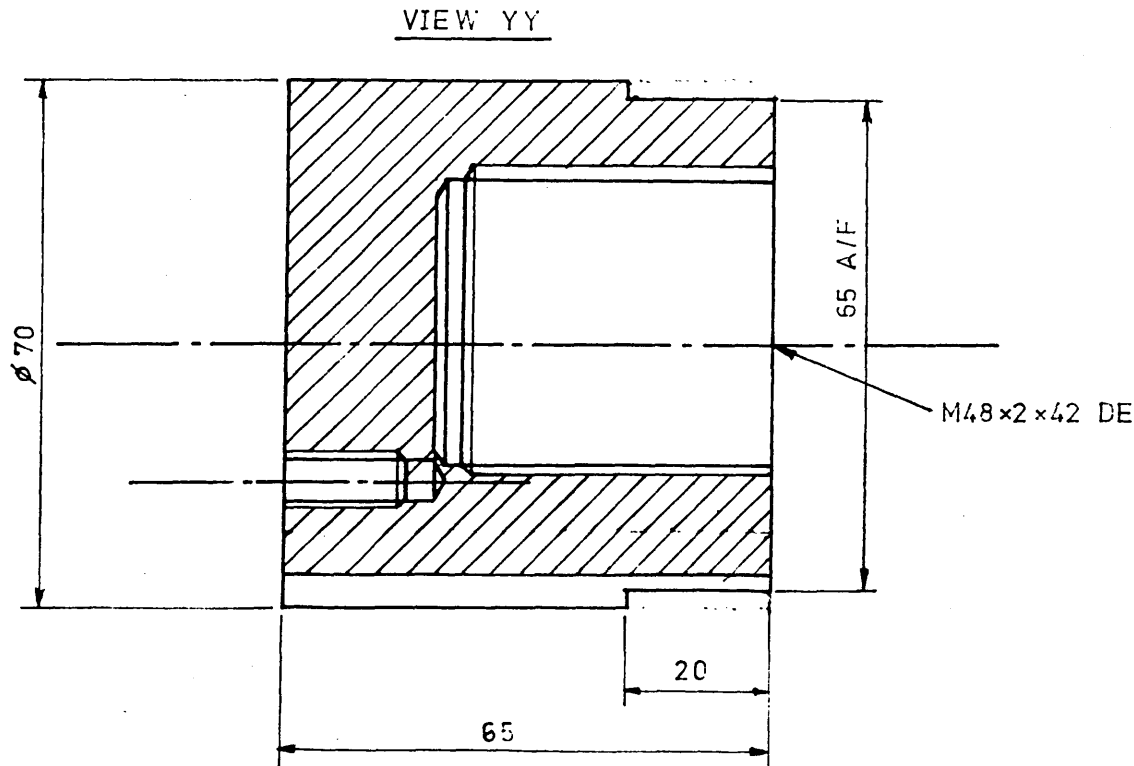
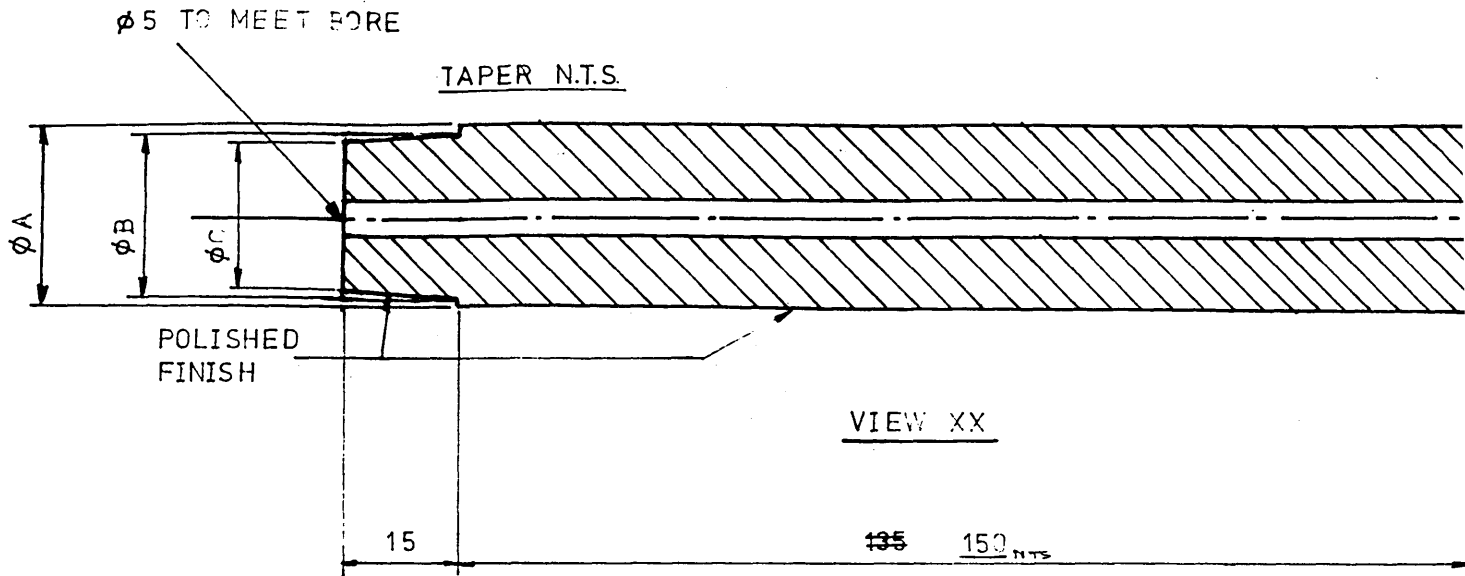
FIGURE 8. Variation of side branch length with respect to the internal pressure at two different axial loads.

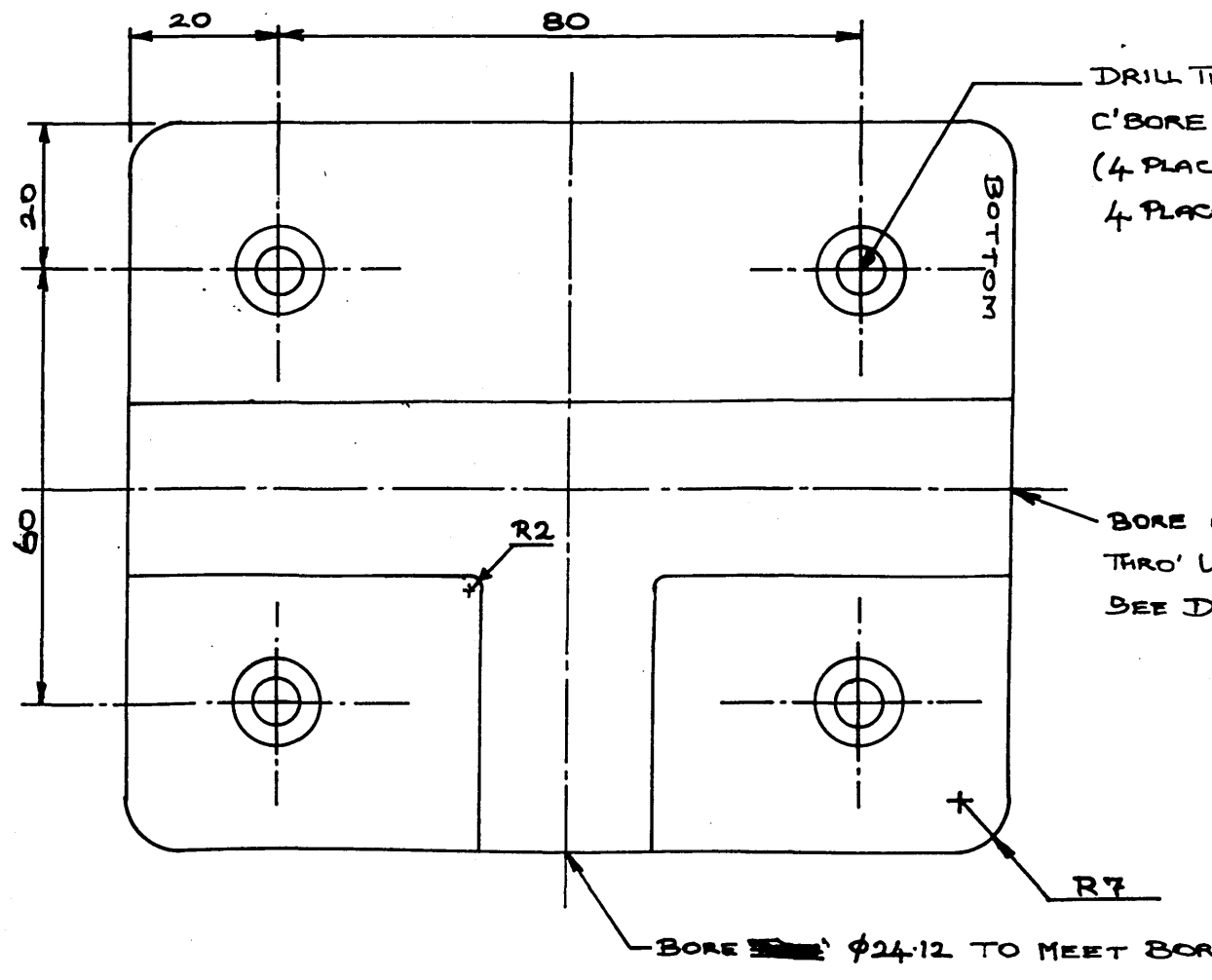
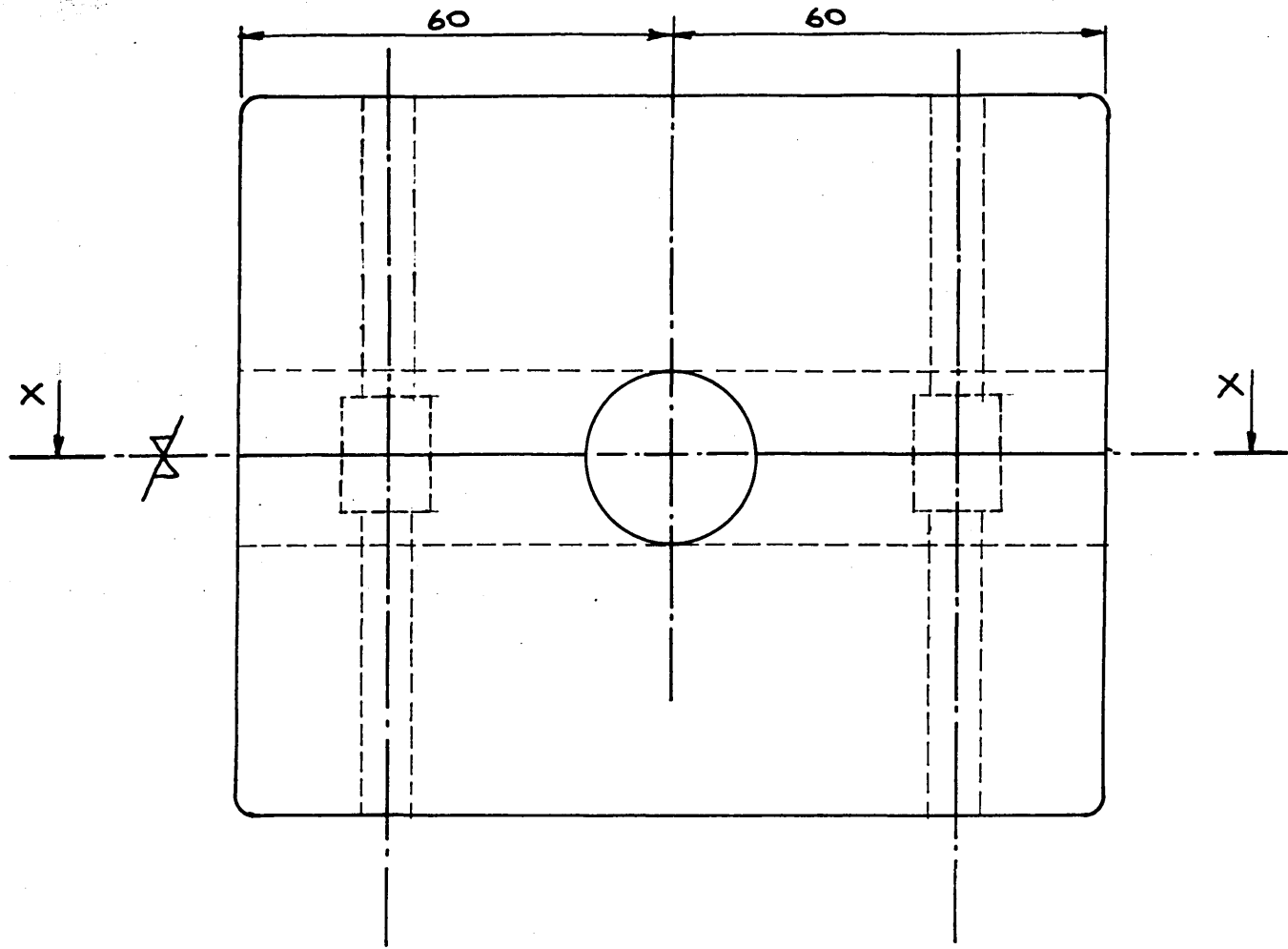
	DIMENSIONS
ϕA	$24.120_{-0.020}^{-0.007}$
ϕB	21.385 ± 0.005
ϕC	21.365 ± 0.005

PLUNGER 2 OFF

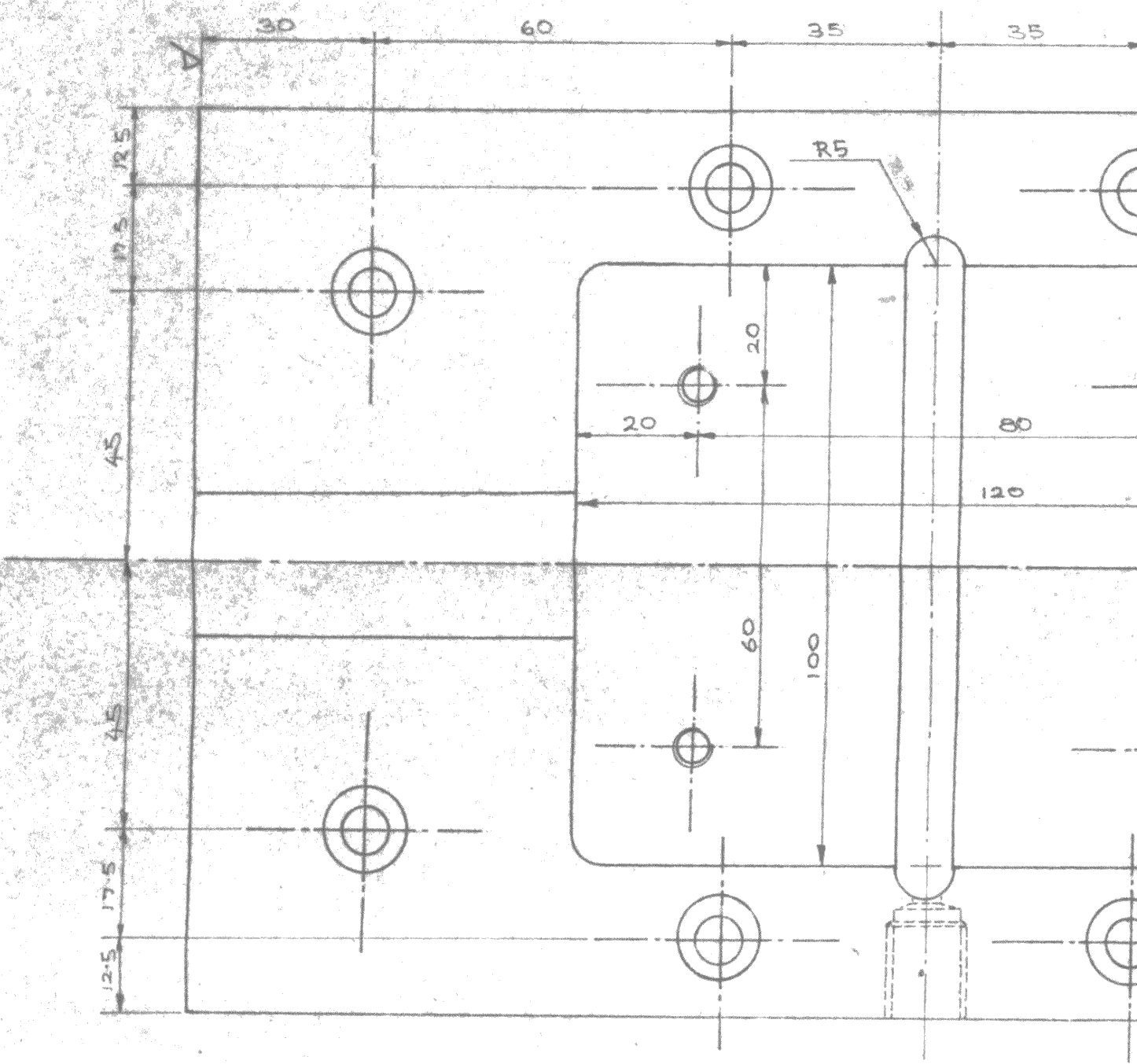
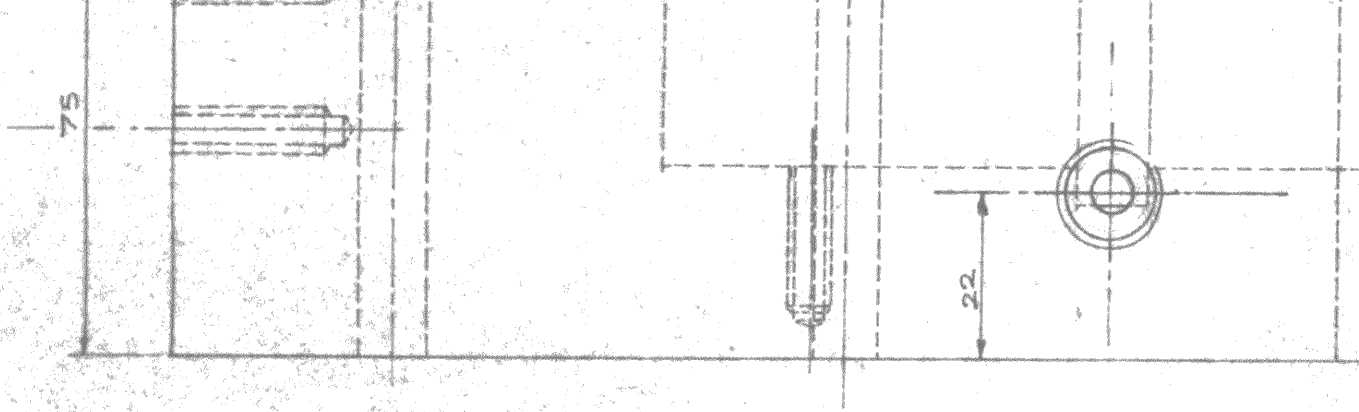
1st ANGLE PROJECTION

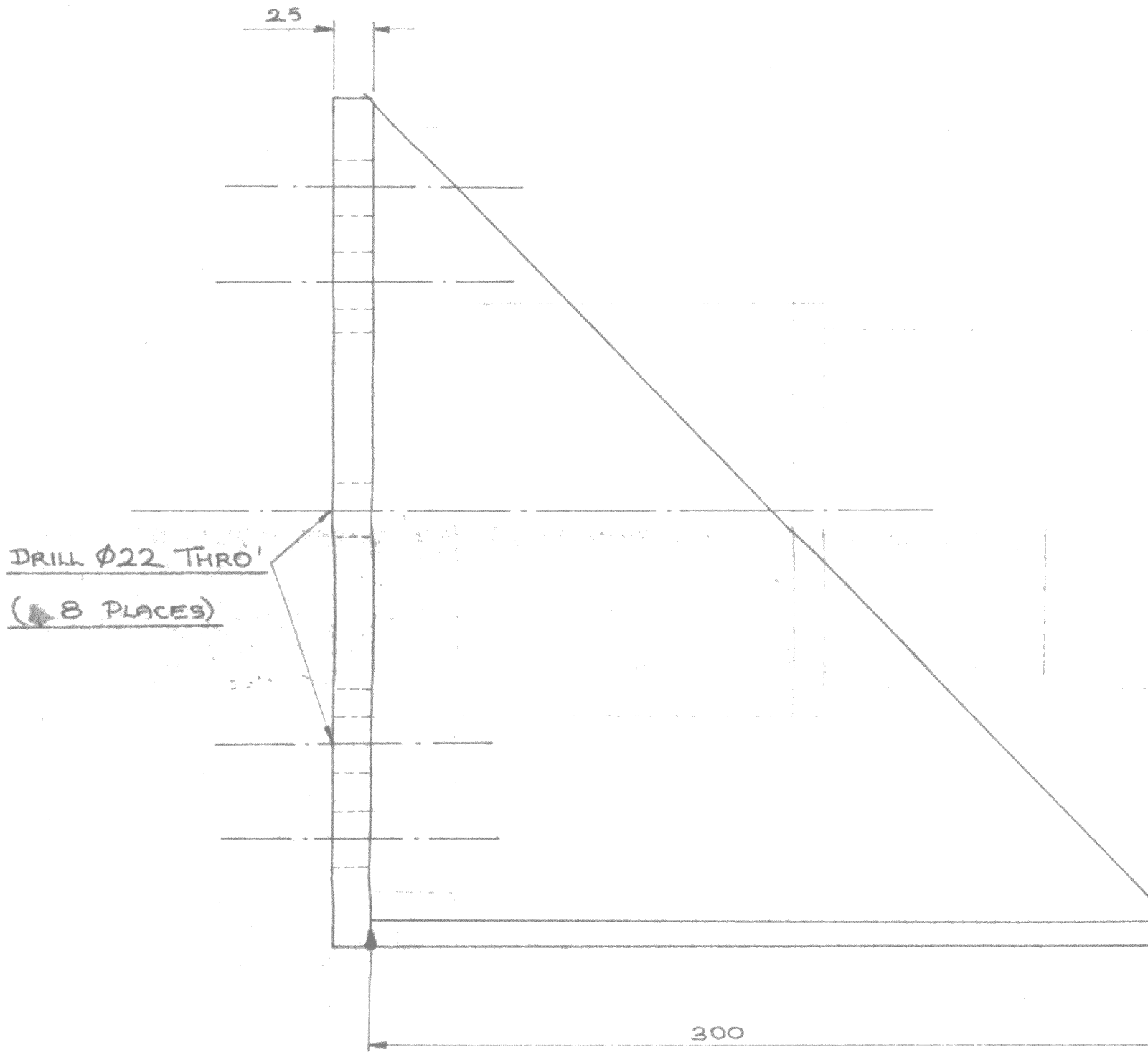
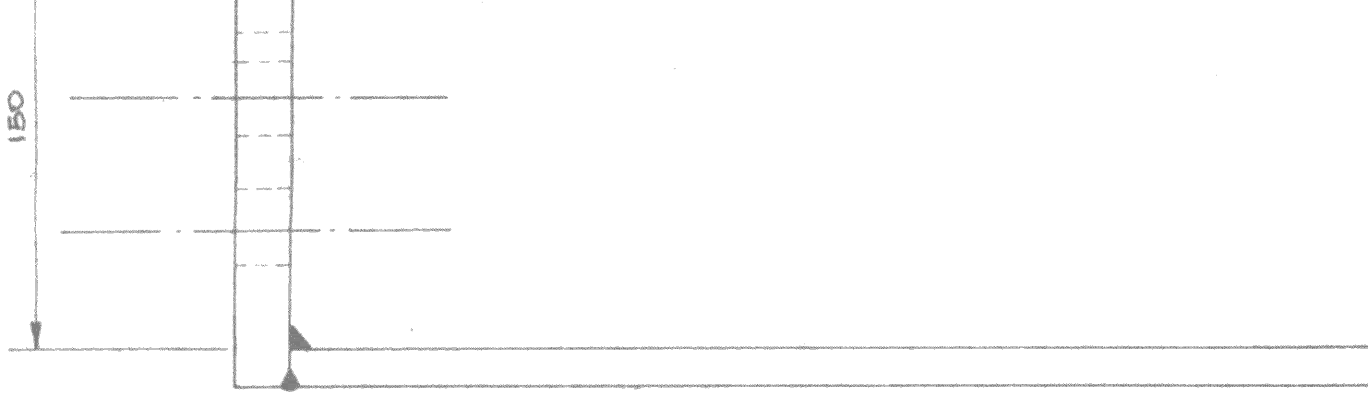
MATL. EN24

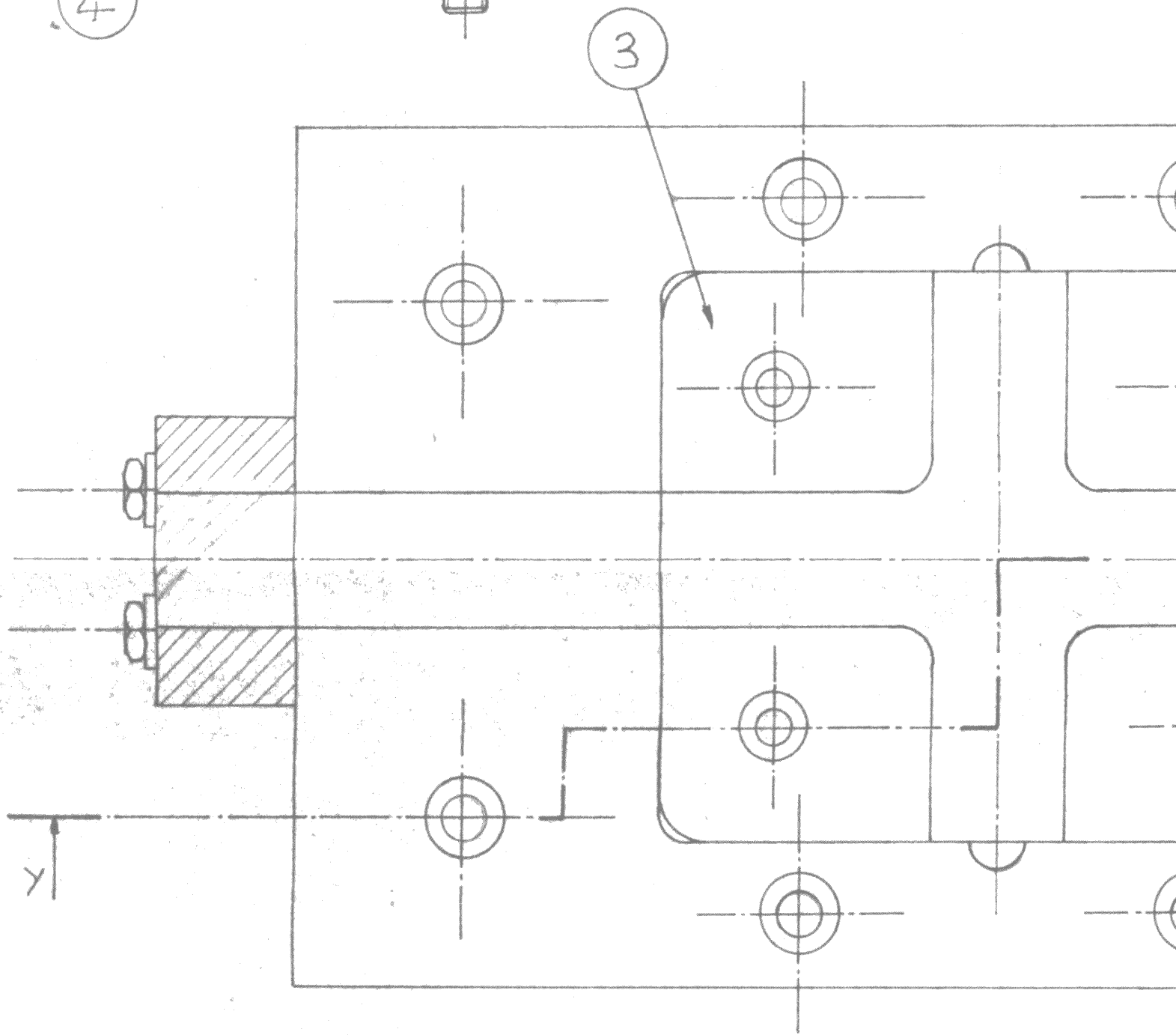
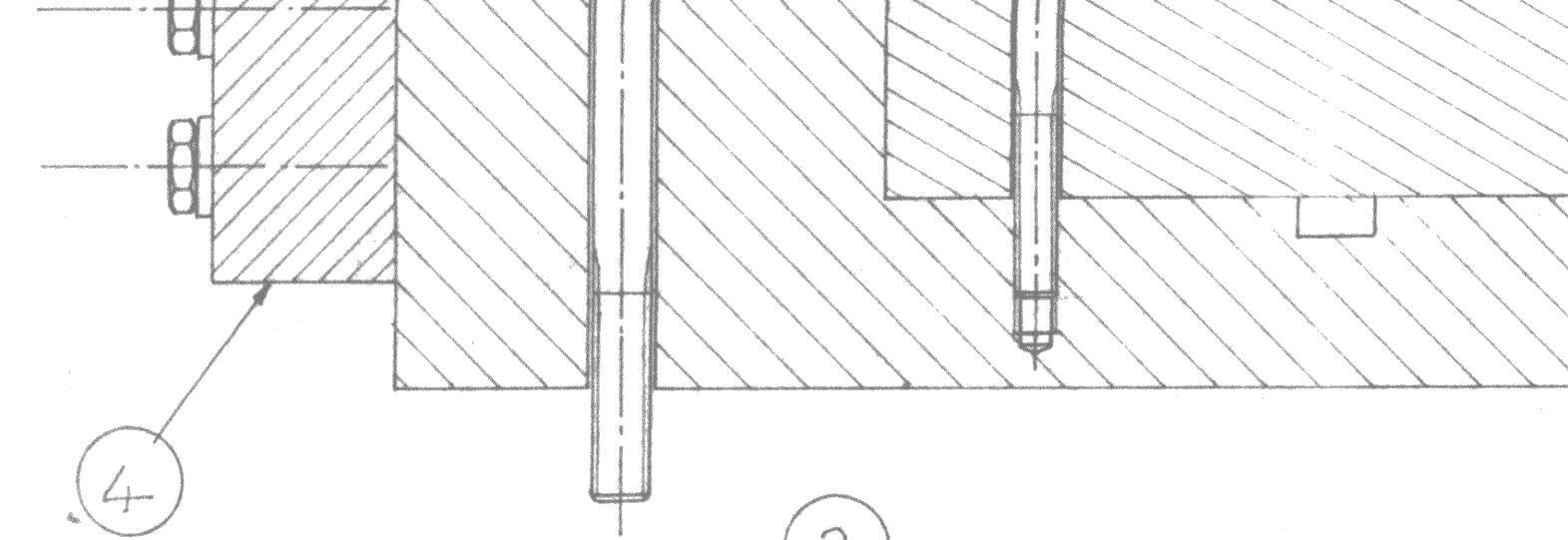




VIEW XX







VIEW XX